PATHOGENESIS OF INFLUENZA IN THE FERRET MODEL: A BASIS FOR IMPROVED INTERVENTION

E.J.B. Veldhuis Kroeze

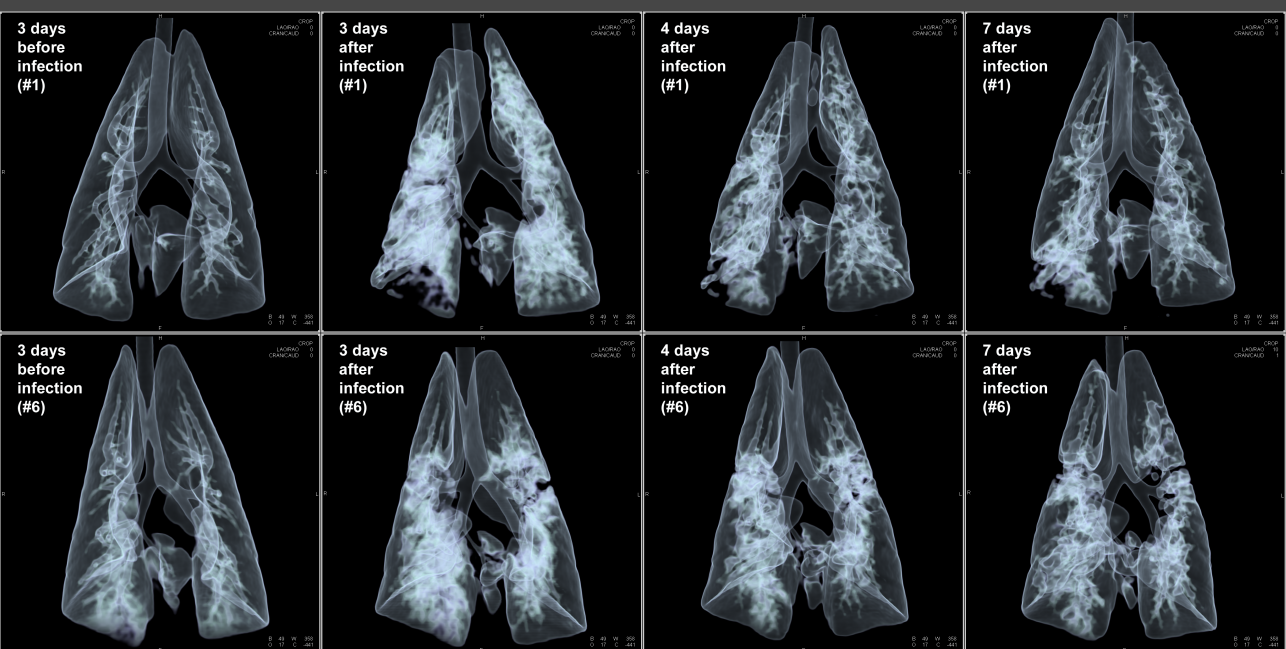

PATHOGENESIS OF INFLUENZA IN THE FERRET MODEL: A BASIS FOR IMPROVED INTERVENTION

PATHOGENESIS OF INFLUENZA IN THE FERRET MODEL:
A BASIS FOR IMPROVED INTERVENTION

Cover
Front: Two rows of four consecutive 3D *in vivo* lung CT-images of two ferrets intratracheally inoculated with the 2009 pandemic H1N1 influenza A virus, compared with their appearance at autopsy.
Back: Exhibition with touchscreen of the former 'Zweetkamer' in the new educational center Erasmus MC Rotterdam.

ISBN: 978-94-6233-605-6
Lay-out & print: Gildeprint, Enschede

This thesis is supported by:

VIROCLINICS BIOSCIENCES B.V.
www.viroclinics.eu

PATHOGENESIS OF INFLUENZA IN THE FERRET MODEL: A BASIS FOR IMPROVED INTERVENTION

Pathogenese van influenza in het frettenmodel: een basis voor verbeterde interventie.

Proefschrift

ter verkrijging van de graad van doctor aan de Erasmus Universiteit Rotterdam op gezag van de rector magnificus

Prof. dr. H.A.P. Pols

en volgens besluit van het College voor Promoties.

De openbare verdediging zal plaatsvinden op woensdag 3 Mei 2017 om 9.30 uur

door

Edwin Johannes Bertus Veldhuis Kroeze

geboren te ’s-Gravenhage

Erasmus University Rotterdam

PROMOTIECOMMISSIE:

Promotores:	Prof. dr. A.D.M.E. Osterhaus
	Prof. dr. T. Kuiken
Overige leden:	Prof. dr. W. Baumgärtner
	Prof. dr. S. Herold
	Prof. dr. G.F. Rimmelzwaan

PATHOGENESIS OF INFLUENZA IN THE FERRET MODEL:
A BASIS FOR IMPROVED INTERVENTION

Pathogenese van influenza in het frettenmodel:
een basis voor verbeterde interventie.

Dedicated to my great-grandfather Johan (Joe) Veldhuis Kroeze
(Kampen NL, Aug 17, 1883 – Ripon Ca, USA, Jan 28, 1920)
who died from acute respiratory distress syndrome
during the Spanish flu pandemic

Edwin Johannes Bertus Veldhuis Kroeze, 2017

CONTENTS

CHAPTER 1

General introduction

CLASSIFICATION OF INFLUENZA VIRUSES AND SUMMARY OF THEIR HOST RANGE

Influenza viruses (family *Orthomyxoviridae*) may cause respiratory disease in humans and animals worldwide. Within the family of *Orthomyxoviridae*, four genera of influenza viruses are recognised based on different antigenic and structural characteristics: A, B, C, and D, which also largely determine their respective host ranges.

Influenza A viruses (IAVs) are endemic in a large variety of mammalian and avian species. Although in principle all bird species may be infected with IAVs, waterfowl and poultry play a special role in their epidemiology. In addition to endemic IAV infections in a particular species, IAV sporadically can jump the species barrier into another species, causing either individual cases of infection or more or less extensive epidemics. Such introduction of a novel strain or subtype of IAV into the human population with variable levels of pre-existing immunity can lead to localised epidemics or worldwide pandemics with variable infection rates and mortalities. Seasonal influenza viruses circulating in the human population cause annual epidemics, which in the temperate climate zones occur predominantly in the winter months.

Influenza B viruses (IBVs) can cause similar disease in humans as seasonal IAVs. Whilst IBV infections were considered to be restricted to humans, in recent years IBV has also been found in seals (1, 2), and in pigs (3). IBVs are classified in lineages and strains, with the two currently lineages being B/Yamagata and B/Victoria.

Influenza C virus can cause mild upper respiratory tract (URT) illness in humans, and can infect pigs as well (4). Influenza B and C virus are not implicated in causing pandemics. **Influenza D virus** is the most recent recognised genus, detected since 2011 in pigs and cattle only (5).

GENOME AND CATEGORISATION OF INFLUENZA A VIRUS

The following sections of this introductory chapter are limited to IAVs, as all studies in this thesis have focused on this influenza virus genus. IAV is an enveloped virus containing a negative-sense single-stranded RNA genome in eight segments (polymerase basic 2, ***PB2***; polymerase basic 1, ***PB1***; polymerase acidic, ***PA***; haemagglutinin, ***HA***; nucleoprotein, ***NP***; neuraminidase, ***NA***; matrix 1 and 2, ***M***; non-structural 1 and 2, ***NS***). These eight gene segments encode for eleven or twelve different viral proteins: **RNA polymerase complex** (*PB1, PB2* and *PA*), **N40 protein** of unknown function (*PB1*), receptor-binding glycoprotein **haemagglutinin** (*HA*), RNA-binding **nucleoprotein** (*NP)*, sialic acid (SA)-destroying enzyme **neuraminidase** (*NA*), ribonucleoprotein-interacting **matrix protein** (*M1*), **ion channel protein** (*M2*), **nuclear export protein** also known as

non-structural protein 2 (*NS2*), interferon (IFN)-antagonising **non-structural protein 1** (*NS1*). In addition, some viruses express the pro-apoptotic protein **PB1-F2** (*PB1*). The viral envelope that encloses the gene segments and carries glycoproteins HA and NA on its surface is formed by a lipid bilayer originating from the infected host cell's membrane upon release of a new infectious virus particle.

IAVs are classified in subtypes on basis of antigenic differences of their HA and NA. To date, 18 HA subtypes (H1-H18) and 11 NA subtypes (N1-N11) are recognised. Sixteen different HA subtypes (H1-H16) and nine different NA subtypes (N1-N9) have been detected mostly in wild waterfowl, where they are considered to replicate asymptomatically in the intestine. In contrast, IAVs of the subtypes H5 and H7 can mutate into a highly pathogenic form in poultry, which induces systemic disease and high mortality rates. H17N10 and H18N11 are the most recently detected IAV subtypes found in asymptomatic New World fruit bats (*Sturnira sp. a*nd *Artibeus sp.*) in 2012 and 2013, respectively (6-8). However, there is ongoing scientific debate whether these bat-derived H17N10 and H18N11 viruses should be classified as influenza A H17/18N10/11-like viruses because of their relative antigenically distant HA and NA genes compared with those of the previously recognised H and N subtypes (9-11).

IAVs subtypes are further classified into different strains, based on host species, geographical location, and year of origin (12). All subtypes are given a chronological strain number. For example, A/equine/Newmarket/2/1993 (H3N8) denotes strain 2 of an H3N8 subtype isolated from a horse in Newmarket in 1993, and A/Perth/16/2009 (H3N2) denotes strain 16 of an H3N2 subtype isolated from a human in Perth in 2009. The host species is not included in the name of the virus strain if it is from humans. Usually, for avian IAVs (AIVs), a prefix is given to indicate the virus' pathogenicity in chickens e.g., H5N1 highly pathogenic avian influenza virus (HPAIV) or H7N9 low pathogenic avian influenza virus (LPAIV).

HOST RANGE OF INFLUENZA A VIRUSES

The host range of established endemic IAV infections is remarkably broad compared to the host ranges of genera B, C, and D, as it includes: humans, wild and domestic birds, domestic pigs, horses, domestic dogs, and most recently New World bats. Wild waterfowl (mainly geese, ducks, swans, gulls, and waders) are regarded the original reservoir of all IAVs, from which mammalian virus strains are derived. Many sporadic infections of various IAVs have been detected in carnivores, cetaceans, non-human primates, bats, uneven-toed and even-toed ungulates, rodents, lagomorphs, and anteaters. Multiple epidemics with considerable mortality rates of avian-origin IAVs have occurred in populations of harbour seals (*Phoca vitulina*) (13-15).

INFLUENZA IN HUMAN BEINGS

1. Epidemiology of seasonal influenza

Two seasonal IAVs, subtypes H1N1 and H3N2, have circulated (together with IBV) globally amongst humans since 1977 and account for up to 500,000 mortalities every year (16). In 2009, the seasonal H1N1 virus was replaced by the 2009 pandemic H1N1 IAV. Such replacement of the previously circulating seasonal subtype commonly occurred when a new pandemic IAV was introduced in the population. An exception was the reintroduction of H1N1 IAV in 1977 as the ''Russian flu'', which has continued to co-circulate with H3N2, as seasonal IAVs. Each year, small antigenic changes (**antigenic drift**) in the HA gene and/or NA gene, resulting from continuous point mutations, provide an escape from pre-existing immunity of the human population. The genes of IAV have high mutation rates because their RNA polymerase complex has no proofreading activity (17). The glycoprotein HA is the major antigenic constituent of IAV. Pre-existing neutralising antibodies drive positive selection of these spontaneous escape mutants and result annually in new seasonal influenza virus infections and outbreaks. Influenza is an acute infectious disease without chronic latent infections and is maintained within the population by continuous human-to-human transmission. Infections occur in winter months of temperate climate regions when decreased levels in relative air humidity stabilise infectious aerosols and are thus considered to favour viral transmission (18, 19). Seasonality is less prominent in tropical and subtropical regions where these viruses circulate throughout the year. The prevalence of disease peaks in school-age children, whereas influenza-associated morbidities that require hospitalisations prevail in young children < 2 years of age and in the elderly > 65 years of age. Infection rates and severity of induced disease depend, besides susceptibility and age of the individual, on the levels of pre-existing immunity and on the virulence of the virus. Risk factors associated with developing severe disease such as pneumonia are: underlying cardiovascular and pulmonary conditions reduced immune status, metabolic and neoplastic diseases, and pregnancy. The cumulative interpandemic seasonal mortality rates usually surpass the mortalities due to pandemics.

2. Epidemiology of pandemic influenza and avian influenza

When a major change (**antigenic shift**) in the HA gene and/or NA gene in a human IAV occurs, attributed to the introduction of an IAV or one or more of gene segments from an animal reservoir a new IAV with pandemic potential may emerge. This may be due to direct zoonotic infections, or an intermediate animal species may be involved. The 1918 and 2009 pandemic H1N1 IAVs involved introductions of a whole virus with all eight gene segments into the human population. Prerequisites for such a new IAV gaining

pandemic proportions are: (a) efficient human-to-human transmission in (b) a relatively immunologically naive human population, permitting high infection rates.

Influenza pandemics are usually designated according to the geographic location of first emergence of the new virus. During the last century four influenza pandemics originating from antigenic shifts have occurred: the 1918 H1N1 pandemic (''Spanish flu'') from introduction of presumed avian IAV, the 1957 H2N2 pandemic (''Asian flu'') and the 1968 H3N2 pandemic (''Hong Kong flu''), both from reassortants of human and avian IAVs, and the 2009 H1N1 pandemic (''Mexican flu'') from a swine IAV (complex reassortant of swine, human, and avian IAVs) (20), all of which caused significant morbidity and mortality. Indeed, the Spanish flu was so severe that a quarter of the world's population was affected by illness during the pandemic and an estimated 50 million people died, plummeting the life expectancy of Americans by 11.8 years from 1917 to 1918 (21). Highest mortality rates prevailed in previously healthy young adults in the age range of 18-34 years, associated with acute respiratory distress syndrome (**ARDS**) and bacterial super-infections (22, 23).

The Mexican influenza virus, mostly designated as ''H1N1 pdm09 IAV'' or ''**pH1N1 IAV**'', was first identified in April 2009 in Mexico and caused an estimated 151,700–575,400 deaths (24) in its first year of global circulation. Mortalities occurred in 0.5% of cases with severe respiratory disease (25), which prevailed in infected older children and young adults. People > 60 years of age were less infected than these younger people, which has been attributed to protective cross-immunity from exposure to pre-1950 H1N1 strains (26, 27). Although the elderly experienced fewer infections, the case fatality rate in this age group was high. Common risk factors associated with developing severe disease such as pneumonia were: obesity, underlying respiratory (asthma) and cardiovascular conditions, diabetes mellitus, smoking, and pregnancy or immediate post-partum period (28-30).

In May of 1997 in China (Hong Kong), **H5N1 HPAIV** was first shown to have crossed the species barrier from chickens to infect humans (31, 32). H5N1 IAVs continue to circulate in wild birds and poultry in Asia, Africa, and Europe, and occasionally infect and kill humans. This avian virus replicates in the lower respiratory tract (LRT) of humans, inducing acute pneumonia, severe respiratory disease and potentially fatal ARDS. To date (July 19, 2016), there have been 854 confirmed human infections of which 450 people died. This corresponds to a current case fatality rate of 53% for H5N1 HPAIV-infected humans. Highest mortality rates prevailed in previously healthy teenagers. In 2015, 39 fatal human cases of H5N1 HPAIV were reported in Egypt alone (33). Most human cases of H5N1 HPAIV-infections had a history of recent exposure to potentially contaminated environments, particularly live poultry markets. Infected humans are regarded poorly infectious to other people, as sustained transmission of H5N1 HPAIV among people is not apparent. However, there is concern that if this pathogenic virus

gains human transmissibility through mutations and/or reassortments, it could evolve into a pandemic virus (34-36).

In March of 2013 in China, another avian-origin influenza virus, **H7N9 LPAIV,** spread to humans. Infected people, with a predisposition for middle-aged to older men, suffered from severe respiratory disease. To date (July 19, 2016), there have been 793 laboratory-confirmed human infections of which 319 people died. This corresponds to a current case fatality rate of 40% for H7N9 LPAIV-infected humans (37). Common underlying medical conditions in hospitalised patients were: coronary heart disease, hypertension, diabetes mellitus and chronic obstructive pulmonary disease (COPD) (38). Like H5N1 HPAIV, most human cases of H7N9 LPAIV had a history of recent exposure to potentially contaminated environments, such as live poultry markets. Although limited human-to-human H7N9 LPAIV transmission could not be entirely excluded in a few clusters of cases, no evident sustained human-to-human transmission has been reported for H7N9 LPAIV (37), but again concern remains that reassortments or mutations may give rise to a new pandemic virus (39).

3. The disease

3a. Uncomplicated influenza: pathogenesis, clinical signs and symptoms, and pathological changes

Pathogenesis of uncomplicated influenza

The pathogenesis describes the process of development of disease. Commonly, infectious aerosols or droplets expelled into the air by infected people are deposited in the URT and LRT of permissive people. Indirect virus transmission via manipulation of freshly contaminated object surfaces (fomites) followed by oronasal or conjunctival self-inoculation is considered another route of infection (40). The virus particle attaches with its surface glycoprotein HA to the host's cell surface receptors, the sialic acid (SA) terminated glycans. Human adaptation of IAVs such as seasonal IAV entails preferential attachment to glycan receptors terminating in SA linked to galactose (Gal) by an α-2,6 SA-linkage (''human type IAV receptors''). These α-2,6 SA-linked receptors are expressed on epithelial cells throughout the human respiratory tract (nasal mucosa, paranasal sinuses, pharynx, trachea, bronchi, bronchioles, and alveoli) but their abundance varies according to anatomical location (41). In contrast, avian IAVs' HA preferentially attach to α-2,3 SA-linked receptors (''avian type IAV receptors'') expressed on epithelial cells of the respiratory and intestinal tract of aquatic birds (42). Confirmed by virus attachment studies using seasonal influenza virus-histochemistry (43), epithelial cells targeted by seasonal IAVs are localised within the nasal cavities, trachea, bronchi, bronchioles and alveoli (type I pneumocytes). The attachment is most abundant to ciliated epithelial

cells of the nose, trachea and bronchi. Following viral attachment, epithelial cells can be infected and constrained into actively replicating the virus. Release of newly-synthesised infectious virus particles still anchored to the hosts' cell membrane by their HA occurs actively by enzymatic cleavage of the receptors' sialic acid (SA) by viral neuraminidase (NA). Absence of NA activity results in aggregates of virus particles and loss of infectivity.

Viral replication typically peaks around 2 days after infection in the nasopharynx, to decline slowly in the following days. Even after the infectious virus can no longer be recovered, viral antigen and RNA can be detected in cells and secretions of infected individuals for several days (44).

Virus infection and replication commonly result in cell death (or cell lysis; ''cytolytic effect'') directly by necrosis, or indirectly by cytokine-mediated and/or inflammatory cell-induced apoptosis. Viral infection and damage to cells and tissues incite inflammatory responses characterised by localised infiltration of inflammatory cells (that may exacerbate cell and tissue damage) and localised and systemic release of pro-inflammatory cytokines and other acute phase proteins. This process results in acute inflammation of the URT; e.g., rhinitis (coryza), sinusitis, pharyngitis, and partially of the LRT; e.g., tracheitis and bronchitis, but also results in systemic responses such as fever and altered haematological values.

Clinical signs and symptoms of uncomplicated influenza

Seasonal influenza is typically characterised by URT infections (nose, throat) evidenced by sudden onset of local signs and symptoms like nasal congestion and a runny nose (rhinorrhoea), sore throat, non-productive cough, but also includes more generalised signs and symptoms like high fever, muscle ache (myalgia), headache, chills, and general malaise. Aerosols and droplets expelled during sneezing and coughing are highly infectious. These signs and symptoms are due to viral replication causing mucosal inflammation and to systemic release of pro-inflammatory cytokines (45, 46). The severity of these acute symptoms can vary but endure usually for a week (47), whereas malaise may last longer.

Diagnosis of influenza involves direct demonstration of replication competent infectious virus by viral culture, or demonstration of viral antigens or viral genetic material by PCR, or indirectly by demonstration of a fourfold increase in titre of specific antibodies in paired sera or respiratory secretions (48). Additionally, tissues sampled by intravitam biopsies (or during autopsy) may be used to confirm IAV infection by means of *in situ* hybridisation (ISH) or immunohistochemistry (IHC). The aetiological differential diagnoses of influenza-like illness (ILI) include: IBVs, ICVs, parainfluenza viruses (PIV), respiratory syncytial virus (RSV), human metapneumovirus (HMPV), and *Mycoplasma pneumoniae*. IAVs are isolated in about one-third of patients with ILI during peaks of seasonal influenza epidemics (49).

Pathological changes of uncomplicated influenza

Infections with seasonal IAVs usually induce a form of uncomplicated influenza. Uncomplicated influenza entails a mild and transient inflammation of typically the URT, potentially involving rhinitis, paranasal sinusitis, pharyngitis, laryngitis, but can extend deeper into the LRT, involving tracheitis and bronchitis, that correspond to the pattern of seasonal influenza virus attachment (50). From 1 day after onset of symptoms, corresponding histological lesions such as epithelial vacuolar degeneration with oedema and loss of cilia, epithelial desquamation, hyperaemia, oedema, hemorrhage, and lymphohistiocytic infiltration of the *lamina propria* can be detected. Already from 2 days after onset of symptoms onward, epithelial regeneration indicative of repair can be present (51, 52). Respiratory epithelial repair has shown to be complete in 10 days in animal models (53), although it may take 1 month to heal (44).

3b. Viral pneumonia: pathogenesis, clinical signs and symptoms, and pathological changes

Pathogenesis of viral pneumonia

The primary complication of influenza is extension of viral infection and inflammation to the lungs, reaching the alveoli (51). In contrast to damage to the conducting airways of the URT and LRT, damage to the alveoli directly impairs gas exchange. Like cellular damage in uncomplicated influenza, alveolar epithelial cell (AEC) damage is induced by direct cytolytic effects of viral infection and by indirect effects of the host immune response (54). These alveolar epithelial cells, composed of type I pneumocytes that firmly seal the walls of the air-filled alveolar lumina, and of type II pneumocytes that resorb fluid from the alveolar lumina, constitute the main stronghold of the barrier between air and blood stream, i.e., the alveolar epithelial-endothelial barrier (**EEB**). Thus, loss of pneumocytes allows fluid from the adjacent capillaries to leak into the alveolar lumen, which leads to respiratory dysfunction and may initiate ARDS. ARDS is an aspecific syndrome that can complicate different acute causes of severe lung damage or shock.

Risk factors predisposing for viral pneumonia include specific or generalised compromised immunity, age > 65 years, pre-existing cardiovascular and pulmonary disease, diabetes mellitus, and pregnancy (55). People not exposed previously to immunity-inducing IAV antigens, from vaccines or from natural priming by cross immunity-inducing IAV strains, lack protective specific IgG in serum and alveolar lining fluid (56-58). Concentrations of specific immunoglobulins in the alveolar lining fluid match those of serum. Long-term immunosuppressive medication in organ transplant patients is a cause of reduced generalised immunity. Chronic pre-existing pulmonary diseases such as COPD, asthma and interstitial fibrosis may reduce the defense against respiratory pathogens. Hypertension associated with cardiovascular disease and

pregnancy is believed to increase the risk for pulmonary oedema to develop when the alveolar epithelial cells are damaged after infection (59). Many fatal cases of ARDS were complicated by bacterial infections (60, 61) that aggravate inflammation of the lung and may lead to sepsis.

According to virus attachment studies using virus-histochemistry, **pH1N1 IAV** attaches to ciliated epithelial cells of nasal conchae, trachea, bronchi, bronchioles, and to type I pneumocytes (43). In severe pneumonia and fatal cases of pH1N1 IAV infections a change in the receptor binding specificity from α-2,6 SA-linked (''human type'') to α-2,3 SA-linked glycan receptors (''avian type'') present on ciliated bronchial cells and alveolar type II pneumocytes is observed. After natural infection, pH1N1 antigens are predominantly expressed in type II pneumocytes, and less in alveolar type I pneumocytes and alveolar macrophages, and in airway epithelium (29). The cell tropism of pH1N1 IAV for the LRT likely predisposes for development of severe pneumonia, whereas the cell tropism for the URT likely predisposes for viral transmission. Comparable with seasonal IAV infection, shedding of pH1N1 IAV peaks in the first 2 days of disease and lasts for 5-7 days after onset of disease, whereas prolonged shedding is observed in infants and the elderly, immunocompromised patients and in patients suffering from ARDS (44).

According to virus attachment studies using virus-histochemistry, **H5N1 HPAIV** attaches mainly to non-ciliated epithelial cells of the LRT; the bronchioles and type II pneumocytes of alveoli (62). Evidenced by positive IHC and ISH, virus-infected type II pneumocytes and tracheal epithelial cells are associated with pathological changes in the respiratory tract (63). During H5N1 HPAIV infections, extra-respiratory complications may occur, more likely resulting from the interaction of ARDS and multi-organ dysfunction syndrome (MODS) (64), rather than from viraemia and viral dissemination. The pathogenesis of MODS is attributed to haemodynamic disturbances and hypercytokinaemia, and may include liver, kidneys, gastro-intestinal tract, and cardiovascular tract. Nonetheless, there is evidence for limited extra-respiratory replication of H5N1 virus in people: in some cases, H5N1 virus has been isolated from the cerebrospinal fluid and H5N1 antigen has been demonstrated by IHC and/or ISH in neurons of the brain, intestinal epithelial and mononuclear cells, lymphocytes of lymph node tissue, Kupffer cells of the liver, fetal macrophages and cytotrophoblasts of the placenta, and in fetal pneumocytes (63).

The high pathogenicity of H5N1 HPAIV may originate in part from the susceptibility of its HA to host proteases, as is valid for infection of chickens. For IAVs to be infectious, their HA must be cleaved into two subunits, HA1 and HA2 (55, 65). In contrast to a single arginine at the cleavage site of seasonal IAVs' HA cleavable by trypsin-like proteases of the respiratory and gastrointestinal tract, the HA of H5N1 HPAIV possesses multiple basic amino acids at its cleavage site and may be cleaved by ubiquitously present

furin-type proteases. This may explain H5N1 HPAIV's ability to cause extra-respiratory infection, resulting in increased pathogenicity.

Additional viral virulence factors of H5N1 HPAIV in humans include: the RNA polymerase complex and NA protein permitting fast and efficient viral replication, the NS1 that antagonises interferon (IFN) production in virus-infected cells, and the PB1-F2 protein responsible for inducing apoptosis and proinflammatory cytokines, such as TNF-α (66). Indeed, elevated serum cytokine concentrations in patients correlated to high oropharyngeal H5N1 viral loads and poor prognosis (67).

H7N9 LPAIV can bind to both α-2,3 SA-linked glycan receptors (avian type) and α-2,6 SA-linked glycan receptors (human type), and attaches to epithelial cells of both URT and LRT. According to virus attachment studies using virus-histochemistry, **H7N9 LPAIV** attaches to both type I and type II pneumocytes in the alveolus (68, 69). In acute serum samples of H7N9-infected patients, increased levels of proinflammatory cytokines and chemokines are detected. High replication of H7N9 LPAIV *in vitro* is attributed to blocking of the induction of antiviral IFN-β by the viral NS1 protein (70).

Clinical signs and symptoms of viral pneumonia

The clinical signs and symptoms of IAV-associated pneumonia and ARDS in general include: high fever, general malaise, laboured breathing (dyspnoea) that may aggravate over time, cyanosis, and coughing up blood (haemoptysis). Multi-organ failure and death (mortality rate up to 60%) may occur as soon as 48 hours after onset of symptoms. Viral pneumonia may be complicated by opportunistic bacterial co-infections that aggravate the clinical disease.

Similar clinical signs and symtoms were reported for **pH1N1 IAV**-infected people who developed pneumonia during the 2009 pandemic. Fatal cases were associated with ARDS, concomitant bacterial infections, and multi-organ failure. The median time from onset of symptoms to death varied from 8 - 12 days (28-30).

Other acute signs and symptoms besides those typical for viral pneumonia reported by people infected with **H5N1 HPAIV** included abdominal pain, chest pain, diarrhoea and rare neurologic symptoms. The incubation period of H5N1 HPAIV infections ranged from 2-5 days, whereas the time from onset of symptoms to death varied from 2 - 9 days (71, 72).

People with severe viral pneumonia from **H7N9 LPAIV** infection also showed vomiting and diarrhoea. The incubation period after exposure to live poultry was estimated at 5 days. ARDS was the most common complication with a median time from the onset of illness to ARDS development of 7 days (38).

Pathological changes of viral pneumonia

Gross pathological changes in influenza viral pneumonia are characterised by extensive consolidation and swelling of the pulmonary parenchyma and variable degree of hemorrhage. The lung surface may show rib imprints upon opening of the thorax. The main histological lesion of acute viral pneumonia is diffuse alveolar damage (**DAD**) characterised by necrosis and desquamation of the alveolar epithelial cells, flooded alveolar lumina with oedema fluid admixed with variable quantities of fibrin strands, neutrophils, macrophages and erythrocytes. The fibrin-rich oedema fluid may be inspissated to form characteristic hyaline membranes lining the alveolar septa. In general, the alveolar septa are thickened due to hyperemia of alveolar capillaries, interstitial oedema, and due to infiltrates of mainly neutrophils, macrophages and lymphocytes, and occasional eosinophils. Alveolar septa may be necrotic, possibly due to ischaemia-inducing fibrinous thrombo-emboli that may be present in pulmonary blood vessels as well.

If patients survive the initial 2 weeks, the histopathology of chronic viral pneumonia is characterised by type II pneumocyte hyperplasia indicative of re-epithelisation, interstitial fibrosis of the septa infiltrated by mainly lymphocytes and plasma cells. Eventually, squamous metaplasia may occur (47). Inflammation of the bronchioles is characterised by epithelial necrosis, and infiltration by variable numbers of mainly neutrophils and lymphocytes. The often-concurrent bacterial infection causes a pyogenic inflammatory reaction, i.e., a suppurative bronchopneumonia, that differs morphologically from a typical virus-induced interstitial pneumonia, as it is characterised by a prominent infiltration of neutrophils, which commonly congregate and lyse to form pus within bronchi, bronchioli and alveoli.

Similar typical histopathological findings of DAD were reported for people infected with **pH1N1 IAV, H5N1 HPAIV** and **H7N9 LPAIV**. Additionally reported for pH1N1 IAV cases was haemophagocytosis in draining lymph nodes, and pulmonary thromboemboli (29).

4. Influenza interventions

Intervention options against influenza entail prevention by vaccination or administration of antiviral medication prophylactically or therapeutically. Vaccination is among the most effective methods of influenza prevention. Immunisation may be induced by inactivated or live-attenuated influenza virus vaccines (**LAIVs**). Inactivated vaccines usually contain purified viral HA, and additionally may contain an aspecific immune response enhancing adjuvant, whereas LAIVs contain a vaccine virus capable of limited replication. Inactivated seasonal influenza vaccines are tri- or quadrivalent, containing three or four antigenic types of HA matching the current circulating strains of H1N1 and H3N2 IAVs, and IBVs. Antibodies against the HA glycoprotein prevent virus binding

to the cell receptor and are effective at preventing infection. Vaccinations have shown an efficacy of 70-90% in preventing disease in normal healthy young adults, with moderately lower efficacy rates in the elderly who exhibit lower serum antibody responses (55). The combined effects of relatively rapid decline in antibody titres and of antigenic drift of seasonal influenza viruses require yearly updated vaccinations against seasonal influenza in people from high risk groups. Candidate vaccines against avian influenza in humans, including adjuvanted inactivated and recombinant H5N1 vaccines, have been developed and elicit protective immune responses in animal models, and are currently in clinical evaluation.

Two classes of antiviral drugs are available for prophylaxis and therapy of influenza virus infection. The adamantane class of antivirals (amantadine [Symmetral] and rimantadine [Flumadine]) are matrix 2 ion channel blockers and effective against IAVs, but their relative toxicity and rapid development of viral resistance limits current application, and thus they are not recommended by the Centers for Disease Control and Prevention (CDC) for clinical use (73). The class of neuraminidase inhibitors (NAI) (zanamivir [Relenza®], oseltamivir [Tamiflu®], peramivir [Rapivab®], and laninamivir [Inavir®]) are effective against both IAVs and IBVs. In 2009, oseltamivir resistance and even multi-NAI resistance of mutated pH1N1 IAVs were detected in patients receiving prolonged antiviral treatment, in particular patients under immunosuppressive therapy (74, 75).

A recent development entails **antiviral antibody** preparations for prophylactic and/or therapeutic medication against influenza. The aim is to produce monoclonal antibodies directed against epitopes conserved in different subtypes of influenza viruses that may allow for a universal efficacy against IAVs regardless of differences in classic antigenicities (55).

AIMS AND OUTLINE OF THIS THESIS

Although clinical disease and associated lesions (also necrosis, also haemodynamic changes) of the respiratory tract due to IAV infections are well known, the pathogenesis of ARDS is not yet fully understood. ARDS is a fatal complication of influenza virus infection, and accounts for many influenza-related mortalities. At the **starting point** of this thesis, the mechanism of pulmonary oedema formation, as one of the hallmarks of influenza-induced ARDS, was unknown. Pulmonary oedema as a representative lesion of ARDS was of major interest in this thesis as it is an acute lesion that is easily detectable in histopathology. The intricate chronic process of scarring fibrosis that may develop subsequent to acute alveolar damage is outside the scope of this thesis.

Several factors (cellular integrity, inflammatory cells, and cytokines) are known to influence the homeostasis of the EEB preventing or permitting oedema to develop. The obvious question that arose at the start of this thesis was: what is the mechanism by which influenza virus induces pulmonary oedema? Therefore the **main aim of this thesis** was unravelling the pathogenesis of influenza-induced ARDS and pulmonary oedema formation, to ultimately pinpoint the most significant pathogenic factors. A better understanding of the pathogenesis, especially identifying the most important causative pathogenic factors is essential in the development of new intervention strategies. Improved intervention options will likely reduce the recurrent global burden of seasonal influenza epidemics and pandemics.

The **ferret** (*Mustela putorius furo*) has shown to be very susceptible to infections with human and avian IAVs and associated diseases, and it has been used to study human influenza since the 1930s, and is regarded by many as the most suitable animal available to mimic human influenza. According to literature reviews summarised in this thesis, various mammalian animal species' susceptibility and sensitivity to IAV infections were assessed in comparison to ferrets. Overall, intratracheally inoculated ferrets were concluded to be particularly suited to model influenza-induced ARDS. This model of experimental intratracheal (IT) IAV inoculation of ferrets is simply referred to as 'the ferret model' throughout this thesis. Although models merely approximate the truth, the benefits of a good animal model are to provide better insights in the vast array of intricate host responses to infectious inflammatory diseases. Often there are no *in vitro* alternatives to study such host responses.

Throughout several scientific publications that constitute this thesis' chapters 2 to 6, the term 'necropsy' is used. Classically, necropsy is the preferred terminology in veterinary medicine designating post-mortem examination. However as recently argued by Law and colleagues, it is time to set dogma and tradition aside for the sake of better communication in the contexts of comparative pathology and One Health initiatives (76). **Autopsy** (''the act of seeing with one's own eyes, from Greek: aut- + opsis'' (77)) commonly used in human medicine, is currently regarded the preferred universal terminology designating post-mortem examination regardless of the species. In adherence, 'autopsy' will be applied in the remainder of this thesis.

The **outline** of this thesis according to chapter numbers is as follows: In this **chapter 1**, a brief introduction was given on influenza A viruses in general, followed by a description of the epidemiology, clinical signs and symptoms, pathogenesis, and the main types of influenza-induced lesions in the respiratory tract. In **chapter 2**, the basic development of influenza-induced ARDS, including pulmonary oedema formation, is reviewed and analysed mainly from a histological and cellular perspective. This leads to the novel interpretation that the alveolar lining epithelium is the main stronghold

of the EEB against leakage of plasma fluids into the pulmonary airspace. In **chapter 3**, the susceptibility of various animal species to influenza virus infections and subsequent disease is reviewed. This host-specific susceptibility is an important determinant for the suitability of a laboratory animal species to model influenza-induced ARDS. Variables involved in using experimental animals in influenza research are outlined and summarised in a table with pros and cons inherent to the commonly used animal models. In **chapter 4**, the pathogenesis of influenza virus infections in the ferret model is evaluated and described, exemplified by inoculations with human IAV isolates: 2009 pH1N1 IAV and 2013 H7N9 AIV. In **chapter 5**, a novel approach to quantify alterations in aerated lung tissue in pH1N1-IAV-inoculated ferrets is presented. The method of repeated computed tomography (CT)-scanning of inoculated and acutely inflamed ferret lungs is validated and described as proof of principle and potential additional read-out parameter in influenza research. In **chapter 6**, several practical applications of the ferret model to assess the efficacy of human influenza vaccines with novel administration routes and adjuvant formulations are outlined, including quantification of altered ferret lung aeration by CT-scanning as correlate of protection. In **chapter 7**, the summarising discussion, the findings and conclusions from previous chapters are discussed and integrated with existing knowledge culminating in perspectives on future research regarding pathogenesis and intervention strategies of influenza-induced ARDS. In **chapter 8**, a thesis summary in Dutch is given. In **chapter 9**, scientific literature references concerning all chapters are listed. A list of abbreviations, *Curriculum vitae*, PhD portfolio, list of publications, and acknowledgements, are provided as **addenda** to this thesis.

CHAPTER 2

Pathogenesis of ARDS

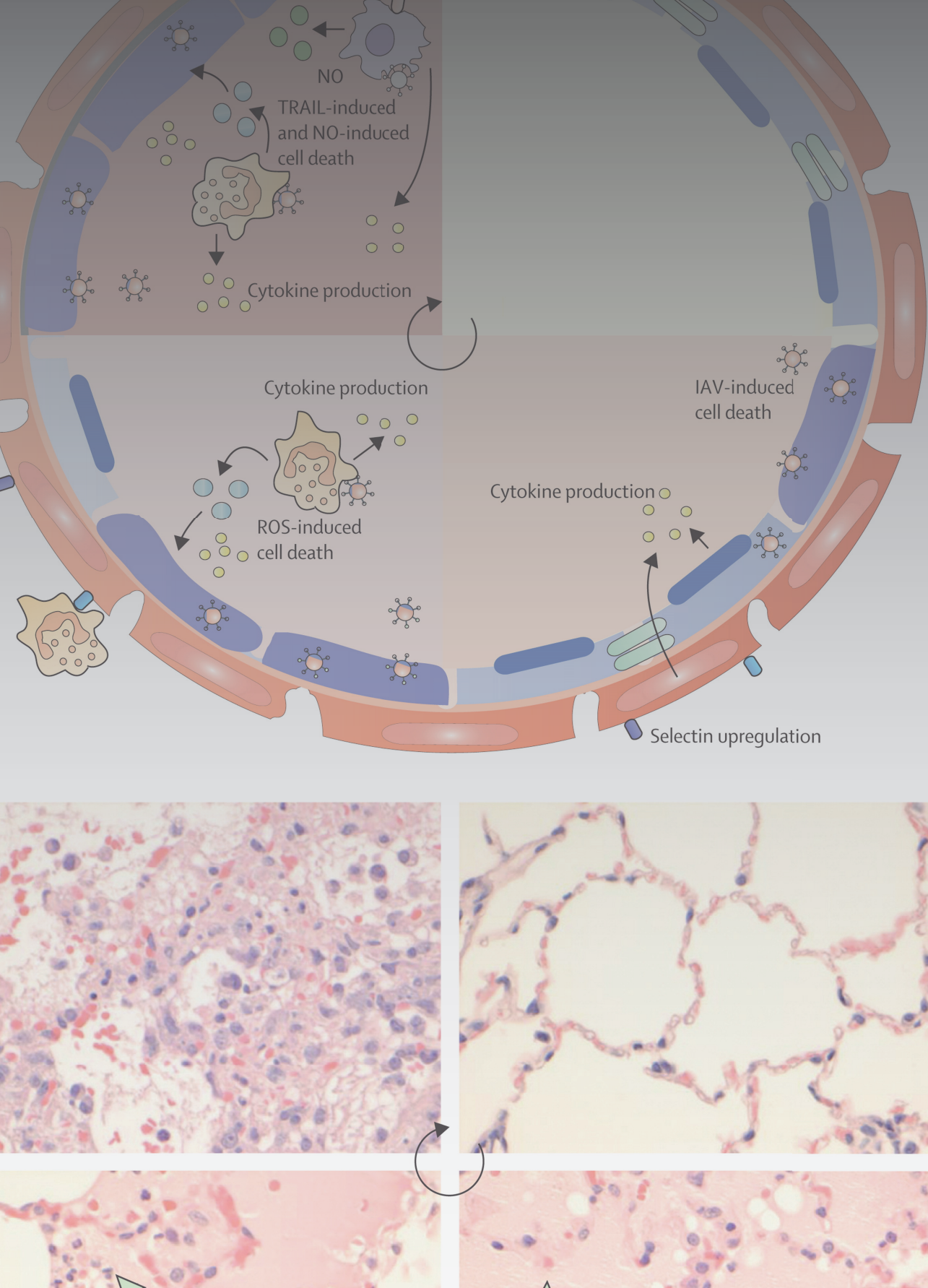
NO
TRAIL-induced
and NO-induced
cell death
Cytokine production
Cytokine production
ROS-induced
cell death
IAV-induced
cell death
Cytokine production
Selectin upregulation

2.1

Pathogenesis of influenza-induced acute respiratory distress syndrome

K.R. Short[1], E.J.B. Veldhuis Kroeze[1,2], R.A.M. Fouchier[1] & T. Kuiken[1]

Lancet Infectious Diseases 2014; 14: 57-69

Affiliations
[1]Department of Viroscience, Erasmus Medical Center, Rotterdam, The Netherlands
[2]Viroclinics Biosciences B.V., Rotterdam, The Netherlands

SUMMARY

ARDS is a fatal complication of influenza infection. In this Review we provide an integrated model for its pathogenesis. ARDS involves damage to the EEB, fluid leakage into the alveolar lumen, and respiratory insufficiency. The most important part of the EEB is the alveolar epithelium, strengthened by tight junctions. Influenza virus targets these epithelial cells, reducing sodium pump activity, damaging tight junctions, and killing infected cells. Infected epithelial cells produce cytokines that attract leucocytes—neutrophils and macrophages—and activate adjacent endothelial cells. Activated endothelial cells and infiltrated leucocytes stimulate further infiltration, and leucocytes induce production of reactive oxygen species (ROS) and nitric oxide (NO) that damage the barrier. Activated macrophages also cause direct apoptosis of epithelial cells. This model for influenza-induced ARDS differs from the classic model, which is centred on endothelial damage, and provides a rationale for therapeutic intervention to moderate host response in influenza-induced ARDS.

INTRODUCTION

Influenza A virus is a respiratory pathogen that substantially affects human health worldwide. Seasonal viruses circulating in the human population cause annual epidemics with about 500 000 deaths per year (16). A novel strain of influenza A virus without pre-existing immunity in the population could cause a global pandemic with variable mortality; the 2009 H1N1 pandemic caused 151,700–575,400 deaths in its first year of circulation (24), whereas the 1918 H1N1 pandemic caused more than 40 million deaths (78). There is concern that newly emerging strains of influenza A virus from animal reservoirs (e.g., avian-origin H5N1 and H7N9 viruses) could gain efficient transmissibility in human beings and cause a severe pandemic (39, 79). To mitigate the severity of such a pandemic, the mechanisms by which influenza A causes respiratory disease need to be understood.

The main complication of influenza virus infection is viral pneumonia, which often occurs together with, or is followed by, bacterial pneumonia (22, 23, 51, 80-82). In this Review, we focus on primary viral pneumonia, which can then lead to ARDS (38, 83-86). Clinically, the acute phase of ARDS is characterised by cyanosis, hypoxaemia, pulmonary oedema, and increasing respiratory failure over time, resulting in multiorgan failure and a high mortality rate (up to 60%) (87). In addition to influenza A virus, various other disorders—e.g., sepsis, pneumonia, trauma, and aspiration of gastric contents—can cause ARDS (88). A major cause of respiratory failure in the acute phase of ARDS is damage to the epithelial–endothelial barrier of the pulmonary alveolus, where gas exchange takes place (**Figure 2.1.1**). Damage to this barrier results in flooding of the alveolar lumen with proteinaceous oedema fluid containing fibrin, erythrocytes, and inflammatory cells. This oedema fluid reduces alveolar gas exchange and can result in severe respiratory insufficiency, as noted in patients with ARDS (88).

Much of the understanding of damage to the EEB in the acute phase of ARDS comes from studies of bacterial sepsis, in which the first site of damage is the endothelium (88-90). This model might not be appropriate for influenza virus, which first infects the epithelium. Additionally, although some reviews have focused on different factors of influenza-virus-induced lung damage —including viral virulence factors (91), cytokine production (92), and pathological changes (47)— no review has brought these features together. We review the available literature on the interaction between influenza A virus and key cell types present in the pulmonary alveolus in the acute phase of ARDS. Specifically, we focus on the roles of pulmonary epithelial and endothelial cells, neutrophils, and macrophages in damage to the EEB to develop a new conceptual framework for influenza-induced ARDS.

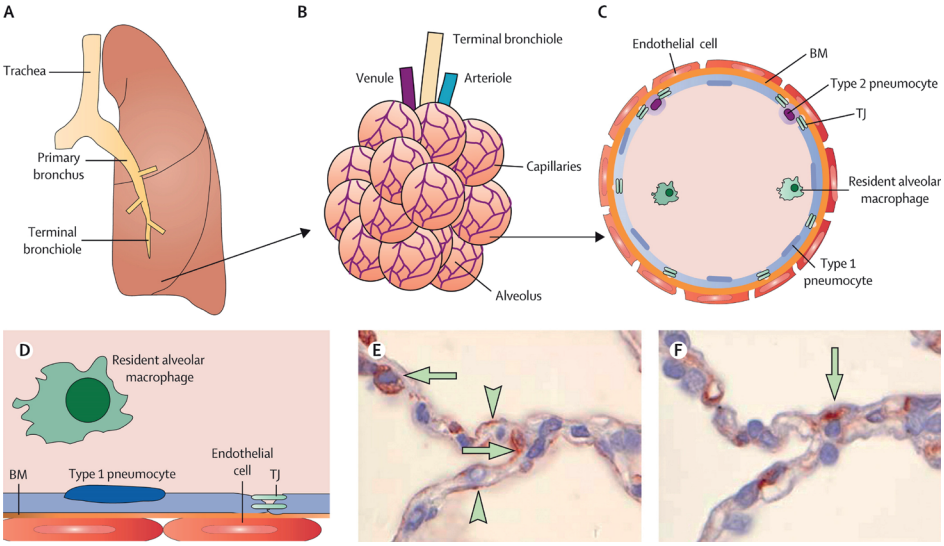

Figure 2.1.1 Schematic representation of the EEB in the human respiratory tract. (A) In the lower respiratory tract, the trachea divides into primary bronchi and several levels of bronchi and bronchioles until the terminal bronchioles. (B) Each terminal bronchiole supplies an acinus of about 2000 alveoli. The alveolar walls contain a network of pulmonary capillaries, supplied with blood coming from pulmonary arterioles and draining into pulmonary venules. (C) Each alveolus contains several alveolar macrophages and is lined by flat type 1 pneumocytes and cuboidal type 2 pneumocytes. The pneumocytes lie on a basement membrane, which is directly juxtaposed to or fused with the basement membrane of the pulmonary capillaries, which are lined by endothelial cells. (D) Gas exchange between blood in pulmonary capillaries and air in alveolar lumina takes place across the EEB, consisting of the alveolar epithelial layer, basement membrane or membranes, and pulmonary endothelial layer. (E) Specific staining for pankeratin stains type 1 pneumocytes (arrowheads) and type 2 pneumocytes (arrows) in a normal human alveolus (reduced by 13% from ×1000). (F) Specific staining for von Willebrand factor stains capillary endothelial cells (arrow) in a serial section of the same tissue shown in part E (reduced by 13% from ×1000). BM=basement membrane. TJ=tight junction.

EPITHELIAL CELLS

Among the first cells that influenza virus encounters after entering the alveolus are epithelial cells, either type 1 or type 2 pneumocytes. Type 1 pneumocytes are flat cells that cover 95% of the alveolar surface and allow easy diffusion of gas between air in the alveolar lumen and blood in the capillaries. Type 2 pneumocytes are cuboidal cells that secrete lung surfactant, which is important to reduce alveolar surface tension. Tight junctions at the sites where adjoining epithelial cells meet reduce the permeability of the alveolar epithelial cell layer. Tight junctions are composed of different proteins, including claudins and zona occludens 1, 2, and 3 (93). More than 90% of the resistance to protein transport across the EEB arises from the alveolar epithelium (94). By limiting

protein transport, the epithelium maintains osmotic pressure across the barrier and prevents pulmonary oedema (87).

A second mechanism by which the alveolar epithelium keeps the alveolar lumen free of fluid is through the action of ion channels and membrane proteins, which include the amiloride-sensitive epithelial sodium channels (ENaCs), the cystic fibrosis transmembrane conductance regulator, and many different aquaporins. The best characterised ion channel in the lung is the ENaC, which is present on the apical surface of both type 1 and type 2 pneumocytes (95, 96). This channel is complemented by an Na^+/K^+ ATPase on the basolateral cell surface. Na^+ ions entering the channel at the apical surface are translocated to the basolateral cell surface, where Na^+/K^+ ATPase pumps them into the underlying interstitium (where present). The presence of Na^+ in the interstitium creates an osmotic gradient that removes water from the alveolar lumen through aquaporins and intracellular pathways in alveolar epithelial cells, thus preventing pulmonary oedema (95, 96).

Not only are pneumocytes a crucial component of the EEB, but they are also target cells for infection by influenza A virus. Influenza A binds to its target cell by attachment of viral haemagglutinin to a sialosaccharide on the cell surface. The expression of sialosaccharides differs for different pneumocytes: type 1 pneumocytes express predominantly α-2,6-linked sialosaccharides, generally preferred by human influenza viruses, whereas type 2 pneumocytes express mainly α-2,3-linked sialosaccharides, generally preferred by avian influenza viruses (41, 50, 62). Consistent with the tropism of avian influenza viruses for α-2,3-linked sialosaccharides, autopsy findings of patients who died from influenza H5N1 showed that H5N1 virus antigens are most prominent in type 2 pneumocytes (97-99). By contrast, autopsy findings of fatal cases of infection with 2009 pandemic H1N1 virus (which has dual tropism for both α-2,3-linked and α-2,6-linked sialosaccharides (100)) showed antigen expression for pandemic H1N1 virus in both type 1 and type 2 pneumocytes (29). These virus-dependent differences in attachment are dependent on specific aminoacid residues in the receptor-binding domain of the haemagglutinin globular head. Positions 190 and 225 (influenza A H1 virus) and positions 226 and 228 (influenza A H2 and H3 viruses) are the main determinants of receptor specificity for pandemic influenza viruses (101). Mutations at these positions also define the receptor-binding preference of the influenza A H5N1 virus (102). Thus, the type of alveolar epithelial cell targeted might differ between influenza A strains.

Very early after infection, influenza A virus causes fluid accumulation in the alveolar lumen by direct inhibition of ENaCs (**Figure 2.1.2**) (103). *In vitro* exposure of type 2 pneumocytes to influenza A/Puerto Rico/8/1934 (H1N1) for 1 h decreased ENaC activity while maintaining the integrity of the epithelium (103). This decrease in activity was due to activation of protein kinase C and phospholipase by the viral haemagglutinin (103, 104). The M2 ion channel of influenza virus might also inhibit the activity of ENaCs on

epithelial cells by triggering the production of ROS and subsequently activating protein kinase C (105). Consistent with these findings, rats infected with influenza virus and then intratracheally given saline solution had significantly less fluid clearance from the lungs at 2 h after infection than did uninfected rats (103).

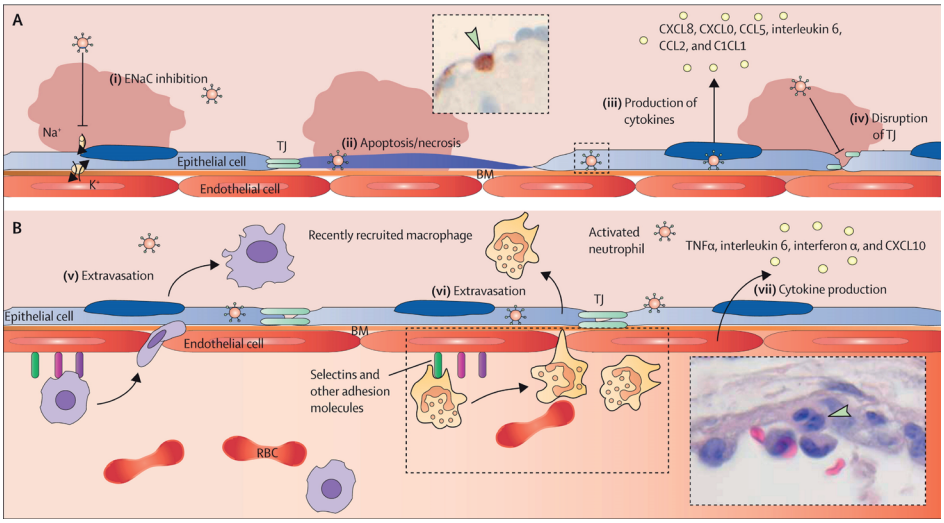

Figure 2.1.2 The role of alveolar epithelial and endothelial cells in influenza-induced ARDS. (A) In the early stages of ARDS, influenza A virus can inhibit the action of ENaCs (i) on alveolar epithelial cells. Later in infection, influenza virus can trigger the apoptosis or necrosis (ii) of alveolar epithelial cells, cytokine production (iii), and disruption of tight junctions (iv). Ultimately, these changes lead to the accumulation of proteinaceous fluid in the alveolus (pink). Specific staining for influenza A nucleoprotein shows influenza A H5N1 infection (inset) of an alveolar epithelial cell (arrowhead) in human lung tissue after 24 h (reduced by 22% from ×400). (B) After influenza A virus infection, the capillary endothelial cells enable the extravasation of monocytes (v) and neutrophils (vi) into the alveolus via the upregulation of adhesion molecules such as E-selectin and P-selectin. The inset shows adhesion of neutrophils (arrowhead) and other leucocytes to the endothelium of a pulmonary blood vessel from a ferret, 4 days after *in vivo* infection with influenza A H5N1 (Haematoxylin and eosin (H&E) stain, reduced by 22% from ×800). The endothelium can produce various proinflammatory cytokines (vii) in response to influenza A. In both (A) and (B), epithelial cells represent both type 1 and type 2 pneumocytes. ARDS=acute respiratory distress syndrome. ENaC=amiloride-sensitive epithelial sodium channel. BM=basement membrane. RBC=red blood cell. TJ=tight junction. TNF=tumour necrosis factor.

At a later stage of infection, death of epithelial cells induced by influenza A virus plays a major part in damage to the EEB by destruction of the physical epithelial layer (106). Both types of cell death—apoptosis and necrosis—have been reported in post-mortem tissues of patients with ARDS induced by influenza virus (107, 108). The mechanisms by which influenza virus induces cell death have been shown *in vitro* (109-111), although

typically for bronchial or bronchiolar epithelial cells rather than alveolar epithelial cells. Infection of a human bronchiolar epithelial cell line (NCL-H292) with reassortant influenza A/England/939/69 (H3N2) resulted in caspase-8-dependent apoptosis (109). Influenza virus can induce epithelial cell apoptosis through various different pathways, including the activation of protein kinase R, which subsequently upregulates proapoptotic genes (e.g., *FAS*) (112). Alternatively, viral neuraminidase can activate transforming growth factor β to its active form, which then induces apoptosis by interacting with its cognate receptors (113). The expression of non-structural protein 1 (NS1), derived from influenza A/Hong Kong/483/97 (H5N1), is also sufficient to induce epithelial cell apoptosis in a caspase-dependent manner (111). By contrast with influenza-virus-induced apoptosis of NCL-H292 cells, infection of primary human bronchial epithelial cells with a mouse-adapted strain of influenza A/Puerto Rico/8/1934 (H1N1) resulted in necrosis (110). The viral polymerase complex (particularly the nucleoprotein) could contribute to influenza-virus-induced cell death by removal of the cap structures of host-cell mRNA (so-called cap snatching), which reduces the amounts of capped host mRNAs that are translated into functional proteins (114). Because of the important role of the epithelium in minimisation of pulmonary oedema, the loss of epithelial cells as a result of influenza-virus-induced cell death has a major role in damaging the architecture of the lung.

The effects of epithelial cell death on damage to the EEB could be compounded by the ability of influenza virus to damage tight junctions of epithelial cells. Specifically, some H5N1 strains might directly disrupt tight junctions through a PDZ-ligand-binding motif present in the ESEV consensus sequence in the carboxyl terminus of viral NS1 (115). This sequence mediates binding of viral NS1 to host proteins such as scribble and DLG1, which are important to the formation of tight junctions (115). Accordingly, infection of Madin-Darby canine kidney (MDCK) cells with viruses possessing the ESEV motif disrupts the formation of tight junctions (115). However, the expression of the ESEV motif is limited to a subset of influenza A strains (115). Thus, direct targeting of tight junctions by viral NS1 might not occur in all influenza virus infections.

Finally, in influenza virus infection, epithelial cells produce cytokines that can subsequently damage the EEB. Post-mortem analysis of a fatal case of influenza virus H5N1 pneumonia showed the production of tumour necrosis factor α (TNFα) by alveolar epithelial cells (116). Findings from in-vitro studies suggest that influenza-virus-infected alveolar epithelial cells produce other cytokines in addition to TNFα (**Table 2.1.1**) (109, 110, 117-125). Generally, data from in-vitro studies must be interpreted with caution because results can differ dependent on the influenza virus strain and cell type used, and because many studies use primary cells or cell lines derived from the trachea, bronchus, or bronchiole (rather than from the alveolus). Findings of studies with primary human type 2 pneumocytes suggest that the increased production of CXCL10, interleukin 6, and CCL5 after infection with H5N1 (compared with infection with a seasonal H1N1 strain)

Table 2.1.1 Cytokine production by cell type after influenza A virus infection of epithelial cells

	Cell description or source	Influenza A strain	Cytokines produced upon influenza A infection
Human primary airway epithelial cells[117]	Derived from main bronchi and lobar or segmental bronchi of patients after surgical lung resections	A/Port Chalmers/72 (H3N2)	Interleukin 8
Human primary type 2 pneumocytes[118]	Isolated from human non-tumour lung tissue	A/Hong Kong/483/97 (H5N1), A/Vietnam/1194/04 (H5N1), A/Vietnam/3046/04 (H5N1), A/Hong Kong/54/98 (H1N1)	Interleukin 6, interferon β,* CXCL10, and CCL5 (Hong Kong/483/97 strain, Vietnam/1194/04 strain); interleukin 6, interferon β,* CXCL10, and CCL5* (Vietnam/3046/04 strain, Hong Kong/54/98 strain)
Primary mouse airway epithelial cells[119]	Derived from the lungs of naïve BALB/C mice	A/PR/8/34 (H1N1)	CCL2 and CCL5
Normal human bronchial or tracheal epithelial cells[110]	Commercially available primary cells	A/PR/8/34 (H1N1)	Interleukin 8
U1752[110]	Cell line derived from a lung tumor originally diagnosed as a small-cell carcinoma	A/PR/8/34 (H1N1)	Interleukin 8, CXCL1, and CCL5
BEAS-2B[120]	Cell line derived from normal human bronchial epithelium obtained from autopsy of non-cancerous individuals.	A/Scotland/20/74 (H3N2)	Interleukin 8, CCL5, and interleukin 6

Table 2.1.1 Cytokine production by cell type after influenza A virus infection of epithelial cells (continued)

	Cell description or source	Influenza A strain	Cytokines produced upon influenza A infection
Primary ferret pulmonary epithelial cells[121]	Derived from the trachea of naïve ferrets	A/Brisbane/59/07 (H1N1), A/Mexico/4482/09 (H1N1), A/Wisconsin/67/05 (H3N2), A/Vietnam/1204/03 (H5N1)	Interferon β,* CXCL9,* CXCL11,* CXCL10,* TNFα,* interleukin 6,* interleukin 8,* and CXCR3* (Brisbane strain); interferon β,*CXCL9,* CXCL10,* TNFα,* interleukin 6,* interferon α, and CXCR3* (Mexico strain); interferon β,* CXCL9,* CXCL10,* TNFα,* interleukin 6,* interferon α* CXCL11,* interleukin 8*and CXCR3* (Wisconsin strain); interferon β,*CXCL9,* CXCL10,* TNFα,* interleukin 6,* interferon α,* CXCL11,* interleukin 8,* and CXCR3* (Vietnam strain)
A549[122]	Cell line derived from lung carcinomatous tissue	A/WSN/33 (H1N1)	TNFα,* interleukin 1β,* interleukin 6,* interleukin 8, and CCL5*
A549[123]	Cell line derived from lung carcinomatous tissue	A/New Caledonia/20/99 (H1N1), A/Beijing/353/89 (H3N2)	CCL2, CCL5, CXCL10, and interleukin 8
A549[110]	Cell line derived from lung carcinomatous tissue	A/PR/8/34 (H1N1)	Interleukin 8, CXCL1, CCL5, and CCL2
NCl-H292[124]	Cell line derived from a lymph node metastasis of a pulmonary mucoepidermoid carcinoma.	H3N2	Interleukin 6, interleukin 8, and CCL5

Table 2.1.1 Cytokine production by cell type after influenza A virus infection of epithelial cells (continued)

	Cell description or source	Influenza A strain	Cytokines produced upon influenza A infection
NCI-H292[125]	Cell line derived from a lymph node metastasis of a pulmonary mucoepidermoid carcinoma.	A/Sisen/2/92 (H3N2)	Interleukin 6, interleukin 8, and CCL5
NCI-H292[109]	Cell line derived from a lymph node metastasis of a pulmonary mucoepidermoid carcinoma.	Reassortant virus: A/Puerto Rico/8/34 (H1N1) x A/ England/939/69 (H3N2)	Interleukin 6, interleukin 8, and CCL5

*Determined by mRNA expression. TNF=tumour necrosis factor.

could contribute to increased disease severity (118). However, the mechanism by which these or other cytokines damage the EEB is unclear. ENaC activity can be decreased by cytokines such as interleukin 1β (126). Tight junctions can also be disrupted by cytokines such as TNFα (127). Several cytokines produced by alveolar epithelial cells in response to influenza virus infection are also chemotactic, or can upregulate the expression of cell adhesion molecules on pulmonary endothelial cells, and thus enable the extravasation of leucocytes (128). These cells can then damage the EEB.

ENDOTHELIAL CELLS

Endothelial cells are the most abundant cell type in the lung, constituting 30% of the total cell population (129). In the alveolus, endothelial cells line the capillaries that form a network in the alveolar walls. On their apical side, endothelial cells are in direct contact with circulating blood and form the site of attachment for recruited inflammatory cells. After appropriate activation, endothelial cells express cell adhesion molecules, which bind to their cognate ligands on leucocytes and mediate leucocyte extravasation (87). On their basolateral side, endothelial cells lie on a basement membrane, which is closely apposed to (or even fused with) the epithelial basement membrane (129). This intimate contact suggests that endothelial cells are strongly affected by signals and virus particles released from epithelial cells and inflammatory cells in the alveolar lumen. Activation of the endothelium by these signals and virus particles is essential to mediate an effective immune response against influenza A. However, activation of the endothelium might play a part in damage to the EEB and contribute to pulmonary oedema.

Influenza virus infection can upregulate the expression of endothelial adhesion molecules (e.g., E-selectin, P-selectin, ICAM1, and VCAM1), thereby enabling the recruitment of leucocytes to the alveolus (**Figure 2.1.2**) (130, 131). The presence of a large number of neutrophils and macrophages could damage the EEB through various mechanisms. Infection with influenza A H5N1 virus results in increased expression of E-selectin and P-selectin on human endothelial cells compared with infection with 1918 pandemic H1N1 or a seasonal H1N1 strain (131). This differential activation of the endothelium might help to account for the increased leucocyte recruitment that occurs in H5N1 influenza virus infection (132) and the consequent increase in alveolar damage. Influenza virus infection can also trigger cytokine production by pulmonary endothelial cells. Seasonal H3N2 and H1N1 viruses trigger the production of interleukin 6, CXCL9, and CXCL10 by human umbilical-vein endothelial cells (133, 134), whereas infection with H5N1 virus can trigger the production of CXCL10, TNFα, and interleukin 6 (131). Findings of murine studies have shown that influenza-virus-induced activation of the pulmonary endothelium contributes to disease severity in mice infected with

2009 pandemic H1N1 or seasonal H1N1 viruses (135). Specifically, the pulmonary endothelium produced cytokines such as CCL2, CXCL10, interferon α, interleukin 6, TNFα, and interferon γ in response to influenza A virus and recruited leucocytes to the lung during infection (135). Accordingly, inhibition of endothelial-induced cytokine production and leucocyte recruitment by treatment with a sphingosine-1-phosphate agonist significantly improved survival rates after infection with influenza virus (135). Unfortunately, the mechanism by which endothelial-derived cytokines could have damaged the EEB in influenza virus infection is unknown (135). Nevertheless, these findings emphasise the important role that endothelial activation has in influenza-virus-induced damage of the alveolus.

Influenza A virus might also damage the EEB by directly infecting endothelial cells, triggering cell death, and thereby creating sufficient endothelial damage to mediate pulmonary oedema (130, 136, 137). *In vitro*, the presence of a multibasic cleavage site in haemagglutinin enables the productive replication of H5N1 viruses in endothelial cells (131). In poultry, haemagglutinins with a multibasic cleavage site enable systemic virus replication because these haemagglutinins can be cleaved by ubiquitously expressed proteases, by contrast with haemagglutinins with monobasic cleavage sites that depend on trypsin-like proteases expressed only in the airways and gastrointestinal tract (138). However, unlike the epithelial layer, the endothelial layer is not as important a barrier to fluid leakage from the capillary lumen to the alveolar lumen. Together with the basement membrane, the endothelial layer constitutes only 10% of the resistance to protein transport (which maintains osmotic pressure) across the EEB (94). Therefore, damage to the endothelial layer alone is not a key cause of pulmonary oedema. Exposure of sheep to endotoxin caused moderately severe injury to the lung endothelium but no pulmonary oedema, probably because the alveolar epithelium remained morphologically and functionally intact (139). Furthermore, although H5N1 influenza virus and other influenza virus strains infect endothelial cells of human beings and laboratory mammals *in vitro* (130, 131, 133, 136, 140, 141), little evidence suggests that influenza virus infection of the endothelium occurs *in vivo*. Findings of post-mortem studies of fatal human cases show no infection or rare infection of endothelial cells by H5N1 and other influenza virus strains (29, 51, 142). Similarly, findings of many detailed pathological studies of H5N1 and other influenza virus strains in laboratory mammals also show no evidence for endotheliotropism (143), and extensive infection of the endothelium is seen only when H5N1 virus is given to cats through the intestine (144). Together, these results suggest that influenza virus infection of endothelial cells is absent or rare in human beings and other mammals. Thus, endothelial activation plays a more important part than does direct infection of endothelial cells with influenza virus in damage to the alveolar EEB.

NEUTROPHILS

Neutrophils arrive in the pulmonary alveolus within 1 day of influenza virus infection (132), where they join residential leucocytes such as alveolar macrophages. Neutrophils are short-lived, phagocytic granulocytes that, in response to proinflammatory stimuli, extravasate from the blood into the alveolar lumen. Extravasation of neutrophils has several steps: rolling along the endothelium, adherence to selectins and adherins on endothelial cells, and migration through both the endothelial and the epithelial layer into the alveolar lumen (145). This migration can cause temporary damage to the EEB, but is not sufficient to cause pulmonary oedema (145-147).

After entering the alveolar lumen, neutrophils become activated in response to locally present cytokines and pathogens. Activated neutrophils can phagocytose pathogens. The resulting phagosome can fuse with intracytoplasmic primary, secondary, and tertiary granules, which contain various toxic compounds to kill phagocytosed pathogens. These toxic compounds can be released extracellularly after contact with indigestible material (e.g., immune complexes deposited on a basement membrane), phagocytosis of membranolytic substances (e.g., urate crystals), or fusion of the granules with the phagosome before it is completely closed (87, 148-150). In addition to phagocytosis, neutrophils can trap and kill pathogens by forming neutrophil extracellular traps (NETs), which consist of extracellular DNA studded with histones, chromatin, and antimicrobial compounds (151). The importance of neutrophils in limiting the replication and spread of influenza virus is shown by the fact that mice depleted of neutrophils have increased virus titres in the lungs and extrapulmonary sites compared with control mice (152).

However, neutrophils might also have an important role in damage to the EEB. In human cases of ARDS, neutrophil concentrations in bronchoalveolar lavage (BAL) fluid are positively correlated with disease severity (153). Similarly, pulmonary lesions in influenza-virus-infected mice are reduced by blocking of neutrophil recruitment to the lungs (154). Although several mechanisms have been proposed as to how neutrophils might damage the EEB in ARDS, those best characterised for influenza virus infection are the ability of neutrophils to produce ROS, cytokines, and NETs (**Figure 2.1.3**).

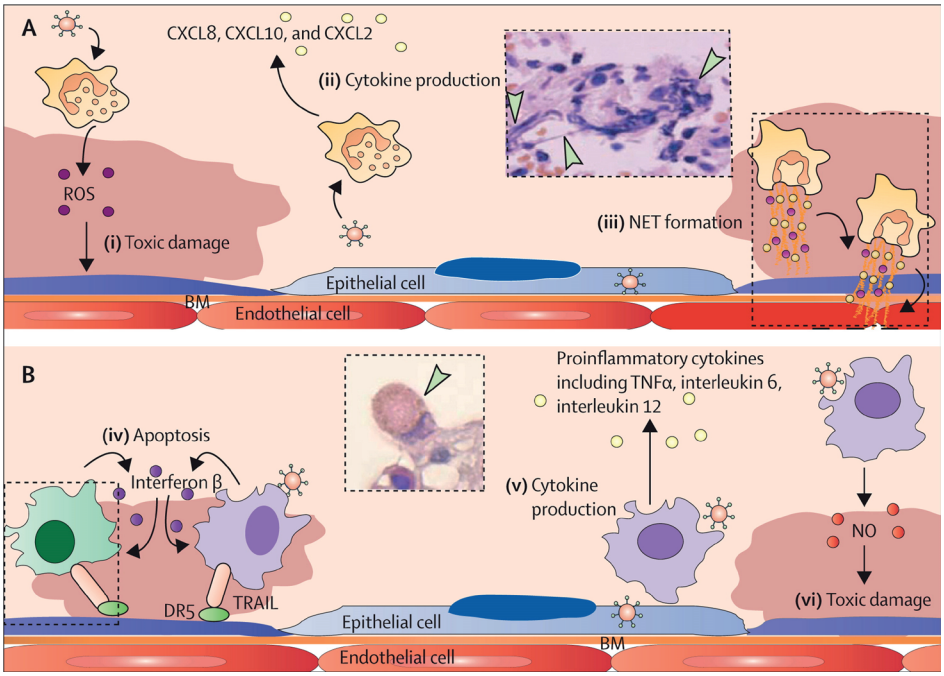

Figure 2.1.3 The role of neutrophils and macrophages in influenza-induced ARDS. (A) Neutrophils can damage the EEB in influenza virus infection via the production of ROS (i). In response to influenza virus infection, neutrophils also produce cytokines (ii), which can then indirectly damage the EEB. The production of NETs (iii) can also damage epithelial and endothelial cells. The inset shows NETs (arrowheads) in large blood vessels of a mouse after in-vivo infection with influenza virus (H&E stain). (B) Macrophages can damage the EEB directly by influenza-induced expression of TRAIL, which interacts with DR5 (iv) to cause epithelial cell apoptosis. TRAIL expression is triggered by interferon β. In response to influenza virus, macrophages also produce various cytokines (v) that can indirectly damage the EEB. The inset shows a macrophage (arrowhead) interacting with an alveolar epithelial cell in human lung tissue, 24 h after *ex-vivo* infection with influenza A H5N1 virus (H&E stain, reduced by 33% from ×500). Finally, influenza A induces macrophages to mediate the production of NO (vi) and the subsequent formation of peroxynitrite, which can damage the EEB. In both (A) and (B) epithelial cells represent both type 1 and type 2 pneumocytes. Newly recruited macrophages are depicted in dark pink, and resident alveolar macrophages are depicted in green. Accumulation of proteinaceous fluid in the alveolus is shown in pink. ARDS=acute respiratory distress syndrome. BM=basement membrane. ROS=reactive oxygen species. NET=neutrophil extracellular trap. TNF=tumour necrosis factor. NO=nitric oxide. DR5=death receptor 5. TRAIL=tumour-necrosis-factor-related apoptosis-inducing ligand. Inset of part iii reproduced from Narasaraju and colleagues (155) by permission of Elsevier.

Neutrophils can produce ROS (e.g., superoxide) through NADPH oxidase, a multicomponent enzyme complex consisting of proteins in the cytosol and cytochrome b558 on the membrane of secondary granules. Fusion of secondary granules with phagosomes or the plasma membrane results in production of ROS in the phagosome or extracellular environment (156). Accordingly, ROS can not only kill pathogens such

as influenza virus, but also damage the alveolus (157, 158). Consistent with this notion, removal of superoxide (by injection of superoxide dismutase) protected mice from lethal influenza virus infection (159). Similarly, influenza virus infection caused less tissue damage in NADPH-oxidase-deficient mice than in wild-type mice (160).

Myeloperoxidase is present in primary granules and enables the production of hypochlorous acid from hydrogen peroxide and free chloride ions. Myeloperoxidase, interacting with the macrophage mannose receptor, can trigger macrophages to release ROS and cytokines (161). These effects can not only inactivate influenza virus (162), but also damage the EEB (163). Accordingly, influenza virus infection causes less disruption of the pulmonary architecture and less pulmonary oedema in myeloperoxidase-deficient mice than in wild-type mice (164). Additionally, myeloperoxidase-deficient mice also showed increased expression of claudin 9 and claudin 18-1 (164), suggesting that myeloperoxidase could damage the EEB by disrupting tight junctions. How important myeloperoxidase-induced damage is to influenza-virus-induced mortality is not clear; although survival did not differ between wild-type and *Mpo*$^{-/-}$ mice inoculated with a high viral dose, the knockout mice had a trend for prolonged survival at a lower dose (164).

Neutrophils might indirectly damage the EEB by producing cytokines. Influenza virus infection triggers neutrophils to produce CXCL2 and interleukin 8 (165), both of which recruit additional neutrophils to the site of infection. Neutrophils are also the key producers of CXCL10 after influenza virus infection (166). Influenza virus infection caused less pulmonary injury and mortality in CXCL10-deficient mice than in wild-type mice. Neutrophil-derived CXCL10 might act in an autocrine fashion and bind to its receptor CXCR3, which is expressed on neutrophils. In doing so, CXCL10 triggers the generation of superoxide and enhances chemotaxis towards CXCL2 (166). Accordingly, treatment of ferrets with a CXCR3 antagonist reduced the severity of clinical signs after H5N1 virus infection (167).

Neutrophils might also damage the EEB through the production of NETs (155). Mice infected with influenza A/Puerto Rico/8/1934 developed NETs both in the lumina of alveoli and in terminal bronchioles in areas of tissue damage, and attached to the endothelium in areas of haemorrhage (155). These results suggest that NETs could damage both alveolar epithelial and endothelial cells. The role of influenza virus in the production of NETs *in vivo* was supported *in vitro* by co-incubation of neutrophils and influenza-virus-infected epithelial cells (155). However, the survival rate of mice deficient in peptidyl arginine deiminase 4 (an enzyme that is essential for formation of NETs did not differ substantially from that of wild-type mice after influenza virus infection (168), suggesting that formation of NETs might not be crucial for damage to the EEB.

MACROPHAGES

Like neutrophils, macrophages are an important component of the innate immune response against influenza virus infection. Macrophages ingest pathogens and infected or apoptotic cells. Phagocytosed pathogens are then killed through a so-called respiratory burst and the production of ROS and NO. Macrophages can also produce a broad range of both proinflammatory and anti-inflammatory cytokines. Within the alveolus, two types of macrophages need to be distinguished. The first type are the alveolar macrophages, which are long-lived resident cells that occur at a density of about seven per alveolus (169). They typically express an alternatively activated phenotype to minimise pulmonary inflammation in response to innocuous pathogens, while still protecting the lung from more virulent pathogens (170). Their importance in control of influenza virus infection is shown by the fact that depletion of alveolar macrophages before influenza virus infection leads to increased viral replication and disease severity (155). In influenza virus infection, alveolar macrophages are soon outnumbered by monocytes that are attracted to the alveolus by chemokines (e.g., CCL2, CCL5, and CXCL10). These monocytes migrate from the blood to the alveolar lumen, where they differentiate into macrophages. This second type of macrophages—recently recruited macrophages—typically have a classically activated phenotype. Although blocking of monocyte recruitment to the lung leads to increased virus replication (171), recently recruited macrophages could also have an important role in damage to the EEB. After influenza virus infection, mice deficient in CCR2 (the receptor for CCL2, which mediates monocyte chemotaxis) had reductions in both monocyte recruitment to the lungs and severity of pulmonary lesions (172). The main mechanisms for damage by recently recruited macrophages are related to release of tumour-necrosis-factor-related apoptosis-inducing ligand (TRAIL, also known as TNFSF10), production of NO, and production of proinflammatory cytokines (**Figure 2.1.3**).

After infection with influenza A/Puerto Rico/8/1934 recently recruited macrophages express TRAIL, which interacts with death receptor 5, a protein that is upregulated on alveolar epithelial cells in influenza virus infection; this interaction induces apoptosis of these cells. Accordingly, inhibition of TRAIL reduced the rate of epithelial cell apoptosis, the amount of pulmonary oedema, and the mortality rate of mice infected with influenza A virus (173). TRAIL production is dependent on activation of protein kinase R by influenza A virus, and subsequent production of interferon β. Autocrine interaction of interferon β with its receptor (interferon α, β, and ω receptor) triggers the production of TRAIL in a JAK–STAT-dependent manner (174). In accordance with this pathway, blocking of interferon β signalling in mice impaired TRAIL production and reduced alveolar epithelial damage after influenza virus infection (174).

Macrophages—and, to a lesser degree, neutrophils—that are stimulated by proinflammatory cytokines express inducible nitric oxide synthase (NOS2), which mediates the production of NO (158). NO can combine with superoxide to form peroxynitrite, which can both kill pathogens (175) and damage cells (176). Inhibition of NOS2 activity reduced the extent of pneumonia and mortality rate after lethal influenza virus infection (177). These findings complement the finding that, unlike wild-type mice, NOS2-deficient mice do not develop pneumonia after influenza virus infection (178). Karupiah and colleagues (178) suggested that NOS2 expression contributes more to severity of pneumonia than to cytopathic effects of influenza virus infection, because increasing viral titres in NOS2-deficient mice by blocking of interferon γ still did not induce mortality. The findings of this study emphasise the importance of pulmonary damage induced by NO in influenza virus infection.

The production of cytokines by macrophages is broad (**Table 2.1.2**) (132, 179-191), and depends on both strain of influenza virus and type of macrophage. The importance of these cytokines to protect against influenza virus is shown by the fact that viral NS1 acts at several levels to interfere with interferon production and interferon-mediated induction of antiviral proteins (192). For example, the Asp92Glu mutation in NS1 renders H5N1 IAV relatively insensitive to interferon α, interferon γ, and TNFα (193). Typically, however, H5N1 strains induce higher concentrations and a more diverse repertoire of cytokines in macrophages than do other influenza A strains (132, 180, 185, 186), and whereas this induction represents an important component of the antiviral response, it could also contribute to the hypercytokinaemia and subsequent pulmonary dysfunction reported in some human cases of influenza H5N1 infection (180). Human monocyte-derived macrophages—perhaps representative of recently recruited macrophages—produce significantly higher concentrations of proinflammatory cytokines than do human alveolar macrophages upon ex-vivo influenza virus infection (186, 191). Any macrophage-mediated, cytokine-induced pulmonary damage could therefore come mainly from recently recruited macrophages. However, the many different roles of cytokines in influenza virus infection, and the redundancy in many cytokine-signalling pathways, results in contradictory findings from experimental inoculations of influenza virus in mice deficient in specific cytokines (194, 195). Which macrophage-induced cytokines are most important in damage to the EEB, whether this damage is direct or indirect and the mechanism of this damage are unclear.

Table 2.1.2 Cytokine production after influenza A virus infection of human monocyte-derived and alveolar macrophages

	Influenza A strain
Infection of monocyte-derived macrophages	
Interleukin 1β[132, 179-181]	A/HK/486/97(H5N1),* A/Beijing/353/89(H3N2), A/PR/8/34(H1N1), A/Vietnam/1203/04(H5N1),* A/HK/54/98(H1N1),* A/Vietnam/3212/04(H5N1),* A/Thailand/16/04(H5N1), A/Thailand/SP/83/04(H5N1)
Interleukin 10[180]	A/HK/486/97(H5N1)*
Interleukin 12[132, 180]	A/HK/486/97(H5N1),* A/HK/483/97(H5N1),* A/HK/1174/98(H3N2),* A/Thailand/16/04(H5N1), A/Thailand/SP/83/04(H5N1), A/South Carolina/1/18(H1N1), A/Texas/36/91(H1N1)
CCL3[180, 182-184]	A/HK/486/97(H5N1),* A/HK/483/97(H5N1),* A/HK/1174/98(H3N2),* A/Beijing/353/89(H3N2), A/Vietnam/1203/04(H5N1),* A/Vietnam/3212/04(H5N1),* A/HH/01/09(H1N1), A/California/07/04(H3N2), A/Thailand/1(Kan-1)/04(H5N1)
CCL4[132, 180]	A/HK/486/97(H5N1),* A/HK/483/97(H5N1),* A/Thailand/16/04(H5N1), A/Thailand/SP/83/04(H5N1)
CCL2[180, 182, 183, 185]	A/HK/486/97(H5N1),* A/HK/483/97(H5N1),* A/Vietnam/HN3028(H5N1),* A/California/04/09(H1N1),* A/HK/403946(H1N1),* A/Beijing/353/89(H3N2), A/Vietnam/1203/04(H5N1),* A/Vietnam/3212/04(H5N1),* A/Thailand/16/04(H5N1), A/Thailand/SP/83/04(H5N1)
CCL5[180, 182, 183, 186, 187]	A/HK/486/97(H5N1),* A/HK/483/97(H5N1),* A/Beijing/353/89(H3N2), A/Vietnam/1203/04(H5N1), A/Thailand/1(Kan-1)/04(H5N1),* A/PR/8/34(H1N1)*
Interferon α[179-181, 188, 189]	A/HK/486/97(H5N1),* A/Beijing/353/89(H3N2), A/Finland/553/09(H1N1),* A/PR/8/34(H1N1), A/Thailand/1(Kan-1)/04(H5N1)*
Interleukin 6[132, 181, 184, 185, 187]	A/Vietnam/HN3028(H5N1),* A/California/04/09(H1N1),* A/HK/415742(H1N1),* A/HK/403946(H1N1),* A/PR/8/34(H1N1), A/Vietnam/1203/04(H5N1), A/HH/01/09(H1N1), A/California/07/04(H3N2), A/Thailand/1(Kan-1)/04(H5N1), A/Thailand/16/04(H5N1), A/Thailand/SP/83/04(H5N1)

Table 2.1.2 Cytokine production after influenza A virus infection of human monocyte-derived and alveolar macrophages (continued)

	Influenza A strain
Interferon β[179-182, 188, 189]	A/HK/486/97(H5N1),* A/HK/483/97(H5N1),* A/HK/54/98(H1N1),* A/HK/1174/98(H3N2),* A/Beijing/353/89(H3N2), A/Finland/553/09(H1N1),* A/PR/8/34(H1N1), A/Vietnam/1203/04(H5N1),* A/Vietnam/3212/04(H5N1),* A/Thailand/1(Kan-1)/04(H5N1)*
TNFα[179-182, 185, 186, 188-191]	A/HK/486/97(H5N1), A/HK/483/97(H5N1), A/HK/54/98(H1N1), A/HK/1174/98(H3N2), A/Beijing/353/89(H3N2), A/Vietnam/1203/04(H5N1), A/Vietnam/1194/04(H5N1), A/Thailand/MK2/04(H5N1), A/Vietnam/3046/04(H5N1), A/Vietnam/HN3028(H5N1),* A/California/04/09(H1N1),* A/HK/415742(H1N1),* A/PR/8/34(H1N1), A/HK/403946(H1N1),* A/Vietnam/3212/04(H5N1),* A/HH/01/09(H1N1), A/California/07/04(H3N2), A/Thailand/1(Kan-1)/04(H5N1), A/Thailand/16/04(H5N1), A/Thailand/SP/83/04(H5N1), A/Finland/553/09(H1N1),* A/PR/8/34(H1N1)*
CSF2[132]	A/Thailand/16/04(H5N1), A/Thailand/SP/83/04(H5N1)
CSF3[132]	A/Thailand/16/04(H5N1), A/Thailand/SP/83/04(H5N1)
Interleukin 4[180]	A/HK/483/97(H5N1)*
Interferon γ[185]	A/Vietnam/HN3028(H5N1),* A/California/04/09(H1N1),* A/HK/403946(H1N1)*
TGFβ[191]	A/Netherlands/602/09(H1N1),* A/Vietnam/1194/04(H5N1)*
Interleukin 7[180]	A/HK/483/97(H5N1)*
Interleukin 18[179]	A/Beijing/353/89(H3N2)
Interferon λ[182, 188]	A/Finland/553/09(H1N1),* A/Vietnam/3212/04(H5N1),* A/HK/483/97(H5N1)*
CXCL10[182-184, 186-188]	A/Finland/553/09(H1N1),* A/Vietnam/1203/04(H5N1), A/New Caledonia/20/99(H1N1), A/HH/01/09(H1N1), A/California/07/04(H3N2), A/Thailand/1(Kan-1)/04(H5N1), A/HK/483/97(H5N1), A/Beijing/353/89(H3N2), A/Vietnam/3212/04(H5N1),* A/HK/54/98(H1N1)*
CCL8[189]	A/Thailand/1(Kan-1)/04(H5N1),* A/PR/8/34(H1N1)*

Table 2.1.2 Cytokine production after influenza A virus infection of human monocyte-derived and alveolar macrophages (continued)

	Influenza A strain
CXCL11[189]	A/Thailand/1(Kan-1)/04(H5N1),* A/PR/8/34(H1N1)*
Infection of alveolar macrophages	
CXCL10[186]	A/HK/483/97(H5N1)
TNFα[186]	A/HK/483/97(H5N1)
CCL5[186]	A/HK/483/97(H5N1)*
Interferon β[186]	A/HK/483/97(H5N1)*
Interleukin 6[186]	A/HK/483/97(H5N1)*
CCL2[186]	A/HK/483/97(H5N1)*

*Determined by mRNA expression. TNF=tumour necrosis factor. TGF=transforming growth factor.

CONCLUSIONS & PERSPECTIVES

In this Review, we set out the main cell types and mechanisms involved in influenza virus infection of the lung that lead to the following model for influenza-virus-induced damage to the EEB (**Figure 2.1.4**). Upon entering the alveolus, influenza virus infects its main target, epithelial cells, which undergo apoptosis or necrosis, opening the epithelial layer. Influenza-virus-infected epithelial cells also produce cytokines (e.g., CCL2, CCL5, and CXCL10) that recruit neutrophils and monocytes to the alveolus by direct chemotaxis. Activation of endothelial cells in influenza virus infection results in the upregulation of adhesion molecules for leucocyte extravasation and the production of cytokines such as CCL2, CXCL10, interferon α, interleukin 6, TNFα, and interferon γ. Both processes further attract neutrophils and macrophages to the alveolus. Recruited neutrophils produce ROS, which can cause tissue damage. Neutrophils also produce cytokines in response to influenza virus infection. In particular, the production of CXCL10 could damage the EEB by triggering the production of superoxide or enhancing neutrophil chemotaxis. Recruited macrophages can damage the EEB in three ways. First, they can express TRAIL, which interacts with death receptor 5 on the epithelial cell and induces epithelial cell apoptosis. Second, by the activation of NOS_2, recruited macrophages can increase concentrations of NO and peroxynitrite, which cause tissue

damage. Third, they are important producers of proinflammatory cytokines, which further exacerbate the inflammatory response and could damage the EEB.

The pathogenesis of influenza-virus-induced ARDS is centred on the alveolar epithelium. This framework contrasts with the classic model of ARDS pathogenesis, in which lung vascular endothelium is thought to be the main target. An important cause of ARDS in the classic model is bacterial sepsis, which differs in two important ways from influenza virus infection. First, the typical pathological agent in sepsis, lipopolysaccharide (LPS), enters the alveolus through the blood circulation (89), whereas influenza virus enters through the airways. Second, the main target of LPS is the endothelial cell (89), whereas that of influenza virus is the epithelial cell. Because many *in vitro* and *in vivo* models used to study the pathogenesis of ARDS make use of LPS that the endothelial cell has received such attention is not surprising. However, irrespective of whether the cause of ARDS is sepsis, a respiratory virus such as influenza virus, or another pathological agent, its pathogenesis is highly dependent on damage to the alveolar epithelium, which is mainly responsible for maintaining the osmotic pressure across the EEB (94).

This new model for influenza-virus-induced ARDS has implications for pathogenesis research, both by identification of topics of particular interest and by exposure of gaps in our knowledge. Can this framework, which is based on information from various sources, be validated in one experimental system? By which mechanisms does influenza virus induce cell death in alveolar epithelial cells? Which factors establish whether apoptosis or necrosis occurs? How is this mechanism affected by cell type (ie, type 1 or type 2 pneumocytes)? By which mechanisms do cytokines produced by epithelial cells, endothelial cells, and recently recruited macrophages damage the EEB? Which are the most important mechanisms by which endothelial cells are activated; direct contact with influenza virus, cytokines produced by influenza-virus-infected epithelial cells, or cytokines produced by other cell types? At which stage of damage to the EEB are influenza virus particles released into the systemic circulation, and on which factors is this release dependent? Does influenza virus infection damage the basement membrane? If so, how? What effect does this damage have on re-epithelialisation? Which characteristics in influenza-virus-induced damage to the alveolar epithelium are crucial to establish whether re-epithelialisation or fibrosis occurs? How do the above mechanisms vary between different influenza virus strains? Which host factors define whether a patient with influenza goes on to develop ARDS? How is the difference in main target (epithelium *vs* endothelium) between influenza-virus-induced ARDS and sepsis-induced ARDS shown in disease progression, response to intervention, or clinical outcome? Findings that patients with sepsis-induced ARDS have higher concentrations of procalcitonin and interleukin 6 on days 1 and 2 after diagnosis of ARDS, more severe

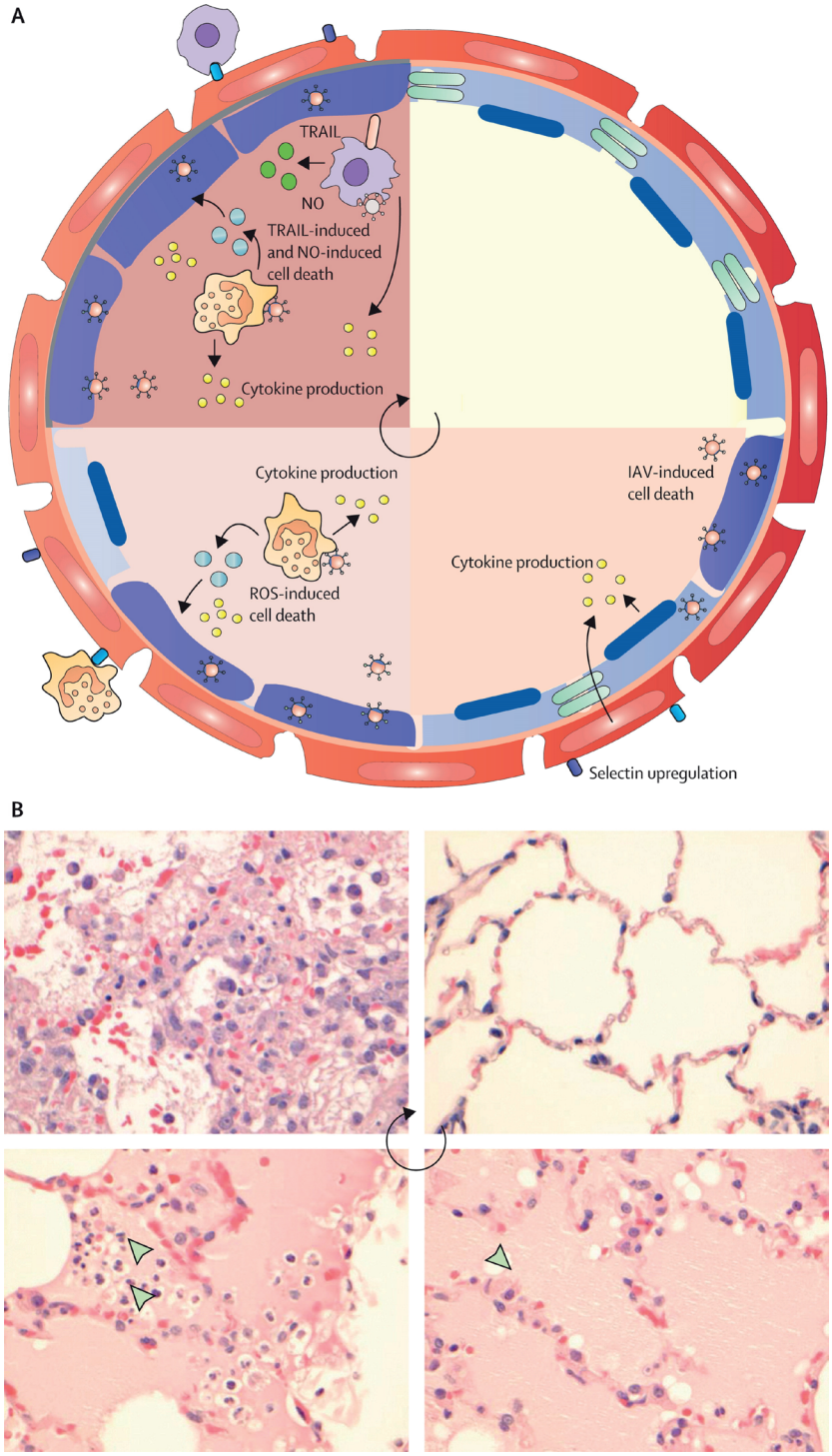

Figure 2.1.4 Pathogenesis model and histopathology of influenza-induced ARDS.

← **Figure 2.1.4 Pathogenesis model and histopathology of influenza-induced ARDS.** (A) A schematic model of the pathogenesis of influenza-induced ARDS. In a healthy lung, the alveolar lumen is free of fluid to ensure optimum gas exchange (upper right quadrant). After infection, influenza A virus induces epithelial cell death, resulting in leakage of proteinaceous fluid into the alveolar lumen (lower right quadrant). Influenza virus also induces cytokine production by epithelial and endothelial cells, and selectin upregulation on endothelial cells. Selectin upregulation on endothelial cells enables extravasation of neutrophils, which are among the first cells recruited to the lung in influenza virus infection (lower left quadrant). Neutrophils damage the EEB via the release of toxic granules and cytokine production, resulting in increased leakage of proteinaceous fluid into the alveolar lumen. Selectin upregulation on endothelial cells enables extravasation of macrophages, which damage the barrier via the production of NO, TRAIL, and cytokines (upper left quadrant). In addition to proteinaceous fluid and infiltrating leucocytes, the progressive damage to the EEB results in fibrin deposition and haemorrhage into the alveolar lumen. (B) Histopathology panel shows representative stages of ARDS in a ferret lung 4 days after infection with influenza A H5N1. The upper right quadrant shows normal air-filled alveoli from an uninfected ferret. The lower right quadrant shows alveoli abundantly filled with proteinaceous fluid, visible as homogeneous pink material (arrowhead). The lower left quadrant shows alveoli filled with proteinaceous fluid mixed with infiltrating leucocytes, mainly neutrophils (arrowheads). The upper left quadrant shows alveoli filled with proteinaceous fluid mixed with macrophages, erythrocytes, and fibrin strands. Additionally, the alveolar walls are disrupted (H&E stain, reduced by 24% from x400). ARDS=acute respiratory distress syndrome. IAV=influenza A virus. NO=nitric oxide. TRAIL= tumour-related apoptosis-inducing ligand.

disease, and higher mortality than do patients with non-septic ARDS lend support to the notion that different causes of ARDS can result in different clinical outcomes (196-198).

The model described in this Review also provides a rationale to choose therapeutic targets to minimise the tissue-damaging response against influenza virus infection of pulmonary alveoli (199, 200). Potential therapeutic targets for influenza-virus-induced ARDS are the alveolar epithelium, infiltrating leucocytes, and the overall proinflammatory response. Growth factors such as keratinocyte growth factor (KGF) (199) and hepatocyte growth factor (HGF) (201) help to protect and restore alveolar epithelium. Inhibitors of the CXCL10–CXCR3 axis reduce infiltration of neutrophils and induction of ROS production (166, 167). Apocynin, an inhibitor of NADPH oxidase 2, also reduces production of ROS (202, 203). Celecoxib and mesalazine, cyclo-oxygenase-2 inhibitors, reduce cytokine dysfunction and prevent apoptosis (204). Gemfibrozil, an agonist of peroxisome proliferator-activated receptor α, reduces the release of proinflammatory cytokines (204). Mesenchymal stem cells moderate inflammatory response, improve alveolar fluid clearance, and maintain integrity of lung epithelium and endothelium in pneumonia (200). Lung stem cells have been identified that undergo rapid proliferation and radiate to areas of alveolar damage and express markers typical of alveoli after sublethal influenza virus infection in mice. Understanding of the signals that trigger this cell proliferation and radiation, and apparent regeneration of alveolar structures, could be useful to develop new therapies for treatment of influenza-virus-induced ARDS. Furthermore, therapies should promote re-epithelialisation in the absence of widespread fibrosis (which can result in decreased lung function and increased ventilator

dependence) (205). However, treatments that limit influenza-virus-induced damage in mice might not necessarily produce equivalent effects in human beings. Therefore, prevention of damage to the alveolus in influenza virus infection needs an approach that combines knowledge obtained with use of experimental infection in laboratory animals together with clinical data.

Influenza-virus-induced ARDS has a high case fatality rate, despite intensive hospital care, development of lung-protective ventilation strategies, and the use of extracorporeal membrane oxygenation (ECMO). Therapies directed against the virus are often not adequate to cure the disease because the lung damage remaining after the virus infection has been abrogated is too severe to resolve by itself. Only through better understanding of the mechanism by which this damage develops and is repaired can therapeutic strategies be developed to improve the outcome of this intractable complication of influenza.

Search strategy and selection criteria

We identified relevant articles by searching PubMed and Google Scholar with the search terms “epithelial cell”, “influenza”, “macrophages”, “neutrophils”, “endothelial cells”, “H5N1”, “tight junctions”, “interferon”, “alveolar macrophage”, “sodium channel”, “lung damage”, “ENaC”, “cytokines”, “necrosis”, “post-mortem”, “NETs”, “reactive oxygen species”, “nitric oxide”, “toxic damage”, “myeloperoxidase”, “NADPH”, “peroxynitrite”, “acute lung injury”, “apoptosis”, “ARDS”, and “cytokine storm”. We reviewed relevant articles that were found in these searches, articles cited by those found, and articles present in our own files. Only English-language articles that were published before July 2013 were included.

Acknowledgments

KRS, RAMF, and TK wrote the Review. EJBVK, RAMF, and TK edited the Review. KRS prepared the figures and EJBVK took the histology images. We thank Lonneke Leijten for doing Pankeratin and von Willebrand factor staining. We thank Judith van den Brand for the provision of histology sections and Debby van Riel for the provision of histology sections and critical reading of the Review. KRS is supported by an NHMRC CJ Martin post-doctoral fellowship (1054081). RAMF is supported by NIH/NIAID contract HHSN266200700010C. TK is supported by European Union FP7 ANTIGONE contract 278976.

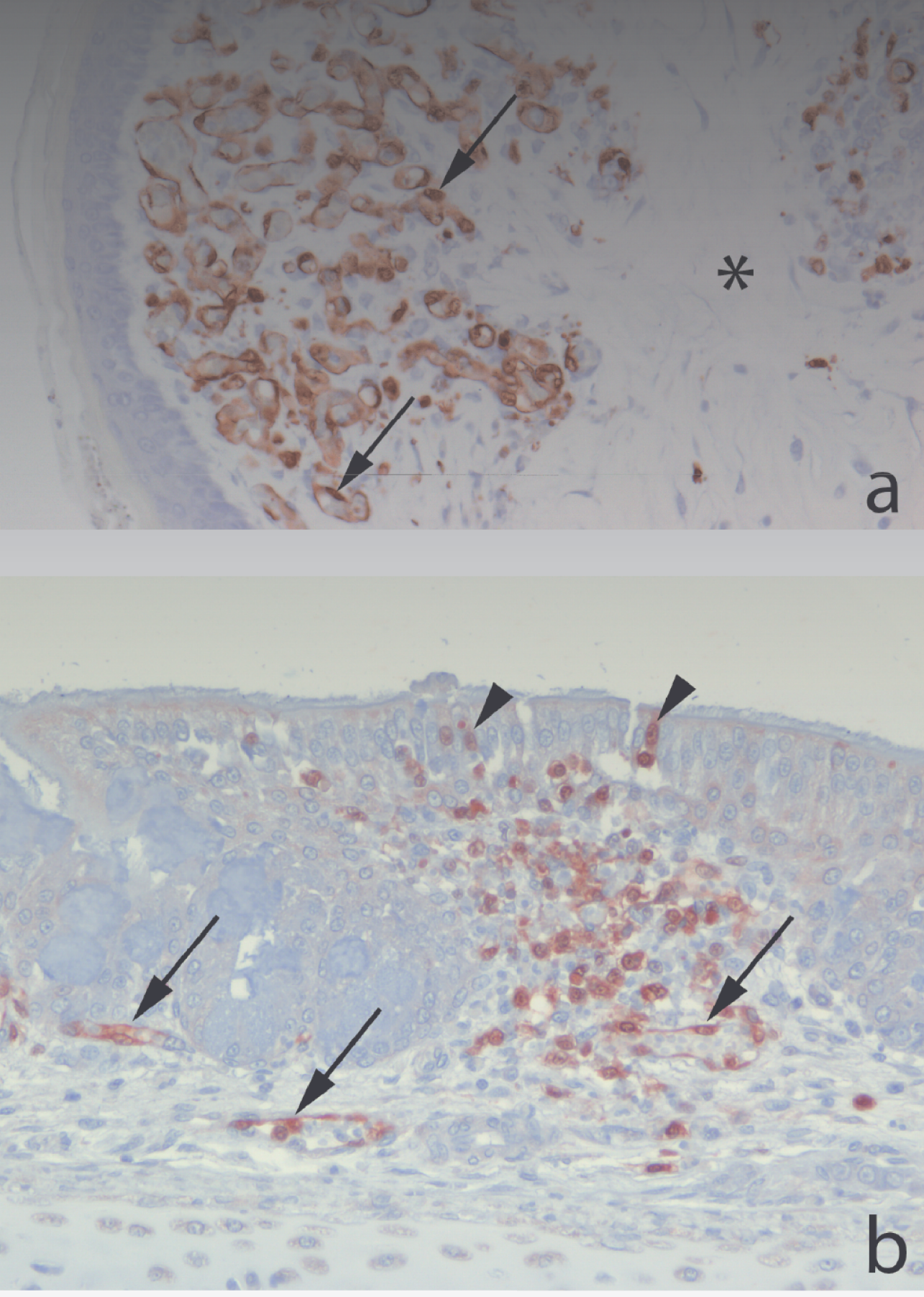
a
b

2.2

Influenza virus and endothelial cells: a species specific relationship

K.R. Short[1,2], E.J.B. Veldhuis Kroeze[1,3], L.A. Reperant[1], M. Richard[1] & T. Kuiken[1]

Frontiers in Microbiology 2014; 5: 653

Affiliations
[1]Department of Viroscience, Erasmus Medical Center, Rotterdam, The Netherlands
[2]School of Biomedical Sciences, University of Queensland, Brisbane, QLD, Australia
[3]Viroclinics Biosciences B.V., Rotterdam, The Netherlands

ABSTRACT

Influenza A virus infection is an important cause of respiratory disease in humans. The original reservoirs of IAV are wild waterfowl and shorebirds, where virus infection causes limited, if any, disease. Both in humans and in wild waterbirds, epithelial cells are the main target of infection. However, influenza virus can spread from wild bird species to terrestrial poultry. Here, the virus can evolve into highly pathogenic avian influenza. Part of this evolution involves increased viral tropism for endothelial cells. HPAIV infections not only cause severe disease in chickens and other terrestrial poultry species but can also spread to humans and back to wild bird populations. Here, we review the role of the endothelium in the pathogenesis of influenza virus infection in wild birds, terrestrial poultry and humans with a particular focus on HPAIVs. We demonstrate that whilst the endothelium is an important target of virus infection in terrestrial poultry and some wild bird species, in humans the endothelium is more important in controlling the local inflammatory milieu. Thus, the endothelium plays an important, but species-specific, role in the pathogenesis of influenza virus infection.

Keywords: influenza virus, endothelial cells, highly pathogenic avian influenza, zoonotic infection, poultry

INTRODUCTION

IAV is a negative-sense RNA virus of the Family *Orthomyxoviridae*. IAVs can be classified into different subtypes based on antigenic differences in the two surface glycoproteins of the virus, the HA and NA. Each year, antigenic changes (or "drift") in the HA and NA result in a seasonal outbreak of IAV in the human population. However, when there is a dramatic change in the HA and/or NA, often originating from the avian reservoir, global pandemics can result. In the last 100 years there have been four IAV pandemics in the human population: the 1918 H1N1 pandemic, the 1957 H2N2 pandemic, the 1968 H3N2 pandemic and the 2009 H1N1 pandemic. These pandemics have all caused significant morbidity and mortality. Indeed, the 1918 H1N1 virus was so severe that life expectancy in the U.S.A. dropped by 11.8 years from 1917 to 1918 (21). The constant threat of a future IAV pandemic highlights the need to study and understand IAV pathogenesis not only in humans, but also in the virus' natural avian reservoirs. The original reservoirs of IAV are wild waterfowl (order Anseriformes—which includes geese, ducks, and swans) and shorebirds (order Charadriiformes—which includes gulls and waders). Sixteen different HA subtypes and 9 different NA subtypes of IAV have been recorded in wild waterfowl. A subset of these different IAV strains can then spread from wild bird populations to terrestrial poultry (order Galliformes). Here, IAV can cause a mild or subclinical infection of the respiratory and/or gastrointestinal tract, and is thus referred to as a low pathogenic AIV. LPAIVs of the H5 and H7 subtypes can subsequently evolve in poultry to become HPAIVs, which typically cause a fatal and systemic infection. LPAI and HPAI viruses can cause respiratory infection in humans, with HPAIVs occasionally reported in extra-respiratory organs.

The pathogenesis of IAV infection differs markedly between wild waterbirds, terrestrial poultry and humans. In all three host groups, endothelial cells play a key role in disease pathogenesis—either as the primary cellular target of viral infection or as orchestrators of the anti-viral immune response. Here, we review the currently available literature on the role of the endothelium in the pathogenesis of IAV (in particular H5N1 HPAIVs) in terrestrial poultry, wild birds and humans. Specifically, we will compare the ability of IAV to infect and/or "activate" the endothelium across these different host groups.

TERRESTRIAL POULTRY (ORDER GALLIFORMES)

Typically, terrestrial poultry infected with LPAIVs display limited clinical signs and with no evidence of endothelial cell infection (rather the virus preferentially infects epithelial cells of the respiratory tract) (206). However, viruses of the H5 and H7 subtype can

evolve in terrestrial poultry to become HPAIVs. This evolution typically occurs via the addition of a multi-basic cleavage site in the viral HA. This then allows the HA to be cleaved (a prerequisite for viral infection) by the ubiquitously present furin family of enzymes. In contrast, LPAIVs can only be cleaved by trypsin like enzymes that are present within the respiratory and digestive tract. Upon evolution to HPAIV, the cell tropism of IAV changes dramatically. Studies on naturally or experimentally infected chickens show that HPAIVs can infect the endothelium in a variety of different organs including, but not limited to, the lung, heart, brain, and spleen (207-216) (**Figure 2.2.1**) This endothelial cell tropism can be so striking that in chickens infected with H5N1, IAV antigen is more prevalent in the endothelial cells of the respiratory and intestinal tract than in the epithelial cells of the same tissues (215). Similarly, in Galliformes other than chickens viral antigens are predominant in the vascular and capillary endothelial cells of various tissues including the lung, liver, brain, skeletal muscle, pancreas, heart, kidney, spleen, and bursa (217-221). The endothelial tropism of HPAIVs is determined, at least in part, by the presence of the multi-basic cleavage site in the HA, as the removal of these basic amino acid residues reduces endothelial tropism (65). The polarity of virus budding may also contribute this distinct pattern of viral infection (222).

The endothelial tropism of HPAIVs in chickens and other Galliformes has important pathological ramifications. Firstly, IAV infection of chicken endothelial cells is associated with the apoptotic death of these cells (209). The loss of endothelial cells is likely to contribute to the oedema and hemorrhaging observed in the wattle, comb, lungs and legs of chickens infected with HPAIVs (216, 223). A loss of endothelial cells can also detrimentally affect blood coagulation (212, 213). Damage to endothelial cells activates the extrinsic coagulation cascade and facilitates the microthrombosis. This can then lead to disseminated intravascular coagulation (DIC) whereby the coagulation cascade become “hyper-activated,” resulting in thrombocytopenia, widespread hemorrhaging and ischaemia. Consistent with a role for DIC in the pathogenesis of HPAIVs in chickens, Muramoto and colleagues demonstrated that chickens intravenously infected with H5N1 display both microthrombosis and thrombocytopenia (212). Similarly, chickens infected intranasally with H5N1 display microthrombosis in the lung within 24 h post-infection. It has also been suggested that the replication of HPAIVs in endothelial cells could disrupt the innate immune response, thermoregulation (224) and facilitate the systemic spread of the virus to parenchymal cells of the brain, skin, and visceral organs (225). Together, these features help account for the rapid and high mortality rates of HPAIVs in Galliformes. For example, in chickens death typically occurs within 2 days post-infection, often in the absence of visible clinical signs (215). Similarly, during an outbreak of a H7N1 HPAIV in Italy, turkeys and guinea fowl (reared on litter) had a 100% mortality rate within a mere 48–72 h of becoming symptomatic (226).

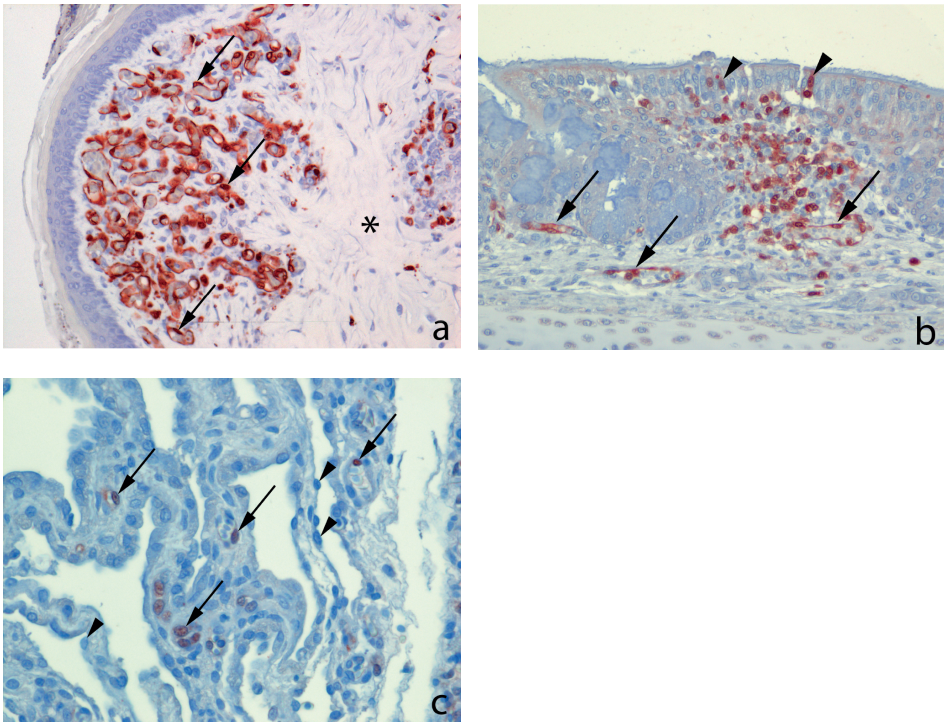

Figure 2.2.1 Endotheliotropism and epitheliotropism of IAVs in chickens. Virus distribution in: **(A)** endothelial cells of the wattle of a chicken naturally infected with H7N7 HPAIV. Brown-reddish staining antigen indicative of viral replication is present in many endothelial cell nuclei (arrows) and cytoplasm lining the small blood vessels. The dermis is expanded by oedema (asterisk). (original magnification 200×, in van Riel and colleagues (216) **(B)** Epithelial cell nuclei (arrowheads) and in endothelial cells (arrows) of the nasal mucosa of a chicken 24 h after experimental intranasal (IN) infection with 10^5 $TCID_{50}$ of H5N1 HPAIV A/Indonesia/05/2005, illustrating both epitheliotropism and endotheliotropism of the virus (original magnification 200×). **(C)** Endothelial cell nuclei (arrows) of the lung interstitium 24 h after infection of the same chicken as in (B), the alveolar lining epithelial cells nuclei (arrowheads) do not stain positive for viral antigen (original magnification 400×). (IHC for IAV-NP with hematoxylin counterstain).

WILD BIRDS (ORDER ANSERIFORMES AND CHARADRIIFORMES)

In wild birds, LPAIVs normally present as a sub-clinical infection with little involvement of the endothelium in disease pathogenesis (225, 227). Prior to the emergence of H5N1 HPAIVs, there was only one recorded incidence of a HPAI strain being detected in wild birds (228). It was therefore assumed that HPAI strains were unlikely to transmit back to the wild bird population and cause disease following their emergence in poultry. However, since 2002 the H5N1 HPAIV strain has caused infection and mortality in a variety of wild birds. Unlike LPAIVs, H5N1 viruses in wild birds do not infect intestinal

epithelial cells. Instead, the virus predominantly infects cells in the respiratory tract and other organs (**Tables 2.2.1** and **2.2.2**) and infection can be associated with severe necrosis and inflammation (215, 229-232). H5N1 viruses display, at most, limited tropism for the endothelium in wild birds (**Tables 2.2.1** and **2.2.2**), and it is therefore unlikely that endothelial cell infection plays a major role in disease pathogenesis. However, one notable exception to this trend is black swans (233). Upon infection with H5N1 A/whooper swan/Mongolia/244/05 AIV, 100% (*n* = 5) of black swans succumbed to disease within 2–3 days (as seen during H5N1 infection of chickens, this was often observed in the absence of clinical signs of disease) (233). IHC showed that the endothelial cells throughout the body were the primary target of IAV infection, and the presence of IAV antigen was associated with multiorgan necrosis and mild acute inflammation (233). Although a tropism for the endothelium is observed in other species of swans, this does not appear to be as pronounced as that seen in the black swan (233-237). For example, viral antigen was detected infrequently or not at all in the endothelial cells of whooper swans (233, 235) and trumpeter swans (233) following either a natural or experimental infection with H5N1. Similarly, whilst endothelial cells of mute swans were positive for IAV, and widespread hemorrhage was recorded, this was only detected in 3 out of 12 birds (236). Thus, although the ability of H5N1 HPAIV to infect endothelial cells contributes to the severity of the disease observed in black swans this does not necessarily hold true for other species of swans or wild birds.

HUMANS

In humans, the primary cellular targets of IAV are epithelial cells in the respiratory tract. Seasonal IAVs, which are adapted to and circulate in the human population, typically infect ciliated cells in the upper respiratory tract, trachea and bronchi (43, 50). In contrast, HPAIVs such as H5N1 preferentially infect the lower respiratory tract, specifically club cells and alveolar type II pneumocytes (50, 62). This differential tropism reflects, in part, the ability of H5N1 viruses to bind to α-2,3-linked sialosaccharides (expressed on type II pneumocytes) whilst seasonal IAVs typically display a preference for α-2,6-linked sialic acid (41, 50, 62). Within the lower respiratory tract, alveolar epithelial cells are in close proximity to the underlying endothelium. Indeed, in the human alveolus there is on average only 0.5 µm separating the airspace from the capillary (88). During IAV infection the endothelium is therefore likely to be exposed to free virus particles produced by infected and damaged epithelial cells. It is often suggested that—like chickens and black swans—IAV infects human endothelial cells, and that this contributes to disease pathogenesis (131, 136, 141). For example, *in vitro* studies using primary human lung microvascular endothelial cells demonstrated

Table 2.2.1 Endothelial tropism of H5N1 in Anseriformes as determined by immunohistochemistry

Order	Species	Infection[a]	Location of viral antigen	Virus	Endothelial cell infection recorded?
Anseriformes[234]	Bar-headed goose (*Anser indicus*)	N	Brain	N/A	Occasional positive endothelial cell within the gut mucosa and lung
Anseriformes[230]	Canada goose (*Branta canadensis*)	E	Brain; Heart; Intestine; Kidney; Lung; Pancreas; Proventriculus; Sciatic nerve; Skeletal muscle; Spina; Spleen; Trachea and Ventriculus	A/chicken/ Vietnam/14/2005 (H5N1)	Positive endothelial cells detected in sciatic nerve (1/5 geese) and respiratory tract (3/5 geese)
Anseriformes[233]	Cackling goose (*Branta hutchinsii*)	E	Adrenal gland; Brain; Liver and Pancreas	A/whooper swan/ Mongolia/244/05 (H5N1)	
Anseriformes[234]	Canada goose (*Branta canadensis*)	N	Lung	N/A	
Anseriformes[238]	Canada goose (*Branta canadensis*)	E	Trachea; Tracheal cartilage; Lung; Cerebrum; Cerebellum; Ventricles; Medulla oblongata; Spinal cord; Heart; Pancreas; Esophagus; Proventriculus; Duodenum and Ceca	A/chicken/ Vietnam/14/05 (H5N1)	A few endothelial cells in scattered capillaries
Anseriformes[223]	Domestic geese (*Anser anser domesticus*)	E	Nasal cavity; Heart; Brain; Alimentary tract; Pancreas; Liver and Spleen	A/chicken/Hong Kong/220/97 (H5N1)	

Table 2.2.1 Endothelial tropism of H5N1 in Anseriformes as determined by immunohistochemistry (continued)

Order	Species	Infection[a]	Location of viral antigen	Virus	Endothelial cell infection recorded?
Anseriformes[218]	Embden geese (*Anser anser domesticus*)	E	Brain; Pancreas and Heart	A/chicken/Hong Kong/220/97 (H5N1)	
Anseriformes[237]	Greylag goose (*Anser anser*)	E	Brain	A/chicken/Korea/IS/06 (H5N1)	
Anseriformes[234]	Hawaiian goose (*Branta sanvicensis*)	N	Lung	N/A	
Anseriformes[233]	Black swan (*Cygnus atratus*)	E	Brain and viscera	A/whooper swan/Mongolia/244/05 (H5N1)	IAV antigen detected primarily in endothelial cells of blood vessels in brain and viscera
Anseriformes[234]	Coscoroba swan (*Coscoroba coscoroba*)	N	Brain and Lung	N/A	
Anseriformes[233]	Mute swan (*Cygnus olor*)	E	Adrenal; Brain; Heart; Intestine; Kidney; Liver; Lung; Pancreas; Proventriculus; Spleen and Trachea	A/whooper swan/Mongolia/244/05 (H5N1)	
Anseriformes[236]	Mute swan (*Cygnus olor*)	E	Adrenal; Brain; Bursa; Caecum; Eye; Gonad; Heart; Kidney; Liver; Lung; Nasal cavity; Peripheral nerves; Proventriculus; Spina; Spleen and Trachea	A/Cygnus cygnus/Germany/R65/2006 (H5N1)	Endothelial tropism detected in 3/12 swans in various organs incl. nasal concha, vascular endothelium in intestine

Table 2.2.1 Endothelial tropism of H5N1 in Anseriformes as determined by immunohistochemistry (continued)

Order	Species	Infection[a]	Location of viral antigen	Virus	Endothelial cell infection recorded?
Anseriformes[237]	Mute swan (*Cygnus olor*)	E	Viral antigen infrequently identified in the Small and Large Intestines; Kidney; Epidermis and Pulp of feather follicles.	A/chicken/Korea/IS/06 (H5N1)	Viral antigen infrequently identified in vascular endothelium in intestine, heart and nasal cavity
Anseriformes[233]	Trumpeter swan (*Cygnus buccinators)*	E	Brain and Visceral organs	A/whooper swan/Mongolia/244/05 (H5N1)	
Anseriformes[233]	Whooper swan (*Cygnus cygnus*)	E	Adrenal; Brain; Heart; Intestine; Kidney; Liver; Lung; Pancreas; Proventriculus; Spleen and Trachea	A/whooper swan/Mongolia/244/05 (H5N1)	
Anseriformes[235]	Whooper swan (*Cygnus cygnus*)	N	Adrenal; Cerebellum; Gonad; Heart; Kidney; Liver; Lung; Pancreas; Peyer's Patches; Proventriculus; Spina; Spleen; Thyroid and Trachea	N/A	A few endothelial cells were positive within the spleen, bone marrow, Peyer's patches and lungs
Anseriformes[239]	Call ducks (*Anas platyrhyncha var domestica*)	E	Cerebrum; Cerebellum; Brain stem; Epithelium of feathers; Epithelium of beak; Pancreas; Liver; Heart and Skeletal muscle	A/chicken/Yamaguchi/7/04 (H5N1)	A few positive endothelial cells were recorded. Organ not stated

Table 2.2.1 Endothelial tropism of H5N1 in Anseriformes as determined by immunohistochemistry (continued)

Order	Species	Infection[a]	Location of viral antigen	Virus	Endothelial cell infection recorded?
Anseriformes[229]	Commercial domestic ducks in Korea	N	Heart; Pancreas; Peripheral nerves and ganglia; Kidney; Skeletal myofibres; Elastic fibres of tunica media in the artery	N/A	Pulmonary endothelial cells infected
Anseriformes[223]	Domestic ducks (*Anas platyrhynchos*)	E	No viral antigen detected	A/chicken/Hong Kong/220/97 (H5N1)	
Anseriformes[240]	Eastern Zhejiang white geese	E	Brain, Pancreas, Lung, Spleen and Kidney	A/Bar-headed Goose/ Qinghai/0510/05 (H5N1)	
Anseriformes[237]	Mandarin duck (*Aix galericulata*)	E	Nasal cavity; Brain and Pancreas	A/chicken/Korea/ IS/06 (H5N1)	
Anseriformes[218]	Pekin ducks (*Anas platyrhynhcos*)	E	No viral antigen detected	A/chicken/Hong Kong/220/97 (H5N1)	
Anseriformes[215]	Pekin duck (*Anas platyrhynchos*)	E	Sinus; Air sac; Ependyma; Meninges; Spleen; Bursa; Thymus; Conjunctiva; Lymphoid foci; Marrow; Periosteum; Feather sheath and follicle epidermis; Feather pulp and Myocardium Skeletal Muscle	A/duck/Sleman/ BBVW-1003-34368/2007 (H5N1)	

Table 2.2.1 Endothelial tropism of H5N1 in Anseriformes as determined by immunohistochemistry (continued)

Order	Species	Infection[a]	Location of viral antigen	Virus	Endothelial cell infection recorded?
Anseriformes[215]	Pekin duck (*Anas platyrhyncos*)	E	Infraorbital sinus; Air sacs; Bursa; Thymus; Conjunctiva and Feather pulp	A/duck/Sleman/ BBVW-1003-34368/2007 (H5N1)	
Anseriformes[241]	Pekin duck (*Anas platyrhynchos*)	E	Nasal cavity; Trachea; Lung; Heart; Brain; Adrenal gland; Enteric tract; Pancreas; Liver; Kidney; Spleen; Thymus, Skeletal muscle; Proventiculus	A/Thailand PB/6231/04 (H5N1)	
Anseriformes[241]	Pekin duck (*Anas platyrhynchos*)	E	Nasal cavity; Trachea; Lung; Heart; Brain; Adrenal gland; Enteric tract; Pancreas; Liver; Kidney; Bursa; Thymus, Skeletal muscle; Proventiculus	A/Crow/ Thailand/04 (H5N1)	
Anseriformes[241]	Pekin duck (*Anas platyrhynchos*)	E	Nasal cavity; Trachea; Lung; Heart; Brain; Adrenal gland; Enteric tract; Pancreas; Liver; Kidney; Spleen; Bursa; Thymus, Skeletal muscle; Gizzard; Proventiculus	A/Egret/ HK/757.2/02 (H5N1)	
Anseriformes[237]	Ruddy shelducks (*Tadorna ferruginea*)	E	Nasal cavity, Lung; Heart; Brain; Peripheral Nerves	A/chicken/Korea/ IS/06 (H5N1)	

Table 2.2.1 Endothelial tropism of H5N1 in Anseriformes as determined by immunohistochemistry (continued)

Order	Species	Infection[a]	Location of viral antigen	Virus	Endothelial cell infection recorded?
Anseriformes[240]	Shaoxing ducks	E	Pancreatic glands; Brains; Lungs	A/Bar-headed Goose/ Qinghai/0510/05 (H5N1)	
Anseriformes[231]	Tufted duck (*Aythya fuligula*)	N	Brain and neural tissue; Nasal mucosa; air vesicles and parabronchi, Liver, Pancreas; Adrenal glands; Ovarian follicular cells; Proventriculus and ventriculus	N/A	Endothelium of small vessels in the nasal mucosa positive in 2/17 ducks
Anseriformes[242]	Tufted duck (*Aythya fuligula*)	E	Brain, Caecal tonsil; Lung; Skeletal muscle; Heart; Spleen; Liver; Airways (trachea and main bronchus)	A/turkey/ Turkey/1/05 (H5N1)	
Anseriformes[243]	Wood duck (*Aix sponsa*)[b]	E	Brain; Adrenal glands; Testicles; Kidneys; Liver, Small intestines; Heart; Skeletal muscles; Pancreas and Air sacs	A/Whooper Swan / Mongolia/244/05 (H5N1) or A/Duck Meat /Anyang/01 (H5N1)	Endothelial cells in the brain

[a]E, Experimental; N, Natural. [b]Viral antigen recorded in birds that died during the experiment.

Table 2.2.2 Endothelial tropism of H5N1 in Charadriiformes as determined by immunohistochemistry

Order	Species	Infection[a]	Location of viral antigen	Virus	Endothelial cell infection recorded?
Charadriiformes[233]	Herring gull (*Larus argentatus*)	E	Adrenal Gland; Cerebellum; Heart and Pancreas	A/whooper swan/ Mongolia/244/05 (H5N1)	
Charadriiformes[233]	Herring gull (*Larus argentatus*)	E	Cerebrum and Pancreas	A/duck meat/ Anyang/01 (H5N1)	
Charadriiformes[243]	Laughing gull[b] (*Leucophaeus atricilla*)	E	Brain, Pancreas, Adrenal glands, Heart (minimal), Lungs (minimal), Air sacs (minimal), Thymus (minimal), Kidneys (minimal), Small intestines (minimal) and Eyes (minimal)	A/Whooper Swan/ Mongolia/244/05 (H5N1) and A/ Duck Meat/ Anyang/01 (H5N1	Viral antigen frequently detected in endothelial cells in brain
Charadriiformes[218]	Laughing gulls (*Leucophaeus atricilla*)	E	None	A/chicken/Hong Kong/220/97 (H5N1)	
Charadriiformes[244]	Laughing gulls (*Leucophaeus atricilla*)	E	None	A/chicken/Hong Kong/220/97 (H5N1)	

[a]E, Experimental; N, Natural. [b]Viral antigen recorded in birds that died during the experiment.

that endothelial cells can be infected by seasonal H3N2 IAV, with infection ultimately resulting in increased endothelial cell permeability (136). Others have suggested that IAV infection of the pulmonary endothelium is a unique feature of infection with H5N1 viruses, as H5N1 strains are able to efficiently infect and replicate in human microvascular endothelial cells whereas other IAV strains do not (131, 136, 141). However, in spite of these *in vitro* studies, there is limited evidence suggesting that IAV infection of human endothelial cells occurs *in vivo*. Post mortem analysis of patients who succumbed to H5N1 did not demonstrate the presence of virus in pulmonary endothelial cells (142). Similarly, endothelial cells were only very infrequently infected in a limited number of patients infected with fatal pandemic 2009 H1N1 (29). Whilst one recent study in mice recorded endothelial cell infection (245), in most animal models of human infection IAV infection of the endothelium is rarely observed (143) (**Figure 2.2.2**). Together, these data suggest that infection of endothelial cells by IAV is unlikely to contribute to disease severity in humans.

Although human endothelial cells are not infected by IAV *in vivo*, endothelial cells may still play an important role in the pathogenesis of IAV in humans. During IAV infection pulmonary endothelial cells are thought to be the most important source of cytokines in the lung (135). Specifically, in a mouse model of influenza, treatment with a SIP1 receptor agonist reduced IAV-induced mortality by blocking endothelial cell cytokine and chemokine production (135), suggesting a key role for endothelial cells in IAV pathogenesis. It has also been shown that the IAV-induced inflammatory response (namely the production of TNFα, IL-6 and IL-1β) upregulates trypsin production (246). The increased amount of trypsin then damages the tight junction protein zona-occludens 1 that is found between endothelial cells and increases endothelial permeability (246). However, it is important to note that this is unlikely to account for the pulmonary oedema observed during severe IAV infection as it is epithelial, not endothelial, cells that play the most important role in ensuring that the alveolus remains free of fluid (94). Pro-inflammatory cytokines, derived either from the endothelium or other cells in the lung, may also contribute to the development of thrombosis during IAV infection (137, 247). For example, treatment of human umbilical vein endothelial cells with TNFα significantly increased platelet binding to the cells by promoting the interaction between the F11 receptor on platelets and the F11 receptor on endothelial cells (247). This observation is supported by epidemiological evidence from the 2009 H1N1 pandemic, whereby 5.9% of patients hospitalised for influenza virus infection had thrombotic vascular events (248).

In addition to mediating cytokine production, endothelial cells may also indirectly control the inflammatory response in the lung during IAV infection via the expression of adhesion molecules, such as E-selectin, P-selectin, ICAM1, and VCAM1, on their apical surface. These adhesion molecules can bind to various leukocytes and mediate their

ravasation to the infected lung. The increased expression of E/P-selectin expression on human endothelial cells following exposure to H5N1 (132) may therefore account for the increased inflammatory response (and lung lesions) associated with this virus. In sum, whilst human endothelial cells are not infected with IAV, endothelial cells still play an important role in the pathogenesis of IAV in humans.

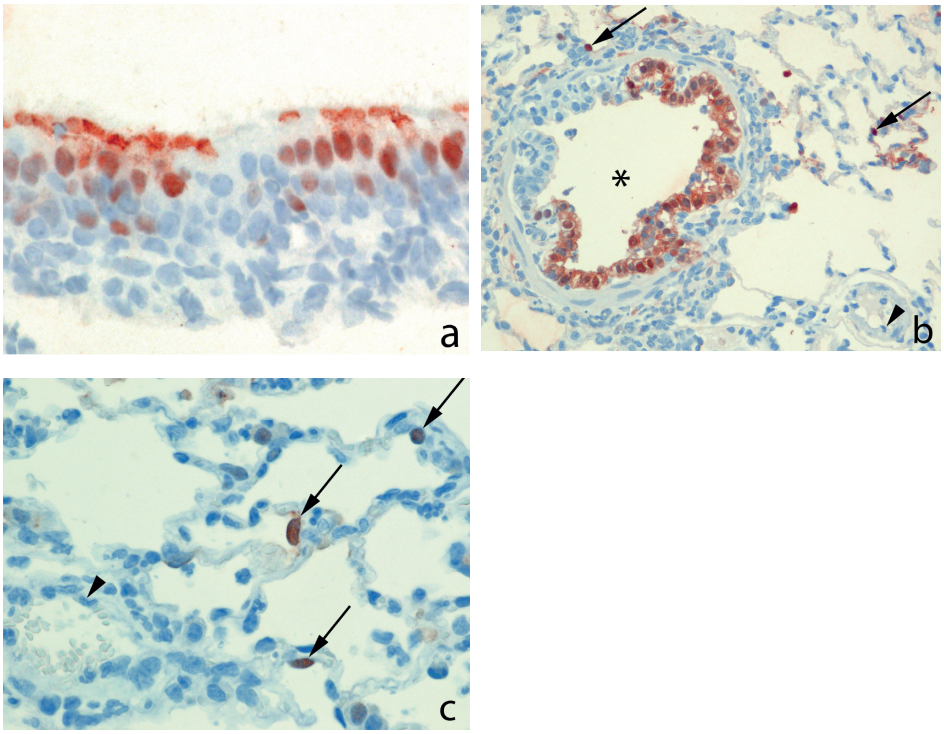

Figure 2.2.2 Epitheliotropism of IAVs in ferrets. IAV distribution in: **(A)** Epithelial cell nuclei and apical cytoplasm of the nasal respiratory mucosa of a ferret 24 h after experimental intranasal infection with 10^6 $TCID_{50}$ of seasonal influenza H3N2 A/Netherlands/177/2008 (original magnification 800×). **(B)** Epithelial cells of a bronchiole (asterisk) and in few alveolar lining epithelial cell nuclei (arrows) of a ferret lung 24 h after experimental intratracheal infection with 10^6 $TCID_{50}$ of influenza pH1N1 A/Netherlands/602/2009. The blood vessel lumen lining endothelial cell nuclei (arrowhead) do not stain positive for viral antigen (original magnification 200×). **(C)** Alveolar lining epithelial cell nuclei (arrows) of a ferret lung 24 h after experimental intratracheal infection with 10^6 $TCID_{50}$ of H5N1 HPAIV A/Indonesia/05/2005. The blood vessel lumen lining endothelial cell nuclei (arrowhead) do not stain positive for viral antigen (original magnification 400×). Brown-reddish staining antigen indicative of viral replication was present only in epithelial cells of ferret respiratory tract, not in ferret endothelial cells. (IHC for IAV-NP with hematoxylin counterstain).

ENDOTHELIAL CELL INFECTION IN CATS

Upon the initial emergence of H5N1 viruses, mortality in cats was observed in areas where the viruses were spreading in wild and domestic birds. This suggested that cats were susceptible to infection. This was unusual as cats have long been considered to be refractory to IAV infection. H5N1 viruses administered to cats intratracheally resulted in productive infection of many organs, including the respiratory tract, with parenchymal and epithelial cells as the primary targets for viral replication (249). These studies demonstrated that domestic cats could indeed develop clinical disease upon H5N1 HPAIV infection. Cats and other carnivores can be exposed to H5N1 viruses by feeding on sick or dead birds. In order to mimic this route of infection, Reperant and colleagues (144) administered H5N1 HPAIV to the small intestine of cats using enteric-coated capsules (the use of which avoided accidently exposing the respiratory tract to the inoculum). Three days post-infection H5N1 infected cats became lethargic and began to display severe clinical signs. Surprisingly, IHC demonstrated that there was an overwhelming infection of endothelial cells in virtually every organ of infected cats, in a pattern reminiscent of that observed in chickens. In contrast, parenchymal cells were rarely infected. In particular, infection of respiratory epithelial cells was not observed, despite massive infection of the pulmonary endothelium. The virus used to infect the cats via the intestine had been isolated from the liver of infected chickens, and may have accumulated mutations potentially responsible for such difference in tissue tropism. However, analyses of the viruses used to infect, and recovered from, cats inoculated intra-tracheally and via the intestine, revealed no coding differences associated with the difference in tropism. These data suggest that the route of virus exposure may influence the role of the endothelium in the pathogenesis of influenza virus in mammals.

CONCLUSIONS AND FUTURE DIRECTIONS

Endothelial cells play important but distinct roles in the pathogenesis of IAV in wild birds, poultry and humans. Whilst endothelial cells are infected by HPAIVs in chickens and swans, in humans they are more important in driving and controlling the inflammatory response in the lung. It is important to note that endothelial cells in both chickens and swans may also influence the inflammatory response to IAV. It has already been suggested that the overwhelming endothelial tropism of H5N1 viruses in poultry may disrupt the innate immune response (224). However, the details of this ‘disruption’ have been hard to elucidate due to the limited availability of reagents to study the avian immune response. This remains a key research priority for the future. In addition, what makes the endothelial cells of chickens and black swans (and not those of other

wild bird species and humans) so permissive to H5N1 viruses *in vivo* remains to be determined. It is likely that as research and the availability of reagents for studying avian species continues to grow new roles for endothelial cells in pathogenesis of IAV will be discovered. However, what is clear at present is that endothelial cells contribute to the severity of IAV infections across multiple different species.

Acknowledgments

We thank Judith van den Brand and Debby van Riel for the provision of histology sections. The authors declare that the research was conducted in the absence of any commercial or financial relationships that could be construed as a potential conflict of interest. Kirsty R. Short is supported by an NHMRC C. J. Martin post-doctoral fellowship (1054081). Thijs Kuiken is supported by European Union FP7 ANTIGONE

CHAPTER 3

Natural and experimental susceptibility of mammalian species to influenza
A virus infection and disease

3.1

Sporadic influenza A virus infections of miscellaneous mammal species

E.J.B. Veldhuis Kroeze[1,2] & T. Kuiken[1]

In: *Animal Influenza, 2nd edition, Chapter 23, edited by D.E. Swayne[3] 2016*

Affiliations
[1]Department of Viroscience, Erasmus Medical Center, Rotterdam, The Netherlands
[2]Viroclinics Biosciences B.V., Rotterdam, The Netherlands
[3]Southeast Poultry Research Laboratory, U.S. Department of Agriculture's Agricultural Research Service, Athens, Georgia, USA

ABSTRACT

Influenza viruses can infect a wide range of mammals, including carnivores, cetaceans, non-human primates, bats, ungulates, rodents, lagomorphs, and anteaters. We here provide a comprehensive overview of the sporadic influenza virus infections reported in these species. Besides a special section on highly pathogenic avian influenza virus subtype H5N1, which has the ability to cause severe disease in multiple mammalian species, and an in-depth discussion of the new bat-origin subtypes H10N17 and H11N18, we deal with all other influenza virus subtypes known to infect mammals. For each host-virus pair, we describe the history, clinical and pathological features, epidemiology, molecular virology, public health risk, and control measures. The scale of current global changes makes for a dynamic process, in which the sporadic infection of today may develop into the endemic situation of tomorrow.

Keywords: Influenza A Virus, H5N1, Carnivores, Marine mammals, Cetaceans, Non-human primates, Bats, Ungulates, Rodents, Lagomorphs.

INTRODUCTION

From the original wild bird reservoir, IAVs have crossed the species barrier at some time or other in the past and established endemic IAV infections in humans, domestic pigs, horses, and, most recently, domestic dogs. However, there seem to be few limits with regard to the range of mammalian species that IAVs can infect. This may be in part due their use of ubiquitous sialosaccharides as the receptor for virus attachment, and their ability to efficiently suppress the host innate immune response. This chapter provides an overview of the many mammals for which there is evidence of sporadic infections by diverse IAVs, namely carnivores, cetaceans, non-human primates, bats, uneven-toed and even-toed ungulates, rodents, lagomorphs, and anteaters.

A game changer in recent years has been the discovery of IAV infection in New World bats. Not only do these IAVs appear to be endemic in these bat populations, but also they are subtypes that are not represented in the wild bird reservoir. Therefore they appear to represent an additional original reservoir of IAVs, and are only included in this chapter because of their recent discovery.

The characteristics that are shared by mammalian species in which IAV has become endemic are large population numbers and aggregation in enclosed spaces (public buildings for human beings, barns for domestic pigs, stables for horses, and kennels for domestic dogs). In these species, IAV infection is present in the population continuously, and the virus has adapted to its host species. At the other end of the scale are mammalian species in which IAV infections are limited to sporadic cases in individual animals due to cross-species transfer, exemplified by the spread of pandemic H1N1 IAV from humans to their pet cats and ferrets. Intermediate between these two extremes are mammalian species in which efficient IAV transmission appears to be possible, but for some reason does not result in persistence of the virus in the population. The multiple reports of avian IAV epidemics in harbour seals (*Phoca vitulina*) are a clear example of this.

However, the situation can change rapidly. Who would have thought 20 years ago that an avian IAV like H5N1 would have wreaked such havoc among such a wide range of mammals, or that domestic dogs would harbour their own canine-adapted IAV? The scale of global change in animal populations and the ecosystems that they inhabit, together with the plastic nature of IAV, has resulted in a dynamic situation. Therefore the information presented in this chapter should be viewed as a snapshot of the current situation. Today's sporadic infection may be tomorrow's endemic situation.

H5N1 HPAIV INFECTIONS IN MISCELLANEOUS MAMMAL SPECIES

The H5N1 HPAIV that emerged in Asia in 1996 in poultry has shown the capacity to infect a wide range of mammalian species, including humans. In these species, the virus may spread to multiple organs beyond the respiratory tract, resulting in severe disease and death. Natural infections have been reported in multiple species of wild and domestic carnivores (250-264) (**Tables 3.1.1** and **3.1.2**), domestic pigs (265), black-lipped pikas (*Ochotona curzoniae*) (266), and donkeys (267) (**Table 3.1.3**). Serological evidence of natural infection or exposure to H5N1 HPAIV has been recorded in brown rats (*Rattus norvegicus*) (268, 269), raccoons (*Procyon lotor*) (270), and horses (268). Furthermore, experimental H5N1 HPAIV infections (not extensively discussed here) have been performed in laboratory mice, laboratory rats, laboratory hamsters (271-275), ferrets (*Mustela putorius furo*) (273, 276, 277), cynomolgus macaques (*Macaca fascicularis*) (278-280), red foxes (*Vulpes vulpes*) (281), cattle (*Bos taurus*) (282), and laboratory rabbits (266).

Two concerns about the many sporadic cases of mammalian H5N1 HPAIV infection are that they form a source of infection for humans, and they provide the opportunity for the virus to adapt to allow efficient mammal-to-mammal transmission. Until now there has been no concrete evidence of H5N1 HPAIV spreading from infected wild or domestic mammals to humans. With regard to efficient mammal-to-mammal transmission, the only strong evidence has been the probable tiger-to-tiger spread of H5N1 HPAIV at a zoo in Sri Racha, Thailand, in 2004 (262). Therefore the main source of H5N1 HPAIV infection for humans continues to be poultry, in which the virus continues to circulate in eastern Asia and northern Africa (33). The first indication that H5N1 HPAIV could spread from birds to mammals other than humans was in December 2003, when fatal H5N1 HPAIV infection was reported in two tigers (*Panthera tigris*) and two leopards (*Panthera pardus*) from a zoo in Suphanburi, Thailand (251). This was followed by a second outbreak in October 2004 in Sri Racha, Thailand, which involved the death or euthanasia of 147 tigers (262). Affected felids had high fever, respiratory distress, and (in some cases) nervous signs, and died with serosanguinous nasal discharge 3 days after the onset of clinical signs (**Figure 3.1.1**). Autopsy revealed severely congested and hemorrhagic lungs, which corresponded microscopically with bronchointerstitial pneumonia and co-localisation of influenza virus antigen expression in pneumocytes. Extra-respiratory spread of the virus was demonstrated by meningoencephalitis and hepatitis, co-localised with influenza virus antigen expression in neurons and hepatocytes, respectively (251, 262). The felids were initially infected as a result of feeding on fresh poultry carcasses – the H5N1 HPAIV isolates from felids at both zoos were very similar to H5N1 HPAIV strains circulating in poultry at the time (283). It is likely that tiger-to-tiger transmission of H5N1 HPAIV also occurred at Sri Racha, because the outbreak continued after the feeding of fresh

poultry carcasses had been stopped. There was limited evidence of H5N1 HPAIV spread to humans. Five zookeepers at Sri Racha were placed under surveillance after showing influenza-like signs (284). However, only 2 of 58 zookeepers and veterinarians, neither of whom had shown clinical signs, had anti-H5N1 HPAIV antibodies in their serum 6 weeks after the outbreak (262).

H5N1 HPAIV infections were reported not only in Thailand, but also in Cambodia and China. In December 2003 there was an outbreak of H5N1 HPAIV in 26 species of birds, including birds of prey, in Phnom Tamao Wildlife Rescue Centre, Cambodia. During this outbreak, two lions (*Panthera leo*), two tigers, two Asiatic golden cats (*Catopuma temminckii*), three leopards, and one clouded leopard (*Neofelis nebulosa*) exhibited anorexia and lethargy for 5–7 days, but neither respiratory illness nor mortality. Serum samples were collected from one tiger, one leopard, one Asiatic golden cat, and one clouded leopard, and had neutralising antibody titers of 10–40 against H5N1 HPAIV. The H5N1 HPAIV isolates from the zoo birds were phylogenetically highly similar to those from poultry in Cambodia, and it was assumed that infected poultry carcasses used as a food source both for birds of prey and for felids were the source of infection (250). In 2005, a tiger at a zoo in Shanghai, China, died with similar clinical and pathological findings to those in tigers from Thailand. The H5N1 HPAIV isolate from the tiger's lung belonged to clade 2.2, and was phylogenetically almost identical to that isolated in the same year from a migratory duck at Poyang Lake, China. However, it was not reported whether the tiger had consumed chickens or wild birds (256).

Table 3.1.1 Virological evidence of natural influenza A virus infection in mammals of the suborder Caniformia (dog-like carnivores). Only reports where the virus was detected by virus isolation or RT-PCR are listed.

		Virus				Tissue tropism[a]					
Family	Species	Origin	Subtype	Morbidity	Mortality	Respiratory	Extra-respiratory	Sustained intraspecies transmission	Region[b]	Period	References
Canidae	Domestic dog	Human	H3N2	yes[a]	no	yes	no	yes[a]	AS, EU	1970-71	(285-288)
		Avian	H5N1	yes	yes	yes	yes	no	AS	2004	(261)
		Human / Canine	H3N1	yes	no	yes	no	no	AS	2009-10	(289)
		Human	pH1N1	yes	no	yes	yes[d]	no	AS, NA	2009	(290-292)
		Swine / Avian	H5N2	yes	no	yes	yes[e]	yes[a]	AS	2009	(293-295)
		Avian	H9N2	yes	no	yes	no	no	AS	2010-12	(296)
		Human / Canine	H3N2	yes	no	yes	no	yes[a]	AS	2013	(297)
	Raccoon dog	Avian	H5N1	yes	yes	yes	–[c]	–	AS	2005	(258)
	Red fox	Avian	H5N1	–	–	yes	yes	–	EU	2006	(281, 298)
Ursidae	Giant panda	Human	pH1N1	yes	no	yes	yes[e]	no	AS	2009	(299)
Mephetidae	Striped skunk	Human	pH1N1	yes	yes	yes	no	no	NA	2009-10	(300)
Mustelidae	American badger	Human	pH1N1	yes	no	yes	no	no	NA	2009	(301)
	American mink	Avian	H10N4	yes	yes	yes	yes[e]	yes	EU	1984	(302)
		Avian	H5N1	yes	no	–	yes	no	EU	2006	(252, 257, 264)
		Swine	H3N2	yes	yes	yes	no	–	NA	2007	(303)
		Human / Swine	H3N2	yes	yes	yes	no	yes	EU	2009	(304, 305)
		Swine	H1N2	yes	yes	yes	no	yes	NA	2010	(306)
		Human	pH1N1	yes	yes	yes	no	yes	EU	2010-11	(305, 307, 308)
	Black-footed ferret	Human	pH1N1	yes	no	yes	no	no	NA	2009	(301)

Table 3.1.1 Virological evidence of natural influenza A virus infection in mammals of the suborder Caniformia (dog-like carnivores). Only reports where the virus was detected by virus isolation or RT-PCR are listed. (continued)

Family	Species	Virus		Morbidity	Mortality	Tissue tropism[a]		Sustained intraspecies transmission	Region[b]	Period	References
		Origin	Subtype			Respiratory	Extra-respiratory				
	Domestic ferret	Human	unspecified IAV	yes	yes	yes	yes[e]	yes	EU, NA	1940s	(309, 310)
		Swine	H1N1	yes	yes	yes	yes[e]	yes	NA	2008	(311)
		Human	pH1N1	yes	yes	yes	no	no	NA	2009	(312-316)
	Stone marten	Avian	H5N1	yes	yes	yes	yes	no	EU	2006	(254)
Phocidae	Harbour seal	Avian	H7N7	yes	yes	yes	yes	yes	NA	1979-80	(13, 317-319)
		Avian	H4N5	yes	yes	yes	yes	yes	NA	1982-83	(320)
		Avian	H4N6	yes	yes	yes	no	yes	NA	1991	(14)
		Avian	H3N3	yes	yes	yes	no	yes	NA	1992	(14)
		Avian	H3N8	yes	yes	yes	yes	yes	NA	2011	(15)
		Avian	H10N7	yes	yes	yes	yes[f]	yes	EU	2014	(321-323)
	Harp seal	Avian	H3N8	–	–	yes	–	–	NA	2005-07	(324)
	Northern elephant seal	Human	pH1N1	no	no	yes	no	yes, restricted	NA	2010	(325)

[a] Also based on results of experimental infections.

[b] AS, Asia; EU, Europe; NA, North America.

[c] –, not determined or not recorded.

[d] Tonsil was reported positive by IHC.

[e] Conjunctivitis and/or ocular discharge was reported.

[f] Spleen was reported PCR positive by Krog and colleagues (323).

Table 3.1.2 Virological evidence of natural influenza A virus infection in mammals of the suborder Feliformia (cat-like carnivores). Only reports where the virus was detected by virus isolation or RT-PCR are listed.

Family	Species	Virus		Morbidity	Mortality	Tissue tropism[a]		Sustained intraspecies transmission	Region[b]	Period	References
		Origin	Subtype			Respiratory	Extra-respiratory				
Felidae	Domestic cat	Avian	H5N1	yes	yes	yes	yes	yes	AS, EU, ME	2004-12	(253, 255, 260, 263, 326-328)
		Human	pH1N1	yes	yes	yes	no	no	NA, EU	2009	(329-331)
		Canine	H3N2	yes	yes	yes	–[c]	yes	AS	2010	(332, 333)
	Cheetah	Human	pH1N1	yes	no	yes	no	no	NA	2009	(334)
	Leopard	Avian	H5N1	yes	yes	yes	yes	yes	AS	2003	(251)
	Tiger	Avian	H5N1	yes	yes	yes	yes	yes	AS	2003-05	(251, 256, 262)
Viverridae	Owsten's palm civet	Avian	H5N1	yes	no	yes	yes	no	AS	2005	(259)
	Bornean binturong	Human	pH1N1	yes	no	yes	no	no	NA	2009	(301)

[a]Also based on results of experimental infections.

[b]AS, Asia; EU, Europe; NA, North America; ME, Middle East.

[c]–, not determined or not recorded.

Table 3.1.3 Virological evidence of natural influenza A virus infection in mammals of the orders Perissodactyla (Equidae), Artiodactyla (Bovidae, Camelidae, and Cervidae), and Cetacea (Balaenopteridae and Delphinidae). Only reports where the virus was detected by virus isolation or RT-PCR are listed.

Family	Species	Virus		Morbidity	Mortality	Tissue tropism[a]		Sustained intraspecies transmission	Region[b]	Period	References
		Origin	Subtype			Respirator	Extra-respiratory				
Equidae	Domestic donkey	Avian	H5N1	yes	no	yes	no	no	ME	2009	(267)
Bovidae	Domestic cattle	Swine	H1N1	yes	no	yes	no	suspect	EU	1959	(339, 340)
		Human	H3N2	yes	no	yes	no	suspect	EU, AS	1968, 1971	(340, 341)
	Domestic sheep	Human	H2N2	yes	no	yes	yes[d]	suspect	EU	1959-60	(339, 340)
Camelidae	Bactrian camel	Human	H1N1	yes	yes	yes	yes[e]	yes	AS	1978-88	(342)
		Equine	H3N8	no	no	yes	no	–[c]	AS	2012-13	(343)
Cervidae	Reindeer	–	–	–	–	–	–	–	AS	1970s	(340)
Balaenopteridae	Common minke whale	Avian	H1N3	–	no	yes	yes	–	South Pacific Ocean	1975-76	(344, 345)
Delphinidae	Long-finned pilot whale	Avian	H13N2, H13N9	yes	no	yes	yes[f]	no	NA coastal waters	1984	(346, 347)

[a]Also based on results of experimental infections.

[b]AS, Asia; EU, Europe; NA, North America; ME, Middle East.

[c]–, not determined or not recorded.

[d]Virus was isolated from fetus also.

[e]Conjunctivitis and/or ocular discharge was reported.

[f]Virus was isolated from hilar lymph node also.


1

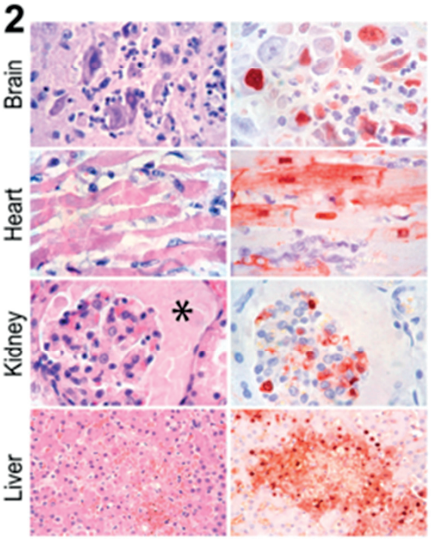
2
Brain
Heart
Kidney
Liver

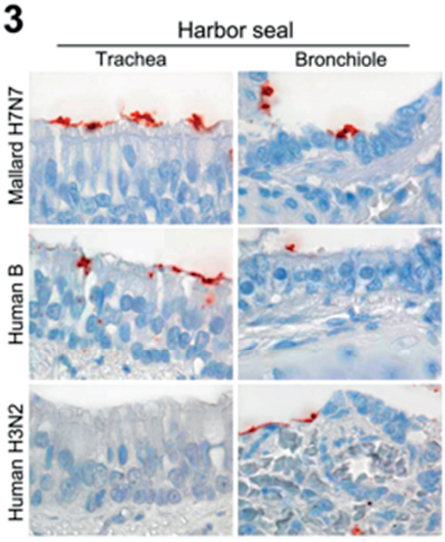
3
Harbor seal
Trachea
Bronchiole
Mallard H7N7
Human B
Human H3N2

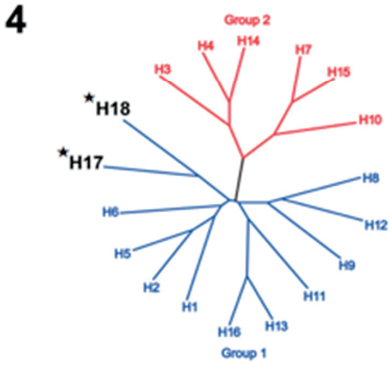
4
Group 2
H4
H14
H7
H3
H15
H18
H10
H17
H8
H6
H12
H5
H9
H2
H11
H1
H16
H13
Group 1

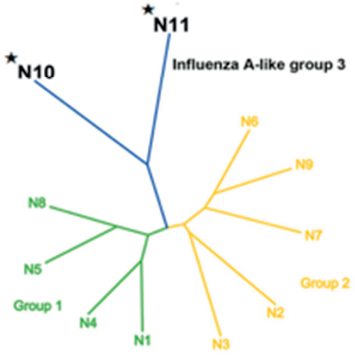
N11
N10
Influenza A-like group 3
N6
N9
N8
N7
N5
Group 2
Group 1
N2
N4
N1
N3

← **Figure 3.1.1 Natural infection of tigers with H5N1 highly pathogenic avian influenza virus in Sri Racha, Thailand, in 2004.** Affected animals had high fever, respiratory distress, and—in some cases—nervous signs, and died with serosanguinous nasal discharge. Photograph courtesy of Dr Roongroje Thanawongnuwech, Chulalongkorn University, Thailand.

← **Figure 3.1.2 Systemic histological lesions in domestic cats after experimental H5N1 HPAIV infection.** Necrotising inflammatory foci are present in multiple tissues stained with H&E in the left column. Influenza virus antigen (red-brown staining) is present in serial sections of the same tissues, stained for nucleoprotein by IHC in the right column. Reprinted from: The American journal of Pathology, January 2006, Vol. 168, No. 1, p. 176-83, Rimmelzwaan GF, van Riel D, Baars M, Bestebroer TM, van Amerongen G, Fouchier RA, Osterhaus, AD, Kuiken, T. Influenza A virus (H5N1) infection in cats causes systemic disease with potential novel routes of virus spread within and between hosts, with permission from Elsevier.

← **Figure 3.1.3 Low pathogenic avian influenza A virus (H7N7), human seasonal influenza A virus (H3N2), and human influenza B virus show different degrees of attachment to the trachea and bronchiole of a harbor seal (*Phoca vitulina*).** Red staining indicates virus attachment to the epithelial cell surface. Reprinted from: Ramis AJ, van Riel D, van de Bildt MWG, Osterhaus A, Kuiken T. Influenza A and B virus attachment to respiratory tract in marine mammals. Emerg Infect Dis [serial on the Internet]. 2012 May [date cited]. Available from http://dx.doi.org/10.3201/eid1805.111828

← **Figure 3.1.4 Phylogenetic trees displaying the hemagglutinin (HA) and neuraminidase (NA) genes of bat-derived H17N10 and H18N11 influenza viruses (with stars) compared to the relative distance of HAs and NAs of all previously known influenza A virus subtypes.** Reprinted from: Trends in Microbiology, April 2014, Vol. 22, No. 4, p. 183-91, Wu Y, Wu Y, Tefsen B, Shi Y, Gao GF. Bat-derived influenza-like viruses H17N10 and H18N11, with permission from Elsevier.

Starting in 2004, there were several reports from all around the world of domestic cats with natural H5N1 HPAIV infection – from Thailand in 2004 (260, 327), Germany and Austria in 2006 (253, 255, 335), Iraq in 2006 (263), Indonesia in 2006 (328), and Israel in 2012 (326). Most of these reports indicated that contact with or feeding on infected birds was the route of infection, and described severe clinical disease or death in the cats. Five days after eating a pigeon, a cat in Thailand developed high fever, dyspnea, and depression, and it died 2 days later (260). Several cats on the German island of Rügen were infected by an H5N1 HPAIV that belonged to clade 2.2 (336) and was genetically very similar to an isolate from a dead whooper swan (*Cygnus cygnus*) from the same area (253, 335). Several cats in Israel showed respiratory signs, weakness, and subsequently died after feed- ing on turkey carcasses. The H5N1 HPAIV found in the cats was similar to that from the turkeys (326). In contrast, no overt clinical disease was observed in several cats that had pharyngeal swabs positive for H5N1 HPAIV by PCR after contact with infected birds at an animal shelter in Austria (255).

Experimental H5N1 HPAIV infection, either by intratracheal inoculation or by feeding on infected chicks, showed that cats were susceptible to both severe respiratory disease and widespread extra-respiratory complications. Cats developed not only a severe bronchointerstitial pneumonia, but also severe necrosis and inflammation in the brain,

heart, liver, kidney, spleen, adrenal glands, and intestine, co-localised with influenza virus antigen expression in epithelial and mesenchymal cells of these tissues (**Figure 3.1.2**) (249, 337, 338). In addition, hemorrhagic pancreatitis was observed in naturally infected cats (263).

Serological evidence that cats are exposed to or infected with H5N1 HPAIV depends on the situation in poultry. In geographical regions where H5N1 HPAIV was endemic in poultry, the following proportions of cats were found to be seropositive: 8 of 111 (7%) in central Thailand (348), 100 of 500 (20%) on Java and Sumatra (349), and 9 of 25 (36%) in endemic areas of Egypt (268). In contrast, no cats were found to be seropositive in areas of Europe where H5N1 HPAIV had occurred in birds as an epidemic (350, 351).

Guidelines for prevention and management of H5N1 HPAIV infections in pet cats were published by Kuiken and colleagues (352) and by the European Advisory Board on Cat Diseases (353). In areas where H5N1 HPAIV has been detected in poultry or wild birds, cat owners should avoid feeding uncooked poultry meats, and keep cats indoors to prevent contact between their pets and infected birds or their droppings. In suspected cases of H5N1 HPAIV infection in cats, veterinarians and cat own- ers should maintain stringent hygienic measures with regard to animal handling, and quarantine and test the affected cat(s). An inactivated, adjuvanted heterologous H5N6 AIV vaccine has been shown to protect cats against fatal disease from H5N1 HPAIV infection (338).

H5N1 HPAIV infection has also been reported in domestic dogs, but the associated disease appears to be milder than in cats. There is only one case report of natural H5N1 HPAIV infection in a dog (261). Like cats, feeding on infected birds probably infected the dog. It developed high fever, dyspnea, and lethargy 5 days later, and died the following day. Autopsy revealed severe pulmonary congestion and oedema, which correlated histologically with interstitial pneumonia and influenza virus antigen expression in pulmonary alveolar cells. Extra-respiratory spread of virus was demonstrated histologically by multifocal hepatic necrosis and tubulonephritis, which co-localised with influenza virus antigen expression in hepatocytes and epithelial cells of the glomeruli and renal tubules, respectively. The H5N1 HPAIV isolated from lung, liver, kidneys, and urine was genetically similar to that recovered earlier from a tiger in Thailand (261). In experimental H5N1 HPAIV infections in dogs, clinical signs ranged from transient fever and conjunctivitis (354) to anorexia, fever, conjunctivitis, laboured breathing, cough, and death in one of six dogs (355). In contrast to the fatal case reported by Songserm and colleagues (261), virus replication and associated lesions in experimentally infected dogs were restricted to the respiratory tract. The high percentage of dogs with specific antibodies to H5N1 influenza virus suggests that dogs are commonly infected with or exposed to the H5N1 HPAIV in areas where the virus is endemic in poultry (160 of 629 dogs (25%) in central Thailand (348), and 4 of 25 dogs (16%) in endemic areas of Egypt (268).

There is one report of H5N1 HPAIV infection associated with die-off in raccoon dogs (*Nyctereutes procyonoides*), which belong to the family Canidae (356). About 100 of a total of 1000 raccoon dogs from a fur farm in China died with respiratory disease, diarrhea, or both in 2005. Genetic and molecular characterisation identified the viruses, which were isolated from the lungs of two of the dead raccoon dogs, as H5N1 HPAIV. It was assumed that chicken carcasses fed to the raccoon dogs were the source of infection (356). None (0%) of 102 free-living raccoon dogs sampled in South Korea in 2011 had antibodies against IAVs (357).

Red foxes (*Vulpes vulpes*), which belong to the family Canidae, are an important predator on and scavenger of wild and domestic birds, and may potentially be exposed to H5N1 HPAIV by this route. An H5N1 HPAIV (A/fox/Azerbaijan/1413/2006) was isolated from a fox in Azerbaijan in 2006 (298). Experimental infections show that red foxes excrete virus from the throat for up to 7 days after inoculation. Ingestion of infected chicks causes subclinical infection or mild pneumonia, whereas intratracheal inoculation causes severe pneumonia, myocarditis, and encephalitis. Together these results demonstrate that red foxes might play a role in virus dispersal (281). There is one report of fatal H5N1 HPAIV infection in Owston's palm civets (*Chrotogale owstoni*), a globally threatened species belonging to the family Viverridae. It involved three Owston's palm civets that were kept together in captivity at a national park in Vietnam in 2005. They showed anorexia and neurological signs, including hind limb paralysis, for 1 or 2 days before death. Pathological examination revealed interstitial pneumonia, meningitis, cerebral oedema, and multifocal hepatic necrosis. H5N1 HPAIV was detected by virus isolation, RT-PCR, and IHC in all of these tissues, as well as in kidney and intestine, demonstrating systemic viral infection. Although the H5N1 HPAIV from the Owston's palm civets was similar to that in poultry, and undiagnosed poultry deaths were reported in the surroundings of the park, the civets were not fed on bird carcasses, so the source of infection remains unknown (259, 358).

There are reports of single cases of H5N1 HPAIV infection in a stone marten (*Martes foina*) (254) and an American mink (*Mustela vison*) (257), both of which belong to the family Mustelidae. The stone marten was from the Isle of Rügen, north Germany, and the American mink was from south Sweden. Both animals were free-living, had neurological signs, and were identified in 2006. They were probably infected as a result of feeding on infected wild birds. Histopathological examination of the stone marten revealed encephalitis and pancreatic necrosis, co-localised with influenza virus antigen expression in neurons and pancreatic acinar cells, respectively (254). Surprisingly, neither pneumonia nor influenza viral antigen were observed in the lungs, which contrasts with the pneumotropism of H5N1 HPAIV in most other mammals. Molecular

characterisation of the Swedish mink isolate (A/Sweden/mink/V907/2006) revealed no specific adaptation to mammals (252, 264).

There is only serological evidence of H5N1 HPAIV infection in raccoons (*Procyon lotor*), which belong to the family Procyonidae. In total, 10 (0.9%) of 1088 healthy free-living raccoons that were sampled in Japan between 2005 and 2009 had virus-neutralizing antibodies to H5N1 IAV, but not to viruses of other hemagglutinin (HA) subtypes, including H1, H3, H7, and H9. During that period, Japan experienced two outbreaks of H5N1 HPAIV on poultry farms and one in free-living swans. Therefore it is likely that the raccoons became infected or exposed by feeding on infected bird carcasses (270).

There is also only serological evidence of H5N1 HPAIV infection in brown rats (*Rattus norvegicus*), belonging to the family Muridae. Hemagglutination-inhibiting antibodies to H5N1 IAV were found in some brown rats sampled at live poultry markets in Hong Kong during the 1997 H5N1 HPAIV outbreak (269), and in 1 (1.4%) of 72 brown rats sampled in Cairo, Egypt, and the surrounding area after H5N1 HPAIV became endemic in poultry there in 2006 (268). Experimentally, not only laboratory rats, but also laboratory mice (*Mus musculus*), of the family Muridae, and hamsters (*Mesocricetus auratus*), of the family Cricetidae, develop both a productive infection and associated lesions upon H5N1 HPAIV inoculation (273-275).

There is one report of H5N1 HPAIV infection in free-living black-lipped pikas (*Ochotona curzoniae*), of the family Ochotonidae, which together with rabbits and hares belong to the order Lagomorpha. Evidence of H5N1 HPAIV infection was found in black-lipped pikas sampled between August 2006 and December 2007 in their natural habitat around Qinghai Lake, China (266), where there had been a large-scale outbreak of H5N1 HPAIV infection in migratory birds (240, 359, 360). Initially, hemagglutination-inhibiting antibodies to H5N1 IAV were detected in 11 (13%) of 82 pikas. Subsequently, H5N1 HPAIV was isolated from brain, lung, and rectum samples from 5 (3%) of 147 newly caught pikas. Phylogenetically, these isolates could be divided into a mixed/Vietnam H5N1 lineage and a wild bird Qinghai-like H5N1 lineage. Presumably the black-lipped pikas contracted these viruses from wild birds at common weed-foraging sites. Experimental infection of rabbits (*Oryctolagus cuniculus*), of the family Leporidae, resulted in a productive infection and interstitial pneumonia, with influenza virus antigen expression in epithelial cells of nasal turbinates, trachea, and lungs (266). Recently, the host range of H5N1 HPAIV has been extended to include donkeys (*Equus africanus asinus*), which together with horses (*Equus ferus caballus*) belong to the family Equidae. In an Egyptian village in 2009, H5N1 HPAIV was isolated from pooled nasal swabs from three donkeys with mild respiratory disease. These donkeys showed coughing, fever, and serous nasal discharge for 72 hours. Onset of these respiratory signs was 1 week after an outbreak of H5N1 HPAIV infection in poultry in the same village. Phylogenetic analysis of the

isolate from the donkeys showed close homology to the lineage of Egyptian H5N1 HPAIV viruses circulating in poultry and humans. Subsequently, antibodies against H5N1 IAV were found in 27 (26%) of 105 donkeys from areas where H5N1 HPAIV was endemic in poultry. Possible routes of infection included aerosol exposure to bird faeces, feed or water contaminated with bird faeces, or direct contact with infected birds. Concerns were raised that donkeys commonly housed with poultry might spread a mammal-adapted H5N1 HPAIV to humans (267). In a later serological survey, El-Sayed and colleagues (268) found antibodies against H5N1 not only in donkeys but also in horses from H5N1-endemic areas in and around Cairo.

Although cattle (*Bos taurus*), of the family Bovidae, may be naturally infected with IAV (340, 341), there are no reports of natural H5N1 HPAIV infection in cattle. Experimentally, four calves that were inoculated intranasally with H5N1 HPAIV from a naturally infected cat had a subclinical infection with low virus excretion from the nose. There was no firm evidence of calf-to-calf transmission; although one of two sentinel calves housed together with the inoculated calves seroconverted, the nasal swabs of both sentinel calves remained negative for H5N1 HPAIV RNA throughout the experiment (282).

OTHER INFLUENZA A VIRUSES IN MISCELLANEOUS MAMMAL SPECIES

Influenza A viruses in the order Carnivora, suborder Caniformia

Various species belonging to the order Carnivora, suborder Caniformia, have been infected with IAV (**Table 3.1.1**), and are described in detail in the following sections.

Influenza A viruses in the family Canidae

Sustained circulation of canine-adapted IAVs is a recent phenomenon. In 2002, an H3N8 IAV originating from horses caused an outbreak of respiratory disease in a pack of 92 English foxhounds in the UK. Although the route of transmission is not known, the dogs were housed adjacent to horse stables, and had recently been fed the meat of two euthanised horses (361). Two years later, another horse-origin H3N8 IAV caused an outbreak of respiratory disease in greyhound dogs in Florida, USA (362). Starting in 2007, an H3N2 low-pathogenicity avian influenza virus originating from birds caused respiratory disease outbreaks in dogs in South Korea (363), China (364), and Thailand (365). These H3N8 and H3N2 viruses have now adapted to their new hosts, are able to spread efficiently in domestic dog populations, and are the recognised etiological agents of this new disease – canine influenza.

In contrast to these dog-adapted IAVs, it has been recognised for years that human-origin IAVs may sporadically jump the species barrier and infect domestic dogs. Experimentally, the susceptibility of dogs to human H1N1 IAV infection was demonstrated as early as 1959 (366), and natural infection was first demonstrated in 1975, when human H3N2 IAV was isolated from affected dogs (285, 286). Studies showing serological responses in dogs to human H3N2 IAV (285, 367, 368) also suggested that there was transmission of virus from humans to dogs. Both natural and experimental human H3N2 IAV infections in dogs are usually subclinical (286-288, 368-370), although they may cause transient fever (287). Human H3N2 IAV was transmitted to sentinel dogs housed together with experimentally inoculated dogs (287). When the most recent influenza pandemic, caused by pandemic H1N1 IAV (pH1N1), occurred in humans, it was also reported in domestic dogs in China (290) and the USA (291). The pH1N1-positive dog from the USA had clinical evidence of pneumonia, with fever, coughing, and anorexia. pH1N1 IAV had been confirmed in the dog's owner 1 week previously. Experimental inoculation of the canine isolate from China into dogs resulted in mild clinical signs and inefficient dog-to-dog transmission (292). In contrast, inoculation of a human isolate of pH1N1 into dogs did not cause infection (371).

Recently, two reassortants of pH1N1 and H3N2 canine influenza virus (CIV) have been isolated in South Korea from nasal swabs from domestic dogs with respiratory signs. The first reassortant, H3N1, had the HA gene segment of H3N2 CIV and the remaining seven gene segments of pH1N1. Experimental inoculation into dogs resulted in a subclinical infection with virus shedding from the nose. At autopsy, the severity of pneumonia was intermediate between the mild lesions of pH1N1 IAV infection and the marked lesions of H3N2 CIV infection (289). The second reassortant, H3N2, had the M gene segment of pH1N1 and the remaining seven gene segments of H3N2 CIV. Experimental infection of dogs resulted in similar virus shedding, dog-to-dog transmission, and severity of pneumonia as classic H3N2 CIV infection (297).

In 2009, an H5N2 LPAIV was isolated in China from nasal swabs from domestic dogs with respiratory signs (293, 294). Experimentally infected dogs shed virus, had transient fever, and developed mild respiratory signs (294). The virus was transmitted from infected dogs both to sentinel dogs (294) and to a cat and chickens (295).

An H9N2 LPAIV was detected by culture and PCR in 13 (2.2%) of 588 juvenile to young adult domestic dogs with clinical signs (coughing, vomiting, fever) in Guangxi, China, in 2010 and 2011. Serologically, up to 45% of dogs tested positive. The virus, known as A/canine/Guangxi/1/2011 (H9N2), showed more than 98.5% genetic homology with Eurasian-lineage H9N2 LPAIV (296). Dogs could be infected by intranasal inoculation (372), but not by feeding on infected chickens (373). Although virus was recovered from nasal turbinates, trachea, and lung in association with a mild pneumonia, infection was subclinical and no virus was shed from the URT. In contrast, intranasally inoculated

dogs in another experiment (373) had mild respiratory signs, shed virus from the nose, and infected sentinel dogs. Concerns were raised that dogs may contribute to further spread, and adaptation to mammals, of this widely circulating Eurasian LPAIV.

Control of influenza in domestic dogs should include routine hygiene measures, such as isolation of infected dogs to prevent virus spread to other animals (374). Because dogs are susceptible to avian IAV infection, live in close proximity to humans, and may have access to poultry at live animal markets, especially in South-East Asia, they are potential intermediate hosts for virus spread to humans. Furthermore, because dogs are susceptible to both human and avian IAVs, they have the potential to serve as a "mixing vessel" in which new reassortants may arise, as has been seen recently for reassortant H3N1 and H3N2 IAVs (289, 297).

Influenza A viruses in the family Ursidae

Bears are long-lived, wide-ranging, opportunistic animals that one would expect to be easily exposed to infectious agents from a wide range of animals and humans. However, reports of exposure to IAVs in bears are rare. There is one report of weak positive IAV (and influenza B virus) serum antibody titers in a juvenile captive Eurasian brown bear (*Ursus arctos arctos*) from Croatia, suggesting exposure to infected humans (375). More compelling evidence of infection with IAVs was found in giant pandas (*Ailuropoda melanoleuca*) by Li and colleagues (299). In 2009, during the human H1N1 pandemic, three captive giant pandas from a conservation center in Sichuan Province, China, showed clinical signs of respiratory disease. A nasal swab taken from one animal tested positive by PCR for the HA gene of pH1N1, and by culture for IAV. Phylogenetic analysis of the virus isolate suggested human-to-panda transmission without significant adaptation. All three pandas received 75 mg of oseltamivir twice daily for 5–6 days, recovered, and seroconverted to pH1N1 (299).

Influenza A viruses in the family Ailuridae

There is a report of weak positive IAV-nucleoprotein antibody titers by agar gel immunodiffusion in one of 73 captive red pandas (*Ailurus fulgens*) from China (356). The source or type of influenza virus was not specified.

Influenza A viruses in the family Mustelidae

The American mink (*Mustela vison*) is a mustelid species that is kept in captivity in large numbers for its fur. Recently this species has been placed in a separate genus (*Neovison vison* or *Vison vison*) from the domestic ferret (*Mustela putorius furo*) and the European mink (*Mustela lutreola*), based on molecular phylogeny (376). The susceptibility of American mink to IAV infection has been recognised for several decades. In the late 1970s and early 1980s, antibodies against human H3N2 and H1N1 IAVs were detected

in farmed mink from Japan (377, 378). Inoculation of mink with human H3N2 IAV resulted in a productive infection with respiratory signs, and transmission to contact mink. Productive infection of mink also resulted from inoculation of human H1N1, swine H1N1, equine H1N2, and avian H3N2 and H4N1 IAVs (379). In similar experiments (380, 381), inoculation of different avian (H3N8, H5N3, H7N2, H7N7, H8N4, and H11N4) or mammalian (human and swine H1N1, and equine H2N2) IAVs also resulted in productive infection, with transmission to contact mink.

In 1984, H10N4 IAV, probably of avian origin, caused an outbreak of severe respiratory disease with 100% morbidity and 3% mortality in 100,000 mink on neighbouring farms in Sweden (302). Clinical signs included anorexia, sneezing, coughing, and nasal and ocular discharge. Pathological examination of fatal cases showed an acute interstitial pneumonia. Experimental infection in mink induced similar clinical signs and pathological changes, with transmission to sentinel mink separated by a wire fence. The presumed origin of the virus was wild birds (corvids, gulls, and ducks) that were attracted to the tops of the open wire cages by offal fed to the mink (302). Interestingly, comparative infections of mink with either H10N4 IAV (A/mink/Sweden/3900/1984) or H10N7 IAV (A/chicken/Germany/N/1949) revealed that only H10N4 IAV was transmitted to sentinels, and that it caused more severe pneumonia than H10N7 IAV (382, 383). Recent full-genome analysis of the viruses showed that the NS gene of H10N4 IAV may have contributed to its virulence for mink by helping the virus to evade the innate immune response (384).

In 2006 and 2007, swine H3N2 IAV was associated with increased respiratory disease and mortality in mink farmed in Nova Scotia, Canada. Clinical signs included dry cough, and pathological examination of fatal cases revealed interstitial pneumonia and bronchiolitis. The virus isolated from affected mink was related to a triple reassortant swine IAV that had emerged in 2005. The presumed route of transmission was the feeding of uncooked meat by-products, including ground swine lung from parts of Canada where swine H3N2 IAV was known to occur (303).

In 2009 and 2010, a human/swine reassortant H3N2 IAV caused an outbreak of respiratory disease in mink on 18 farms in Denmark. Clinical signs included sneezing, coughing, and hemorrhaging from the nose, and the average mortality rate was 1.2%. The HA and NA genes of the isolated virus were homologous with human H3N2 IAV, and the six remaining genes were homologous with a circulating swine H1N2 IAV. These findings suggest that mink are susceptible to infection by both swine and human IAVs, and may act as a "mixing vessel" (304). The probable source of infection was feeding of raw offal, including swine tracheas and lungs. All of the affected mink farms received this offal from the same slaughterhouse. The outbreak, which lasted for 10 weeks, may have been sustained by continued feeding of infected offal, by horizontal transmission, or both (305).

In 2010 and 2011, human pH1N1 IAV caused respiratory disease outbreaks on several mink farms in Denmark, Norway, and the Netherlands (305, 307, 308). Clinical signs included nasal discharge, coughing, and sneezing in vixens, and dyspnea in kits. Mortality rates in kits ranged from 14% in Norway to 30% in the Netherlands. Pathological examination of dead kits showed severe acute interstitial pneumonia. Phylogenetic analysis revealed that the virus isolated from Norwegian mink closely resembled human pH1N1 IAV from 2009 that circulated among people in Norway during the winter of 2010–2011. However, respiratory symptoms were not reported for the Norwegian mink farmers at the time of the outbreaks, and feeding of pig offal was considered the most likely source of infection. Dutch mink farmers were suffering from an influenza-like illness at the time of the outbreaks. It was not reported whether mink on Dutch farms were directly exposed to swine or fed on raw swine offal (307, 308). In 2010, avian/swine reassortant H1N2 IAV caused respiratory disease on a farm in the Mid- western USA that had 15 000 mink. Clinical signs included persistent severe respiratory distress, and hemorrhaging from the nasal and oral orifices, and mortality rates were approximately 3%. Pathological examination of fatal cases revealed a hemorrhagic broncho-interstitial pneumonia associated with H3N2 IAV and hemolytic *Escherichia coli*. Phylogenetic analysis revealed that the virus had a matrix gene and a nucleoprotein gene that showed genetic relatedness to the swine lineage of IAV. The source of the infection appeared to be feeding of raw turkey meat; no swine offal was fed, and there were no swine herds nearby (306).

Conclusions from the above reports are that American mink are highly susceptible not only to infection, but also to severe disease caused by human, avian, and swine IAVs, and that efficient mink-to-mink transmission is possible. Thus mink may serve as “mixing vessels” that facilitate the reassortment of IAVs from different host species (304). In addition, commonly recurring sources of infection include open housing, allowing contact with wild birds, and feeding of raw products from IAV-infected animals, such as swine and poultry. Consequently, the use of housing that prevents contact with wild birds, and the cooking of animal products prior to feeding (306) are important measures for prevention of influenza in American mink.

The domestic ferret (*Mustela putorius furo*) originates from the European polecat (*Mustela putorius*), and has been used since the 1930s in animal models for IAV infection in humans. In part this can be explained by the similarity in the pattern of IAV attachment to different parts of the ferret and human respiratory tracts (62). The ferret proved highly susceptible to infection with both human (385) and swine IAVs (386). Furthermore, human IAV infection in ferrets induced similar clinical signs to those observed in humans, namely fever, lethargy, anorexia, and nasal catarrh. In contrast, swine IAVs induced more severe disease, and death. In 1934, Shope provided detailed, accurate, and well-illustrated descriptions of the associated lesions in affected

ferrets, both grossly and microscopically (386). IAV transmission was demonstrated from ferrets to humans (387), and among ferrets, both by direct contact (388) and by air (389). Numerous studies on vaccine efficacy, antiviral products, pathogenesis and transmission, and virus reassortment, all relating to IAVs, have been performed in ferrets (390-400). In these studies, inoculation of many human and avian IAVs resulted in productive infection and disease.

Based on the above information, one would therefore expect natural IAV epidemics in ferrets to be common. However, even individual cases of natural IAV infection in ferrets, let alone epidemics, are rarely reported. Fisher and Scott reported natural IAV infection in ferrets in 1944 (309). Subsequently, Bell and Dudgeon reported an outbreak of IAV infection in two ferret colonies in Sussex, in the UK, in February 1947 (310). The affected ferrets exhibited nasal and ocular discharge, blepharosynechia, sneezing, lethargy, and fever for about 7 days, and eight ferrets died. Remarkably, none of these animals exhibited gross lung lesions at autopsy, although their nasopharynges were congested. The animal attendants had influenza-like symptoms immediately before and during the outbreak, and were assumed to be the source of infection. The widespread seroconversion against IAV in these group-housed ferrets suggested that there was efficient ferret-to-ferret transmission of IAV (310).

There were multiple cases of pH1N1 IAV in pet ferrets in the USA in 2009. The affected ferrets displayed mild to severe respiratory disease, and some died. Clinical signs included fever, lethargy, sneezing, and coughing. In all cases, humans in the household were suffering from influenza, and were the probable source of infection (312-315). Ferrets that were infected experimentally with pH1N1 IAV showed similar clinical signs, and at autopsy exhibited multifocal necrotising bronchointerstitial pneumonia (316, 399).

Natural infection of ferrets with swine IAVs was not reported until 2009, when there was an outbreak of contemporary reassortant swine H1N1 IAV in a ferret colony in the USA (311). Ferrets showed typical respiratory signs, and at autopsy exhibited bronchointerstitial pneumonia with necrotising bronchiolitis. The genetic characterisation of the isolated virus suggested that swine was the source of infection.

In October and November 2009, pH1N1 IAV infection occurred in an American badger (*Taxidea taxus*) and a black-footed ferret (*Mustela nigripes*) that were housed separately in a zoo in California, USA. Clinical signs included lethargy, inappetence, dyspnea, nasal discharge, and coughing. The American badger was euthanised due to the severity of disease, and at autopsy exhibited bronchopneumonia with IAV antigen expression. pH1N1 IAV was identified in lung samples from the American badger and swabs from the black-footed ferret by PCR and sequencing. Humans were assumed to be the source of infection (301).

Serological evidence of pH1N1 IAV infection was found in free-ranging northern sea otters (*Enhydra lutris kenyoni*), with an estimated age range of 2–19 years, captured off the coast of Washington, USA, in August 2011. ELISA revealed that 21 (70%) of 30 sea otters had detectable IgG (>200 mg/dL) for rHA of pH1N1 (A/Texas/05/2009); 22 (73%) of these 30 animals had HI antibody titers of ≥ 40 against pH1N1 virus (401). The source of infection remains unknown, although potential contact between pH1N1-IAV-infected northern elephant seals (*Mirounga angustirostris*) (325) and sea otters was considered to be one possibility, as their feeding ranges and breeding areas along the North-East Pacific coast overlap (401).

Influenza A viruses in the family Procyonidae

There is serological evidence of natural avian IAV infection in raccoons (*Procyon lotor*). Of 730 free-living raccoons sampled between 2004 and 2006 in several states of the USA (California, Texas, Louisiana, Maryland, Wyoming, and Colorado), 2.4% had antibody to avian IAVs of the subtypes H10N7, H4N6, H4N2, H3, and H1 (402). Presumably they were infected by direct or indirect contact with infected wild waterbirds. Intranasal inoculation of avian H4N8 IAV (A/chicken/Alabama/1975) into raccoons resulted in subclinical infection with nasal shedding up to 14 days post infection (dpi), and transmission to sentinel raccoons (402). In another experiment, exposure of raccoons to avian H4N6 IAV via drinking and washing water only led to a productive infection at a high dose, and exposure via infected eggs and waterfowl carcasses did not lead to infection (403). These results, together with the peridomestic nature of raccoons, suggest that this species is capable of infecting poultry and swine (402).

Influenza A viruses in the family Mephetidae

Between December 2009 and January 2010, eight striped skunks (*Mephitis mephitis*) died on a mink farm near Vancouver, Canada. Autopsy of two of these animals showed splenomegaly and pneumonia on gross examination. Histopathological findings included rhinitis, bronchopneumonia with intralesional bacteria, multifocal interstitial pneumonia, and plasmacytosis of lymph nodes and spleen. Both pH1N1 IAV and Aleutian disease virus were identified in organ samples by PCR and sequencing. The cause of death was determined as primary influenza viral pneumonia with secondary bacterial infection. The presumed source of both viruses was the population of co-habiting farmed American mink, some of which had nasal discharge. However, the possibility of direct IAV transmission from humans to striped skunks could not be excluded (300).

Influenza A viruses in the families Phocidae, Odobenidae, and Otariidae

Reports of natural IAV infection are more frequent in pinnipeds – a mammalian clade of the order of carnivores that includes the Odobenidae (walruses), the Phocidae (true seals), and the Otariidae (fur seals and sea lions).

There have been repeated avian IAV outbreaks in harbour seals (*Phoca vitulina*), with efficient seal-to-seal transmission and high mortality. The first recorded outbreak, involving H7N7 AIV, occurred on Cape Cod Peninsula, New England, USA, in the winter of 1979–1980 (13, 317, 318). Clinical signs included dyspnea, lethargy, emphysema of the neck, and frothy white to red discharge from the nose and mouth. More than 400 harbour seals, mostly juveniles, died, with an estimated mortality rate of 20% (13). This high number suggests efficient seal-to-seal transmission, yet apparently the virus was not able to persist in the harbour seal population. Autopsy showed pneumonia characterised by necrotising bronchitis and bronchiolitis, and hemorrhagic alveolitis (13). H7N7 AIV was isolated at high titers from the lung and at lower titers from the brain of diseased harbour seals. Experimentally infected harbour seals also developed pneumonia, but this was less severe than in natural cases (318). Antibodies against this virus were found in sera of gray seals (*Halichoerus grypus*) from Nova Scotia, Canada, more than 500 miles from Cape Cod, but no mortality of gray seals was reported (13). Although avian in origin, the virus replicated more efficiently in mammals (ferret, cat, and pig) than in birds (chicken and turkey), thus suggesting adaptation to mammals. This included accidental human infection during a seal autopsy, which resulted in conjunctivitis, but no human-to-human transmission (319). Experimental conjunctival inoculation in squirrel monkeys also induced conjunctivitis, along with respiratory disease and systemic viral spread (404). The source of the virus was not determined, but was suggested to be waterbirds such as terns (*Sterna* species), as they were known to harbour IAVs and to associate with harbour seals in water and on land. Possible factors contributing to the outbreak were abnormally high population densities and unseasonably high temperatures, which led harbour seals ashore (13).

In the winter of 1982–1983, there was an out- break of avian-origin H4N5 IAV infection in harbour seals from the New England coast, USA. Approximately 60 harbour seals died, and the mortality rate was estimated to be 2–4%. Histopathological examination revealed a necrotising bronchopneumonia, and H4N5 IAV was isolated from lungs, hilar lymph nodes, and brains of affected harbour seals. Interestingly, this virus did replicate in duck intestines upon intranasal inoculation, in contrast to earlier avian-origin IAV isolates from mammals (320).

In January 1991 and January 1992 there were outbreaks of avian-origin IAV infection of the subtypes H4N6 and H3N3, respectively, in harbour seals from Cape Cod, Massachusetts, USA. Autopsy showed subcutaneous emphysema and acute interstitial pneumonia, acute hemorrhagic pneumonia, or both (14).

From September to December 2011, there was an outbreak of avian-origin H3N8 IAV in harbour seals from New England, USA. A total of 162 harbour seals were found dead, and autopsy showed acute pneumonia. Based on genetic analysis, the virus isolated from the lungs was closely related to H3N8 IAV circulating in waterfowl (15). Interestingly, an avian-origin H3N8 IAV had been detected by PCR in a harp seal (*Phoca groenlandica*) caught in coastal waters of the North-West Atlantic Ocean several years previously (324). It was not reported whether this seal had respiratory disease. The harbour seal H3N8 IAV had a D701N amino acid substitution in the PB2 protein. This substitution was also found in H5N1 HPAIV infecting humans (405, 406), and indicates adaptation to virus replication in mammals. Based on agglutination assays, this virus had an affinity not only for avian-type sialic acid α2,3-galactose (SAα2,3)-linked receptors, but also to human-type sialic acid α-2,6 galactose (SAα-2,6)-linked receptors. These mammalian adaptations pose an increased risk of human infection (15).

More recently, between March and October 2014, an outbreak of avian-origin H10N7 IAV infection in harbour seals spread southward along the North-Western European coasts of Sweden, Denmark, Germany, and the Netherlands (321-323). Unusually high numbers of dead stranded seals (around 2000 in total) were found. Similar pulmonary lesions of acute bronchointerstitial pneumonia with emphysema to those reported earlier in the North American outbreaks were found. The virus was detected in the lungs (321-323) and spleen (323). The HA and NA genes of this seal virus were genetically closely related to those of H10N7 IAVs recently found in migratory ducks from Georgia, Egypt, and the Netherlands (322).

In April 2010, human-origin pH1N1 IAV infection was detected in northern elephant seals (*Mirounga angustirostris*) from California, USA. The virus was isolated from nasal swabs from 2 of 42 apparently healthy adult females, which had just come ashore after months at sea. Genetic sequencing of the seal isolate revealed more than 99% homology with pH1N1 IAV that had emerged in humans in 2009. Humans were the most likely source of infection, although human exposure at sea was limited to shipping vessels. Possible adaptation of this isolate to elephant seals was assumed, as replication was normal in MDCK cell cultures, but inefficient in human tracheobronchial epithelial cells compared with human pH1N1 IAV reference strains. Specific antibodies to pH1N1 IAV were detected in sera collected from elephant seals after April, whereas sera collected earlier were all negative (325). All of the above-mentioned pinniped species belong to the family Phocidae. In addition to virological evidence of IAV infection, there are many articles reporting the presence of antibody against IAV in sera of pinnipeds (**Table 3.1.4**). This serological evidence has been found not only in pinniped species belonging to the family Phocidae, but also in Pacific walruses (*Odobenus rosmarus divergens*), belonging to the family Odobenidae, and South American fur seals (*Arctocephalus australis*), belonging to the family Otariidae. These serological data indicate that the susceptibility

of pinnipeds to IAV infection of both human and avian origin involves more species than those in which IAV infection has actually been detected.

The ability of avian IAVs to transmit efficiently among harbour seals and cause high mortality is unusual. To investigate this, Ramis and colleagues determined the pattern of IAV attachment to the respiratory tract of the harbour seal (**Figure 3.1.3**). They found abundant attachment of avian IAVs to tracheal and bronchial epithelial cells, which is consistent with efficient seal-to-seal transmission. In the same study, they also found scarce attachment of avian IAVs to bronchiolar and alveolar epithelial cells of harbour seals (417). This was paralleled by rare expression of SAα-2,3 receptors in harbour seal lungs (15). These findings do not fit with the reports of high mortality of harbour seals (13, 317), although they are consistent with the low pathogenicity seen in experimental infections with AIV H7N7 in harbour seals (13). One possible explanation is that the natural avian IAV epidemics in seals were aggravated by co-infecting agents, such as *Mycoplasma* species (13).

Influenza A viruses in the order Carnivora, suborder Feliformia

Various species of the order Carnivora, suborder Feliformia have been infected with IAV (**Table 3.1.2**), and are described in detail in the following sections.

Influenza A viruses in the family Felidae

Unlike canine influenza in dogs, there is no evidence of sustained transmission of a cat-adapted IAV among domestic cats. Historically, cats were not even considered susceptible to disease from IAV infection (393, 418). However, like dogs, pet cats live in very close contact with humans. Indeed, following the human 1968 H3N2 IAV pandemic, naturally exposed cats had HI titers of > 40 against human H3N2 IAV, suggesting susceptibility to infection. Experimentally, cats were shown to develop a subclinical infection after inoculation not only with human H3N2 IAV, but also with avian H7N3, swine H1N1, and seal H7N7 IAVs, and with human influenza B virus (285, 393, 419).

The idea that IAV infection does not cause disease in cats was proved to be incorrect with the emergence of H5N1 HPAIV in cats (see above). In addition to the pathogenicity of this avian virus infection for cats, human-origin pH1N1 IAV was also reported to cause severe respiratory disease in cats, both in the USA (329, 330, 420-424) and in France (425). In most of these cases, the cat owners or their family members had been diagnosed with pH1N1 IAV and were considered to be the source of infection for the cats. Some cats died from the infection. At autopsy, they were found to have severe necrotising bronchointerstitial pneumonia associated with pH1N1 IAV (329, 330).

Experimentally inoculated cats showed similar lesions, and transmitted the virus to in-contact sentinel cats (426). Although most cases involved single animals, there was one outbreak in Italy in which 25 of 90 cats in a colony died. The lungs of two cats that

Table 3.1.4 Serological evidence of natural influenza A virus infection in marine mammals of the order Carnivora, clade Pinnipedia (Phocidae, Otariidae, and Odobenidae), and of the order Cetacea (Balaenopteridae and Delphinidae). Only reports where antibody to influenza A virus in serum was detected are listed.

Family	Species	Virus		Morbidity	Mortality	Number positive/total number (%)	Serological assay[a]	Sustained intraspecies transmission	Region[b]	Period	References
		Origin (likely)	Subtype								
Phocidae	Baikal seal	Avian	H3N2	–[c]	–	2/7 (29)	ELISA & HI	no	AS	1998	(407)
	Caspian seal	Human	H3N2	–	–	28/ 77 (36)	ELISA & HI	suspect	AS	1993, 97-98, 2000	(408)
	Gray seal	Avian	H7N7	–	–	–	–	–	NA	–	(13)
	Harp seal	–	unspecified IAV	no	no	33/183 (18)	NP-ELISA	no	AS, Barents Sea	1991-92	(409)
	Hooded seal	–	unspecified IAV	no	no	8/100 (8)	NP-ELISA	no	AS, Barents Sea	1991-92	(409)
	Kuril harbour seal	Avian	H3, H6	–	–	15/211 (7)	ELISA & HI	no	AS	1998, 2003-05	(410)
	Northern elephant seal	Human	pH1N1	no	no	adults: 20/44 (40) pups: 14/71 (19)	HI	yes, restricted	NA	2010	(325)
	Ringed seal	Avian	H3, H7	no	no	1/ 32 (3)	DID & HI	no	NA	1984	(411)
		–	unspecified IAV	–	–	23/ 903 (2.5)	NP-ELISA	–	NA	1984-97	(412)
		Avian	H3N2, H7N7	–	–	H3N2: 5/ 6 (83) H7N7: 1 6 (17)	ELISA & HI	no	AS	2002	(407)

Table 3.1.4 Serological evidence of natural influenza A virus infection in marine mammals of the order Carnivora, clade Pinnipedia (Phocidae, Otariidae, and Odobenidae), and of the order Cetacea (Balaenopteridae and Delphinidae). Only reports where antibody to influenza A virus in serum was detected are listed. (continued)

Family	Species	Virus		Morbidity	Mortality	Number positive/ total number (%)	Serological assay[a]	Sustained intraspecies transmission	Region[b]	Period	References
		Origin (likely)	Subtype								
	Seal (unspecified species)	Avian	H1, H3, H4, H7, H12	–	–	10/338 (3)	HI	no	Bering Sea	1978-88	(413)
		Avian	H4	–	–	1/757 (0.1)	HI	no	EU	1988	(413)
Otariidae	South American fur seal	–	H1N1	–	–	1/37 (3)	HI	no	SA	2004	(414)
Odobenidae	Pacific walrus	Avian	H10, N2, N3, N5, N6, N7	–	–	8/38 (21)	AGID	no	NA	1994-96	(415)
Balaenopte-ridae	Common Minke whale	–	unspecified IAV	–	–	7/140 (5)	ELISA	no	AS, Western North Pacific	2000-01	(416)
Delphinidae	Beluga whale	–	unspecified IAV	–	–	5/418 (1.2)	NP-ELISA	–	NA	1991-92	(412)
	Dall's porpoise	–	unspecified IAV	–	–	2/34 (5)	ELISA	no	AS, Western North Pacific	2000-01	(416)

[a]NP-ELISA, nucleoprotein enzyme-linked immunosorbent assay; HI, hemagglutination inhibition; DID, double agar immunodiffusion; AGID, agar gel immunodiffusion.

[b]AS, Asia; EU, Europe; NA, North America; SA, South America.

[c]–, not determined or not recorded.

died of severe respiratory disease showed necrotising bronchointerstitial pneumonia associated with pH1N1 IAV. Of the surviving cats, 21 animals had serum antibodies to pH1N1 IAV, and two had PCR-positive nasal swabs. Taken together, these findings were strongly indicative of cat-to-cat transmission of pH1N1 IAV (331).

Serological screening of cats for antibodies to pH1N1 IAV yielded variable results. Of sera collected from pet cats during the 2009–2010 influenza season, 22.5% from Ohio, USA (*n* = 400) (427) and 21.8% from the southern and Midwestern states of the USA (*n* = 78) (428) had hemagglutination-inhibiting (HI) antibodies to pH1N1 IAV, suggesting that cats are highly susceptible to pH1N1 IAV infection. In contrast, only 1.2% of sera collected from cats (*n* = 1080) during the same period in southern China had antibodies to pH1N1 IAV by NP-specific ELISA (429), and only 1.93% of sera collected from cats (*n* = 1150) in Germany in 2010–2011 had anti- bodies to pH1N1 IAV by virus neutralisation assay (430). Feral cats appeared to be less likely to become infected with pH1N1 IAV than pet cats.

Only 0.43% of sera collected from feral cats (*n* = 200) in Florida between November 2008 and July 2010 had antibodies to pH1N1 IAV by ELISA (431), and in a survey of cats (*n* = 1140) in north-east China, only 11% of sera from feral cats had antibodies to pH1N1 IAV, compared with 30.6% of sera from pet cats (432).

Similar short-lived influenza epidemics in cats, but now from H3N2 CIV, occurred in South Korea in 2010 in two large animal shelters. These shelters housed dogs as well as cats, and both epidemics coincided with or were preceded by H3N2 CIV infections in dogs. It is likely that there was virus transmission from dogs to cats, followed by rapid cat-to-cat transmission. In one shelter, which had 60 cats, there was 47% morbidity and 22% mortality; in the other shelter, which had 50 cats, there was 100% morbidity and 44% mortality. Clinical signs in cats included high fever, lethargy, dyspnea, and coughing. At autopsy, the lungs showed severe bronchopneumonia, and the isolated virus was nearly identical to H3N2 CIV based on sequencing of all eight gene segments (332, 333). Experimental H3N2 CIV infection of cats resulted in similar clinical signs and severe necrosuppurative bronchointerstitial pneumonia, co-localised with abundant influenza virus antigen in bronchial epithelial cells (332). Both for pH1N1 IAV and for H3N2 CIV, housing many cats together appeared to be a risk factor for efficient cat-to-cat transmission of virus.

There is concern that cats, like dogs, might act as an intermediate host for AIV and either facilitate its adaptation to mammals or transmit the virus to humans (337, 428). Given the recent reports of IAV transmission from birds, dogs, and humans to cats, and the potential for efficient cat-to-cat trans- mission of such viruses, cats need to be included in influenza monitoring programs to protect public health (418).

Infection with pH1N1 IAV occurred in four captive cheetahs (*Acinonyx jubatus*) in an animal park in California, USA, in November 2009. Clinical signs included ptyalism,

anorexia, and lethargy. An IAV isolated from swabs taken from one animal had 100% homology by sequence analysis with human isolates of pH1N1 IAV. The animals' keeper had an influenza-like illness and was considered likely to be the source of infection (334).

Serological evidence of infection with an unspecified IAV was detected in one of 16 wild Pallas's cats (*Felis [Otocolobus] manul*) on the Daurian Steppe of Russia in 2010–2011. The exact source of IAV exposure for these cats was not known, although they may have had contact with horses, dogs, cats, and house mice in remote human settlements. Furthermore, the Pallas's cats occupied fox burrows and preyed upon Daurian pikas (*Ochotona daurica*) and voles (*Microtus* species) (433). Interestingly, both red foxes (*Vulpes vulpes*) (281) and black-lipped pikas (*Ochotona curzoniae*) (266) were found to be susceptible to H5N1 IAV infections.

Influenza A viruses in the family Viverridae

In autumn 2009, severe respiratory disease occurred in a Bornean binturong (*Arctictis binturong penicillatus*) in a zoo in California, USA. Clinical signs included lethargy, inappetence, dyspnea, nasal discharge, and coughing. The animal was euthanised because it had severe disease, and autopsy showed interstitial pneumonia. By PCR and sequencing, pH1N1 IAV was identified in lung samples from an American badger (*Taxidea taxus*) and in swabs from a black-footed ferret (*Mustela nigripes*) that were housed separately at the same zoo and were suffering from respiratory disease during the same time period. It was assumed that humans were the source of infection (301).

Influenza A viruses in non-swine species in the order Artiodactyla

Despite the fact that the order Artiodactyla (even-toed ungulates) contains about 220 species, many of which are important domestic or hunted animals, IAV infection has been reported only sporadically in a few species other than domestic and wild pigs (*Sus scrofa*) belonging to the family Suidae. Evidence of infection with or exposure to IAVs has been reported in cattle (*Bos taurus*), sheep (*Ovis aries*), goats (*Capra aegagrus hircus*), yak (*Bos grunniens*), and water buffalo (*Bubalus bubalis*), which belong to the family Bovidae, in alpaca (*Lama pacos*), which belongs to the family Giraffidae, and in reindeer (*Rangifer tarandus*), fallow deer (*Dama dama*), and European roe deer (*Capreolus capreolus*), which belong to the family Cervidae (**Table 3.1.3**) (339, 340, 367, 434-438). The only epidemics of severe respiratory disease caused by IAV infection in non-swine artiodactyls were reported in Bactrian camels (*Camelus bactrianus*), which belong to the family Camelidae (342). Influenza in domestic and wild pigs is not treated extensively in this chapter.

Possibly the first IAV to be isolated from ruminants was from a sheep in Hungary in 1960 (339, 340), followed by several H3N2 IAV isolations from cattle in Russia from the early

1970s to the 1980s (340). These viruses were isolated during outbreaks of respiratory disease in sheep and cattle that coincided with pandemics and circulation of H2N2 IAV Asia/1957 and H3N2 Hong Kong/1968 in humans.

Romvary and colleagues reported the isolation of Asian H2N2 IAV (A/Borzsony/111/1960) from an adult sheep and her mature fetus suffering from respiratory disease in Hungary in 1960 (339). This coincided with the H2N2 IAV Asia/1957 pandemic in humans. Respiratory disease was observed in several flocks of sheep. To confirm the susceptibility of sheep to human IAVs, lambs were intratracheally inoculated with egg-adapted strains of H2N2 and PR8 H1N1 IAVs. This resulted in fever, anorexia, coughing, dyspnea, and lassitude. Autopsy at 7 dpi revealed viral pneumonia both macroscopically and histologically, as well as marked immune responses to the inoculated strains (339). However, it was not reported whether IAV was re-isolated from inoculated sheep. Reisolation was attempted by McQueen and Davenport in 1963, when they infected several 3- to 10-week-old lambs intratracheally with the Hungarian sheep isolate H2N2 IAV (A/Borzsony/111/1960) and PR/8/1934 H1N1 IAV. The lambs showed febrile responses but no respiratory signs, and no virus could be re-isolated from nasal swabs taken at 2 and 3 dpi, or from lungs and tracheas at autopsy 3 dpi. Homologous antibody titers were detected in the sera from all inoculated lambs (439). During a major H2N2 influenza epidemic in humans in Ireland in January 1961 (440), cattle sera taken between early 1960 and summer 1961 were screened for antibodies against H2N2 IAV. No compelling evidence of spread to cattle was found, as all of the sera were negative (441).

Naturally occurring antibodies against H3N2 IAV were detected in 16 of 28 cattle, 5 of 12 goats, two water buffalo, and one yak–zebu cross in Nepal and India, which were sampled between 1972 and 1973 (436). This coincided with the circulation of H3N2 IAV (A/England/42/1972, closely related to A/Hong Kong/1/1968) among humans in India and Nepal (442). The animals were not reported to exhibit any signs of disease. Experimental inoculation of H3N2 IAV into yak induced mild signs of respiratory disease, including coughing and malaise, for 6 dpi (436). A more severe influenza-like illness was observed in 3- to 4-week-old calves that were experimentally inoculated with cattle strain H3N2 IAV (A/calf/Duschanbe/55/1971) isolated from a calf in Russia. For 4 dpi the calves had nasal discharge and coughed. The virus was shed from the nose for 7 dpi. Similar infections of calves with human H3N2 IAV isolates did not induce signs of respiratory disease (341). IAV infections in cattle were reported to be associated with cases of acute reduction in milk production, known as “milk drop syndrome” (443-446). A case–control study of a dairy herd in Devon, UK, showed that rising antibody titers against human H1N1 IAV (A/England/333/1980) and H3N2 IAV (A/England/427/1988) were associated with sudden milk drop, signs of respiratory disease, and higher rectal temperatures compared with controls (444).

In contrast to sporadic reports of IAV in other ruminants, many outbreaks of severe respiratory disease associated with human H1N1 IAV infection were recorded in Bactrian camels on farms throughout Mongolia between 1978 and 1988. During a severe epidemic in the winter of 1979–1980, 4000 camels showed signs that included fever, coughing, bronchitis, and nasal and ocular discharge. Clinical signs typically lasted for 5–7 days. Some camels aborted, and the mortality rate was 9.1%. Isolates of H1N1 IAV from nasopharyngeal swabs from affected animals induced respiratory disease in experimentally inoculated serologically naive camels. Genetic sequence anal- ysis of the isolates revealed that the PB1, HA, and NA genes were almost identical to a human H1N1 IAV isolate from 1977 that was closely related to a UV-light-inactivated reassortant (USSR/77 × PR/8/34) H1N1 vaccine strain used in Mongolian people in Leningrad, whereas the remaining genes originated from the H1N1 PR/8 laboratory strain. It was speculated that humans were the source of infection in camels, because the epidemic in camels coincided with a mild influenza H1N1 epidemic among vaccinated Mongolian children (342). During that same time period and in the same region as the outbreaks in Mongolian camels in 1985, an H1N1 IAV was isolated from a child with respiratory disease. This isolate was genetically almost identical to the camel H1N1 IAV (447) suggesting that this H1N1 IAV reassortant was capable of crossing the species barrier.

Following the surge of the 2009 H1N1 pandemic, concerns were raised that pilgrims gathering at the Hajj might infect dromedary camels (*Camelus dromedarius*, belonging to the family Camelidae) in Saudi Arabia, and that returning pilgrims might infect dromedary camels in their countries of origin (448). However, there were no subsequent reports that substantiated these concerns. Although parainfluenza-3 virus has been associated with respiratory disease in dromedary camels (449), antibodies against IAVs have not been reported to date in sera of dromedary camels.

Very recently, an H3N8 IAV was isolated from one of 460 nasal swabs collected from healthy Bactrian camels from Mongolia between January 2012 and January 2013. Phylogenetic analysis of the isolate indicated that it was a relatively recent horse-to-camel transmission of an IAV closely related to equine H3N8. In Mongolia, recurring equine H3N8 IAV epidemics arise in areas occupied by many free-ranging horses and Bactrian camels. Camel-to-camel transmission has not been reported to date (343).

Serological screening has been performed on other members of the family Camelidae. Antibodies against IAV were detected in more than 100 Peruvian alpacas (*Lama pacos*), with a prevalence of 4% (438). More recent serological screenings for antibodies against IAV, including human H1N1 and equine H3N8, in wild vicuñas (*Vicugna vicugna*) and llamas (*Lama glama*) from Argentina were negative (450, 451).

Influenza A viruses in the order Cetacea

Reports of natural exposure to IAVs are rare in cetaceans, the mammalian order that includes whales, dolphins, and porpoises (**Table 3.1.3**). Avian-origin H1N3 IAV was isolated from several lungs and one liver collected from live-caught minke whales (*Balaenoptera acutorostrata*) on a whaler in the South Pacific during 1975–1976. The virus was identified by electron microscopy and was cultured in eggs. The NA protein was antigenically most close to AIV. No associated signs of disease were reported (344, 345).

H13N2 and H13N9 AIVs were isolated from a long-finned pilot whale (*Globicephala melaena*, currently *G. melas*) in association with two mass stranding events along the coast of Cape Cod peninsula, USA, in 1984 (346). One of the diseased and disorientated pilot whales was caught alive, euthanised, and examined. It was extremely emaciated and had sloughed skin. Gross autopsy revealed enlargement of the hilar lymph node, hemorrhagic lungs, and a small friable liver. Although AIVs of H13N2 and H13N9 subtypes were isolated from the hilar lymph node and lungs, there was no evidence that AIV infection had caused these lesions. Genetic and antigenic properties of the pilot whale AIV isolates suggested that they originated from gulls (346). Indeed, 28 years after the original isolation, the gull origin of the pilot whale H13N2 AIV isolate was confirmed by genomic analysis (347). In contrast to other duck-enterotropic H13 gull isolates, these viruses were apparently sensitive to low pH, as they did not replicate or induce disease in orally inoculated ducks. They did replicate in the lower intestine of ducks when rectally inoculated, thereby avoiding the acidic milieu of the proventriculus. The two isolates also replicated in the nose of intranasally inoculated ferrets. Fecal–oral transmission from shedding gulls to feeding whales was proposed as a possible route of transmission (346). Such transmission may be facilitated by gulls and whales feeding concurrently on the same fish species during so-called "multi-species feeding frenzies." Accidental ingestion as a route of transmission is also a possibility, since it is not unusual for whole birds to be caught in the mouth of a baleen whale during such feeding frenzies, and case reports of birds being ingested by baleen whales have been published (452, 453).

Serological evidence of IAV infection in cetaceans has been reported for minke whales, Dall's porpoises (*Phocoenoides dalli*), and belugas (*Delphinapterus leucas*) (**Table 3.1.4**). Interestingly, the five positive beluga sera originated from a relatively small sample of 34 belugas from one population from the same area (Baffin Island, Nunavut, Canada), sampled between 1991 and 1992. No antibodies against IAV were detected in 76 narwhals (*Monodon monoceros*) or four bowhead whales (*Balaena mysticetus*) from the same survey (412).

Influenza A viruses in non-human primates

Only three published articles present virological evidence of natural IAV infection in non-human primates (NHPs) (**Table 3.1.5**). First, in 1971 Johnsen and colleagues (454) reported an H3N2 IAV (A/Hong Kong/1968) epidemic in a colony of white-handed gibbons (*Hylobates lar*) from Thailand. The virus was initially introduced into the colony by experimental inoculation of a few selected animals, but after 2–3 weeks it developed into an epidemic in the colony. The gibbons suffered from mild to fatal respiratory disease. Clinical signs consisted of fever, serous to purulent rhinitis, coughing, anorexia, depression, and gastrointestinal disturbances. Autopsy of the four fatal cases revealed dark red, oedematous lungs, which corresponded to necrohemorrhagic pneumonia demonstrated by histological examination (454). Second, in 1975, Malherbe and colleagues isolated an unspecified influenza-like virus from the throats of 3 of 20 healthy yellow baboons (*Papio cynocephalus*) that had been imported into the USA from Kenya (455). Third, one of 48 oral swabs from pet and free-ranging urban macaques (*Macaca fascicularis* and *M*. *nemestrina*) from Cambodia was found to be PCR-positive for IAV (456).

Serological evidence of IAV infection in NHPs has been reported in several articles (**Table 3.1.6**). These data suggest that NHPs are commonly exposed to and infected with IAV, but are relatively resistant to development of disease. Possible sources of IAV for both captive and free-living NHPs are humans, with whom NHPs often have close contact. However, other sources of IAV (e.g., birds) cannot be excluded.

Experimental inoculation of IAV has shown that multiple NHP species are susceptible to both IAV infection and associated disease. In the 1920s and 1930s, chimpanzees (*Pan troglodytes*) developed signs of influenza-like illness after inoculation with nasal washings from human patients with influenza (459, 460). In 1969, Kalter and colleagues inoculated H3N2 IAV into baboons (*Papio* species), which transmitted the virus to sentinel baboons but did not develop overt respiratory disease (461). Several other NHP species have been found to be susceptible to experimental IAV infection and to develop respiratory disease. The most commonly studied species are squirrel monkeys (*Saimiri sciureus*) (462-468) and cynomolgus, rhesus, pigtailed, and bonnet macaques (*Macaca* species) (288, 395, 469-478).

Influenza A viruses in the order Chiroptera

Traditionally, the original reservoir of all IAVs was considered to be wild waterbirds (479). This dogma was recently overturned by the discovery of IAVs with new HA (H17 and H18) and NA (N10 and N11) subtypes in frugivorous bats from Central and South America (6, 7) (**Table 3.1.5**). This was very surprising, because previously there had only been a single published report of IAV infection in bats (which belong to the order Chiroptera),

Table 3.1.5 Virological evidence of natural influenza A virus infection in mammals of the order Primates (Cercopithecidae and Hylobatidae) and Chiroptera (Vespertilionidae and Phyllostomidae). Only reports where the virus was detected by virus isolation or RT-PCR are listed.

Family	Species	Virus		Morbidity	Mortality	Tissue tropism[a]		Sustained intraspecies transmission	Region[b]	Period	References
		Origin	Subtype			Respiratory	Extra-respiratory				
Cercopithecidae	Yellow baboon	–[c]	influenza-like 'myxo'-virus	no	no	yes	–	–	NA (African import)	1974	(455)
	Macaque	–	Unspecified IAV	no	no	yes	–	no	AS	2011	(456)
Hylobatidae	White-handed gibbon	Human	H3N2	yes	yes	yes	no	yes	AS	1970?	(454)
Vespertilionidae	Common noctule bat	Human	H3N2	–	–	yes	–	no	AS	1977	(457, 458)
Phyllostomidae	Little yellow-shouldered bat	–	H10N17	no	no	yes	yes	– (suspect)	CA	2009-10	(6)
	Flat-faced fruit-eating bat	–	H11N18	no	no	yes	yes	– (suspect)	SA	2010	(7)

[a]Also based on results of experimental infections.

[b]AS, Asia; EU, Europe; NA, North America; SA, South America; CA, Central America.

[c]–, not determined or not recorded.

Table 3.1.6 Serological evidence of natural influenza A virus infection in mammals of the order Primates (Homidae, Hylobatidae, and Cercopithecidae). Only reports where antibody to influenza A virus in serum was detected are listed.

Family	Species	Virus		Morbidity	Mortality	Number positive/total number (%)	Serological assay[a]	Sustained intraspecies transmission	Region[b]	Period	References
		Origin (likely)	Subtype								
Homidae	Chimpanzee	Human	H1N1, H2N2	no	no	H1N1(PR8): 8/56 (14) H2N2: 23/56 (41)	HI	no	NA (captive)	1960s	(480)
		Human	pH1N1, H3N2	no	no	pH1N1: 218/305 (71.5 H3N2: 34/305 (11.2)	HI	no	EU (captive)	1986-2000	(481)
Homidae	Orangutan	Human	H1N1, H2N2	no	no	H1N1 (PR8): 4/22 (18) H2N2: 10/22 (45)	HI	no	NA (captive)	1960s	(480)
		Human	pH1N1, H3N2	no	no	pH1N1: 34/179 (19.0) H3N2: 10/179 (5.6)	HI	no	EU, AS (captive)	1994-98	(481)
Homidae	Gorilla	Human	pH1N1, H3N2	no	no	pH1N1 & H3N2: 3/77 (3.9)	HI	no	EU (captive zoo)	–[c]	(481)
Hylobatidae	Gibbon	Human	H1N1, H2N2	no	no	H1N1(PR8): 2/9 (22) H2N2: 3/9 (33)	HI	no	NA (captive)	1960s	(480)
Cercopithe-cidae	Baboon	Human	H1N1, H2N2	no	no	H1N1(PR8): 13/122 (11) H2N2: 1/122 (0.8)	HI	no	NA (captive) and AF (wild)	1963-64	(480)
		Human	unspecified IAV	no	no	12/14 (86)	CF	–	NA (captive)	1966	(482)
	Rhesus macaque	Human	H1N1, H2N2	no	no	H1N1 (PR8): 5/48 (10) H2N2: 1/48 (2)	HI	no	NA (captive)	1960s	(480)

Table 3.1.6 Serological evidence of natural influenza A virus infection in mammals of the order Primates (Homidae, Hylobatidae, and Cercopithecidae). Only reports where antibody to influenza A virus in serum was detected are listed. (continued)

Family	Species	Virus		Morbidity	Mortality	Number positive/total number (%)	Serological assay[a]	Sustained intraspecies transmission	Region[b]	Period	References
		Origin (likely)	Subtype								
		Human	unspecified IAV	no	no	159/171 (93)	CF	–	NA (captive)	1966	(482)
	African green monkey	Human	unspecified IAV	no	no	94/141 (67)	CF	–	NA (captive)	1966	(482)
	Tonkean macaque	Human	unspecified IAV	no	no	wild: 5/15 (33) captive: 2/ 11 (18)	RDIA	no	AS (pet & wild free-ranging)	1999	(483)
	macaque	Human / Avian	H1N1, H3N2, H9N2	no	no	33/163 (20)	NP-ELISA & HI	no	AS (pet & urban free-ranging)	2011	(456)

[a]NP-ELISA, nucleoprotein enzyme-linked immunosorbent assay; HI, hemagglutination inhibition; CF, complement fixation; RDIA, rapid dot-immunobinding assay.

[b]AS, Asia; EU, Europe; NA, North America.

[c]–, not determined or not recorded.

when an H3N2 IAV was cultured and isolated from the lungs of insectivorous common noctule bats (*Nyctalus noctula*) from Kazakhstan (457).

The first IAV of previously unknown subtype, H17N10, was detected in little yellow-shouldered bats (*Sturnira lilium*) from Guatemala by next- generation sequencing of rectal swabs and internal organs, including lungs, liver, intestines, and kidneys. The second IAV of previously unknown subtype, H18N11, was detected in a flat-faced fruit bat (*Artibeus planirostris*) from Peru by next-generation sequencing of rectal swabs and intestines (liver and spleen were negative). The consistent detection of virus in intestinal and rectal swabs suggested that these new bat-origin IAVs replicated in the intestine. The viruses could not be propagated in cell cultures or eggs. No clinical signs were reported in these bats, which were caught alive (6, 7).

Serological analysis of several Peruvian bat species, including *Artibeus* species, yielded a high percentage (50%, 55 of 110) of sera that contained specific antibodies against recombinant H18 and N11 proteins by ELISA. Likewise, specific antibodies against recombinant H17 protein were detected by ELISA in 38% (n=86) of 228 sera from eight bat species from Guatemala collected during 2009–2010 (7). Tong and colleagues interpreted these high seroprevalences of identical bat IAV infections in multiple species from distant geographic locations spanning several years as being indicative of widespread endemic infections with sustained bat-to-bat transmission in New World bats (7). However, no virological evidence was found for such new IAVs from a large survey of 26 species of bats from Central Europe, in the Old World (484). These bat IAVs contain newly discovered gene segments that encode the major surface envelope proteins HA (H17 and H18) and NA (N10 and N11). They differ in form and function from all previously known HAs (H1–H16) and NAs (N1–N9). The bat H17 showed on average 45% amino-acid-sequence similarity to HAs from known IAV subtypes. Sequence motifs of the sialic acid (SA) receptor-binding site were identified in bat H17 IAV, although position changes in specificity for galactose–SA linkage indicated a ligand preference other than SA receptors (6). Zhu and colleagues indeed showed that the presumed receptor-binding site of HA H17 was highly acidic, making it unfavourable for binding of the negatively charged SA receptors (9). Unlike the HA gene and internal genes, the bat N10 was extraordinarily divergent from known NAs. It showed only 24% amino-acid-sequence similarity to other IAV NA subtypes. Interestingly, this sequence similarity was even lower than the similarities between NAs from IAV and influenza B virus (6). Otherwise, the crystal structure of N10 resembled other IAV NA structures (e.g., the highly conserved N-glycosylation site N146 shared in all IAV NAs). However, enzymatic MUNANA assays showed a lack of typical neuraminidase activity (485).

Bat H18 showed 49.1% amino-acid-sequence similarity with other HA subtypes, and only 60.2% sequence similarity with H17. The bat N11 NA (more accurately referred to as “NA-like protein” or NAL) had only 29.6% identity with all other NAs (7). Furthermore,

the HAs H17 and H18 showed no specific binding to sialosides evaluated by sialoside microarray and glycan ELISA (7, 9), and it was also found that N10 and N11 NA-like proteins did not bind or cleave SAs (7, 485). In contrast to non-bat IAVs, these results indicate that bat H18N11 and H17N10 IAVs do not mediate host cell attachment and release via SA receptors. The receptors or mechanisms that these bat IAVs use for host cell attachment, fusion, entry, and release have yet to be identified (6, 7, 486).

The amino acid sequences of the remaining internal genes of H17N10 and H18N11 IAVs showed most of the known functional sequence motifs of other IAVs. The polymerase complex proteins (PB2, PB1, PA, and NP) of both showed functional viral transcription by means of reporter minigenomes in human and primate cells. This transcription was abrogated when PB1 was removed from the minigenome (6, 7). Furthermore, it was determined that the N-terminal domain of PA (PAn) from H17N10 has manganese or magnesium ion-dependent endonuclease activity producing small RNA primers essential for initiation of viral gene transcription like any other IAVs (487).

Phylogenetic analysis of the primary genetic sequences of the HA molecules of bat H17 and H18 indicated that they belong to group 1 HAs (together with H1, H2, H5, H6, H8, H9, H11, H12, H13, and H16), and not to group 2 HAs (H3, H4, H7, H10, H14, and H15). The more divergent NA-like molecules N10 and N11 did not belong to either of the existing NA groups 1 and 2, but were categorised as a separate influenza A-like group 3 (**Figure 3.1.4**) (8). Although their internal genes were almost the same as known IAVs, Wu and colleagues proposed that on the basis of the different NA and HA genes these viruses should be renamed as “influenza-like viruses” (8). The origins of the NALs are not known, but they might be derived from an unknown influenza type other than influenza A, B, or C, either extinct or yet to be identified (485). The positions of the six internal genes of bat H17N10 in the phylogenetic tree were between the IAV and influenza B virus split. However, they were more closely related to IAV-type genes (6). Tong and colleagues concluded from their findings that these newly discovered IAVs needed to have evolved in bats for a long period of time (7). Briefly, these findings included higher viral genetic diversity than was previously known to exist, divergence into multiple HA and NA subtypes with a presumed SA-independent alternative mechanism or receptor for host cell entry and release, and a widespread geographic distribution of these two monophyletic bat IAVs.

The two major surface proteins, HA and NA, of bat H17N10 and H18N11 IAVs lacked typical cell attachment and cleavage functions. However, their more conserved internal genes responsible for viral transcription were shown to be functional *in vitro*. These genes are considered to be potentially inter- changeable with known IAVs that contain classical functional HAs and NAs. This raised serious scientific and public health questions about whether such genomic reassortments could occur, thereby possible generating an infectious influenza virus capable of causing disease in species other than the bat species

in which they were detected (6-8). Furthermore, bats are known to harbour many viruses with considerable zoonotic disease potential (488, 489), and are sometimes regarded as a "treasure trove" hosting many unknown viruses (488). Indeed discoveries of new viruses in bats are ongoing (490, 491). In general, bats possess specific characteristics that could favor the evolution and spread of novel viruses, including IAV. Belonging to the taxonomic order Chiroptera that contains approximately 1150 species worldwide, bats are long-lived globally abundant mammals, which migrate and inhabit urban, rural, and natural environments, with possible contacts with humans, livestock, and other wildlife. Furthermore, they exhibit clustered roosting in extremely high densities in multi-species colonies, practically guaranteeing bat-to-bat transmission of viruses (488). Bats have to be considered as a novel potentially important mammalian reservoir of influenza viruses.

Influenza A viruses in the orders Rodentia and Lagomorpha

Although there are about 2300 species in the order Rodentia and around 80 species in the order Lagomorpha (492), natural IAV infection has very rarely been reported in species belonging to these two orders (268, 275, 367, 493). Specific antibodies against IAV indicating infection with human IAV were detected unequivocally by HI and complement fixation tests in one domestic rabbit (*Oryctolagus cuniculus*) and one chipmunk (*Tamias striatus*). This was part of a serological screening study for antibodies against H3N2 IAV (A/Hong Kong/1/1968) in 6 wild chipmunks, 25 groundhogs (*Marmota monax*), 13 cottontail rabbits (*Sylvilagus* species), 42 snowshoe hares (*Lepus americanus*), and 106 pet rabbits from the Ottawa area, Canada, sampled between 1966 and 1970 (367).

Six of six wild house mice (*Mus musculus*) caught on a gamebird farm in Idaho, USA, during an H5N8 LPAIV outbreak in 2008 were found to be positive for antibodies against IAV by indirect NP-ELISA (493). Six brown rats (*Rattus norvegicus*), one harvest mouse (*Reithrodontomys megalotis*), and one deer mouse (*Peromyscus maniculatus*) that were caught and tested in the same study were all seronegative. Subsequent experimental intranasal inoculation of newly caught serologically naive house mice with AIV isolates from wild birds (H3N6, H3N8, and H4N6) or chickens (H6N2 and H4N8) resulted in virus replication in the nasal turbinate, trachea, and lungs. The virus isolates from the wild birds replicated to higher titers in the mouse tissues than did the chicken isolates. The results indicated that house mice might be a risk factor for transmission of IAV to poultry and gamebird farms (493).

Influenza A viruses in other species

An outbreak of human seasonal H1N1 IAV infection occurred in giant anteaters (*Myrmecophaga tridactyla*, belonging to the family Myrmecophagidae, in the order Pilosa) in Nashville Zoo, USA, in February 2007. All 11 animals in the group exhibited clinical signs of severe nasal discharge and congestion, inappetence, and lethargy. The

isolated virus was identified as IAV and showed more than 99% nucleotide identity with a human seasonal IAV isolate Tennessee/UR06-0119/2007 (H1N1). The anteaters had no contacts except with their keepers, who were suffering from respiratory disease, and presumably were the source of infection (494).

The reports, albeit rare, of IAV infection in reptiles and amphibians emphasise the broad host range of this virus. In 2006, IAV was detected by PCR for IAV-matrix gene in blood samples from 4 of 37 captive crocodilians in Florida, USA, namely a Chinese alligator (*Alligator sinensis*), a Schneider's dwarf caiman (*Paleosuchus trigonatus*), a Nile crocodile (*Crocodylus niloticus*), and a broad-snouted caiman (*Caiman latirostris*). Antibodies to IAV were detected by agar gel immunodiffusion testing in sera of all these animals except for the broad-snouted caiman. These crocodilians were kept in open pens with exposure to wild birds, some of which were eaten, and it is likely that these were the source of infection. This is supported by sequence analysis of the non-structural protein 1 (NS1) gene of the PCR products, which revealed more than 99.7% homology with the NS1 gene from duck isolates (495). One other study, by Mancini and colleagues (496), suggested that there was susceptibility to IAV (and influenza B virus) infection in poikilothermic animals. Antibodies against human H1N1 and H3N2 IAVs and equine H7N7 and H3N8 IAVs were detected by HI assay in sera collected from captive and free-ranging snakes and amphibians from Brazil, namely pit vipers (*Bothrops jararaca* and *B. jararacussu*), Cascavel rattlesnakes (*Crotalus durissus terrificus*), Rococo toads (*Bufo paracnemis*), and American bullfrogs (*Lithobates catesbeianus*, formerly *Rana catesbeiana*) (496).

3.2

Animal models. Influenza virus, methods and protocols

E.J.B. Veldhuis Kroeze[1,2], T. Kuiken[1] & A.D.M.E. Osterhaus[1,2]

Based on:
Influenza Virus, methods and protocols, Chapter 8, edited by Y. Kawaoka[3] & G. Neumann[4].
Methods in Molecular Biology 2012; 865: 127-146

Affiliations
[1]Department of Viroscience, Erasmus Medical Center, Rotterdam, The Netherlands
[2]Viroclinics Biosciences B.V., Rotterdam, The Netherlands
[3]School of Veterinary Medicine, Department of Pathobiological Science, University of Wisconsin-Madison, USA
[4]Influenza Research Institute (IRI), Department of Pathobiological Science, University of Wisconsin-Madison, USA

ABSTRACT

Five well-established animal models in influenza research are discussed in a schematic fashion. Although there are clear parallels between these models, like viruses used, housing and handling conditions under biosafety conditions, routes of virus inoculation, sampling strategies, and autopsy techniques, each of these models involves specific differences in practical applicability that need thorough assessment depending on the scientific question raised. In other words, there is no universal animal model for influenza and depending on the actual question to be answered the model and the experimental conditions should be carefully selected.

Keywords: Influenza, Animal model, Mouse, Ferret, Guinea pig, Macaque, Chicken, Duck, Methods.

INTRODUCTION

Several animal models for human and animal influenza have been established to answer questions related to the pathogenesis of influenza and to the development and testing of intervention strategies like the use of vaccines and antiviral drugs. The most commonly used mammal species are the laboratory mouse (*Mus musculus*; predominantly BALB/c-strain (497-499) and C57BL/6J-strain ("black/6 strain") (500-504), the ferret (*Mustela putorius furo*) (505-509), and the cynomolgus macaque (*Macaca fascicularis*) (278, 279, 510-513), which all exhibit respiratory tract lesions to a lesser or greater extent comparable to those commonly observed in humans and animals with influenza. Several of these models can also be used to study questions related to transmission of influenza viruses. Especially ferrets and, more recently, also guinea pigs (*Cavia porcellus*) (514-521) are used in influenza transmission studies. Other mammalian species used in influenza models include the cotton rat (*Sigmodon hispidus*) (522), the domestic pig (*Sus scrofa domesticus*) (395, 523-525), the golden hamster (*Mesocricetus auratus*) (526) (34), and the domestic cat (*Felis catus*) (249, 337). Frequently used avian species are the White Leghorn chicken (*Gallus gallus domesticus*) for pathogenicity studies (337, 527) and vaccine studies (528), and various species of ducks (Anseriformes) for studies on the geographical spread of influenza (529, 530). In addition, several of these animal models are used to answer basic scientific and practical questions. Each animal model has its advantages and disadvantages and limitations that must be considered in relation to the research question concerned.

MATERIALS & METHODS APPLIED IN ANIMALS MODELS

Animals

All animal experiments are to be approved by an independent expert governmental and/or institutional animal ethics and welfare committee. Laboratory animals need access to fresh species-specific commercial food pellets, with or without supplements, which meet their individual nutritional requirements, and fresh water ad libitum. If animal experiments (including housing, sample handling, and laboratory work) deal with biosafety level 3 (BSL3) classified pathogens, they are performed under BSL3-conditions. The animals are housed accordingly in negatively pressurised and high efficiency particulate air (HEPA)-filtered biocontainment isolation units (usually glove boxes).

General anesthesia is applied for performing virus challenges (intranasal, intratracheal, intra-esophageal, intragastric, intrachoanal), taking nose/throat/rectal/cloacal swabs, blood samplings, nasal washes, subcutaneous or intraperitoneal

implantation of telemetric transponders, and euthanasia (514). Monitoring for clinical signs, such as reduced activity, labored breathing, diarrhea, and body weight loss is performed at predefined regular intervals as indicators of disease. The body temperature may be recorded at regular intervals, ranging from every 5–15 min, using a temperature-logging device implanted in the peritoneal cavity or subcutis (514) 14 days prior to the start of the experiment. Changes in body temperature can individually be calculated by subtracting the mean day and night temperatures measured on 4 successive days during the period before the challenge from the mean day and night temperatures measured after infection (510).

Laboratory mouse strains commonly used are C57BL/6J and BALB/c with a specified pathogens-free (SPF) status, mostly females 6–8 weeks of age. They are group-housed in age-matched study groups in standard filter-top cages or in isolator units.

General anesthesia is induced by means of inhalation of 3% isoflurane in O_2, and is applied also when mice are immunised intramuscularly. Vaccines or other appropriate treatments are administered intramuscularly in the hind legs (maximum injection volume used is 100 µl i.m. equally divided over both hind legs). Blood sampling is performed from the tail vein.

Monitoring for clinical signs and body weight loss is performed at predefined regular intervals as indicators of disease. According to protocol laboratory mice are to be euthanised if they show a postinfection weight loss exceeding 20% (504).

Virus challenge is performed by intranasally instilling a volume of 50 µl phosphate-buffered saline (PBS) that contains generally 10^2–10^4 median tissue culture infective dose ($TCID_{50}$) of mouse-adapted H1N1 strains (e.g., influenza virus A/PR/8/34), or non-mouse-adapted H5N1 HPAIV (e.g., A/Vietnam/1194/04), amongst other IAVs, dosed generally at 10^3 $TCID_{50}$ in 50 µl PBS. Sham challenged control animals are similarly treated with the matching volume of PBS. Virus shedding is monitored post infection in daily serial nose washings and at autopsy.

Euthanasia of laboratory mice is performed under general anesthesia by means of exsanguination from orbital puncture or by cervical dislocation at predefined time points, or according to predefined clinical criteria.

Studies with **ferrets** are carried out with outbred males and/or females, approximately 8 months of age, with body weights ranging from 0.8 to 1.5 kg. The ferrets are housed in study groups of 6–10 animals. For transmission experiments, naïve ferrets are placed in a transmission enclosure adjacent to an inoculated ferret at 1 day postinfection. The animals in these cages are separated by two relatively closely spaced stainless steel grids with low walls on each side that allow unidirectional airflow from the inoculated ferret to the naïve ferret, but prevent direct contact and fomite (e.g., cage bedding material) transmission. Nose and throat swabs are taken from the inoculated and exposed ferrets at predefined daily time points to assess potential horizontal virus transmission.

General anesthesia is induced by intramuscular injection in a hind leg with a mixture of ketamine 12.5 mg/kg body weight and medetomidine–HCl 7.5 mg/kg body weight (which can be antagonised by atipamezole–HCl 0.5 mg/kg body weight). Intramuscular injection of ketamine 25 mg/kg body weight is used for blood sampling, euthanasia, and swabbing throat, nose, and rectum. Anesthesia of ferrets can be induced alternatively by means of inhalation of 5% isoflurane in O_2 (531).

The jugular vein is used for blood sampling and i.v. administration of drugs.

Vaccines or other appropriate treatments are administered intramuscularly in the hind legs (maximum injection volume used is 1 ml equally divided over both hind legs). When a vaccine based on a live-attenuated virus is applied that needs limited replication within the nasal epithelium to induce an adequate protective immunity, this is typically instilled intranasally (0.5 ml equally divided over both nostrils).

Since ferrets in influenza research with a SPF status are not readily available, previous field infections with circulating influenza viruses may have occurred which may interfere with vaccine efficacy and virus challenge studies because of possibly induced cross-immunity against the vaccine or challenge virus. Similarly, infection with Aleutian disease virus (ADV; a parvovirus) can cause interference by means of an altered immune competent status (532). Therefore only animals seronegative for these viruses are used; a limited SPF status.

Virus challenge is performed by intratracheal instillation of influenza virus (dosage in the range of 10^5–10^7 $TCID_{50}$ depending on the virus used) suspended in 3 ml PBS. The challenge virus can also be administered by intranasal instillation of influenza virus (dosage in the range of 10^5–10^7 $TCID_{50}$ depending on the virus used) suspended in 0.3–0.5 ml PBS (equally divided over both nostrils).

Euthanasia of ferrets is performed under general anesthesia usually by means of exsanguination from cardiac puncture.

Cynomolgus macaques, male and/or female, adolescent to young adults (approximately 3 years), colony bred in captivity, body weight ranging from 3.5 to 4.5 kg are most frequently used in influenza infection experiments. The macaques are group housed in study cohorts, either in harem groups (one dominant male with several females) and/or in male groups (peer group of young adults). Commercial macaque food is supplemented with fresh fruit.

General anesthesia is induced by intramuscular injection in one of the legs of a mixture of ketamine 1.0 mg/kg body weight and medetomidine–HCl 0.1 mg/kg body weight (which can be antagonised by atipamezole–HCl 0.25 mg/kg; i.m.).

The inguinal vein usually is used for blood sampling and intravenous drug administration.

Vaccines or other appropriate treatments are administered intramuscularly in the legs (maximum injection volume used is 1.0 ml equally divided over both legs). Live-

attenuated virus vaccines that need limited replication within the nasal epithelium are typically instilled intranasally (volume usually used is 1.0 ml equally divided over both nostrils).

Virus challenge is performed by intratracheal instillation of influenza virus suspended in 3–4 ml PBS (dosage in the range of 10^4–10^7 $TCID_{50}$ depending on the virus used) propagated in monkey kidney (MK) cells or MDCK cells. Virus challenge can also be performed by intranasal instillation of influenza virus (dosage in the range of 10^4–10^7 $TCID_{50}$ depending on the virus used) suspended in 1.0 ml PBS (equally divided over both nostrils). Intranasal or intratracheal inoculation can be combined with application of the virus suspension on the tonsils and conjunctivae (278). Euthanasia of macaques is performed under general anesthesia usually by means of exsanguination from cardiac puncture.

Female **guinea pigs** of the outbred Hartley strain, approximately 8 weeks of age with body weights of 300–350 g, are used predominantly (514-521) in influenza virus transmission models. Guinea pigs in transmission settings are housed each in a standard rat cage (Ancare R20 series) with an open wire top, and are usually kept on a 12 h light/dark cycle. Two cages, one containing the infected animal and the other containing the exposed sentinel animal, are placed with the wire grids facing each other at variable distances without possible physical contact in an environmental chamber (Caron model 6030) with supporting unidirectional airflow. During such transmission experiments, strict measures are to be implemented to prevent aberrant cross contamination between cages. This includes handling of sentinel animals before inoculated animals, changing gloves and sanitizing work surfaces between animal handlings (514, 517, 521). Guinea pigs can be housed also in HEPA-filtered isolation units under BSL3 conditions when infected with, e.g., an H5N1 HPAIV (515).

General anesthesia is induced by a mixture of ketamine (30 mg/kg body weight) and xylazine (2 mg/kg body weight) administered intramuscularly in the gluteal muscles (514).

Blood sampling is performed from the metatarsal vein. Vaccines are administered intramuscularly in the hind legs (gluteal muscles, maximum injection volume used is 0.5 ml, equally divided over both sites). Live-attenuated virus vaccines are inoculated intranasally at 10^6 plague forming units (PFU) in 300 µl solvent (equally divided over both nostrils) (518).

Virus challenge is performed by intranasal instillation of a virus stock that was diluted in PBS to a volume of 300 µl (equally divided over both nostrils) (514). Inoculation doses reported are 10^6 (median egg infective dose) EID_{50} for H1N1 IAV and H5N1 HPAIV (519) and 10^3 PFU for H3N2 IAV and H1N1 (517). Intragastric inoculation of H5N1 HPAI has been performed by means of gavage catheter, 10^6 EID_{50} in 2 ml PBS (515).

Human IAV isolates replicate in both upper and lower respiratory tracts of guinea pigs without further adaptation. The animals shed high levels of virus in nasal secretions that can be transmitted via direct contact and/or droplets and aerosols, to sentinel guinea pigs (514). Inoculation of unadapted A/Panama/2007/99 H3N2 IAV into Hartley guinea pigs did not result in clinical signs. However, this was dependent on the guinea pig strain (514), as similar infection of inbred strain13 guinea pigs resulted in severe disease, including weight loss, lethargy, hair loss, and hypothermia.

Other viruses such as a human isolate of highly pathogenic avian influenza H5N1 did cause slight temporary lethargy in Hartley strain guinea pigs (515). Also, the dose of virus used proved important, as intranasal challenge with high dose of influenza A virus H3N2 in juvenile Hartley guinea pigs resulted in ruffled fur and reduced activity (516). However, since guinea pigs generally do not exhibit clinical signs when challenged with influenza A viruses (514), clinical observations are not always performed routinely. Since infected guinea pigs do not produce burst expulsions like cough or sneeze, the extrapolation of guinea pig transmission data to human transmission does not seem straightforward (517).

Euthanasia of sedated guinea pigs is performed by means of intraperitoneal injection of sodium pentobarbital (514), or by intracardiac injection with Beuthanasia-D solution 1 ml/kg (519) (26), or by exposure to CO_2 gas (520).

SPF White leghorn **chickens** are used in influenza research. In general they are not used to model human influenza. Instead 1-day-old chicks can serve as route of IAV inoculation as infected prey animals in infection experiments in carnivores (e.g., in cats). Alternatively, 6-week-old SPF White Leghorn chickens may be used to determine the intravenous pathogenicity index (IVPI) of influenza viruses. This is performed by intravenous injection in the ulnar vein of 0.1 ml of 10^6 $TCID_{50}$ virus. Clinical signs are monitored for 10 consecutive days, and the animals are considered diseased when displaying one of the following clinical signs: depression, cyanosis of the comb or wattles, respiratory involvement, diarrhoea, oedema of the face/head, and nervous signs. They are considered severely affected if they displayed two or more of these signs. The index is calculated as the mean score per bird per observation (522). Several **duck** species, including the mallard (*Anas platyrhynchos*) (530), males and females, usually between 8 and 11 months of age, are used in infection and transmission experiments. There is a preference for use of Pekin ducks, a breed of domestic duck, that are preferably captive bred and housed indoors since hatching to avoid the risk for inadvertent avian influenza virus infection. Chickens and ducks are usually group-housed in study groups of 4–8 animals. In these bird species, general anesthesia is induced by means of inhalation of 5% isoflurane in O_2, and blood sampling is performed from the jugular or ulnar veins.

Vaccines or other appropriate treatments are administered subcutaneously or intramuscularly (pectoral muscle), with volumes correlated to body weight. Injection

volumes (of vaccines) per body weights are: <1.4 kg: 0.25 ml, 1.4–7 kg: 0.5 ml, >7–12 kg: 0.75 ml, >12–44 kg: 1.25 ml, >44 kg: 2.5 ml (533).

Virus challenge is performed by intratracheal instillation of e.g., 2.5×10^4 $TCID_{50}$ H5N1 HPAIV in 1-day-old chicks, and euthanised 1 dpi for experimental transmission to carnivores. In pathogenicity studies 8 weeks old chickens are inoculated intranasally or intrachoanally with, e.g., 10^4 EID_{50} H5N1 HPAIV in 0.3 ml PBS (534). Ducks in pathogenicity and excretion studies are inoculated with, e.g., 10^4 $TCID_{50}$ H5N1 HPAIV in PBS, 1.5 ml intratracheally and 1.5 ml intraoesophageally (530) but intranasal is the most common inoculation route.

Euthanasia of these avian species is performed under general anesthesia usually by means of exsanguination from cardiac puncture.

Serology

Animal studies on influenza are performed in animals seronegative for circulating seasonal influenza viruses and other relevant influenza virus strains. Serum samples are collected at predefined time points and tested (after treatment with cholera filtrate and heat inactivation at 56°C) for the presence of anti-HA antibodies via the hemagglutination inhibition (HI) assay and for virus-neutralizing antibodies using the (micro-) virus neutralisation (VN) assay. Additionally, ferrets are screened before use for the presence of serum antibodies against Aleutian disease virus. Only seronegative animals are used. Additional confirmation of the absence of virus-specific antibodies can be performed by immunofluorescence assay using MDCK cells infected with influenza A or B viruses (535), or by means of commercially available IAV ELISA kit for detection of antibodies against NP. If animals are screened just prior to inoculation by nasal, oropharyngeal, or cloacal swabs, they need to be RT-PCR negative as well.

Virology

Challenge virus stocks can be either propagated in the allantoic cavity of 10- or 11-day-old embryonating chicken eggs or propagated in MDCK or MK cell cultures. Allantoic fluid is harvested 3 days after inoculation and infectious virus titers are determined in MDCK cell cultures. In cell cultures following development of cytopathic changes, supernatants are collected and cleared by low-speed centrifugation, and infectious titers are similarly determined in MDCK cell cultures. To determine the $TCID_{50}$, 100 ml of tenfold serially diluted culture supernatants are inoculated in quadruplicate or quintuplicate on MDCK cells grown confluently in 96-well microtiter plates (10^5 cells per well) in culture medium [minimal essential medium (MEM) supplemented with 10% fetal calf serum (FCS), 100 IU/ml penicillin, and 100 mg/ml streptomycin]. Before infection, the cells are washed twice with PBS. After 1 h at 37°C, cells are washed twice with infection medium [MEM supplemented with 4% bovine serum albumin (BSA) fraction V, 100 IU/ml penicillin, 100

mg/ml streptomycin, and 4 mg/ml trypsin] in a humid 5% CO_2 atmosphere at 37°C for 6–7 days. To determine the hemagglutination activity, 50 µl volumes of these culture supernatants are serially diluted twofold in PBS in round bottom plates. Subsequently, 25 µl PBS and 25 µl of a 1% suspension of turkey erythrocytes are added. After 1 h incubation at 4°C the haemagglutination patterns are read. HA activity is used as an indicator for infection of the cells in individual wells (535). Infectious virus titers are calculated according to the method of Spearman–Karber (536) or Reed–Muench (537) and expressed as log $TCID_{50}$ per ml. Infectious virus titers can alternatively be assessed using 10-day-old embryonating chicken eggs reported as log median egg infective dose (EID_{50}) per ml, calculated according to the method of Reed–Muench (515, 537). The virus stock is diluted with PBS to obtain the final dose needed for inoculation. Usually a large animal experiment is preceded by a dose finding study that includes fewer animals in total than the definitive experiment to determine the optimal challenge dose of a particular virus, e.g., three to four different challenge groups of six animals each (538). Control animals are sham challenged in the same way with the matching volume of PBS, or PBS-diluted sterile allantoic fluid or cell culture supernatant.

Virus shedding from inoculated animals and/or sentinel animals in transmission experiments can be monitored *in vivo* by collection of serial swabs from oropharynx, nose, rectum, and cloaca, in transport medium daily or at other predefined time points post challenge until euthanasia or death. Virus shedding from the respiratory tract of macaques also can be assessed by collecting lung lavage fluids (LLF). Swabs collected for virus shedding can be stored at −80°C until further analysis. Individual swabs are resuspended by vortexing in 3 ml transport medium for virus isolation. The samples are analyzed for the presence of virus by inoculating MDCK cells with serial tenfold dilutions as stated above. Viral titers are determined according to standard procedures and expressed as log $TCID_{50}$ per ml of swab medium. Additionally, viral RNA can be isolated from 200 µl supernatant of swab medium using the MagNA Pure LC system and detected by a TaqMan assay.

Alternatively, especially in guinea pigs, nasal washes can be taken to determine viral titers. This is performed by instilling 1 ml PBS into the nostrils and collecting liquid runoff in a sterile petri dish before aliquots in tubes are centrifuged for 5 min at 2,000 × *g* and 4°C. The supernatants can be stored at −80°C pending analysis (514).

Virus titers also can be determined in tissues collected at autopsy. Tissue samples from the respiratory tract (e.g., lung, bronchus, trachea, nasal turbinate), and extra-respiratory organs are collected at autopsy and can be processed directly or can be snap-frozen (tissues enclosed in ampules on dry ice containing ethanol, and stored at −70°C/−80°C) pending further processing. During processing, tissue samples are weighed and subsequently homogenised in 1 ml of medium (tissue homogenate medium or MDCK infection medium) by means of the FastPrep system with two ¼

in. (»6.4 mm) diameter ceramic balls or four 3.0 mm diameter steel balls and then resuspended by adding an extra 2 ml medium. Alternatively, a Polytron PT2100 can be used to homogenize tissues in 3 ml of medium. The suspension is then clarified by centrifugation (10 min at 500 × g). The titers of clarified supernatants of homogenised tissues are determined by standard procedures in MDCK cells and expressed as log $TCID_{50}$ per gram of tissue.

A microarray assay to assess differences in mRNA expression profiles can be performed using tissue samples collected at autopsy and immediately stored in RNAlater solution. Several small fresh tissue samples are collected at autopsy; non-lesional samples versus lesional samples, and/or samples of vaccinated/treated animals versus samples of sham-vaccinated/placebo-treated control animals. After storage in RNAlater, total RNA is isolated, purified, labeled, and hybridised on GeneChip Arrays. GeneChip Arrays are readily available for laboratory mice but not yet for ferrets. However, amplified RNA can be hybridised to Affymetrix GeneChip Canine Genome 2.0 Array (531). Arrays are also readily available for the rhesus macaque (*Macaca mulatta*) that bears a close genetic resemblance to the cynomolgus macaque and can be used successfully (473). Among others, differences in gene expression levels of inflammatory mediators like interferons and other cytokines and chemokines can be assessed.

Immunology

To avoid hypersensitivity reactions during virus challenge, vaccine preparations should be free of BSA. This may occur after repeated exposure to this antigen (518).

In ferrets, peripheral blood mononuclear cells (PBMCs) can be collected and isolated from blood samples, and a T-cell proliferation assay can be performed to assess vaccine-induced T-cell responses. PBMCs are isolated from blood samples, collected 4 weeks after vaccination in EDTA tubes by density gradient centrifugation using lymphoprep (can be cryopreserved at −135°C), labeled with 0.3 mM carboxyfluorescein diacetate succinimidyl ester (CFSE) in PBS for 5 min at 37°C, washed twice and resuspended in RPMI medium 1640. 10^5 cells per well are seeded into a 96-well plate with or without the immunogenic compound (200 ng HA content) or phytohemagglutinin (PHA) (1 mg/ml) and incubated at 37°C/5% CO_2 for 6 days. After 2 days, 100 µl supernatant of Concanavalin A-stimulated ferret lymph node cells is added per well. After 4 days cells are washed and stained with a monoclonal antibody against human CD8 (OKT-8)-Pacific Blue. Cells are stained with LIVE/DEAD Aqua Fixable Dead Cell Stain to exclude dead cells. Next, cells are fixed and permeabilised with Cytofix and Cytoperm, and stained with an Alexa Fluor 647-labeled mAb specific for human CD3 (PC3/188A). These CD3- and CD8-specific mAb cross-react with ferret CD3 and CD8. Data are acquired using a FACSCanto-II and analyzed with FACS Diva software. The proliferation of CD3 + CD8−

(and CD3 + CD8+) cells is calculated by subtracting the control CD3 + CD8-(+) CFSElow cells from the HA-stimulated CD3 + CD8-(+)CFSElow cells (505) (9).

Especially in mice, spleens can be harvested for the detection of virus-specific CD8+ cytotoxic T lymphocytes (CTL) by tetramer-staining to assess vaccine-induced T-cell responses. The erythrocytes are removed from single-cell splenocyte suspensions (obtained by using 100 mm cell strainers) with ery-lysis buffer. The cells are washed with 0.5% BSA or 2% FCS in PBS and stained for flow cytometry with antibodies such as CD3e-PerCP, CD8b.2-FITC, ToPro 3-APC, and APC or PE-labeled H-2Db-PE tetramer with the NP366-374epitope ASNENMETH. Cells are analyzed on FACSCalibur with a high throughput sampler in combination with PlateManager and CellQuest Pro software (504).

Pathology

During autopsy, a thorough macroscopic examination is performed. This includes weighing the intact animal and selected organs, and assessment of gross lesions. Preferably the trachea is clamped before opening the thorax to prevent lung collapse to allow for accurate in situ examination of the non-collapsed lung. The lungs are inspected, weighed, and the lung (partially or *in toto*) is collected during autopsy, gently instilled with and immersed in 10% neutral-buffered formalin for a minimum of 2 days to allow for adequate tissue fixation and virus inactivation. Lungs and other organs collected at autopsy are placed in 10% neutral-buffered formalin with an approximate ratio of 1 parts tissue to 9 parts formalin. Avian specific tissues collected at autopsy may include the caudal thoracic or abdominal airsac, proventriculus, and bursa of Fabricius.

At autopsy, fresh samples can be collected for determination of viral loads. These samples may include nose washes with PBS, respiratory tissues ranging from nose to lungs, and additional tissues such as tonsils, tracheobronchial lymph nodes, brain, spleen, liver, kidney, pancreas, intestines, and plasma. Typically, lung virus titers are determined in homogenised pools of lung samples, that are collected in a standardised way (e.g., one sample per lung lobe), not guided by the presence of gross lesions, and weighed (each sample ≈ 0.1 g, so total averaged weight of sampled lung tissue ≈ 0.4–0.5 g per animal). Furthermore fresh spleens can be harvested for the detection of virus-specific CD8+ T cells.

Trimming of formalin-fixed organs and lungs for histopathology is done in a standardised way not guided by the presence of gross lesions. The tissue sections are routinely processed and paraffin embedded and sectioned at 3–4 µm, deparaffinised with xylene and rehydrated with alcohol and stained with haematoxylin and eosin (H&E) for histopathological examination by light microscopy. Additionally, IHC can be applied to visualise viral protein synthesis. For IHC, consecutive slides are cut at 3–4 µm and stained using an immunoperoxidase method with a monoclonal antibody

directed against the NP of IAV. A horseradish peroxidase-labeled goat anti-mouse (e.g., anti-IgG2a) is used as secondary antibody. Endogenous cellular peroxidase is blocked with 3% hydrogen peroxide. The peroxidase is revealed using 2,3-diaminobenzidine (DAB) as a substrate, resulting in a dark brown granular staining in the cytoplasm and especially in the nuclei of influenza virus infected cells, followed by counterstaining with haematoxylin. The peroxidase activity can be revealed alternatively by incubating slides with 3-amino-9-ethylcarbazole (AEC) for 10 min resulting in deep red nuclear staining of infected cells. Lung sections from domestic cats intratracheally inoculated with H5N1 HPAIV are simultaneously stained and serve as positive controls. Negative controls are performed in absence of the primary antibody, substitution of primary antibody by an irrelevant monoclonal antibody of the same isotype (279), and preferably include a negative tissue control comprised of the same tissue of a non-infected animal stained for NP.

Materials; Media and Biochemical Substances

- Tissue Homogenate Medium (storage condition: +4°C, for maximum of 2 weeks): Hank's balanced salt solution containing 0.5% lactalbumin, 10% glycerol, 200 U/ml penicillin, 200 mg/ml streptomycin, 100 U/ml nystatin.
- MDCK Infection Medium (storage condition: +4°C, for maximum of 2 weeks): 500 ml Eagle's minimal essential medium, 10 ml Hepes buffer (1 M), 5.7 ml Sodium bicarbonate solution (7.5%), 5.0 ml l-Glutamine (200 mM), 5.0 ml Penicillin (10,000 IU/ml) and Streptomycin (10,000 mg/ml) solution, 350 ml Trypsin 2.5% (10×), 4.3 ml BSA fraction V (35%), 5.0 ml Amphotericin B (0.25 mg/ml).
- RNAlater, storage conditions: stable at +4°C for 4 weeks, or long term at −20 to −80°C.
- Transport Medium for virology samples (storage conditions: +4°C for 2 weeks, and −20°C for 52 weeks): 430 ml General Virus Transport Medium [500 ml Eagle's minimal essential medium, 10 ml Hepes buffer (1 M), 5.7 ml Sodium bicarbonate solution (7.5%), 5.0 ml l-Glutamine (200 mM), 5.0 ml Penicillin (10,000 IU/ml) and Streptomycin (10,000 mg/ml) solution, 4.3 ml BSA fraction V (35%), 5.0 ml Amphotericin B (0.25 mg/ml)], 50 ml Penicillin (10,000 IU/ml) and Streptomycin (10,000 mg/ml) solution, 8.6 ml BSA fraction V (35%), 20 ml Amphotericin B (0.25 mg/ml).
- Transport medium for virology samples: Hank's balanced salt solution containing 10% glycerol, 200 U/ml penicillin, 200 mg/ml streptomycin, 100 U/ml polymyxin B sulfate, 250 mg/ml gentamicin.
- Viral inoculum, PBS-BA-PS: Viral stock diluted in PBS containing 100 units/ml penicillin, 100 mg/ml streptomycin, and 0.3% BSA.

Suppliers: -standard laboratory reagents: Lonza The Netherlands (NL), Sigma-Aldrich NL, ICN NL; -RNAlater: Ambion USA; -veterinary anesthetics: Eurovet NL, Orion Pharma Finland, Pfizer NL; -temperature loggers: StarrOddi Iceland; -MagNA Pure LC system: Roche diagnostics NL; -IAV antibody ELISA kit: EVL NL; -GeneChips: Affymetrix USA; -RPMI medium: Cambrex USA; -Lymphoprep: Axis-Shield Norway; -cytofix, cytoperm, cell strainers and Facs software: BD pharmingen NL; -human monoclonal CD8 antibody: eBiosciences USA; -labeled human monoclonal CD3 antibody: Santa Cruz Biotechnology USA; -Fastprep system: MP biomedicals Europe; -Polytron PT2100: Kinematica AG Switzerland.

CONCLUDING REMARKS & SUMMARY TABLE

In influenza research, a variety of animal species can be used in animal models for influenza in humans. They show species-specific differences in susceptibility to influenza virus infection or subsequent disease. Thorough knowledge and experience of these animals are necessary to obtain reliable data for extrapolation to humans. In **table 3.2.1** a summary is given of important advantages and disadvantages of the foremost animal species used in influenza research.

Table 3.2.1 Summary of advantages and disadvantages of several animal species in models for influenza in humans, modified from references (143, 539).

	Pro	Con
Laboratory mouse	• Pathology of 1918 H1N1 and H5N1 HPAI influenza viral pneumonia comparable to humans	• Anatomy and histology of respiratory tract and pattern of influenza virus attachment dissimilar to humans
	• Low costs (purchase, maintenance, and reproduction)	• Seasonal human influenza viruses need adaptation to the mouse to replicate sufficiently to cause respiratory lesions
	• Well-characterised genetics; microarray and knockouts readily available	• Unsuitable for live-attenuated vaccines
	• Minimal host variability and background pathology of inbred SPF strains	• Unsuitable for transmission experiments
	• Many available molecular biological reagents	• Reservations about extrapolative value of data
		• Need of animal handling experience
Ferret	• Pathology of influenza viral pneumonia comparable to humans	• Genetically outbred, resulting in host response variability to viral challenge
	• Anatomy and histology of respiratory tract moderately similar to humans and similar pattern of influenza virus attachment	• No SPF animals, so need to confirm Aleutian disease and initial influenza seronegative status
	• Susceptible to human and avian influenza viruses	• Appear more susceptible to developing influenza pneumonia than humans
	• Suitable for transmission experiments	• Systemic disease in avian influenza different from humans
	• Suitable body size for blood and tissue sampling	• Ferret microarrays unavailable, although canine chips prove practical cross-hybridisation
		• Few molecular biological reagents available
		• Need of specific animal handling experience

Table 3.2.1 Summary of advantages and disadvantages of several animal species in models for influenza in humans, modified from references (143, 539).

	Pro	Con
Cynomolgus macaque	• Pathology of influenza viral pneumonia comparable to humans, especially for H5N1, less for seasonal IAVs	• Genetically outbred, resulting in host response variability to viral challenge
	• Anatomy and histology of respiratory tract and immune response similar to humans	• Limited SPF status animals, but need to confirm initial influenza seronegative status
	• Absence of systemic disease in avian influenza similar to humans	• High costs (purchase and maintenance)
	• Microarray readily available	• Ethical concerns
	• Many available molecular biological reagents and cross-reaction with human reagents	• Need of specific animal handling experience
	• Good extrapolative value of data	
Guinea pig	• Suitable for transmission experiments	• Pathology of influenza viral pneumonia dissimilar to humans*
		• Usually no clinical signs after virus challenge
		• Need to confirm initial influenza seronegative status
		• Reservations about extrapolative value of data
		• Need of animal handling experience
Chicken/duck	• Monitoring vectors of avian influenza (ducks)	• Pathology of influenza viral pneumonia dissimilar to humans; so not used to model influenza in humans
	• Confirming pathogenicity of avian influenza viruses (chickens)	• Need to confirm initial influenza seronegative status in pathogenicity studies

* Recent work by Wiersma and colleagues (540, 541) shows the application of intratracheal IAV inoculated isogenic guinea pigs as model for influenza pathogenesis in humans.

CHAPTER 4

Pathogenesis studies on influenza induced ARDS in ferrets

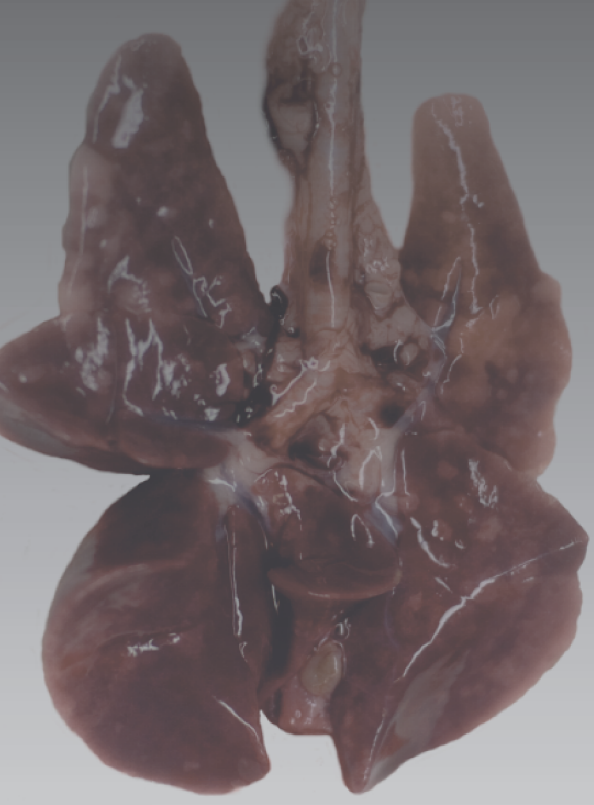

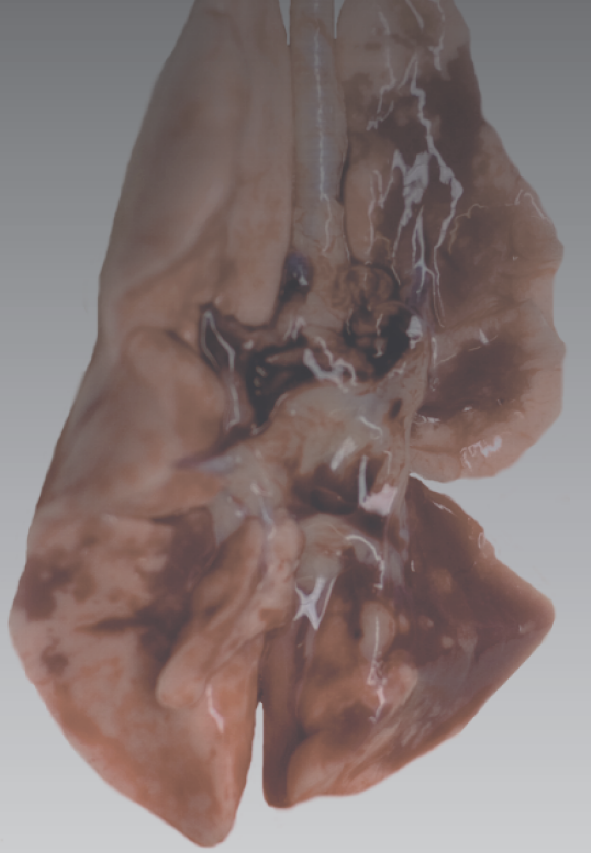

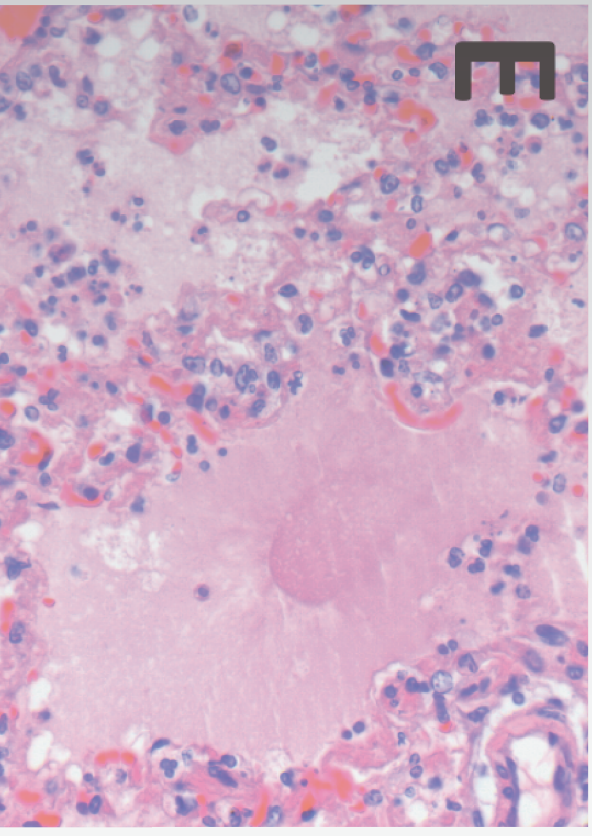
E

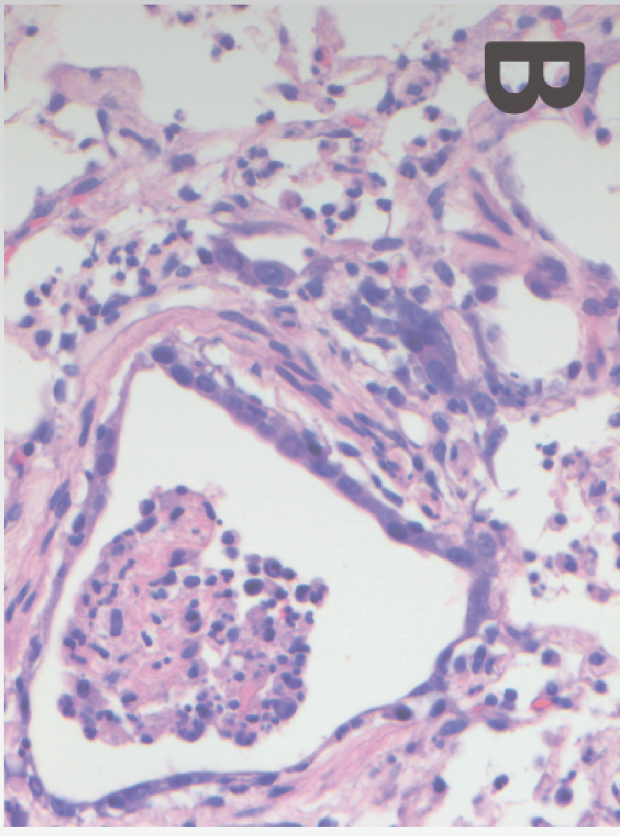
B

4.1

Low pathogenic avian influenza A(H7N9) virus causes high mortality in ferrets upon intratracheal challenge: A model to study intervention strategies

J.H.C.M. Kreijtz[1], E.J.B. Veldhuis Kroeze[1,2], K.J. Stittelaar[2], L. de Waal[2], G. van Amerongen[2], S. van Trierum[1], P.R.W.A. van Run[1], T. Bestebroer[1], T. Kuiken[1], R.A.M. Fouchier[1], G.F. Rimmelzwaan[1,2] & A.D.M.E. Osterhaus[1,2]

Vaccine 2013; 31: 4995-4999

Affiliations

[1]Department of Viroscience, Erasmus Medical Center, Rotterdam, The Netherlands

[2]Viroclinics Biosciences B.V., Rotterdam, The Netherlands

ABSTRACT

Infections with H7N9 LPAIVs have caused more than 100 hospitalised human cases of severe influenza in China since February 2013 with a case fatality rate exceeding 25%. Most of these human infections presented with severe viral pneumonia, while limited information is available currently on the occurrence of mild and subclinical cases. In the present study, a ferret model for this virus infection in humans is presented to evaluate the pathogenesis of the infection in a mammalian host, as ferrets have been shown to mimic the pathogenesis of human infection with influenza viruses most closely. Ferrets were inoculated intratracheally with increasing doses (>10^5 $TCID_{50}$) of H7N9 influenza virus A/Anhui/1/2013 and were monitored for clinical and virological parameters up to four days post infection. Virus replication was detected in the upper and lower respiratory tracts while animals developed fatal viral pneumonia. This study illustrates the high pathogenicity of H7N9 LPAIV for mammals. Furthermore, the intratracheal inoculation route in ferrets proofs to offer a solid model for H7N9 LPAIV induced pneumonia in humans. This model will facilitate the development and assessment of clinical intervention strategies for H7N9 LPAIV infection in humans, such as preventive vaccination and the use of antivirals.

Keywords: H7N9; Avian influenza A; Intervention strategies

INTRODUCTION

Avian influenza viruses have crossed the species barrier on several occasions and with varying impact on human health. From February 2013 onward several human cases with severe respiratory illness were reported from South-East China. The causative agents were rapidly characterised and subtyped as H7N9 LPAIVs that most likely were the result of multiple reassortment events of at least two avian influenza viruses (38, 542). Although the exact source of the human infections with this apparently avian influenza virus remains to be elucidated, sequence analysis has indicated that the viruses have been circulating for a longer period before they recently surfaced (543, 544). Since the first reported human cases, the virus has infected at least 131 humans of which 32 succumbed to the infection with a predilection for older male individuals (545-548). It is the largest outbreak of avian influenza in humans since the introduction of H5N1 HPAIVs in the human population that thus far has resulted in over 600 reported cases with a hospitalised case fatality rate of approximately 60%. The majority of the humans infected with H7N9 LPAIV have presented with severe viral pneumonia and became critically ill (38). The virus has been classified as being low pathogenic based on the genotype (the hemagglutinin does not contain a multi-basic cleavage site) and based on the results of intravenous pathogenicity index (IVPI) testing in chickens and data from poultry and wild birds. However, the clinical manifestation of H7N9 LPAIV infection in humans shows a higher pathogenic phenotype. To further explore this discrepancy and elucidate the pathogenesis of the infection in mammals, we established a model for H7N9 LPAIV induced pneumonia in ferrets (*Mustela Putorius furo*). The ferret model has been used to elucidate the severity of lower respiratory tract infections with various influenza A virus subtypes (506). Preliminary data on intranasal inoculation of ferrets with H7N9 AIV indicates that the virus causes only mild disease (unpublished data) in these animals. However, we have demonstrated in the past that the choice of inoculation route has a major impact on the outcome and severity of influenza virus infection in ferrets (549). Since the vast majority of currently recorded human cases of H7N9 LPAIV infection have been characterised by severe viral pneumonia, replication in the lower respiratory route seems to be the major cause of at least severe human disease. Therefore intratrachael administration of the virus to ferrets would be the route of choice to study the pathogenesis of severe H7N9 LPAIV infection in this mammalian model.

MATERIALS & METHODS

Virus

Influenza virus A/Anhui/1/2013 (H7N9) isolated from a fatal human case in China was kindly provided by the Pandemic Influenza Preparedness (PIP) Framework. The virus had been isolated and passaged three times in embryonated chicken eggs and was subsequently passaged once in MDCK cells. The infectious virus titer was determined as described previously and expressed in tissue culture infectious dose 50% ($TCID_{50}$) (535).

Animals

Healthy outbred female ferrets (*Mustela Putorius furo*), of around 12 months of age and seronegative for antibodies against aleutian disease virus and seasonal influenza viruses were used. About two months prior to the start of the experiment, the animals were anesthetised using a cocktail of ketamine (Alfasan, Woerden, The Netherlands) and domitor (Orion Pharma, Espoo, Finland), and a temperature logger (DST milli-T logger; Star-Oddi, Reykjavik, Iceland) was placed in their peritoneal cavity to record the body temperature every 10 min. The animals were maintained in standard housing, and provided with commercial food pellets and water ad libitum and were placed in BSL-3 isolator units just before inoculation. Ferrets were inoculated intratracheally with influenza virus A/Anhui/1/2013 (H7N9) at a dose of 10^5 (n = 2), 10^6 (n = 3), 10^7 (n = 2) or 10^8 (n = 2) $TCID_{50}$ in a volume of 3 ml. An independent animal ethics committee approved the experimental protocol before the start of the experiments.

Virus replication in the Upper and Lower Respiratory Tract

Nasal and pharyngeal swabs were taken daily during the infection period. After spontaneous death or euthanasia three or four days after inoculation, samples of all lobes of the right lung and the accessory lobe, nasal turbinates, tonsils, trachea, bronchus, tracheobronchial lymph nodes and lungs were collected and snap frozen using a dry ice/ethanol bath and stored at −70 °C until further processing. Tissue samples were weighed and subsequently homogenised with the FastPrep-24 (MP Biomedicals, Eindhoven, The Netherlands) in Hank's balanced salt solution containing 0.5% lactalbumin, 10% glycerol, 200 U/ml penicillin, 200 µg/ml streptomycin, 100 U/ml polymyxin B sulfate, 250 µg/ml gentamycin, and 50 U/ml nystatin (ICN Pharmaceuticals, Zoetermeer, The Netherlands) and centrifuged briefly before dilution. Quadruplicate 10-fold serial dilutions of lung and swab supernatants were used to determine the presence of viral RNA by Taqman and infectious virus titers in confluent layers of MDCK cells as described previously (535).

Histopathological examination and immunohistochemistry

At autopsy all ferrets (n = 9) and their organs were grossly examined by opening the thoracic, abdominal, and cranial cavities. The extent of pulmonary consolidation was assessed based on visual estimation of the percentage of affected lung tissue. The relative lung weight was calculated as proportion of the body weight (lung weight/ body weight × 100). The left lung was routinely collected for histological examination, by means of cutting 4 standard sections per animal (one cross section and one sagittal section from the cranial lobe, and one cross section and one sagittal section from the caudal lobe). Besides the lungs other organs that were sampled for histology included: nasal turbinates, brains including olfactory bulb, tonsil, trachea, tracheobronchial lymphnodes, heart, liver, stomach, small and large intestines, pancreas, spleen, adrenal, kidney, urinary bladder, ovaries, uterus, skeletal muscle (quadriceps), femoral bone marrow. All tissues were immersed in 10% neutral-buffered formalin for fixation, routinely processed, paraffin embedded, cut to 4 µm on glass slides and stained with H&E for histopathological evaluation. Serial sections of the respiratory tract and brains were stained for IAV NP by IHC as described previously (550).

RESULTS

Clinical signs

All infected animals developed fever with a mean peak body temperature of 41.2 °C (SD = 0.53) within 24–48 h post infection. From 2 dpi onwards the animals developed signs of respiratory distress (presented as heavy breathing/dyspnoe) and eventually hunched posture. During the course of infection the animals' food and water intake decreased, resulting in mild emaciation and dehydration. On day 3 post infection the two animals inoculated with 10^8 $TCID_{50}$ and animals inoculated with 10^7 (n = 1) and 10^6 (n = 1) $TCID_{50}$ succumbed. At day 3 post infection the surviving animals were lethargic and by day 4 one additional animal (10^6 $TCID_{50}$) had succumbed whereas one animal (10^7 $TCID_{50}$) was moribund. Autopsies were performed on all the deceased animals and the surviving animals after euthanasia.

Table 4.1.1 Clinical parameters

Nr	Virus dose ($TCID_{50}$)	Day of death	Weight loss (%)	Body temperature	
				Peak (°C)	Time post inoculation (h)
1	10^5	4[a]	11.2	40.8	33
2		4[a]	10.9	41.3	31
3	10^6	4[b]	12.4	41.7	24
4		3[b]	10.3	41.0	24
5		4[a]	14.4	41.3	24
6	10^7	3[b]	9.8	40.1	21
7		4[c]	14.0	41.8	23
8	10^8	3[b]	7.4	41.2	24
9		3[b]	8.8	41.8	16

[a] Sacrificed end experiment

[b] Found dead

[c] Euthananised moribund

Virus replication in the respiratory tract

Pharyngeal swabs from all animals tested positive for virus with the highest virus titers 3 dpi in those obtained from ferrets inoculated with 10^7 or 10^8 $TCID_{50}$: $10^{4.4}$ $TCID_{50}$/ml (SD = 100.1–101.3). Virus replication in the ferrets inoculated with 10^5 or 10^6 $TCID_{50}$ reached peak values 4 dpi (**Figure 4.1.1A**). These data confirmed the detection of viral RNA in the throat by real tie PCR. In seven out of nine animals viral RNA was detected in the nose and this again was confirmed by virus isolation with the peak of virus replication on day 3 post infection: $10^{3.6}$ $TCID_{50}$/ml (SD = 100.4) in the ferrets inoculated with 10^8 $TCID_{50}$ (**Figure 4.4.1B**). On day 4 rectal swabs were taken from the remaining animals and in 40% of the animals viral RNA was detected but no infectious virus could be detected.

All animals tested positive for virus replication in nasal turbinates, tonsils, trachea, bronchus, bronchial lymph nodes and lungs (**Figure 4.1.1C**). In the bronchial lymph nodes and lungs the mean virus titers were highest ($10^{5.7}$–$10^{6.8}$ and $10^{5.0}$–$10^{5.8}$ $TCID_{50}$/g, respectively). Only in the trachea the virus titers were higher for ferrets inoculated with 10^8 $TCID_{50}$: $10^{6.6}$ $TCID_{50}$/g (SD = $10^{1.3}$). Apart from the bronchial lymph nodes and lungs, virus titers were highest in the samples of the ferrets inoculated with 10^7 and 10^8 $TCID_{50}$, illustrating a dose dependency of the H7N9 LPAIV infection.

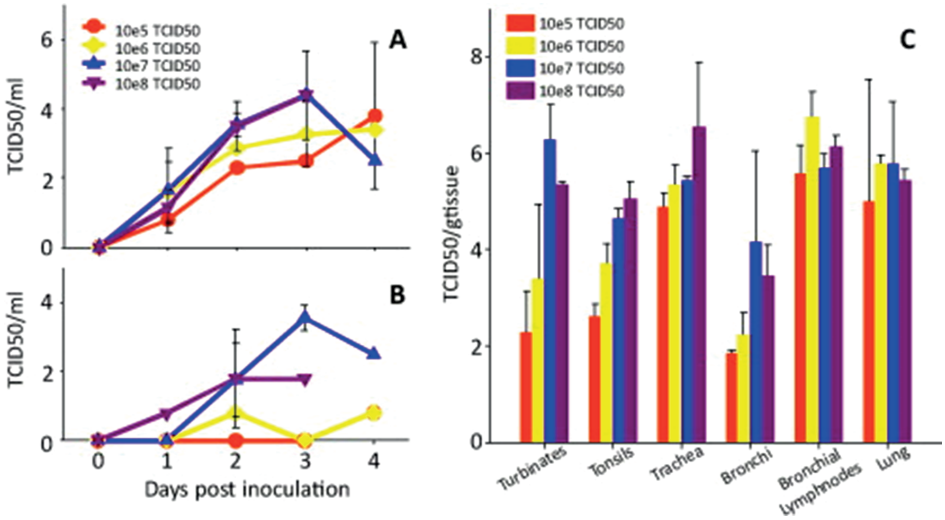

Figure 4.1.1 Virus replication in the respiratory tract. After inoculation with avian influenza A(H7N9) virus, pharyngeal (A) and nasal (B) swabs were taken daily to monitor virus replication at these sites over time. Upon autopsy, samples were taken from the different locations of the respiratory tract for the detection of replication competent virus. To calculate the mean virus titers of the respiratory tract samples (C) the data were combined from the two (10^5, 10^7, 10^8 $TCID_{50}$) or three (10^6 $TCID_{50}$) animals per group.

Histopathological changes and immunohistochemistry

In all the nine animals the foremost macroscopic post-mortem lesions concerned the lungs. The lung lesions ranged from extensive multifocal (**Figure 4.1.2A**) to almost diffuse dark red pulmonary consolidation (**Figure 4.1.2D**) with oedematous frothy fluid oozing from the primary bronchi upon section. The most severely affected lungs additionally displayed a pale mottled aspect, likely due to trapped air. The extent of pulmonary consolidation was assessed based on visual estimation of the percentage of affected lung area from the pleural aspect. All animals were found to have practically empty gastrointestinal tracts combined with a subtle pale reticular pattern of the livers, indicative of hepatic lipidosis due to inappetence. Except for the two lowest dosed animals, all other spleens were slight to moderately swollen and hyperemic. No further macroscopic lesions were encountered (**Table 4.1.1**).

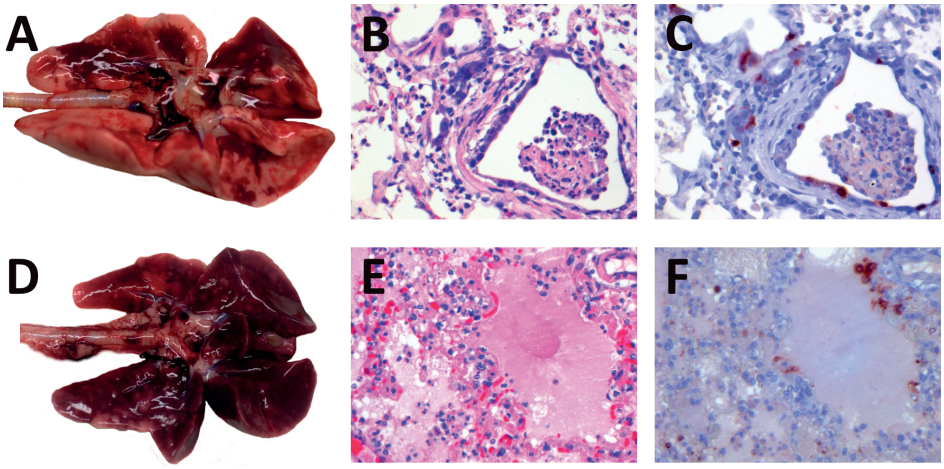

Figure 4.1.2 Representative (histo)pathological changes of the lungs. From left to right, ventral viewed gross lung lesions (A and D), corresponding microscopic lesions serially stained with H&E (B and E) and IHC (C and F) for IAV NP, respectively. The top panel depicts animal#1 which was intratracheally inoculated with 10^5 $TCID_{50}$ Avian influenza A(H7N9) virus, that was grossly affected for approximately 50%. The photomicrographs depict on the right an inflamed bronchiole containing an intraluminal plug of neutrophils and cellular debris, the adjoining inflamed alveoli contain neutrophils and macrophages and some proteinaceous material. The bottom panel depicts animal#8 inoculated similarly with 10^8 $TCID_{50}$, which was grossly affected for approximately 90%, with photomicrographs likewise depicting a bronchiole on the right and adjoining alveoli, but more severely inflamed with necrosis and flooding by intense eosinophilic oedema fluid. The corresponding IHC stains show the influenza virus infected epithelial cells by dark reddish-brown stained nuclei. (Original microscopic magnifications of 400×).

On histopathological examination, the nasal turbinates of the ferrets inoculated with the two highest dosages (n = 4: 10^7 and 10^8 $TCID_{50}$) were moderately inflamed. These rhinitides were characterised by moderate numbers of mainly neutrophils infiltrated within the nasal respiratory epithelium and underlying *Lamina propria*. These lesions co-localised with epithelial cells positive for IAV NP by IHC. The nasal olfactory epithelium was typically not or very mildly affected. None of the other ferrets displayed rhinitis, and the nasal turbinates were negative for influenza A virus NP by IHC (**Table 4.1.2**). The severity of inflammatory lesions in the tracheas was relatively mild, with lesions composed of few neutrophils and lesser lymphocytes within the *Lamina propria.* These occurred in three animals inoculated with the three highest virus doses. These relatively mild lesions co-localised with tracheal epithelial cells positive for IAV NP by IHC, however several tracheas were positive for NP without showing cellular inflammatory reaction. In the bronchi of all animals mild to moderate lesions were present that were mainly limited to epithelial necrosis of the submucosal glands, mostly without affecting

the luminal lining epithelium. The severity and extent of this necrotising bronchial submucosal adenitis was associated and co-localised with the number of glandular cells positive for IAV NP by IHC. The most severe cases of bronchial submucosal adenitis were found in the ferrets inoculated with the two highest virus concentrations. All animals showed inflammatory bronchiolar lesions. These marked to severe bronchiolitides were characterised by intraepithelial infiltrates of neutrophils mainly, with in the most severe cases plugging of bronchioli by sloughed necrotic epithelial cells admixed with mucus containing degenerated neutrophils. In the most severely affected animals nearly all bronchioles were completely denuded. Rather the extent, than the severity of affected bronchioles was associated with virus concentrations inoculated. The necrotising bronchiolitis co-localised with the number of epithelial cells strongly positive for IAV NP by IHC. However, many severely affected bronchioles were completely denuded of their epithelium with only exfoliated cellular debris positive for NP.

Table 4.1.2 Lung parameters & Immunohistochemistry

Nr	Virus dose ($TCID_{50}$)	Relative lung weight[a]	Affected lung (%)	Immunohistochemistry of respiratory tract epithelium[b]					
				Nasal cavity	Tra-chea	Bronchi		Bron-chioles	Alveoli
						Glands	Lining		
1	10^5	2.08	50	–	+	+	+	+	++
2		1.21	30	–	+	+	+	++	++
3	10^6	2.52	50	–	+	++	+	+	++
4		1.74	90	–	++	+	+	+	++
5		1.70	50	–	–	+	+	++	++
6	10^7	3.94	90	+	+	+	+	++	++
7		3.87	90	+	–	+	+	+	++
8	10^8	2.99	90	++	+	++	+	+	++
9		2.28	90	++	–	++	+	++	++

[a] Relative lung weight = (lung weight/body weight) × 100%.

[b] Semiquantative parameter for number of influenza A virus NP positive cells in IHC: **–** = none, **+** = some, **++** = many.

The pattern of inflammation and/or alveolar damage was comparable between all animals, whereas the severity and extent varied in relation to virus doses inoculated. All animals suffered from an acute necrotising (broncho)interstitial pneumonia whilst

the severity combined with the extent ranged from moderate (**Figure 4.1.2B** and **C**) to severe (**Figure 4.1.2E** and **F**). Affected alveoli were centered more or less around inflamed bronchioles in the moderate cases, and were coalescing into extensive affected areas in the more severe cases. Within the affected alveoli the septa were only slightly thickened with some oedema fluid and infiltrated neutrophils, and lesser macrophages and lymphocytes, without noticeable type II pneumocyte hyperplasia. The lining pneumocytes were mostly necrotic and exfoliated in the affected alveolar areas. In the moderate cases the outlines of the affected alveolar septa were present, whereas in the most severe cases the alveolar septa were completely necrotic and their outlines poorly discernable or sometimes even collapsed. The alveolar lumina were markedly flooded by protein rich oedema fluid containing neutrophils, macrophages, erythrocytes, degenerated exfoliated cells or cellular debris, and many fibrin strands. These lesions within the alveoli co-localised with lining and exfoliated pneumocytes strongly positive for IAV NP by IHC. All of the animals' brains including olfactory bulbs were negative for IAV NP by IHC, and histopathology confirmed the slight hepatic lipidosis in all animals. The animals displayed some estrous activity but no bone marrow depression as a result of that and no further abnormalities were observed.

DISCUSSION

Despite the low pathogenic classification of H7N9 LPAIV for poultry, it does cause high morbidity and mortality in ferrets experimentally infected by the intratracheal route. All animals developed clinical signs of severe disease caused by severe viral pneumonia. A higher infectious dose correlated with earlier onset of disease and a more severe outcome and ultimately death within the time frame of the study.

Virus replication was detected both in the upper and lower respiratory tract of all animals in this study, which can be explained by the receptor specificity of the H7 hemagglutinin. The receptor binding pocket mutation Q226L that is found in this virus is associated with a shift in receptor preference of the virus from α2,3 to α2,6-linked sialic acids (38). The exact receptor specificity of the avian influenza A(H7N9) virus has to be determined but it seems that the virus can bind to both α2,3 to α2,6-linked sialic acids. The latter are predominant in the upper respiratory tract, thus correlating with the rhinitis found in the animals inoculated with 10^7 and 10^8 $TCID_{50}$ (n = 4). Most likely, due to the high viral load in these animals, the virus was able to spread more easily from the pharynx to the nasal cavity and was able to replicate there, resulting in inflammation of the nasal turbinates.

Besides replication in the upper respiratory tract the virus was also detected in the lower respiratory tract, most likely associated with the α2,3-linked sialic acids

that are found primarily deep In the lung, thus explaining the severe viral pneumonia observed here. Conclusively the H7N9 LPAIV can infect cells both in the upper and lower respiratory tract, similar to pH1N1 influenza virus (506). H5N1 HPAIVs on the contrary primarily replicate in the lower respiratory tract and are able to spread to the central nervous system (CNS) and other solid organs. In the current study the H7N9 LPAIV did not spread outside the context of the respiratory tract. However the fact that within the respiratory tract the virus could spread to the upper region has implications for the risk assessment of the virus. The receptor distribution and binding of human and avian influenza viruses in the respiratory tract of the ferret is similar to that of humans. And since the virus is capable of spreading upwards through the respiratory tract this increases the risk of virus excretion, which could lead to transmission (43, 50, 551).

In the N9 neuraminidase of the H7N9 LPAIV a deletion was detected. The lack of these five specific amino acids has been associated with enhanced virus replication and alteration of the virus tropism (38). Apart from receptor specificity, the avian influenza A(H7N9) virus has additional pathogenicity markers. The L89V and especially the E627K mutation, associated with enhanced polymerase activity and enhanced virulence in the context of avian influenza A(H5N1) virus, are present in the polymerase protein PB2 of the influenza virus A/Anhui/1/2013 (38). The presence of these markers may account for the severe viral pneumonia that the virus causes in humans and in the ferret model described here.

This study illustrates the potential of the 'low pathogenic' H7N9 LPAIV to infect the lower respiratory tract of mammals and cause severe viral pneumonia in a manner that is comparable to H5N1 HPAIV. This raises questions about whether the pathogenicity classification of avian influenza viruses should not also take into account the pathogenicity phenotype of the virus in mammals. Taken together the data presented in this paper illustrate that intratracheal H7N9 LPAIV infection of ferrets, like other infections with different influenza virus subtypes, can be used to investigate the pathogenesis of this infection in mammals, as well as urgently needed intervention strategies like vaccination and the use of antivirals.

Acknowledgements

The authors would like to thank the Pandemic Influenza Preparedness (PIP) Network and Dr. Shu (CDC, China) and Dr. J. McCauley (Mill Hill, Londen, UK) for providing the avian influenza A(H7N9) virus. D. van Riel, W. van Aert, R. Boom, S. Berkhof and P. Nuijten provided excellent technical assistance. JK and AO are sponsored by ERC Grant Fluplan250136 and ERC GrantARCAS 324634. RF is sponsored by NIAID-NIH contract HHSN266200700010C. PR and TK are sponsored by FP7 contract 278976 ANTIGONE. The authors KS, EVK and LdW are fulltime employed by Erasmus MC spin-off company ViroClinics BioSciences B.V. GvA, GR and AO are part-time employed by ViroClinics BioSciences B.V. of which AO is chief scientific officer.

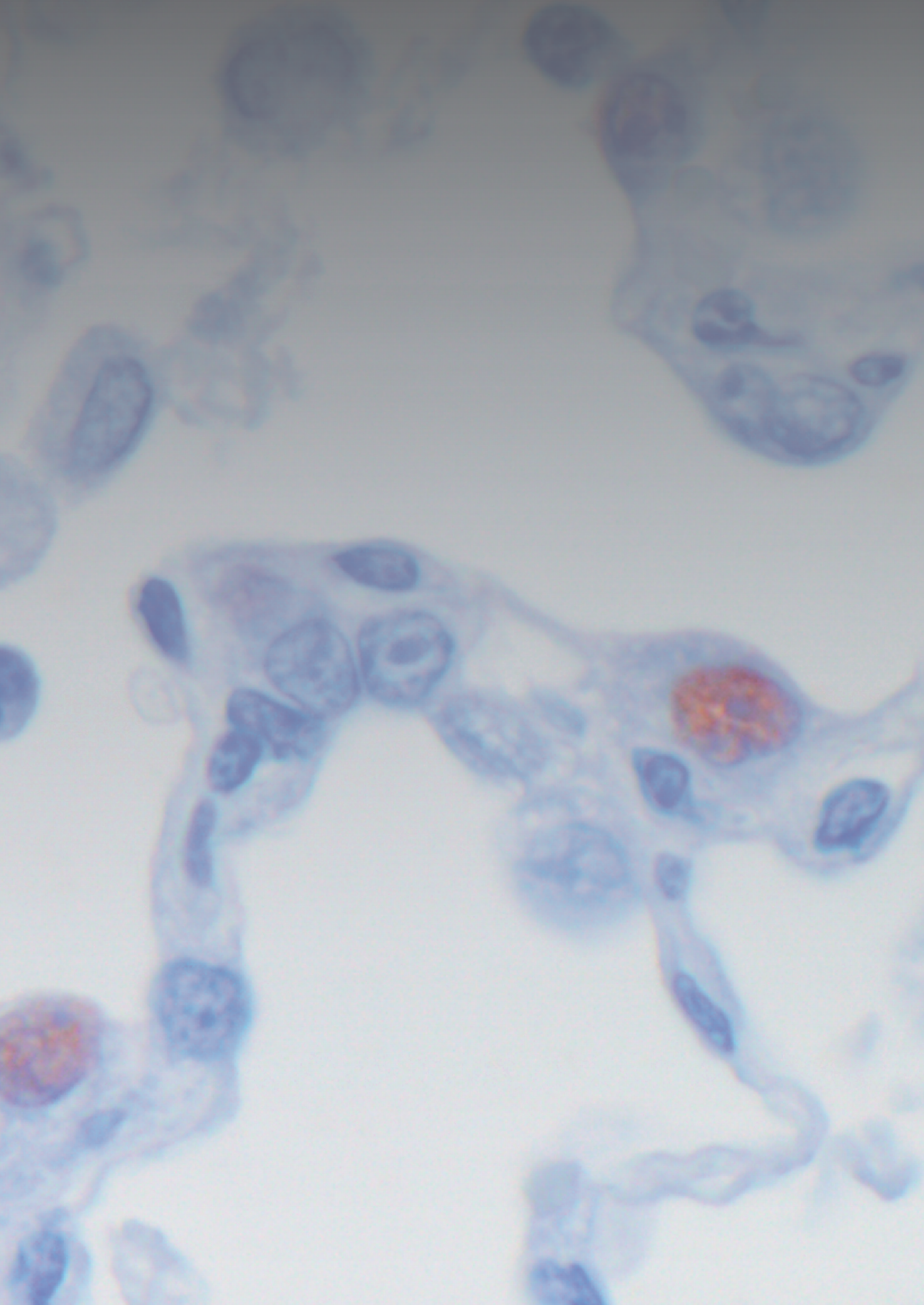

4.2

Multidrug resistant 2009 A/H1N1 influenza clinical isolate with a neuraminidase I223R mutation retains its virulence and transmissibility in ferrets

E. van der Vries[1], E.J.B. Veldhuis Kroeze[1,2], K.J. Stittelaar[2], M. Linster[1], A. van der Linden[1], E.J.A. Schrauwen[1], L.M. Leijten[1], G. van Amerongen[2,3], M. Schutten[1], T. Kuiken[1], A.D.M.E. Osterhaus[1,2], R.A.M. Fouchier[1], C.A.B. Boucher[1] & S. Herfst[1]

PLOS Pathogens 2011; 7: e1002276

Affiliations
[1]Department of Viroscience, Erasmus Medical Center, Rotterdam, The Netherlands
[2]Viroclinics Biosciences B.V., Rotterdam, The Netherlands
[3]Netherlands Vaccine Institute, Bilthoven, The Netherlands

ABSTRACT

Only two classes of antiviral drugs, neuraminidase inhibitors and adamantanes, are approved for prophylaxis and therapy against influenza virus infections. A major concern is that influenza virus becomes resistant to these antiviral drugs and spreads in the human population. The 2009 pandemic A/H1N1 influenza virus is naturally resistant to adamantanes. Recently a novel neuraminidase I223R mutation was identified in an A/H1N1 virus showing cross-resistance to the neuraminidase inhibitors oseltamivir, zanamivir and peramivir. However, the ability of this virus to cause disease and spread in the human population is unknown. Therefore, this clinical isolate (NL/2631-R223) was compared with a well-characterised reference virus (NL/602). *In vitro* experiments showed that NL/2631-I223R replicated as well as NL/602 in MDCK cells. In a ferret pathogenesis model, body weight loss was similar in animals inoculated with NL/2631-R223 or NL/602. In addition, pulmonary lesions were similar at day 4 post inoculation. However, at day 7 post inoculation, NL/2631-R223 caused milder pulmonary lesions and degree of alveolitis than NL/602. This indicated that the mutant virus was less pathogenic. Both NL/ 2631-R223 and a recombinant virus with a single I223R change (recNL/602-I223R), transmitted among ferrets by aerosols, despite observed attenuation of recNL/602-I223R *in vitro*. In conclusion, the I223R mutated virus isolate has comparable replicative ability and transmissibility, but lower pathogenicity than the reference virus based on these *in vivo* studies. This implies that the 2009 pandemic influenza A/H1N1 virus subtype with an isoleucine to arginine change at position 223 in the neuraminidase has the potential to spread in the human population. It is important to be vigilant for this mutation in influenza surveillance and to continue efforts to increase the arsenal of antiviral drugs to combat influenza.

AUTHOR SUMMARY

Recently, a 2009 pandemic A/H1N1 influenza virus was isolated from an immune compromised patient, with antiviral resistance to the neuraminidase inhibitor class of drugs. This virus had an amino acid change in the viral neuraminidase enzyme; an isoleucine at position 223 was substituted for an arginine (I223R). Patients infected with a pandemic virus that is resistant to all neuraminidase inhibitors, would leave physicians without antiviral treatment options, since these viruses are naturally resistant to the other class of antivirals, the adamantanes. To date, it is unknown if this I223R mutant virus is affected in its ability to cause severe disease and to transmit to other humans. Therefore, we have addressed this question by comparing the I223R mutant virus with a wild type reference virus in a ferret pathogenicity and transmission model. We found that the I223R mutant virus was not severely affected in its pathogenicity, although fewer lung lesions and alveolitis scores were found for the I223R mutant virus. In addition, we demonstrated that this virus transmitted efficiently to naive ferrets. Consequently, we conclude that this I223R mutant virus has the potential to cause disease and may spread among humans. Therefore, influenza surveillance for this resistance pattern is advised.

INTRODUCTION

Two classes of antiviral drugs are approved for prophylaxis and therapy of influenza virus infected patients (552). Antiviral therapy against the new (swine-origin) 2009 pandemic A/H1N1 influenza virus relies on the neuraminidase inhibitor (NAI) class of antiviral drugs only, because this subtype is resistant to the adamantane class (amantadine and rimantadine) of drugs (553). In 2009 pandemic influenza viruses, this resistance pattern is mainly caused by an asparagine at amino acid position 31 (N31) in the viral M2 membrane protein. Fortunately, NAI treatment, both as prophylaxis and therapy, has been shown to be effective against most 2009 pandemic H1N1 virus infections so far (554, 555).

To date, the incidence of NAI resistant 2009 pandemic A/ H1N1 viruses is very low. Nevertheless, 565 cases of patients infected with an (H275Y, N1 numbering) oseltamivir (OS) resistant virus have been reported to the World Health Organisation (556). In most of these cases, OS resistance was found in patients receiving prolonged antiviral therapy, in particular patients under immunosuppressive therapy (74). The H275Y mutant viruses are cross-resistant to peramivir (PER), but remain susceptible to zanamivir (ZA). Successful clearance of a H275Y mutant virus from a patient treated with ZA was reported previously (557).

Within the first years after approval of the NAIs in 1999, antiviral resistance in influenza viruses at a population level was rare (0.4%). In clinical trials, the incidence of resistant viruses was higher, varying from 0.4 to 1% in adults and up to 18% in young children (558, 559). However, a dramatic increase, up to 100%, of de novo circulating oseltamivir-resistant A/H1N1 viruses characterised the epidemic seasons of 2007-2008 and 2008-2009 (560, 561). This resistance phenotype was also caused by a H275Y mutation. Remarkably, earlier studies on H275Y mutant H1N1 viruses had characterised these viruses as attenuated and not of clinical importance (562-564). The resistant viruses from 2007-2008 did not seem to be affected in replication capacity, transmissibility and their ability to cause severe disease in humans (565-567). A compensatory role was assigned to the NA amino acid changes V234M, R222Q and D344N (568, 569). These substitutions may have restored the initial loss of NA activity due to the NAI resistance mutation and facilitated the appearance of the H275Y change in the epidemic influenza A/H1N1 viruses that circulated before the 2009 outbreak of the new pandemic virus. Recently, several research groups have studied the fitness of H275Y mutant pandemic influenza A/H1N1 viruses using both *in vitro* and *in vivo* experiments (570-574). Overall, these data indicate that pandemic viruses with the NA H275Y substitution were comparable to their oseltamivir susceptible counterparts in pathogenicity and transmissibility in animal models.

Recently, the identification of a novel multidrug resistant 2009 pandemic A/H1N1 virus was reported, isolated from an immune compromised child with reduced susceptibility to all NAIs (75). An isoleucine to arginine substitution at position 223 in NA (I223R, N1 numbering) was detected in the patient after antiviral therapy with OS had failed due to the emergence of the H275Y mutation and therapy was switched to ZA. This I223R containing isolate, in which the H275Y mutation had disappeared, showed reduced susceptibility to OS (45-fold), PER (7-fold) and ZA (10-fold). *In vitro* analysis showed that reversion of the arginine to isoleucine fully restored NAI susceptibility. In another case, an I223R/H275Y double mutant virus was isolated that showed high resistance to the NAIs (575). In combination with the natural resistance of pandemic A/H1N1 viruses to adamantanes, an infection of such a multi-drug resistant virus leaves physicians without antiviral treatment options. The emergence of this pandemic 2009 A/ H1N1 virus prompted us to investigate the properties of this clinical isolate by evaluating its *in vitro* replication kinetics and its pathogenicity and transmissibility in the ferret model. We here show that this 2009 pandemic influenza A/H1N1 clinical isolate, harboring a neuraminidase I223R substitution retains its virulence and transmissibility, but is less pathogenic than a virus prototype without this mutation. In addition, recombinant NL/602/09 with a single I223R amino acid substitution transmitted as well as its recombinant parental virus, suggesting that no additional mutations are needed

to compensate for the presence of this I223R mutation in the 2009 pandemic A/H1N1 virus backbone.

MATERIALS & METHODS

Ethics statement

Animals were housed and experiments were conducted in strict compliance with European guidelines (EU directive on animal testing 86/609/EEC) and Dutch legislation (Experiments on Animals Act, 1997). All animal experiments were approved by the independent animal experimentation ethical review committee 'stichting DEC consult' (Erasmus MC permit number EUR1821) and were performed under animal BSL3 conditions. Animal welfare was observed on a daily basis, and all animal handling was performed under light anesthesia using ketamine to minimize animal suffering. Influenza virus seronegative 6-month-old female ferrets (*Mustella putorius furo*), weighing 800–1000 g., were obtained from a commercial breeder.

Cells and viruses

MDCK cells were obtained from American Type Culture Collection. MDCK-SIAT1 cells, constitutively expressing the human 2,6-sialyltransferase (SIAT1), were kindly provided by Professor H.D. Klenk, Philipps University Marburg (576). Both cell lines were cultured in Eagle's minimal essential medium (EMEM) (Lonza, Breda, The Netherlands) supplemented with 10% FCS, 100 IU/ml penicillin, 100 mg/ml streptomycin, 2mM glutamine, 1.5mg/ml sodium bicarbonate (Cambrex), 10 mM HEPES (Lonza) and non-essential amino acids (MP Biomedicals Europe, Illkirch, France). In addition, MDCK-SIAT1 cells were cultured in the presence of 1 mg of antibiotic G418/ml. Influenza virus A/Netherlands/2631_1202/2010 (NL/2631-R223) was isolated from a 5-year-old immune compromised child (75). Clonal virus of this isolate was obtained by passaging this virus 3 times under limiting diluting conditions in MDCK cells. Full genome sequencing after the last MDCK passage confirmed the absence of mutations. Influenza A/Netherlands/602/2009 (NL/602) was characterised previously (508). All eight segments of this virus were cloned in a bidirectional reverse genetics plasmid pHW2000 and used to generate recombinant viruses by reverse genetics as described previously (538). The I223R mutation was introduced in the NA gene of NL/602 using QuickChange multi site-directed mutagenesis kit (Stratagene, Leusden, The Netherlands) resulting in recombinant viruses recNL/602-I223R. The presence of this mutation was confirmed by sequencing.

Virus titrations

Virus titers in nasal and throat swabs, homogenised tissue samples, or samples for replication curves were determined by endpoint titration in MDCK cells. MDCK cells were inoculated with 10-fold serial dilutions of each sample, washed 1 hour after inoculation with PBS, and grown in 200 ml of infection medium, consisting of EMEM supplemented with 100 U/ml penicillin, 100 mg/ml streptomycin, 2 mM glutamine, 1.5 mg/ml sodium bicarbonate, 10 mM HEPES, nonessential amino acids, and 20 mg/ml trypsin (Lonza). Three days after inoculation, the supernatants of inoculated cell cultures were tested for agglutinating activity using turkey erythrocytes as an indicator of virus replication in the cells. Infectious-virus titers were calculated from 4 replicates by the method of Spearman-Kaerber (536).

Replication curves

Multi-cycle replication curves were generated by inoculating MDCK or MDCK-SIAT1 cells at a multiplicity of infection (MOI) of 0.001 $TCID_{50}$ per cell. One hour after inoculation, at time point 0, the cells were washed once with PBS, and fresh infection medium was added. The supernatants were sampled at 6, 12, 24, and 48 h post infection and the virus titers in these supernatants were determined by means of endpoint titration in MDCK cells.

Animal experiments

The pathogenesis experiment was done as described previously with some minor changes in the protocol (506). On day 0, the ferrets were inoculated intratracheally with 10^6 $TCID_{50}$ of NL/602 or NL/2631-R223. Throat and nose swabs were collected daily to determine virus excretion from the upper respiratory tract. Animals were weighted daily as indicator of disease and observed for clinical signs. Three animals from each group were euthanised and autopsied at days 4 and 7, and trachea and lung samples were collected to study virus distribution.

Autopsy was done by opening the thoracic and abdominal cavities and examining all major organs. Whilst inflated, all lung lobes (left cranial lobe, left caudal lobe, right cranial-, middle- and caudal lobes and accessory lobe) were evaluated. The extent of consolidation was estimated by visual assessment. The lungs were weighed after the trachea was removed at its bifurcation. The relative lung weights were calculated as proportion of the body weight on day of death (lung weight/body weight x 100). Tissues (~0.4 g) from the right lung were collected for determination of lung virus titers at 4 and 7 dpi. The left lung and trachea were collected for histological examination, and immersed for fixation in 10% neutral-buffered formalin. All samples were sectioned in a standardised way (a total of 4 lung sections per animal; 1 cross section and 1 longitudinal section from both the left cranial and left caudal lobe, and 1 central

tracheal cross section) and routinely processed, paraffin embedded and cut to 4 µm H&E stained slides. The samples were histologically examined for the character and severity of influenza virus–associated lesions without knowledge of the identity of the animals. The extent of alveolitis/ alveolar damage (0=0%, 1≤25%, 2=25-50%, 3=≥50% of a section) and the severity of alveolitis, bronchi(oli)tis (including bronchial submucosal glands) and tracheitis (0 = none, 1 = few, 2 = moderate number, 3 = many inflammatory cells) were scored per slide. The overall histology score for alveolitis is the sum of the scores for the extent and severity of the alveolitis (score 0 to 6).

The transmission experiments were done as described previously (508). The transmission cages were specifically designed to allow transmission experiments to be conducted in negatively pressurised isolator cages (1.6m x 1m x 1m). On day 0, 4 or 2 female ferrets were housed individually in transmission cages (30cm x 30cm x 55cm, W x H x L) and inoculated intranasally with 10^6 $TCID_{50}$ of NL/602, NL/2631-R223, recNL/602 or recNL/602-I223R respectively, divided over both nostrils (2 x 250 µl). On day 1, 4 or 2 naive female ferrets were individually placed in a transmission cage adjacent to an inoculated ferret, separated by two stainless steel grids. Negative pressure within the isolator cage is used to direct a modest (~0.1 m/sec) flow of HEPA filtered air from the inoculated to the naive ferret. This experimental setup was designed to prevent direct contact or fomite transmission, but to allow airflow, thereby permitting transmission via aerosol or respiratory droplets. Nasal and throat swabs were collected on 0, 1, 2, 3, 5 and 7 dpi from the inoculated ferrets and on 0, 1, 2, 3, 5 and 7 days post exposure (dpe) from the naive ferrets. Inoculated ferrets were euthanised at 7 dpi and naive ferrets that were found positive by reverse transcription polymerase chain reaction at 7 dpe were also euthanized (577). Naive animals that remained negative for virus excretion throughout the experiment were euthanised at 15 dpe, and a blood sample was collected for serology. Virus titers in the collected swabs were determined by means of endpoint titration in MDCK cells.

Statistical analysis

For the pathogenesis experiment, statistical analysis was done for each time point, until 4 dpi (when there were still 6 animals present in each group). The Mann-Whitney-U test was used to compare weight losses and virus shedding of the six animals in both groups. P-values less than 0.05 were considered significant.

RESULTS

Sequence comparison of virus isolates

A pandemic 2009 influenza virus with reduced susceptibility to all NAIs that was isolated from a Dutch immune compromised child was studied here. Full genome sequencing of this clinical isolate A/NL/2631_1202/2010 (NL/2631-R223, GenBank accession numbers JF906180-906187) harboring an I223R mutation in the neuraminidase was performed. Since no drug susceptible virus had been isolated from this patient before start of antiviral therapy, the well-characterised NAI-susceptible virus isolate A/ NL/602/2009 (NL/602, GenBank accession numbers CY046940- 046945 and CY039527-039528) was used as a reference virus in all experiments. This reference virus is a representative of pandemic H1N1 viruses that circulated in 2009, with only amino acid changes I108V and V407I (N1 numbering) in NA being unusual among the deposited sequences in the Influenza Research Database (508, 578). Pair-wise comparison revealed, in addition to the amino acid change I223R, 5 amino acid differences in NA (V106I, V108I, N248D, N386D and I407V) and 1 in HA (S203T). The NA and HA amino acid positions are given according to the N1 and H1 numbering. Eleven additional amino acid differences were found in gene segments PB2 (3), PB1 (2), PA (2), NP (3) and NS (1) compared to NL/602. None of these mutations have previously been identified as a virulence marker or as a compensatory mutation involved in restoration of NA activity loss, as a result of the presence of resistance mutations. By studying these isolates, a direct comparison could be made between a NAI susceptible and a novel I223R resistant virus, but such comparison does not address the impact of the single I223R mutation directly. Therefore, we introduced the I223R mutation in the recNL/602 backbone, resulting in the drug-resistant recNL602-I223R, to evaluate the impact of the single I223R mutation on virus replication, virus shedding from the upper respiratory tract and transmissibility in the ferret model.

I223R Harbouring isolate is not attenuated in vitro

Virus replication was studied *in vitro* by multi-cycle replication kinetics of the viruses of interest. For this purpose, MDCK or MDCK-SIAT1 cell cultures were inoculated at a multiplicity of infection of 0.001 $TCID^{50}$ per cell and at fixed time points supernatants were harvested to determine viral titers (**Figure 4.2.1**). Overall, the initial virus replication rates and end point titers were similar for the clinical isolate NL/2631-R223 and recNL/602. A recombinant derivative of NL/602 with the I223R mutation in NA (recNL/602-I223R) replicated to lower peak titers in both cell lines compared to recNL/602 and NL/2631-R223. In addition, initial virus replication of recNL/602-I223R was delayed by 6 to 12 hours in MDCK-SIAT1 cells.

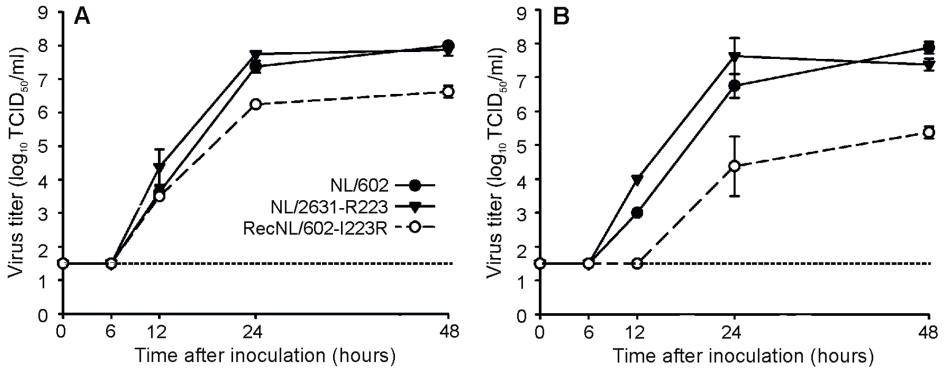

Figure 4.2.1 Replication kinetics in MDCK or MDCK-SIAT1 cells. MDCK (panel A) or MDCK-SIAT1 (panel B) cells were inoculated with 0.001 $TCID_{50}$ virus per cell of recNL/602 (black circles), isolate NL/2631-R223 (black triangles) and recNL/602-I223R (open circles). Supernatants were harvested after 6, 12, 24, and 48 hours post infections and were titrated in MDCK cells. Geometric mean titers and standard deviations were calculated from two independent experiments. The lower limit of detection is indicated by the dotted line.

No marked differences in virus replication in the respiratory tract of ferrets

The pathogenicity of clinical isolate NL/2631-R223 was compared with NL/602 in the ferret model that was previously established to study the ability of influenza viruses to cause pneumonia (506). Two groups of 6 ferrets were inoculated intratracheally with 10^6 $TCID_{50}$ of virus. The animals were weighed daily as an indicator of disease. Over the 7-day period, no significant differences were observed in weight loss between the two groups inoculated with either virus. At 4 dpi, when there were still 6 animals present in each group, the mean percentage of weight loss was 8.2±2.4% and 7.6±6.7% for NL/602 and NL/2631-R223-inoculated animals respectively, not statistically significant (**Figure 4.2.2A** and **B**). In addition, no marked differences were observed for other clinical parameters, such as lethargy, sneezing and interest in food.

Nose and throat swabs were collected daily from the inoculated animals and virus titers were determined by end-point titration in MDCK cells. Infectious virus shedding from the throat was detected from 1 dpi onwards in all ferrets, with similar patterns of virus shedding from the throat of the animals in the two groups (**Figure 4.2.2C**). At 4 dpi, 5 and 4 animals were shedding virus from the nose in the NL/602 and NL/2631-R223 inoculated group respectively (**Figure 4.2.2D**). Sequence analysis confirmed the presence of the I223R mutation in the respiratory samples collected at 7 dpi from the NL/2631-R223 inoculated ferrets.

At 4 and 7 dpi, three animals of each group were euthanised and lungs were collected for virological and pathological examination. At 4 dpi, no marked differences were found between the virus titers for both groups of ferrets (**Figure 4.2.3A**). At 7 dpi, no virus was detected in the lungs of ferrets inoculated with either virus.

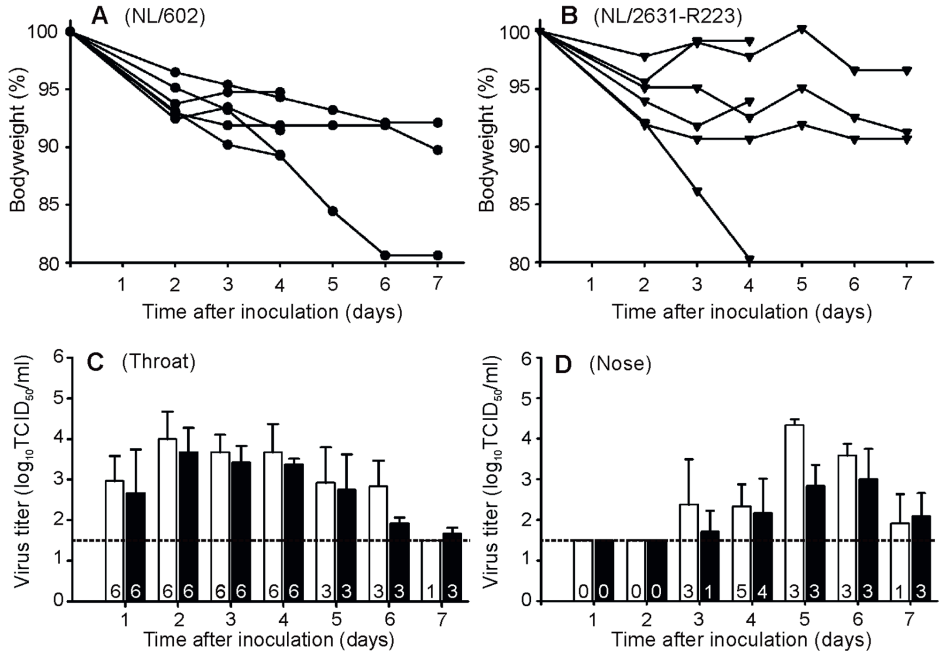

Figure 4.2.2 Ferret relative weight loss and virus shedding from the ferret upper respiratory tract. Ferrets were inoculated intratracheally with 1×10^6 $TCID_{50}$ of NL/602 or NL/2631-R223. Body weights for NL/602 (Panel A) and NL/2631-R223 (Panel B) inoculated animals are depicted as percentage of body weight relative to the time of inoculation. Data are shown for individual animals until the animals were euthanised at 4 or 7 dpi. Virus detection in throat (panel C) and nose swabs (panel D) is indicated for NL/602 (white bars), and NL/2631-R223 (black bars). Geometric mean titers from 6 (day 1 to 4) or 3 animals (day 5 to 7) are displayed and the error bars indicate the standard deviations. The number of influenza virus positive animals per day is depicted in each bar. The lower limit of detection is indicated by the dotted line.

Moderate pathogenicity of I223R harbouring isolate

Gross pathology of the lungs of all animals revealed pulmonary lesions at 4 and 7 dpi (**Figure 4.2.3B**). At 4 dpi, no marked difference was observed between the groups, but at 7 dpi, the percentage of affected lung tissue was higher in the group inoculated with NL/602. The mean relative lung weight increased from day 4 to day 7, with no difference between the animals inoculated with NL/602 or NL/2631-R223 (**Figure 4.2.3C**). Histopathological examination of the lungs showed multifocal to coalescing alveolar damage in both groups characterised by the presence of macrophages and neutrophils within the lumina and thickened alveolar walls. At 4 dpi, the severity of alveolitis did not differ between the two groups (**Figure 4.2.4D**). However, in agreement with the increased percentage of affected lung tissue at 7 dpi (**Figure 4.2.3B**), also higher alveolitis scores were determined for the NL/602 inoculated animals at 7 dpi. (**Figure 4.2.4D**). The bronchial and bronchiolar epithelium from ferrets in both groups showed slight multifocal necrosis with moderate intra-epithelial infiltrates of neutrophils and

multifocal peribronchiolar infiltration of macrophages, lymphocytes, neutrophils and plasma cells. The lumina contained moderate amounts of mucus mixed with cellular debris and few neutrophils. The tracheal epithelium in both groups showed mild neutrophilic infiltrates. The severity of both bronchiolitis and tracheitis increased from 4 to 7 dpi in ferrets infected with both viruses, but the differences in scores between groups were minimal (**Figure 4.2.4E** and **F**).

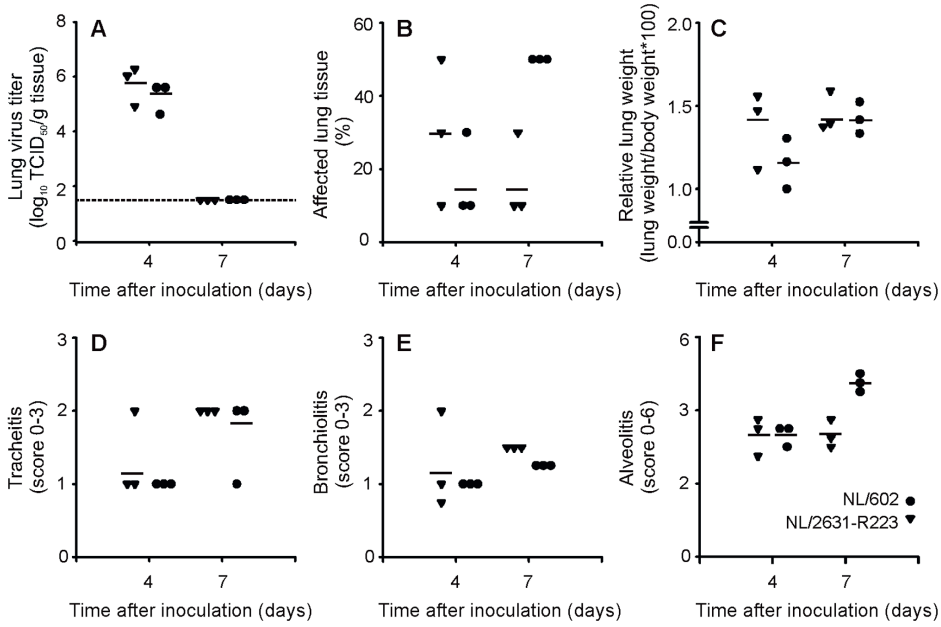

Figure 4.2.3 Semi-quantitative lung scores and histological examination of the infected ferret respiratory tract. Lung virus titers (panel A), percentage of affected lung tissue (panel B) and relative lung weights (panel C) were determined for lungs of ferrets inoculated with NL/2631-R223 (triangles) or NL/602 (circles) that were euthanised at 4 or 7 dpi. Semi-quantitative assessment of the extent and severity of the tracheitis (panel D), bronchiolitis (panel E) and alveolitis (panel F) are shown. Individual values are displayed. In panel A, the lower limit of detection is indicated by a dotted line.

I223R Harbouring isolate is transmissible via aerosols or respiratory droplets

Individually housed ferrets were inoculated with virus isolate NL/2631-R223 or NL/602 and naive animals were placed in a cage adjacent to each inoculated ferret at 1 dpi to allow aerosol or respiratory droplet transmission. All inoculated ferrets started to shed virus at 1 dpi with virus titers up to 10^6 $TCID_{50}$/ml in throat and nose swabs (**Figure 4.2.4A** and **C**).

The naive ferrets became infected, because of aerosol or respiratory droplet transmission, 1, 2 or 3 dpe. In the naive animals, virus was detected in 4 (NL/602), or 3 (NL/2631-R223) out of 4 animals (**Figure 4.2.4B** and **D**). The exposed animal in

the NL/2631-R223 transmission experiment, from which no virus could be isolated, did not seroconvert in the course of the experiment. At 5 dpe, the presence of the I223R mutation was confirmed by sequencing the NA gene of virus isolated from the throat swabs of the positive animals.

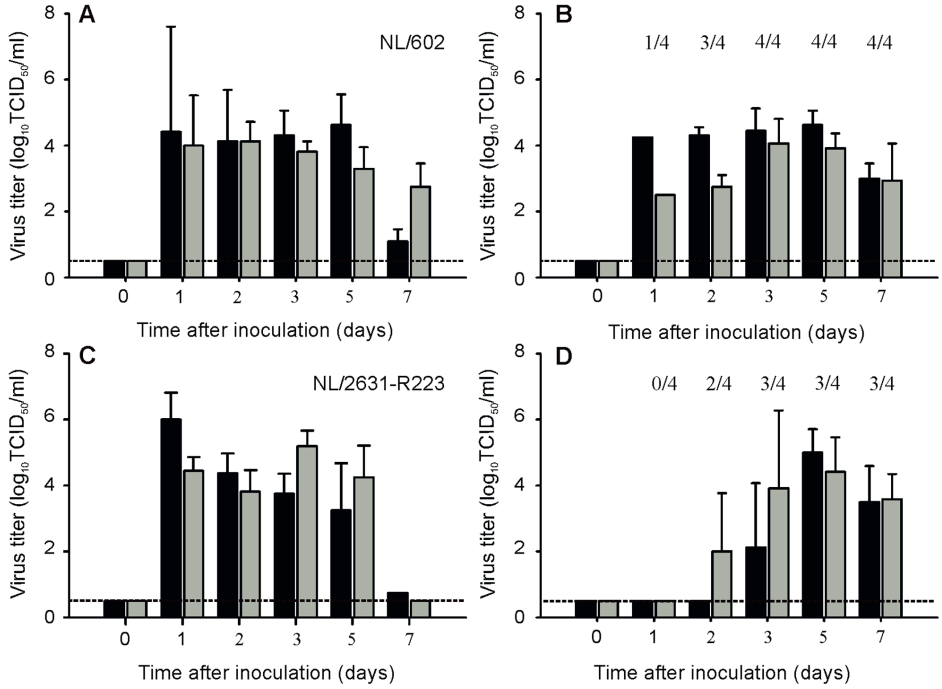

Figure 4.2.4 Transmission of NL/602 and NL/2631-R223 by aerosol or respiratory droplets in ferrets. Virus titers in throat (black bars) and nose swabs (grey bars) are displayed for inoculated (panel A and C) and exposed ferrets (panel B and D). The geometric mean titers of positive samples are displayed and the error bars indicate the standard deviations. The number of positive exposed animals per day is depicted. The lower limit of detection is indicated by the dotted line.

I223R Mutant transmits as well as parenteral reference virus

When the multi-cycle replication kinetics were studied of viruses with or without the I223R substitution in MDCK cells, it was noticed that the recombinant virus in which the I223R mutation was introduced, recNL/602-I223R, replicated to lower titers than its parental virus recNL/602 (**Figure 4.2.1**). To address if this difference in *in vitro* replication capacity could be extrapolated to reduced replication *in vivo*, the ability of recNL/602-I223R to transmit in the ferret model was studied. It was expected that reduced replication in ferrets would impede the virus to transmit to na¨ıve animals, thereby suggesting that compensatory mutations are needed to balance the fitness loss induced by the I223R mutation. In contrast to the results obtained in MDCK cells,

recNL/602-I223R replicated and transmitted as well as recNL/ 602 when evaluated in the ferret transmission model. Inoculated animals started to shed virus from the upper respiratory tract from 1 dpi onwards and transmission was detected in 4 out of 4 (recNL/602), or 2 out of 2 (recNL/602-I223R) naive animals from day 2 onwards (**Figure 4.2.5**). The presence of the I223R mutation in the recNL/602 backbone was confirmed in throat samples obtained from these animals at 5 dpe.

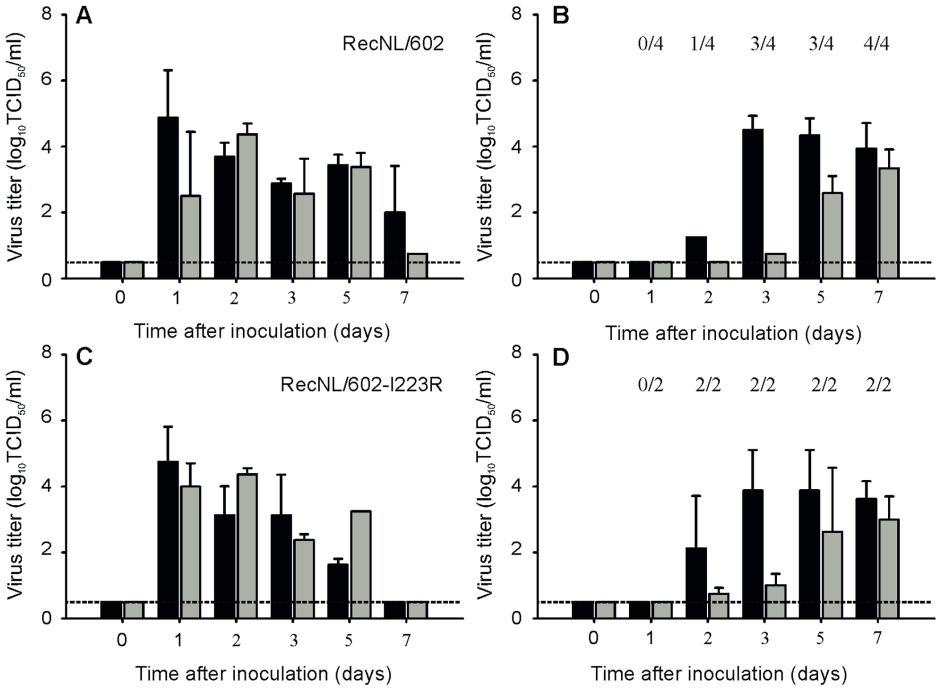

Figure 4.2.5 Transmission of recNL/602 and recNL/602-I223R by aerosol or respiratory droplets in ferrets. Virus titers in throat (black bars) and nose swabs (grey bars) are displayed for inoculated (panel A and C) and exposed ferrets (panel B and D). The geometric mean titers of positive samples are displayed and the error bars indicate the standard deviations. The number of positive exposed animals per day is depicted. The lower limit of detection is indicated by the dotted line.

DISCUSSION

Here, a 2009 pandemic influenza A/H1N1 virus isolate, harboring an I223R multidrug resistance mutation, was characterised by studying its replication capacity in MDCK cells and its pathogenicity and transmissibility in the ferret model. This I223R mutant virus is not attenuated for replication in the ferret respiratory tract and transmitted as well as NAI susceptible reference virus NL/602. Furthermore, it was demonstrated here that compensatory mutations for the I223R mutation are not required, since

recombinant NL/602 with a single I223R change transmitted as efficiently as its parental virus in ferrets.

To date, 2009 pandemic viruses with an amino acid substitution at position 223 have only sporadically been isolated from patients. A I223V/H275Y double mutant was detected in two closely residing patients who were treated with OS (579). Besides the I223R single mutant virus studied here, an I223R/H275Y double mutant was detected in an immune suppressed patient treated with OS and ZA (575). The combination of these mutations resulted in an increased NAI resistance pattern, as compared to the resistance induced by the single mutations. This emphasizes that neuraminidase position 223 is an important marker for antiviral resistance and may be a key residue in the emergence of influenza viruses with resistance to all NAIs, especially in combination with other resistance-associated mutations. So far, the incidence of 2009 pandemic viruses with a 223 change is very low. Notably, 2009 pandemic viruses were reported with a serine to asparagine change at position 247 (580). In combination with the H275Y change, these viruses demonstrated resistance patterns similar to the I223R/H275Y mutant.

In a pathogenesis experiment, no statistical significant differences were found when weight loss was compared of ferrets inoculated with clinical isolates NL/2631-R223 or NL/602 (**Figure 4.2.2A** and **B**). In agreement with high viral loads found in respiratory specimens collected from the patient who was infected with NL/2631-R223, high viral loads were detected in the throat of animals inoculated with the same virus. Overall, identical patterns of virus shedding were observed during the course of the experiment in the throats of animals inoculated with either virus. However, virus shedding from the nose could not be detected in all inoculated animals. Although virus shedding from the nose of NL/ 2631-R223-inoculated animals seem somewhat delayed in comparison with NL/602-inoculated animals, these differences were not significant due to the large variations within groups and small group size after 4 dpi (**Figure 4.2.2C** and **D**).

Both macroscopic and microscopic evaluation of the lungs of the ferrets at 4 dpi revealed no major differences in the percentage of affected lung tissue and relative lung weights between NL/2631-R223 and NL/602 (**Figure 4.2.3B** and **C**). However, at 7 dpi the lungs of ferrets inoculated with NL/2631-R223 had not further deteriorated, whereas the percentage of affected lung tissue had increased to 50% in the NL/602 inoculated animals (**Figure 4.2.3B**). This higher score for affected lung tissue in the NL/602-inoculated animals was also reflected by the higher score for the degree of alveolitis at 7 dpi compared to 4 dpi, whereas the alveolitis scores in the NL/2631-R223-inoculated animals at 4 and 7 dpi were similar. To recapitulate, both viruses replicated to the same extent in the respiratory tract of ferrets, but the NL/2631-R223 seemed less pathogenic compared to the NL/602 virus.

Despite the moderate pathogenicity of NL/2631-R223, this virus transmitted to 3 out of 4 exposed animals via aerosols or respiratory droplets (**Figure 4.2.4B**). This result

is comparable to the data obtained from NL/602, in which 4 out of 4 exposed animals got infected (**Figure 4.2.4D**) (508). This ferret transmission model was designed as a qualitative model for transmission and with the limited number of animals, quantitative information on virus transmission could not be obtained. Therefore, from these experiments it was concluded that both NL/2631-R223 and NL/602 transmitted via aerosols or respiratory droplets, although a delay in virus shedding by approximately 1 day was observed in the naive animals exposed to NL/2631-R223 (**Figure 4.2.4B** and **D**).

When the impact of the single I223R mutation in the recombinant NL/602 backbone on *in vitro* replication kinetics was evaluated, a reduction in virus replication in MDCK cells was noticed (**Figure 4.2.1**). In addition, the initial virus replication of NL/ 602-I223R on MDCK-SIAT1 cells started 6 to 12 hours later as compared to its parental virus (**Figure 4.2.1B**).

These results suggested that compensatory mutations may be required to accommodate the isoleucine to arginine substitution at position 223 in NA and emphasizes the importance of the viral backbone used to study resistance-associated mutations. However, when recNL/602-I223R was tested in the ferret transmission model, the virus transmitted to 2 out of 2 exposed animals (**Figure 4.2.5B**). When these results were compared with transmission data of recNL/602 (**Figure 4.2.5D**) (497), no differences were found in the onset of virus shedding and virus titers that were detected in the collected throat and nose swabs from the exposed animals. This observation demonstrates that the transmissibility of recNL/602-I223R is not significantly diminished or can at least not be studied using a ferret transmission model.

Although these results suggest that introduction of the I223R does not attenuate the virus, it cannot be ruled out that other mutations than 223R in NL/2631-R223 may have compensated for the initial loss of fitness due to the I223R mutation. Sequence comparison revealed 5 amino acid differences between NL/2631-R223 and NL/602. The only amino acid substitution that is located near the active site of the neuraminidase is at position 248, where NL/602 harbors an aspartic acid and NL/2631-R223 an asparagine. Interestingly, neighboring residue 247 has been linked to NAI resistance in combination with the H275Y mutation (580). Further research is needed to study the I223R resistance mechanism in competitive mixture experiments and potential co-mutations on a molecular level (581). To note, small differences between NL/602 and recNL/602 could be observed in replication capacity and transmission patterns in ferrets (**Figure 4.2.4** and **4.2.5**). Previously, differences were also found in pathogenesis experiments, where the wild type NL/ 602 was detected more abundantly in the lower airways of ferrets than recNL/602 (582). These observed differences may be a result of the use of a virus isolate rather than a virus generated by reverse genetics and to a different batch of ferrets used in the different studies. A direct comparison between virus isolates and recombinant viruses can, therefore, not be made.

The different inoculation routes and inoculation doses used for influenza research is subject of debate. The intratracheal route of inoculation is often used to study pathogenicity or to study the efficacy of vaccines to prevent lower respiratory tract infection. In contrast, the intranasal route of inoculation is used when transmissibility is studied. Unfortunately, these inoculation routes and inoculation doses do not accurately mimic the natural way of infection and may mask the fitness differences between the drug- resistant and drug sensitive viruses.

However, the recipient animals in the transmission experiment are infected via the natural route; aerosols or respiratory droplets shed by the donor ferret. The virus secretion pattern, which is the combination of the amount of virus secreted and the duration of virus shedding from the upper respiratory tract, of animals exposed to recNL/602 and rec/NL602-I223R are similar. This suggests that no marked differences in viral fitness are introduced by the single I223R mutation.

The present study demonstrates for the first time that a 2009 pandemic A/H1N1 clinical isolate containing a resistance mutation at position 223 in the NA is not attenuated in its replication capacity and transmissibility in a ferret model. Although the pathogenicity of this virus seems less severe compared to a relevant reference virus in the ferret model, it is unclear whether this moderate pathogenicity has implications for infections with multidrug-resistant viruses in humans. Continuous surveillance is needed to monitor the emergence of (novel) influenza viruses with reduced susceptibility to the NAIs or mutations that may facilitate the emergence of circulating multi drug resistant influenza viruses.

Acknowledgments

We thank Salin Chutinimitkul, Erin Sorrell, Dennis de Meulder and Peter van Run for excellent technical assistance.

Author Contributions

Conceived and designed experiments: EvdV EJVK KJS MS ADMEO RAMF CABB SH. Performed experiments: EvdV EJVK KJS ML AvdL EJAS LML GvA. Analyzed data: EvdV EJVK TK RAMF CABB SH. Contributed reagents/materials/analysis tools: MS CABB. Wrote paper: EvdV EJVK TK RAMF CABB SH.

CHAPTER 5

Pulmonary pathology of pandemic influenza A/H1N1 virus (2009) infected ferrets upon longitudinal evaluation by computed tomography

E.J.B. Veldhuis Kroeze[1,2], G. van Amerongen[1,3], M.L. Dijkshoorn[4], J.H. Simon[1], L. de Waal[1], I. Hartmann[4], G.P. Krestin[4], T. Kuiken[2], A.D.M.E. Osterhaus[1,2] & K.J. Stittelaar[1]

Journal of General Virology 2011; 92: 1854-1858

Affiliations

[1]Viroclinics Biosciences B.V., Rotterdam, The Netherlands

[2]Department of Viroscience, Erasmus Medical Center, Rotterdam, The Netherlands

[3]Netherlands Vaccine Institute, Bilthoven, The Netherlands

[4]Department of Radiology, Erasmus Medical Center, Rotterdam, The Netherlands

ABSTRACT

We investigated the development of pulmonary lesions in ferrets by means of computed tomography (CT) following infection with the 2009 pandemic A/H1N1 influenza virus and compared the scans with gross pathology, histopathology and IHC. Ground-glass opacities (GGOs) observed by CT-scanning in all infected lungs corresponded to areas of alveolar oedema at autopsy. These areas were most pronounced on day 3 and gradually decreased from days 4 to 7 post-infection. This pilot study shows that the non-invasive imaging procedure allows quantification and characterisation of influenza-induced pulmonary lesions in living animals under BSL3 conditions and can thus be used in pre-clinical pharmaceutical efficacy studies.

INTRODUCTION

The ongoing emergence of novel pathogens (583, 584) calls for the concomitant development of animal models that address their pathogenesis and assess the potential of preventive and therapeutic intervention strategies. For example, the emergence of the 2009 pandemic A/H1N1 influenza virus (pH1N1) highlighted the need for the rapid development of animal models that closely mimic the human infection (395, 506, 584). Studies on the pathogenesis of the disease and the timely assessment of the efficacy and safety of the rapidly developed vaccine candidates, antiviral drugs, antibody preparations and immune modulators, largely depend on newly developed animal models (395, 506, 507, 585, 586). However, in these models the assessment of virus-induced lesions is largely based on findings from an arbitrarily chosen time point after experimental infection. When evaluating infections with a peracute onset, significant early findings may be overlooked unless large numbers of animals are sacrificed at consecutive time points. Especially when dealing with outbred animals, like ferrets, evaluation and integration of consecutive findings from different animals may be speculative. In addition, working with highly pathogenic viruses like the pH1N1 virus when it emerged or with the highly pathogenic avian H5N1 influenza viruses, is limited to BSL3 laboratory settings. The complexity of working under these stringent restrictions also limits the possibilities to work with large numbers of animals sacrificed at consecutive time points. To overcome these limitations we performed repeated CT-scans of ferrets under BSL-3 conditions before and during infection with the pandemic H1N1 influenza (2009) virus. The pattern of influenza virus attachment and replication in the ferret respiratory tract is largely similar to that in humans (50, 508), making influenza virus infection of the ferret the model of choice to study human influenza.

METHODOLGY & RESULTS

The ferrets (*Mustela putorius furo*) used were approximately 8 months of age, females, all seronegative for antibodies against circulating influenza viruses and for antibodies against Aleutian disease virus. They were routinely housed and handled under BSL-3^{+} conditions in negatively pressurised and HEPA-filtered biocontainment isolator units, approved by an independent institutional laboratory animal ethics and welfare committee. Animal handling and scans were performed under general injection anaesthesia (ketamine 12.5 mg kg^{-1} and medetomidine-HCl 7.5 µg body weight kg^{-1}). Eight ferrets were inoculated intratracheally with 10^{6} $TCID_{50}$ of pandemic influenza virus A/Netherlands/602/2009 (pH1N1) as described previously (506, 585). The virus was propagated in MDCK cell cultures and the infectious dose was determined as described

previously (508), and titres calculated according to the method of Spearman–Karber (536). Virus shedding was monitored daily by collecting nasal and oropharyngeal swabs that were analysed for determination of viral loads by standard procedures (506), and expressed as log $TCID_{50}$. All animals had detectable levels of virus in their upper respiratory tract (**Figure 5.1**).

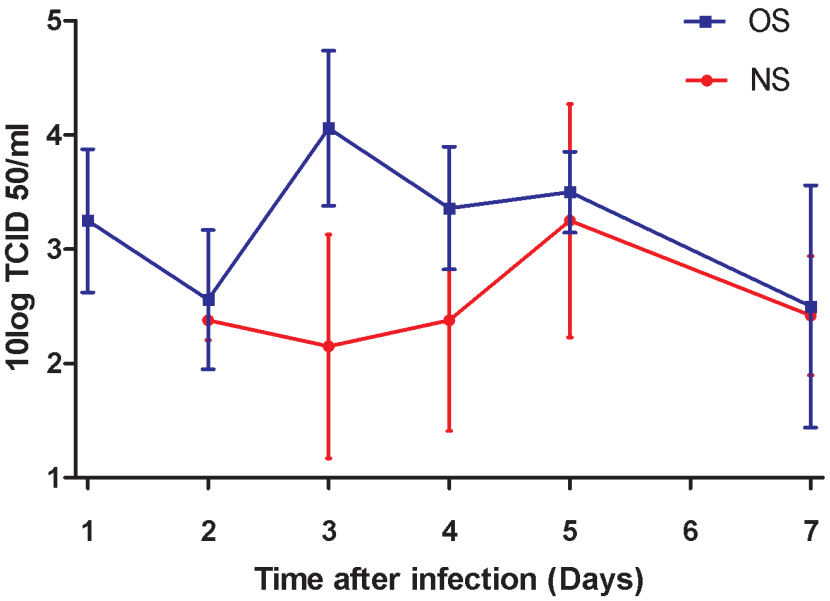

Figure 5.1 Graph depicting the mean virus loads of oropharyngeal swabs (OS) and nose swabs (NS) collected daily from all ferrets after intratracheal infection with 10^6 $TCID_{50}$ pH1N1 A/Netherlands/602/2009 until autopsy on days 4 and 7. Note the oropharyngeal virus peak of $10^{4.06}$ $TCID_{50}$ at 3 dpi, which indicates highest virus shedding from the respiratory tract at 3 dpi. The error bars designate the SD.

The CT-scanner used is a dual-source ultrafast system (Somatom Definition Flash; Siemens Healthcare) with a temporal resolution of 0.075 s and table speed of 458 mm/s, the spatial resolution is 0.33 mm. This CT-scanner requires short acquisition times (≈ 0.22 s) for data recording of an entire ferret thorax. Such a high temporal resolution enables accurate scanning of living ferrets without the necessity of breath holding, respiratory gating or electrocardiogram (ECG) triggering to generate sharp images. During *in vivo* scanning the anaesthetised ferrets were positioned in dorsal recumbency in a perspex biosafety container of approximately 8.3 litre capacity that was purposely designed and built (Tecnilab-BMI) (**Figure 5.2**). The oxygen concentration in the container did not drop below 14 % as measured by oxymetry. All animals had been scanned 3 days prior to virus inoculation to define the uninfected baseline status of the respiratory system.

Four ferrets (#3, #4, #5 and #7) were scanned twice (on days −3 and days 3 or 4), two ferrets (#2 and #8) were scanned three times (on days −3, 4 and 7) and two ferrets (#1 and #6) were scanned four times (on days −3, 3, 4 and 7; **Table 5.1**).

Figure 5.2 An anaesthetised and influenza virus (pandemic H1N1)-infected ferret is monitored for pneumonic (lung) changes by means of CT-scanning, while placed in a perspex biosafety container. The scanner requires very short acquisition times to scan the entire thorax (≈ 0.22 s) that disqualify the need for electrocardiogram (ECG)-triggered or respiratory-gated recordings.

Table 5.1 Scanning and autopsy schedule of the ferrets (*n*=8) before and after influenza virus inoculation

Ferret	Day										
	-3	-2	-1	0*	1	2	3	4	5	6	7
1	CT						CT	CT			CT+MR, autopsy
2	CT							CT			CT+MR, autopsy
3	CT							CT+MR, autopsy			
4	CT						CT, autopsy				
5	CT							CT+MR, autopsy			
6	CT						CT	CT			CT+MR, autopsy
7	CT							CT+MR, autopsy			
8	CT							CT			CT+MR, autopsy

* Intratracheal inoculation with 10^6 $TCID_{50}$ pH1N1 A/Netherlands/602/2009.
CT, CT-scanning; MR, magnetic resonance imaging (MRI)-scanning.

In humans, CT-images have been described previously (587-591) for pulmonary alterations caused by pandemic (2009) H1N1 influenza virus infection and the histopathological nature of these alterations in humans has been evaluated only to limited extent (587, 591). We found consistent bilateral ground-glass opacities in the lungs on all time points of scanning. They were most severe on 3 and 4 dpi and showed a reduction on day 7 (**Figure 5.3**). The post-infectious reductions in aerated pulmonary volumes were measured from 3D CT-reconstructs using lower and upper thresholds

in substance densities of −870 to −430 Hounsfield units (HU). The mean decrease in aerated lung volumes (ALVs) was most pronounced on 3 (26 cm^3) and 4 (24 cm^3) dpi compared with day 3 before infection. On day 7 the mean ALV returned to, and equalled, baseline values (31 cm^3) from day 3 before infection (**Table 5.2**).

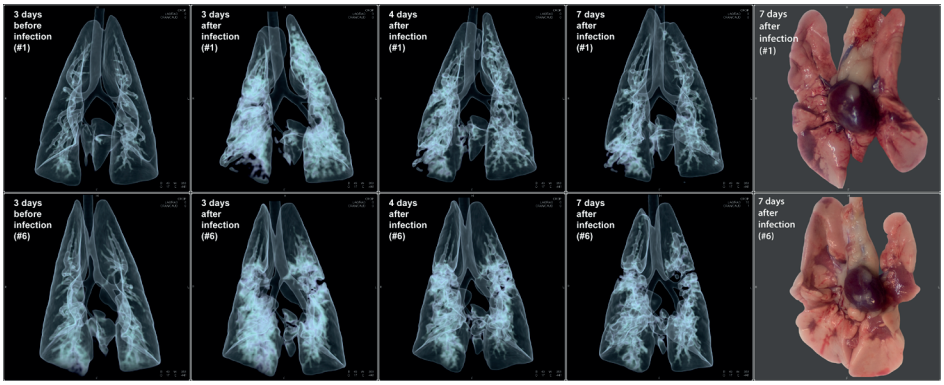

Figure 5.3 Two rows of four consecutive 3D lung CT-images of ferrets #1 and #6. They were recorded *in vivo* under BSL-3^+ conditions, compared with their appearance at autopsy on the far right. At day 3 before infection, the lungs showed the clear aerated baseline condition, at 3 dpi with the 2009 pandemic H1N1 influenza virus marked almost diffuse ground-glass opacities are present that show a gradual reduction towards 7 dpi. The two photographs taken at autopsy on 7 dpi depict the ventral aspect of the lungs, within the centre the hearts still attached to the pulmonary hilus. Both lungs show multifocal reddish consolidated areas of acute inflammation that essentially match with the opacities on the CT-images taken just before autopsy; non-affected aerated lung tissue is light pink in colour.

In addition to CT-scanning, we also performed magnetic resonance imaging (MRI) scanning of the ferrets. The MRI scanner used is a High Definition 3 Tesla clinical scanner (General Electric Healthcare) that requires data acquisition times to such a degree that motionless imaging, without the application of respiratory gating and/or ECG triggering, is only possible post-mortem. Because of this limitation and the lower spatial resolution compared with CT-scanning, the MRI scan proved impractical for use in this animal model and set-up. Accordingly, the MRI results are not presented. However, MRI scanning under BSL-3 conditions could be of value to image other organ systems *in vivo* that are not hampered by heartbeat or respiratory motion.

Within 1 h after euthanasia by exsanguination from cardiac puncture (time needed for post-mortem MRI scanning) the ferrets were submitted for a full autopsy to compare (histo)pathological data with those that were CT-scanned. Animal #4 succumbed spontaneously on 3 dpi and had to be autopsied without prior MRI scanning. The entire intact lungs were instilled with, and submerged in 10 % neutral buffered formalin for fixation and disinfection. The lungs were transversely cut just caudal (approximately 10 mm) of the tracheal bifurcation and matched to the same transversal CT-image.

Additionally from each animal, four similarly cut left lung sections were made not guided by gross lesions. The lung sections were routinely processed, paraffin embedded and 4 µm thin micro-sections were stained with H&E for histopathology. All entire slides were evaluated and scored for the extent of alveolar damage/alveolitis and for the extent of alveolar oedema (0, 0 %; 1, <25 %; 2, 25–50 %; and 3, >50 %). For the detection of influenza A virus-infected cells, additionally serial cut micro-sections were stained for influenza A virus nucleoprotein (NP) as described previously (50).

The pulmonary ground-glass opacities corresponded on histology to extensive alveolar oedema admixed with variable proportions of alveolar macrophages, neutrophils, erythrocytes, fibrin and cellular debris. IIHC staining for viral NP showed infected pneumocytes lining the inflamed and flooded alveoli (**Figure 5.4**). Additionally, there was a moderate necrotising bronchiolitis and similar but milder bronchitis. Despite the return to baseline values in mean ALV on 7 dpi there were still histological lesions mainly in the form of mixed inflammatory cellular infiltrates and type II pneumocyte hyperplasia. Although not statistically significant, the median histopathology scores for the extent of alveolar damage/alveolitis did show a slight decrease from 3 (range 2–3) on day 4 to 2 (range 2–3) on 7 dpi Additionally, matching the improvement in lung aeration is a significant (P = 0.031) decrease in the median extent of alveolar oedema from 3 (range 2–3) on day 4 to 1.5 (range 1–3) on 7 dpi (**Table 5.2**).

Table 5.2 Pandemic H1N1 (2009)-induced lung lesions as measured by CT (aerated tissue) and histopathology (alveolar oedema and alveolar damage)

	Time (days)	Animal no.								Mean (± SD)	Median (range)
		1	2	3	4	5	6	7	8		
Mean aerated lung volume (cm^3)	-3	29 ± 2.2	25 ± 0.4	29 ± 2.7	29 ± 1.8	29 ± 1.7	32 ± 1.2	31 ± 1.9	32 ± 1.2	**31** ± 4.2†	
	+3	24 ± 3.9	–	–	†*	–	28 ± 1.1	–	–	**26** ± 3.6	
	+4	37 ± 2.1	17 ± 1.4	31 ± 1.9	–	15 ± 1.5	36 ± 2.7	20 ± 0.2	14 ± 2.2	**24** ± 9.6	
	+7	48 ± 2.7	11 ± 1.1	–	–	–	33 ± 1.8	–	26 ± 2.3	**31** ± 14†	
Alveolar damage (score 0-3)	+4	–	–	3 (2–3)	–	3 (3–3)	–	3 (3–3)	–		**3** (2–3)
	+7	2 (2–3)	2 (2–3)	–	–	–	3 (2–3)	–	2.5 (2–3)		**2** (2–3)
Alveolar oedema (score 0-3)	+4	–	–	2.5 (2–3)	–	3 (2–3)	–	3 (3–3)	–		**3** (2–3)‡
	+7	1 (1–2)	1.5 (1–2)	–	–	–	2 (1–3)	–	1.5 (1–2)		**1.5** (1–3)‡

* Animal #4 died spontaneously at 3 dpi, † Wilcoxon -3 dpi vs. +4 dpi, P=0.20, ‡ Mann-Whitney +4 dpi vs. +7 dpi, P=0.031.

The ALVs calculated (used lower and upper thresholds in substance densities: −870 to −430 HU) from the 3D CT-reconstructs are presented in cm^3±sd for all animals individually and averaged on the various days. On 7 dpi, the mean ALV returns to, and equals, the mean baseline value on −3 dpi of 31 cm^3. Although not statistically significant, the decrease in lung aeration from baseline value on −3 dpi of 31 cm^3 to 4 dpi 24 cm^3 (P = 0.20). The median extent of alveolar damage/alveolitis (score range 0–3) shows a slight decrease from 3 on 4 dpi to 2 on 7 dpi. The median extent of alveolar oedema (score range 0–3) shows a significant (P = 0.031) decrease from 3 at 4 dpi to 1.5 on 7 dpi.

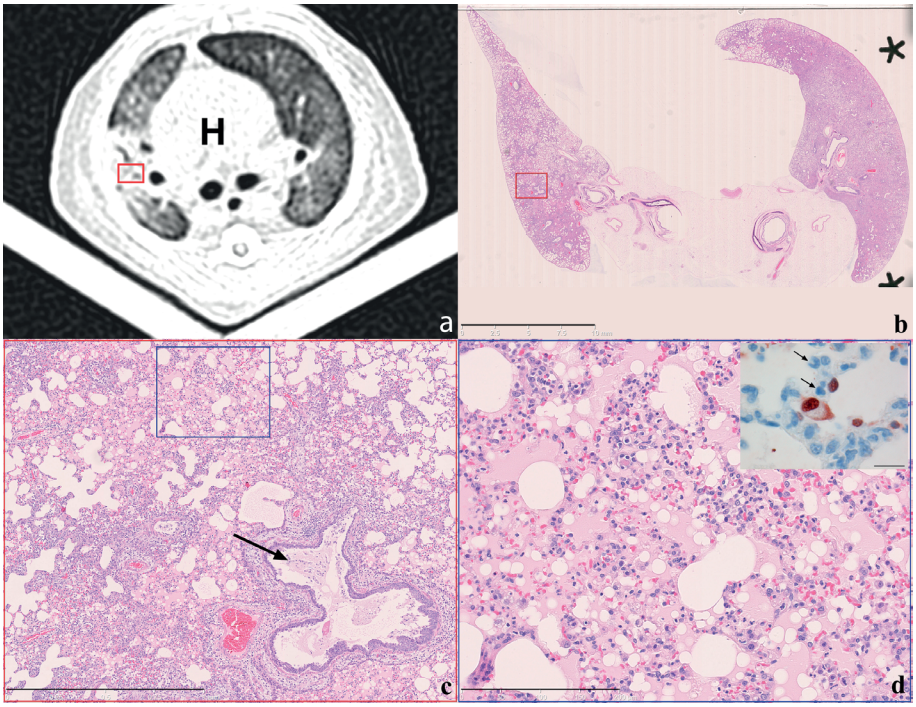

Figure 5.4 Matching CT-scan to histopathology of influenza pH1N1-infected ferret #7 on 4 dpi. (a) Axial CT-image recorded 10 mm caudally of the tracheal bifurcation depicts bilateral pulmonary ground-glass opacities with peribronchovascular predominance. The rounded white heart shadow (H) is visible in the centre enclosed by the darker lung lobes. During scanning the ferret is placed in dorsal recumbency on a V-shaped tray. The red frame indicates the approximate location of micrograph (c). (b) Subgross histological image matching the location of the axial CT-scan. The red frame indicates the exact location of micrograph (c) (H&E-staining; bar, 10 mm). (c) Low magnification micrograph depicting the histological lesions of the right lung corresponding to consolidated ground-glass opacities, they are composed of extensively flooded alveoli and thickened alveolar septa adjacent to a bronchus containing a plug of mucus with few neutrophils and desquamated epithelial cell remnants (arrow). On top right and middle to bottom left, white non-staining still aerated alveoli are present. The blue frame indicates the exact location of micrograph (d) (H&E-staining; bar, 1 mm). (d) Micrograph depicting the damaged alveoli characterised by infiltrated thickened septa and luminal flooding with protein-rich oedema (pink areas) admixed with variable proportions of macrophages, neutrophils, fibrin, erythrocytes and cellular debris (H&E-staining; bar, 200 µm). Insert on top right: high magnification of serially cut IHC-slide from the same area of micrograph (d), depicting thickened alveolar septa infiltrated by neutrophils (arrows) and adjacent dark-brown staining nuclei of influenza virus-infected pneumocytes lining the flooded alveolus (immunoperoxidase-staining for NP of influenza A virus counterstained with haematoxylin; bar, 40 µm).

CONCLUSIONS

We show that monitoring of pulmonary lesions of pH1N1 influenza virus-infected ferrets under BSL3 conditions by consecutive *in vivo* imaging with CT-scanning provides valuable

data on disease progression and severity that closely coincide with post-mortem data obtained at the same time points from euthanised animals. The ground-glass opacities observed by CT-scanning in all infected lungs largely corresponded to areas of alveolar oedema upon autopsy that were most pronounced on days 3 and 4 and decreased towards day 7. As this method involves repeated CT-scans of the same animal instead of sacrificing multiple animals at different time points, it results in a refinement of data collection and a significant reduction in numbers of laboratory animals. In other words the development of respiratory tract lesions of each individual animal can be compared with the situation before infection and followed over time. In this way outbred animals serve as their own baseline control generating more detailed and relevant data per animal. In addition, the assessment of the severity and extent of the lesions over time will lead to more adequate and objective criteria for the time point of euthanasia. The ability of this CT-scanning methodology will not only allow for a more comprehensive study of the pathogenesis of life-threatening infectious diseases, but also of the assessment of the efficacy and safety of vaccination and antiviral strategies against them. In the present pilot study, CT-scan opacities correspond to alveolar oedema, this parameter is among others used as read out in influenza vaccine efficacy studies (390, 550). Obviously this methodology is not limited to studying the respiratory tract, but could also be exploited for new emerging pathogens with their specific target organs in other animal models.

Acknowledgements

The authors E. V. K., G. v. A., J. S., L.d. W., A. O. and K. S. are affiliated with Erasmus MC spinout CRO ViroClinics BioSciences B.V. We thank, Cindy van Hagen, Willem van Aert, Ronald Boom and Rob van Lavieren from ViroClinics Biosciences B.V. for their outstanding technical assistance and virologic analyses, Peter van Run and Lonneke Leijten from the Department of Virology Erasmus MC Rotterdam for their excellent histotechnical work, D. van de Vijver from the Department of Virology Erasmus MC Rotterdam for statistical analyses, Piotr Wielopolski, Gyula Kotek and Sandra van Tiel from the Department of Radiology Erasmus MC Rotterdam for MRI scanning, and Peter Melger from Siemens Healthcare The Netherlands for his technical advice. This study was supported in part by TI Pharma (grant T4-214).

CHAPTER 6

Applications of influenza virus inoculation in the ferret as model of influenza viral pneumonia and intervention studies in humans

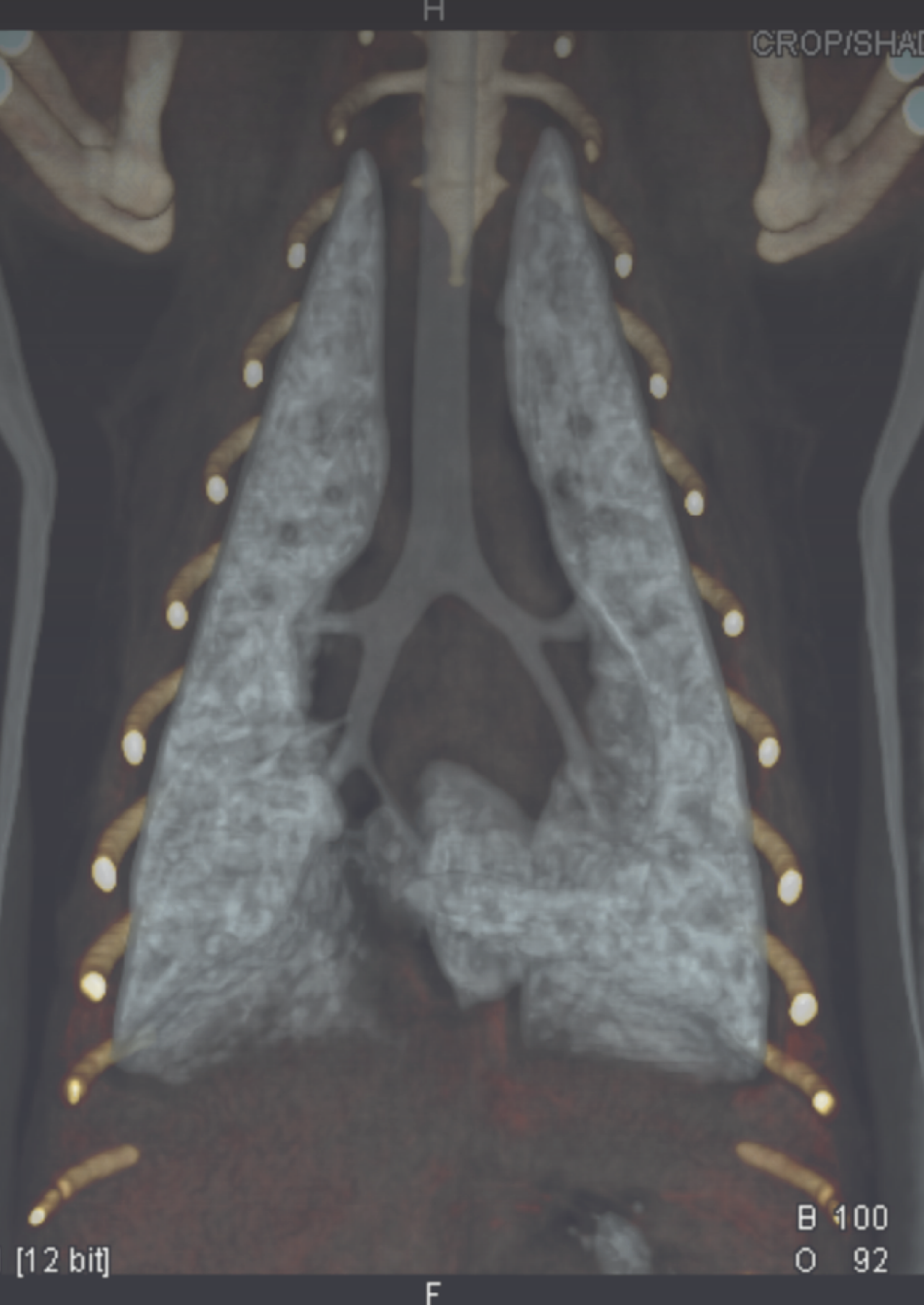
H
CROP/SHAD
B 100
O 92
[12 bit]
F

6.1

Consecutive CT *in vivo* lung imaging as quantitative parameter of influenza vaccine efficacy in the ferret model

E.J.B. Veldhuis Kroeze[1,2], K.J. Stittelaar[1], V.J. Teeuwsen[1], M.L. Dijkshoorn[3], G. van Amerongen[1], L. de Waal[1], T. Kuiken[2], G.P. Krestin[3], J. Hinkula[4,5] & A.D.M.E. Osterhaus[1,2]

Vaccine 2012; 30: 7391-7394

Affiliations

[1]Viroclinics Biosciences B.V., Rotterdam, The Netherlands

[2]Department of Viroscience, Erasmus Medical Center, Rotterdam, The Netherlands

[3]Netherlands Vaccine Institute, Bilthoven, The Netherlands

[4]Department of Radiology, Erasmus Medical Center, Rotterdam, The Netherlands

[5]Eurocine Vaccines AB, Karolinska Institutet Science Park, Solna, Sweden

[6]Division of Molecular Virology, IKE, Linkoping University, Linköping, Sweden

ABSTRACT

Preclinical vaccine efficacy studies are generally limited to certain read out parameters such as assessment of virus titers in swabs and organs, clinical signs, serum antibody titers, and pathological changes. These parameters are not always routinely applied and not always scheduled in a logical standardised way. We used CT-imaging as additional and novel read out parameter in a vaccine efficacy study by quantifying alterations in ALVs in ferrets challenged with the 2009 pandemic A/H1N1 influenza virus.

Vaccination protected from marked variations in ALVS compared to naive controls. The vaccinated group showed a daily gradual mean reduction with a maximum of 7.8%, whereas the controls showed a maximum of 14.3% reduction. The pulmonary opacities evident on CT-images were most pronounced in the sham-vaccinated controls, and corresponded to significantly increased relative lung weights at autopsy. This study shows that consecutive *in vivo* CT-imaging allows for a day-to-day read out of vaccine efficacy by quantification of altered ALVs.

Highlights: We evaluated efficacy of an influenza vaccine by means of CT-scan in the ferret. Longitudinal *in vivo* scanning allows quantification of changes in ALV. Immunisation protects from a significant initial severe increase in ALV seen in unprotected controls. Immunisation protects from major increase of relative lung weight.

Keywords: Influenza; Preclinical vaccine efficacy; Ferret; *In vivo* imaging; CT-scan; Pathology

INTRODUCTION

The field of influenza virus research is in particular an area of new emerging viruses that requires rapid development of animal models needed for pathogenicity studies and assessment of adequate vaccine candidates and antiviral therapies. This was recently illustrated by the emergence of the 2009 pandemic H1N1 IAV (395, 506). Ferrets are being implemented extensively in human influenza virus research. However, influenza virus research is conducted in multiple separate laboratories all with their unique approach how to evaluate vaccine candidates within the ferret challenge model. Substantial differences can be found in all stages and aspects of challenge protocols, study set-ups and read-out parameters. A spectrum of recently published (395, 592-600) infection/challenge protocols showing this diversity is listed in comparison in **Table 6.1.1.** In addition, obviously, different influenza strains are used as challenge virus instigated by the antigenic nature of the vaccine, or alternatively to evaluate efficacy to a heterologous influenza virus challenge. The routes of infection being intranasal, intratracheal or through virus transmission from experimentally infected and shedding ferrets show considerable differences in implementation and outcomes (549). Different viral challenge doses are used, whether or not established in preceding dose-finding studies. However, the challenge doses are pivotal in the interpretation of a challenge outcome. Since, a too robust challenge may prove, false negatively, a poor efficacy of a human vaccine candidate in the ferret model, and vice versa. Furthermore, the duration of the challenge read out period varies, as well as the types of samples collected and frequency of sampling. Often the design of a challenge protocol is based on predefined end points and read outs, or may rely on results from historical experiments.

Because of these variations in the assessment of vaccine efficacy, the comparison of the outcomes of vaccine studies may be hampered; therefore a certain way of standardisation could prove useful by providing clarity.

Recently, we reported that CT-scanning allows quantification and characterisation of influenza-induced pulmonary lesions in living animals (599). We showed that the pulmonary ground-glass opacities observed by CT-scanning corresponded mainly to areas of alveolar oedema, which is a major histological lesion in early influenza-induced pneumonia and can be used to quantify the ALV. The present study was performed to evaluate the immunogenicity and protective efficacy of an adjuvanted inactivated influenza pH1N1 vaccine for intranasal use in the ferret model. A group of six ferrets was intranasally immunised with this vaccine candidate and compared to a second group of six ferrets that received intranasally administered PBS as sham vaccine. These administrations were performed on study days 0, 21 and 42. All animals were subsequently intratracheally challenged with 10^6 $TCID_{50}$ H1N1 inlfuena A/TheNetherlands/602/2009 virus on study day 70. The animals were monitored for vaccine induced serological and

immunological responses and for infection related clinical and virological responses. As novel read out parameter CT-scanning was performed 6 days prior, and daily after, virus inoculation on all twelve ferrets to monitor influenza induced lung damage by quantifying alterations in the ALVs. The animals were sacrificed at 4 dpi to evaluate pathological and virological parameters.

Table 6.1.1 A spectrum of recently published infection/challenge protocols showing divers study set-ups

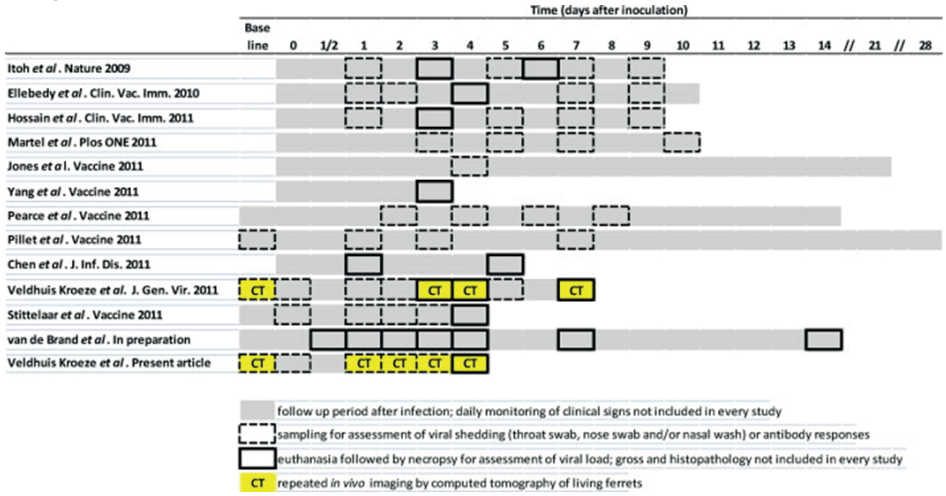

MATERIALS & METHODS

Animals

The ferrets (*Mustela putorius furo*) were females of 8 months of age, seronegative for antibodies against current circulating influenza viruses, and Aleutian disease virus. Housing and handling was performed under BSL3 conditions in negatively pressurised and HEPA-filtered biocontainment isolator units, approved by an independent institutional laboratory animal ethics and welfare committee. General injection anaesthesia (ketamine 8 mg/kg and medetomidine-HCl 7.5 µg/kg body weight) was applied during handling and scanning.

Immunisation

The animals (n = 6) were immunised three times with a 3-week interval with an adjuvanted inactivated vaccine. 200 µl of vaccine was intranasally administered and divided equally over both nostrils. The controls (n = 6) were similarly sham-immunised with 200 µl PBS intranasally.

Challenge virus

All animals were challenged, 4 weeks after the last immunisation, intratracheally with 10^6 $TCID_{50}$ of the 2009 pandemic influenza virus A/Netherlands/602/2009 (pH1N1) in 3 ml PBS, as described previously (506, 585, 600). The virus was routinely propagated in MDCK cell cultures and infectious dose determined as described previously (508), and titres calculated according to the method of Spearman-Karber (536).

CT-scanning

All animals were scanned on −6, 1, 2, 3, and 4 dpi (see also table 6.1.1). A dual-source ultra fast CT-system (Somatom Definition Flash, Siemens Healthcare) was used (temporal resolution: 0.075 s, spatial resolution is 0.33 mm, table speed of 458 mm/s: ferret thorax acquisition time ≈ 0.22 s; enables accurate scanning of living ferrets without the necessity of breath-holding, respiratory gating, or ECG-triggering as previously described (599). Briefly, during scanning the ferrets were in dorsal recumbency in a purpose-built (Tecnilab-BMI) perspex biosafety container of 8.3 L capacity. The post-infectious reductions in ALVs were measured from 3-dimensional CT-reconstructs using lower and upper thresholds in substance densities of −870 to −430 HU.

Pathology

Following euthanasia by exsanguination all animals were submitted for autopsy. The lung lobes were inspected and lesions were assessed while the lung was inflated. The trachea was cut at the level of the bifurcation and the lungs were weighed. The relative lung weight was calculated as proportion of the body weight on day of death (lung weight/body weight × 100).

RESULTS & DISCUSSION

All animals from both groups were scanned 6 days prior to virus inoculation to define the uninfected base-line status of their respiratory system. Consecutive *in vivo* imaging with CT-scanning showed that ferrets intranasally immunised with the vaccine candidate were largely protected against the appearance of pulmonary ground-glass opacities, as is shown by means of transversal CT-images in **Figure 6.1.1.** The ALVs measured from 3D CT-reconstructs likewise showed that the immunised ferrets were protected against major alterations in ALV (group mean ALV ranging from 0.95 to −7.8%) and did not show a temporal increase in ALV on 1 dpi, which was observed in the sham-vaccinated group (group mean ALV ranging from 17.3 to −14.3%) (**Figure 6.1.2**) This sudden and short increase of 17.3% (Mann–Whitney test, two-tailed, P = 0.035) in the unprotected sham-vaccinated animals may result from a virally induced acute respiratory depression

Figure 6.1.1 Consecutive transversal lung CT-images after infection with H1N1 A/Netherlands/602/2009.

← **Figure 6.1.1 Consecutive transversal lung CT-images after infection with H1N1 A/Netherlands/602/2009.** Two columns of consecutive (top to bottom) transversal lung CT-images of one representative immunised ferret (left) and one representative sham-immunised ferret recorded *in vivo* compared with their gross aspect at autopsy (bottom). At day 6 before infection, the lungs showed the clear aerated baseline condition, from 1 dpi with the new pandemic H1N1 influenza virus onwards marked almost diffuse ground-glass opacities appear that show a gradual increase with a plateau on 3–4 dpi. The two photographs taken at autopsy on 4 dpi depict the ventral aspect of the lungs, with the hearts removed. The lungs of the sham-immunised animal (bottom right) show diffuse reddish consolidation indicative of acute inflammation that essentially match the opacities on the CT-images taken just before autopsy; non-affected aerated lung tissue from the immunised animal is light pink in colour (bottom left).

with compensatory hyperinflation. A compensatory increase in respiratory tidal volume by means of hyperinflation is a pathophysiological phenomenon known to occur in respiratory viral infections (601, 602). However, CT-scanning could not discern possible emphysema due to ruptured alveoli as cause of ALV increase. The relative change of ALVs on days 2, 3 and especially 4 after infection did not show significant differences between the two groups. One possible explanation is that over-expansion of the thorax and lungs allows for increased alveolar flooding in excess of base line aeration resulting in approximately unaltered ALVs between the two groups. Another explanation is that the inflamed and oedematous areas were aerated less than normal, but because the unaffected areas of lung were aerated more than normal (hyperinflation or emphysema), the overall ALV values remained approximately unaltered.

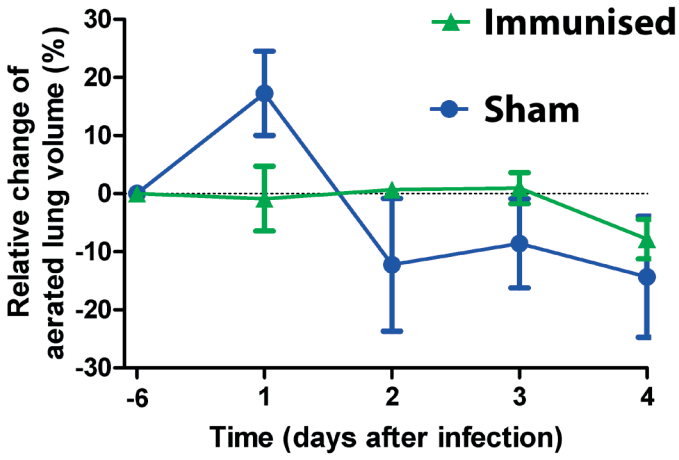

Figure 6.1.2 Changes in aerated lung volume (ALV) after infection with H1N1 A/Netherlands/602/2009. The ALV was calculated using lower and upper thresholds in substance densities of −870 HU for the analysis of 3D-reconstructions of the lung. The percentage change of ALV was calculated using the individual base line ALVs of day 6 against the ALVs of the different days after infection. These data are expressed as mean ± SEM. Animals were intratracheally challenged with 10^6 $TCID_{50}$ H1N1 A/The Netherlands/602/2009 on day 0.

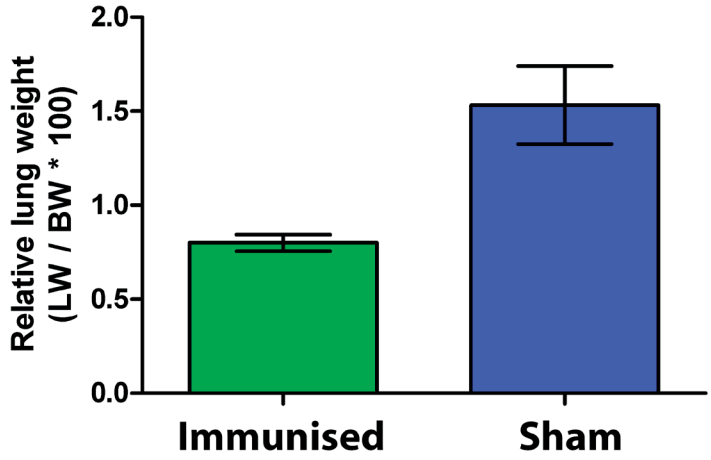

Figure 6.1.3 Relative lung weights. Mean relative lung weights (RLWs, related to body weight; ± SEM) at autopsy (4 dpi) for the immunised group versus the sham-vaccinated control group after infection with H1N1 A/Netherlands/602/2009.

Nevertheless, these ALV profiles provide more detailed knowledge about the influenza-induced respiratory disease development than confined data obtained from a single predefined read out. Moreover, survival and recovery from challenge infection can be included in this set-up and with the opportunity to still measure the development of serum antibody responses upon challenge infection.

Upon autopsy, the relative lung weights (RLWs) of the intranasally immunised ferrets was about 2-fold lower (Mann–Whitney, two-tailed, $P < 0.0047$) as compared to those of the sham-vaccinated animals (**Figure 6.1.3**), which is in agreement with the absence of pulmonary ground-glass opacities. Usually, more severely affected and inflamed lungs with increased amounts of fluid are heavier compared to normal or less affected lungs. This translates within the ferret model in influenza research to RLWs ≤ 1.0 associated with non- to minimally affected lungs and RLWs > 1.0 associated with severe pulmonary inflammation with oedema (390, 600, 603).

In conclusion, the implementation of consecutive CT-imaging enables repeated *in vivo* measurements of lung aeration as parameter to evaluate vaccine efficacy in preclinical protocols. Consecutive day-to-day imaging overcomes the limitations entailed by autopsy at a predefined time point after infection, and the lung capacity can be repeatedly quantified in real-time.

Acknowledgements

We are grateful to Willem van Aert, Ronald Boom, Cindy van Hagen, Rob van Lavieren from ViroClinics Biosciences B.V., Peter van Run from the Department of Virology Erasmus MC Rotterdam, and Dennis de Meulder from the Erasmus Laboratory Animal Science Center Rotterdam for their excellent technical assistance and analyses. The authors EVK, VT, KS, GvA, LdW, and AO are affiliated with Erasmus MC spin-off company ViroClinics BioSciences B.V. The author JH is affiliated with Karolinska Institutet spin-off company Eurocine Vaccines AB.

6.2

Efficacy of live attenuated vaccines against 2009 pandemic H1N1 influenza in ferrets

K.J. Stittelaar[1], E.J.B. Veldhuis Kroeze[1,2], L. Rudenko[3], R. Dhere[4], S. Thirapakpoomanunt[5], M.P. Kieny[6] & A.D.M.E. Osterhaus[1,2]

Vaccine 2011; 29: 9265-9270

Affiliations

[1]Viroclinics Biosciences B.V., Rotterdam, The Netherlands

[2]Department of Viroscience, Erasmus Medical Center, Rotterdam, The Netherlands

[3]Department of Virology, Institute of Experimental Medicine, St Petersburg, Russia

[4]Serum Institute of India Ltd, Hadapsar, Pune, India

[5]Government Pharmaceutical Organisation, Bangkok, Thailand

[6]World Health Organisation, Geneva, Switzerland

ABSTRACT

The advent of the H1N1 influenza pandemic (pH1N1) in 2009 triggered the rapid production of pandemic influenza vaccines, since seasonal influenza vaccines were expected and demonstrated not to provide significant cross-protection against the newly emerged pandemic virus. To increase vaccine production capacity and further evaluate the effectiveness of different candidate pandemic influenza vaccines, the World Health Organisation stimulated the evaluation of different vaccination concepts including the use of live attenuated influenza vaccines (LAIVs). Therefore, we have immunised ferrets intranasally with a single dose of pH1N1-LAIV from different manufacturers. They all induced adequate serum HI antibody titers in the ferrets and protected them against intratracheal wild-type pH1N1 virus challenge: pH1N1 virus replication in the upper respiratory tract and lungs was reduced and no disease signs or severe broncho-interstitial pneumonia were observed in any of the vaccinated ferrets. These data together with the relatively efficient production process emphasize the potential of the LAIV concept for pandemic preparedness.

Highlights: A single intranasal dose of pH1N1-LAIV confers profound protection against 2009 pandemic H1N1 influenza in intratracheally-inoculated ferrets. pH1N1-LAIVs from different manufacturers tested are equally immunogenic and efficacious. This LAIV concept has high potential for pandemic preparedness.

Keywords: Influenza virus H1N1; Ferret; Live attenuated influenza vaccine; Vaccine efficacy

INTRODUCTION

The sudden emergence of the H1N1 influenza pandemic (pH1N1) in 2009 triggered the rapid production of pandemic influenza vaccines, since seasonal influenza vaccines were expected and demonstrated not to provide significant cross-protection against the newly emerged pandemic virus (26, 604, 605). Assessment of antibody cross-reactivity in sera from humans and/or ferrets vaccinated with recent seasonal influenza inactivated vaccines and live attenuated vaccines, did not show significant antibody titers to pH1N1 virus, however an adjuvanted inactivated candidate seasonal H1N1 vaccine administered 4 weeks before immunisation with adjuvanted inactivated candidate pH1N1 vaccine did provide immunological priming in ferrets against pH1N1 virus (550, 585, 605-607). Also the age distribution of severe and fatal human cases of pH1N1 infection indicated priming in humans by exposure to seasonal H1N1 influenza viruses having occurred more than 15 years earlier (605, 608). In view of an expected pH1N1 vaccine shortage at the global level and the anticipated need for broadly protective vaccines, the Strategic Advisory Group of Experts called for the evaluation, production and use of both adjuvanted inactivated virus vaccines and live attenuated influenza vaccines (LAIVs) (609). LAIV concepts described to date include those using cold-adapted (ca) viruses (610-613) and those using viruses with modified NS1, NS2 or M2 genes (586, 614-616). Ca-LAIV is the most developed concept with a LAIV having been used extensively in Russia from 1954 onward in more than 120,000 children and more than 500,000 adults (612, 617-619) and FluMist® being on the market as of 2003 (619). The former are based upon reassortment of seasonal influenza viruses with attenuated ca-strains selected for their ability to replicate at low temperatures, whereas the latter is based on the use of ca viruses that are adjusted to circulating seasonal influenza viruses by reverse genetics techniques.

The use of LAIVs has major advantages, including less complex downstream processing, lower unit cost and higher production yield as compared to inactivated vaccines (620). Furthermore, LAIVs are administered via the intranasal route, which is less invasive than commonly used parenteral routes. LAIVs have been shown to rapidly induce protective systemic antibody and nasal (mucosal) IgA antibody responses as well as cell-mediated immune responses (621). LAIVs developed by Maassab and colleagues (622) have been shown to be safe, genetically stable and do not convert back to the wild-type virus even in immunocompromised mice (623). Although registered LAIVs have been shown to be safe and effective in certain risk-groups like influenza vaccine-naïve children aged 6 to <36 months (624), they are so far not used in immunocompromised individuals.

LAIVs that should protect humans against influenza viruses of animals with pandemic potential, like the H5N1 HPAIVs, are currently being evaluated. Rudenko and

colleagues have tested a live vaccine based on a low pathogenic avian influenza virus of the H5N2 subtype in human trials and showed that the vaccine was well tolerated and that mucosal- as well as protective levels of systemic antibody responses were induced (625). Kobinger and colleagues tested commercially available seasonal 2008–2009 LAIV FluMist® in ferrets against challenge with pH1N1. As indicated above, antibody titers to pH1N1 virus were not detectable, but a specific T cell response was detected (607). Remarkably, upon the heterologous challenge with pH1N1, the vaccinated ferrets exhibited increase in mortality and greater lung damage associated with early up-regulation of interleukin-10. Recently, others have described the production of a LAIV based on a pH1N1 A/California/07/2009 6:2-reassortant with ca-A/AnnArbor/06/1960 and the initial hurdles of poor replication in embryonated eggs through large-plaque selection, sequence modification (626). One or two doses of this LAIV preparation induced a robust antibody response, which correlated with protection from homologous challenging mice and ferrets (627).

Recently, we have shown that the swine-origin wild-type influenza A/California/07/2009 (wt-Cal-pH1N1) virus is a good parental prototype for LAIV-pH1N1 preparation showing neither temperature resistance nor inhibitor resistance and is unable to grow at 25°C (628). A vaccine candidate A/17/California/38/2009, which is an influenza A live attenuated vaccine reassortant (LAIV-pH1N1) based on the temperature sensitive (ts) and ca A/Leningrad/134/17/57 (H2N2) master donor strain (Len/17), was developed as a candidate human vaccine (628). The present study was conducted to evaluate the efficacy of this monovalent (A/17/California/38/2009) LAIV-pH1N1 in a naïve ferret model against challenge with the homologous influenza virus A/Netherlands/602/2009 (pH1N1). The intratracheal route of infection as challenge has been used because recently we showed that this method allows for a reproducible severe influenza pneumonia (506). Three candidate LAIV-pH1N1 preparations tested in this study were produced at three different sites in Russia, Thailand and India.

MATERIALS & METHODS

Vaccines

The monovalent live-attenuated influenza vaccine candidate based on the new H1N1 A/California/2009/38 was prepared through reassortment with temperature sensitive and cold-adapted A/Leningrad/134/17/57 (H2N2) master donor strain as described previously. In this study three different batches of the A/17/California/38/2009 LAIV were used: freeze dried LAIV Russia (series 2.09.11.09; designated as LAIV-Russia-pH1N1), LAIV Thailand (ready to use formulation; designated as LAIV-Thailand-pH1N1), and freeze dried LAIV India (batch number: 143E9003; designated as LAIV-India-pH1N1).

The LAIV-Russia-pH1N1, LAIV-Thailand-pH1N1 and LAIV-India-pH1N1 preparations had a titer of $10^{8.3}$, $10^{7.7}$ and $10^{7.6}$ egg infectious dose 50% (EID_{50}), respectively. The attenuated phenotype of the LAIV-pH1N1 had been demonstrated by completion of the standard protocol for testing in ferrets (629).

Animals

Groups of six healthy outbred male ferrets (*Mustela putorius furo*), approximately 9 months of age and seronegative for antibodies against circulating influenza viruses B, A/H1N1, A/H3N2 and A/pH1N1 by hemagglutination inhibition (HI) assay were used. Two weeks prior to the start of the experiment, the animals were anesthetised using a cocktail of ketamine (Alfasan, Woerden, The Netherlands) and domitor (Orion Pharma, Espoo, Finland), and a temperature logger (DST micro-T ultra small temperature logger; Star-Oddi, Reykjavik, Iceland) was placed in their peritoneal cavity. This device recorded body temperature of the animals every 10 min. During the whole experiment the animals were maintained in negatively pressurised glovebox isolator cages, and provided with commercial food pellets and water ad libitum. The experimental protocol was approved before the start of the experiments by an independent institutional animal ethics committee according to Dutch law.

Intranasal immunization

Three groups of six ferrets each were immunised intranasally with a single human dose of 0.5 ml of LAIV-pH1N1 candidate vaccine divided over two nostrils on study day 0 under anesthesia with ketamin and domitor. To a fourth group of six ferrets, 0.5 ml of PBS was administered intranasally. Blood samples for serum preparation were collected on study days 0, 20 and 28.

HI and VN antibody assays

Serum samples collected prior to immunisation, on day 20 after immunisation and on the day of challenge infection (day 28 after immunisation) were stored at −20 °C. They were tested for the presence of anti-HA antibodies reactive against A/California/4/2009 (rg-Cal-pH1N1) and A/Netherlands/602/2009 (rg-NL-pH1N1) using a HI assay with 1% turkey erythrocytes. For this purpose reverse genetics viruses were used with the HA and NA of the 2009 wild-type pH1N1 viruses and the remaining 6 gene segments of influenza virus A/Puerto Rico/8/34. In addition, the sera were tested for the presence of virus neutralizing antibodies against the same viruses using a virus-neutralisation assay (VN-assay) as previously described (585).

Challenge with wild-type influenza virus A/Netherlands/602/2009

Four weeks after immunisation (day 28), all ferrets were challenged with wild-type influenza virus A/Netherlands/602/2009 (wt-pH1N1) as previously described (550, 585). Briefly, 10^6 $TCID_{50}$ of wt-pH1N1 was diluted in 3 ml of PBS and administered via the intratracheal route under anesthesia with a cocktail of ketamine and domitor.

Virus replication in the upper and lower respiratory tract

On days 0, 1, 2, 3 and 4 after challenge, nose and throat swabs were taken from the animals under anesthesia. Four days after challenge, the ferrets were euthanised by exsanguination under anesthesia after which full-body gross-pathology was performed and lungs were collected. Samples of all lobes of the right lung and the accessory lobe were collected and stored at −70 °C until further processing. Lung samples were weighed and subsequently homogenised with a FastPrep-24 (MP Biomedicals, Eindhoven, The Netherlands) in Hank's balanced salt solution containing 0.5% lactalbumin, 10% glycerol, 200 U/ml penicillin, 200 µg/ml streptomycin, 100 U/ml polymyxin B sulfate, 250 µg/ml gentamycin, and 50 U/ml nystatin (ICN Pharmaceuticals, Zoetermeer, The Netherlands) and centrifuged briefly before dilution.

After collection, nose and throat swabs were stored at −70 °C in the same medium as used for the processing of the lung samples. Quadruplicate 10-fold serial dilutions of lung and swab supernatants were used to determine the virus titers in confluent layers of MDCK cells as described previously (585).

Gross-pathology and Histopathology

The animals were autopsied according to a standard protocol. The trachea was clamped off so that the lungs would not deflate upon opening the pleural cavity. This allowed an accurate visual quantification of the areas of affected lung parenchyma. Samples for histological examination of the left lung and trachea were taken and stored in 10% neutral-buffered formalin (lungs after inflation with formalin), embedded in paraffin, sectioned at 4 µm, and stained with HE for examination by light microscopy. Samples were taken in a standardised way, not guided by changes observed in the gross pathology. Semi-quantitative assessment of influenza virus-associated inflammation in the lung was performed as described previously (**Table 6.2.1**) (506). Slides were examined without knowledge of the identity of the animals.

Statistical analysis

Differences between the vaccinated groups (group 1, 2 and 3) were analyzed statistically using the Kruskal-Wallis test and differences between vaccinated groups (group 1, 2 and 3) compared with the sham-immunised (PBS-treated) control group (group 4) were

analyzed statistically using the Mann–Whitney U test. Differences were considered significant at $P < 0.05$.

RESULTS

Development of HI and VN antibody responses

Twenty days after a single immunisation all ferrets immunised with the respective LAIV-pH1N1 preparations (LAIV-Russia-pH1N1, LAIV-Thailand-pH1N1 and LAIV-India-pH1N1) developed HI antibodies against both the A/California/4/2009 (rg-Cal-pH1N1) and A/Netherlands/602/2009 (rg-NL-pH1N1) strain (titers 320–960, 640–1280 and 280–1120 against rg-Cal-pH1N1, respectively, and titers 320–1120, 560–1280 and 240–1280 against rg-NL-pH1N1, respectively). Eight days later, these HI titers were largely the same or showed a slight decrease (**Figure 6.2.1A**).

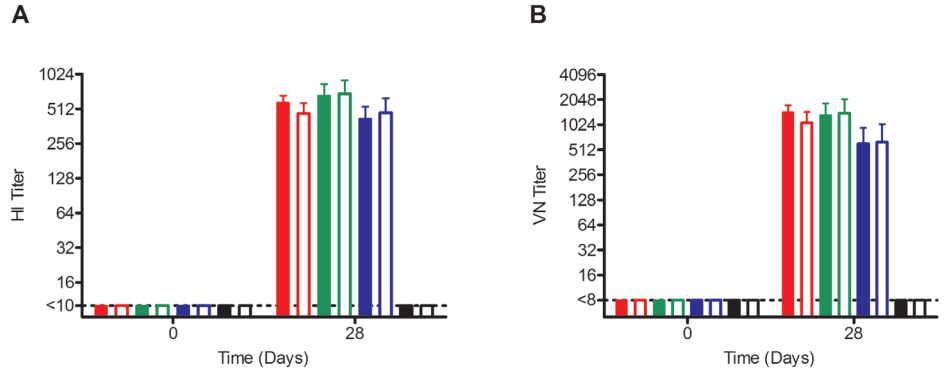

Figure 6.2.1 Development of pH1N1-specific serum HI (A) and VN (B) antibody responses (rg-Cal-pH1N1, solid bars and rg-NL-pH1N1, open bars) in ferrets at 28 days after a single immunisation with different batches of A/17/California/38/2009 pH1N1 LAIV: LAIV-Russia-pH1N1, red; LAIV-Thailand-pH1N1, green; LAIV-India-pH1N1, blue and sham-immunised (PBS-treated), black. The HI and VN antibody titers are presented as group geometric means (6 animals per group) with standard deviation. See text for statistical analysis of the results.

There were no statistical differences between the data obtained with the three different LAIV-pH1N1 preparations or between the HI antibody reactivity against the two rg-pH1N1 strains, neither on day 20 ($P = 0.11$ and 0.23, respectively) nor on day 28 ($P = 0.23$ and 0.31, respectively).

The single immunisation resulted in high levels of VN antibodies against both the rg-Cal-pH1N1 and rg-NL-pH1N1 strain as measured twenty days after immunisation (titers 256–2048, 362–2896 and 181–2048 against rg-Cal-pH1N1, respectively, and 304–2435,

431–3444 and 256–1722 against rg-NL-pH1N1, respectively). Eight days later, these VN titers were largely the same or showed a slight increase (**Figure 6.2.1B**). There were no statistical differences between the data obtained with the three different LAIV-pH1N1 preparations or between the VN antibody reactivity against the two rg-pH1N1 strains, neither on day 20 (P = 0.13 and 0.18, respectively) nor on day 28 (P = 0.19 and 0.32, respectively). The sham-immunised control ferrets (group 4) did not show pH1N1-specific HI or VN antibodies.

Protection against challenge with wild-type A/Netherlands/602/2009 (WT-pH1N1); Clinical signs

Upon challenge, which was performed four weeks after the single immunisation, all 24 ferrets survived the 4 days follow up period (**Table 6.2.1**). The sham-immunised control animals (group 4) developed clinical signs such as lethargy, loss of appetite and dyspnea from 2 dpi onward. These clinical signs were milder in the vaccinated animals (groups 1–3): the control animals (group 4) showed mean body weight loss of 14% (range 10–18%), while mean weight loss in vaccinated animals was significantly lower with 6% (range 0–12%), 8% (range 5–12%) and 7% (range 5–8%) for group 1 (LAIV-Russia-pH1N1; P = 0.024), group 2 (LAIV-Thailand-pH1N1; P = 0.024) and group 3 (LAIV-India-pH1N1; P = 0.004), respectively, while there was no statistical difference between the vaccinated groups (P = 0.692; **Table 6.2.1**). All animals showed an initial temporal rise in body temperature within 24 hours post infection (hpi), which may be considered an acute phase reaction to the intratracheal inoculation (**Figure 6.2.2**). The sham-immunised control animals (group 4) developed fever about 24 hpi with peak temperatures of 39.2 ± 0.6 °C. Of all vaccinated animals only few developed slightly elevated temperature levels and these belonged to group 2 (LAIV-Thailand-pH1N1; one out of six) and group 3 (LAIV-India-pH1N1; three out of six) with peak temperatures between 39.4 and 39.8 °C. Furthermore, the onset of these elevated temperature levels in vaccinated animals was delayed when compared to control animals.

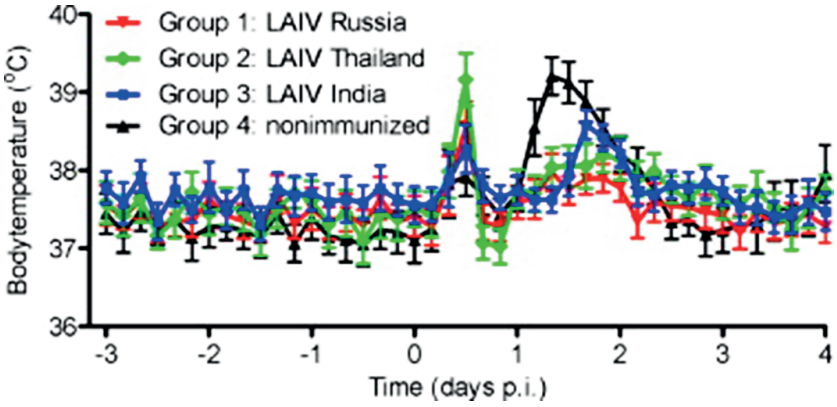

Figure 6.2.2 Body temperature profiles of ferrets following intratracheal challenge with wild-type influenza virus A/Netherlands/602/2009 (pH1N1) as measured by a temperature logger (DST micro-T ultra small temperature logger; Star-Oddi, Reykjavik, Iceland) placed in the peritoneal cavity. The data are presented as group averages (6 animals per group) of 6 h intervals with standard deviation.

Virus replication in the lungs and upper respiratory tract

None of the vaccinated ferrets (groups 1–3) had detectable replication competent virus in the lungs (lower limit of detection $\leq 10^{1.3}$ $TCID_{50}$ per gram tissue) when the animals were euthanised at 4 dpi and also from none of their nasal swabs virus could be isolated. In contrast, at 1 dpi 11 of the 18 vaccinated ferrets had detectable replication competent virus in their throats and these belonged to group 1 (LAIV-Russia-pH1N1; three out of six), group 2 (LAIV-Thailand-pH1N1; four out of six) and group 3 (LAIV-India-pH1N1; five out of six) with titers ranging from 101.0 to $10^{3.0}$ $TCID_{50}$/ml. On 2, 3 and 4 dpi none of the vaccinated ferrets had replication competent virus in their throat except for one animal of group 1 (LAIV-Russia-pH1N1), which started to be positive on 2 dpi up to the end of the experiment with a titer that increased from $10^{1.5}$ to $10^{3.5}$ $TCID_{50}$/ml. The sham-immunised control animals (group 4) showed average lung viral titers of $10^{5.3}$ (range $10^{4.4}$–$10^{6.1}$) $TCID_{50}$ per gram tissue. Virus was detected in the nose of 1–2 animals on 1 and 2 dpi and of five out of six animals on 3 and 4 dpi with titers ranging from $10^{1.5}$ to 10^{5} $TCID_{50}$/ml. One control animal had no replication competent virus in its nose. From throat swabs of all control animals virus could be isolated on 1, 2, 3 and 4 dpi with average titers of $10^{3.4}$, $10^{3.4}$, $10^{4.5}$ and $10^{3.9}$ $TCID_{50}$/ml, respectively. The difference in the frequency of virus recovery from the throat swabs as compared to the nasal swabs could be explained by the fact that with swabs different compartments are sampled and maybe also by the sampling technique.

The reduced virus replication in vaccinated animals corresponded with a reduction in gross pathological changes of the lungs (**Table 6.2.1**).

Table 6.2.1 Efficacy of A/17/California/38/2009 (pH1N1) LAIV in ferrets demonstrated by clinical scoring, virology, gross-pathology and histopathology parameters

		Group 1: LAIV Russia	Group 2: LAIV Thailand	Group 3: LAIV India	Group 4: Sham-immunised
Clinical score	Survival to end experiment	6/6	6/6	6/6	6/6
	Relative body weight loss (%, -1 vs. 4 dpi)	6.2 ± 4.4	7.5 ± 3.6	7.2 ± 1.3	**14 ± 3.2**
Virology	AUC nose swabs (virus titres 1-4 dpi [*]	0 ± 0 [0/6]	0 ± 0 [0/6]	0 ± 0 [0/6]	**3.2 ± 0.6 [5/6]**
	AUC throat swabs (virus titres 1-4 dpi [*]	0.8 ± 1.4 [3/6]	0.5 ± 0.4 [4/6]	0.9 ± 0.9 [5/6]	**11 ± 1.9 [6/6]**
	Lung viral loads (log_{10} $TCID_{50}$/g	≤ 1.3	≤ 1.3	≤ 1.3	**5.3 ± 0.6**
Gross pathology	Estimated % of lung affected	1.7 ± 2.6	2.5 ± 2.7	4.2 ± 2.0	**60 ± 17**
	Relative lung weights	0.5 ± 0	0.6 ± 0.1	0.6 ± 0	**1.1 ± 0.2**
	× normal size of tracheobronchial lymphnode	1.6 ± 0.2	1.8 ± 0.7	2.0 ± 0.5	1.3 ± 0.3
Histopathology	Extent of alveolitis (score 0–3)	0.2 ± 0.3	0.3 ± 0.3	0.3 ± 0.2	**2.4 ± 0.3**
	Severity of alveolitis (score 0-3)	0.2 ± 0.3	0.3 ± 0.3	0.3 ± 0.2	**2.8 ± 0.2**
	Alveolar oedema (% slides positive)	0 ± 0	4.2 ± 10	0 ± 0	**100 ± 0**
	Alveolar haemorrhage (% slides positive)	0 ± 0	0 ± 0	0 ± 0	**83 ± 13**
	Type II pneumocyte hyperplasia (% slides positive)	0 ± 0	0 ± 0	0 ± 0	**88 ± 14**
	Severity of bonchi(oli)tis (score 0–3)	0.8 ± 0.5	1.0 ± 0.1	1.1 ± 0.2	1.5 ± 0.5
	Degree of peribronchial cuffing (score 0–3)	2.0 ± 0.7	2.3 ± 0.5	2.5 ± 0.4	**0.6 ± 0.3**
	Severity of tracheitis (score 0–3)	0.7 ± 0.5	0.5 ± 0.5	0.5 ± 0.5	0.8 ± 0.8

Clinical scores. 6 out of 6 animals of all groups survived the 4 dpi follow up; relative body weight loss as the difference between day -1 and 4 dpi, presented as averages with standard deviation.
Virology. Area under the curve (AUC) for titration results on nose- and throat swab samples, which were collected daily after infection. The data are presented as averages with standard deviation, [*] and with the number of animals showing 1 or more virus positive swabs; lung viral loads are presented as averages with standard deviation or in case all animals of the group were negative in the virus isolation the lower limit of detection of $\leq 10^{1.3}$ $TCID_{50}$ per gram tissue is depicted.
Gross-pathology. Percentage of lung tissue affected, relative lung weight and the estimated enlargement of tracheobronchial lymphnode of ferrets 4 dpi with pH1N1. Results are presented as averages with standard deviation.
Histopathology. Semi-quantitative scoring for histopathology in lungs of ferrets 4 dpi with pH1N1. For the extent of alveolitis and alveolar damage we used: 0, 0%; 1, 25%; 2, 25–50%; 3, >50%. For the severity of alveolitis we scored: no inflammatory cells (0); few inflammatory cells (1); moderate numbers of inflammatory cells (2); many inflammatory cells (3). We also scored for presence of: alveolar oedema (no = 0, yes = 1), alveolar haemorrhage (no = 0, yes = 1) and type II pneumocyte hyperplasia (no = 0, yes = 1). For the severity of bronchiolitis and bronchitis we used: no inflammatory cells (0); few inflammatory cells (1); moderate numbers of inflammatory cells (2); many inflammatory cells (3). Finally, for the degree of peribronchial cuffing we scored: none (0), 1–2 cells thick (1), 3–10 cells thick (2), >10 cells thick (3). All these results are presented as averages with standard deviation.
Noticeable differences are marked bold and underlined. Where applicable see text for statistical analyses of the results.

Gross-Pathology and Histopathology

The principal macroscopic post-mortem lesion concerned the lungs and consisted of multifocal pulmonary consolidation, characterised by reddening and increased firmness of the parenchyme. The extent of consolidation was estimated by visual assessment. In the sham-immunised control group the mean percentage of affected lung tissue was 60% that corresponded to a mean relative lung weight (RLW) of 1.1 (range 0.94–1.32). Whereas in much less affected vaccinated groups LAIV-Russia-pH1N1, LAIV-Thailand-pH1N1, and LAIV-India-pH1N1 the mean percentages of affected lung tissue and corresponding mean RLWs were 1.7% and 0.5 (range 0.47–0.55), 2.2% and 0.5 (range 0.47–0.55), 4.2% and 0.5 (range 0.47–0.55), respectively (**Table 6.2.1**).

On histology the macroscopic pulmonary consolidation corresponded with an acute broncho-interstitial pneumonia. This pneumonia was characterised by the presence of neutrophils and macrophages within the lumina and walls of alveoli, and exfoliation and loss of alveolar epithelium. In addition protein rich oedema fluid, fibrin and extravasated erythrocytes in alveolar spaces and type II pneumocyte hyperplasia were observed in the more severe cases of alveolitis. In comparison of the extent and severity of alveolitis and/or alveolar damage (score range 0–3), the sham-immunised control group was on average the most severely affected scoring 2.4 and 2.8. Vaccinated groups LAIV-Russia-pH1N1, LAIV-Thailand-pH1N1, and LAIV-India-pH1N1 scored for both parameters equally noticeably less with 0.2, 0.3, and 0.3, respectively. In the sham-immunised control group the other parameters related to alveolar damage, such as alveolar oedema, alveolar haemorrhage, and type II pneumocyte hyperplasia were like-wise most prevalent, and absent in the vaccinated groups. The differences between the groups for the averaged scores for bronchi(oli)tis, tracheitis and mononuclear peribronchiolar/perivascular cuffing are summarised in **Table 6.2.1.**

DISCUSSION

Collectively, our data show that vaccination with three different preparations of a monovalent A/17/California/38/2009 live attenuated pandemic H1N1 influenza vaccine induced high levels of HI and VN serum antibody titers as well as protection against a robust pH1N1 challenge in a naïve ferret model. The ferrets were largely protected with one single vaccination against body weight loss, virus replication in both the URT and LRT, and against development of severe pathological changes in the respiratory tract. This indicates that LAIV produced from the parental pandemic virus as described in this ferret model lives up to the primary requirements of vaccines against pandemic influenza virus including the prevention of spread of the influenza virus and mitigation of the severity of disease.

The LAIV-pH1N1 preparations used in the present study were produced at production plants in Russia (group 1), Thailand (group 2) and India (group 3). Although there were slight differences in vaccine formulation and vaccine virus titers, all three induced equivalent antibody titers and protection against challenge. This indicates that indeed pandemic LAIV production capacity can rapidly be expanded taking advantage of production facilities in under-resourced countries (630).

LAIVs have major advantages including less complex downstream processing, lower unit cost and higher production yield as compared to inactivated vaccines. In general, influenza vaccine (inactivated split virus) production from one egg yields a vaccine virus titer of 10^9 EID_{50} translating to a mere single 15 µg vaccine dose. In comparison, a protective dose of LAIV amounts to an approximate increase to 10–100 doses per egg. Furthermore, basically the LAIV is ready for use after one-step purification and it can be distributed as suspension or in freeze-dried form.

The ferrets used in the present study where all confirmed seronegative against circulating influenza A and B viruses before vaccination. The relatively high HI and VN serum antibody levels in the pH1N1 LAIV-vaccinated ferrets at the moment of challenge (28 days after one single immunisation) are important because they are at least of the same order of magnitude as antibody levels found in ferrets vaccinated with MF59-adjuvanted 2009 A/H1N1 inactivated vaccine that had been primed with seasonal vaccine (550, 585). Similar to those ferrets, the pH1N1 LAIV-vaccinated ferrets had no detectable virus in their lungs and there was virtually no virus replication in the URT.

The extent and severity of the lung lesions of the sham-immunised control ferrets (group 4) was consistent with that described previously for pH1N1 influenza virus infection of ferrets and humans (506, 631). Intranasal immunisation with pH1N1 LAIV (groups 1–3) resulted in the strong reduction of alveolar damage, alveolitis, alveolar oedema and haemorrhage, bronchiolar and bronchial lesions as well as the extent of inflammation. Again, this observation is in line with the data found in ferrets immunised with MF59-adjuvanted 2009 A/H1N1 inactivated vaccine that had been primed with seasonal vaccine (550, 585).

For seasonal LAIVs it has been suggested that their efficacy is at least in part associated with the mimicking of a natural infection and thus the induction of a natural immune response. In contrast to seasonal H1N1 and LAIV-pH1N1 that are also restricted to replication in the URT, pH1N1 virus infection in both humans and ferrets shows a deviant severe diffuse alveolar damage caused by replication in epithelia of the LRT (395, 506, 631). However, remarkably LAIV-pH1N1 protects ferrets effectively against LRT damage following a robust intratracheal challenge with pH1N1. These data together with the relatively efficient production process and similar data obtained with pH1N1-LAIV based on the A/AnnArbor/6/60 ca-strain (627) emphasize the potential of the LAIV concept for pandemic preparedness.

Acknowledgements

The Workgroup of this research consisted of the following contributing authors: Koert J. Stittelaar[1], Edwin J.B. Veldhuis Kroeze[1,2], Leon de Waal[1], Geert van Amerongen[1], Judith M.A. van den Brand[2], James H. Simon[1], Irina Kiseleva[3], Natalie V. Larionova[3], Larisa Rudenko[3], Rajeev Dhere[4], Sit Thirapakpoomanunt[5], Marie Paule Kieny[6] and Albert D.M.E. Osterhaus[1,2] [[1]ViroClinics Biosciences B.V., Rotterdam, The Netherlands; [2]Department of Virology, Erasmus Medical Center, Rotterdam, The Netherlands; [3]Department of Virology, Institute of Experimental Medicine, St Petersburg, Russia; [4]Serum Institute of India, Ltd, Pune, Maharashtra, India; [5]Government Pharmaceutical Organisation, Ratchathewi, Bangkok, Thailand; [6]World Health Organisation, Geneva, Switzerland].

The Workgroup thanks P. van Run, L. Leijten, V. Teeuwsen, R. van Lavieren, C. van Hagen, W. van Aert, R. Boom, T. Harmsen and T. Bestebroer for technical assistance, W. Vos for biotechnical assistance and D. van de Vijver for statistical analysis. KJS, EJBVK, LdW, GvA, JHS and ADMEO are employees of ViroClinics Biosciences BV. ADMEO is chief scientific officer of ViroClinics Biosciences BV. The study was supported by the World Health Organisation. The in life phase of the study was conducted by ViroClinics Biosciences BV at the Netherlands Vaccine Institute, Bilthoven, The Netherlands. Management, coordination, sample processing, gross pathology, histopathology and virological analyses were conducted by ViroClinics Biosciences BV, Rotterdam, The Netherlands.

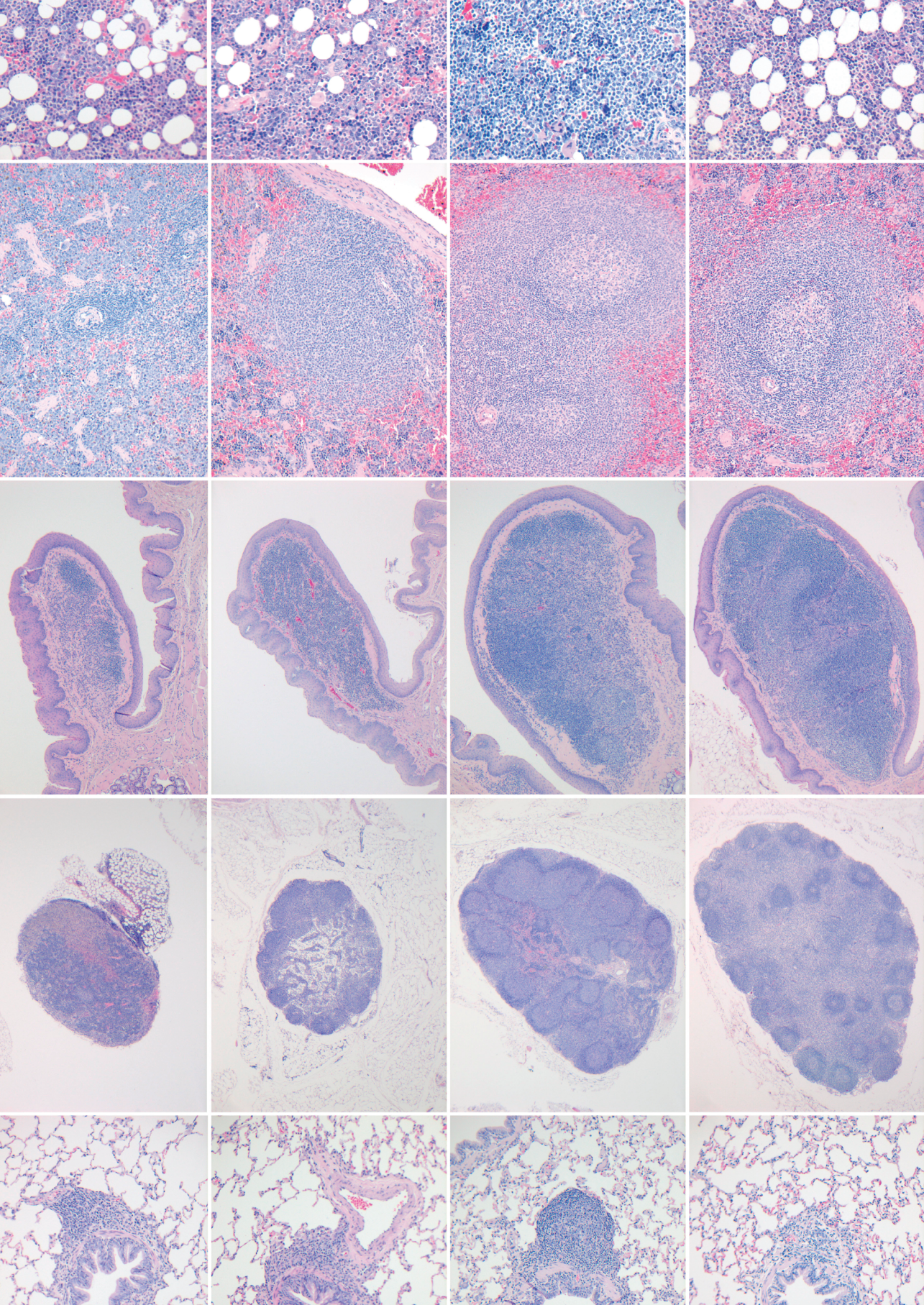

6.3

Synopsis of other applications of the ferret model in influenza intervention studies

Based on:

Intranasally administered Endocine™ formulated 2009 pandemic influenza H1N1 vaccine induces broad specific antibody responses and confers protection in ferrets. *A.K. Maltais[3], K.J. Stittelaar[1], E.J.B. Veldhuis Kroeze[1,2], G. van Amerongen[1], M.L. Dijkshoorn[4], G.P. Krestin[4], J. Hinkula[3], H. Arwidsson[3], A. Lindberg[3] & A.D.M.E. Osterhaus[1,2]*
Vaccine 2014; 32: 3307-3315

Intranasal H5N1 vaccines, adjuvanted with chitosan derivatives, protect ferrets against highly pathogenic influenza intranasal and intratracheal challenge. *A.J. Mann[5], N. Noulin[5], A. Catchpole[5], K.J. Stittelaar[1], L. de Waal[1], E.J.B. Veldhuis Kroeze[1,2], M. Hinchcliffe[6], A. Smith[6], E. Montomoli[7,8], S. Piccirella[8], A.D.M.E. Osterhaus[1,2], A. Knight[9], J.S. Oxford[5], G. Lapini[7], R. Cox[10] & R. Lambkin-Williams[5]*
PLoS One 2014; 9: e93761

Pandemic H1N1 vaccine requires the use of an adjuvant to protect against challenge in naive ferrets. *B. Baras[14], L. de Waal[1], K.J. Stittelaar[1], V. Jacob[14], S. Giannini[14], E.J.B. Veldhuis Kroeze[1,2], J.M.A. van den Brand[2], G. van Amerongen[1], J.H. Simon[1], E. Hanon[14], S.P. Mossman[14] & A.D.M.E. Osterhaus[1,2]*
Vaccine 2011; 29: 2120-2126

Prolonged influenza virus shedding and emergence of antiviral resistance in immunocompromised patients and ferrets. *E. van der Vries[2], K.J. Stittelaar[1], G. van Amerongen[1], E.J.B. Veldhuis Kroeze[1,2], L. de Waal[1], P.L.A. Fraaij[1,11], R.J. Meesters[12], T.M. Luider[12], B. van der Nagel[13], B. Koch[13], A.G. Vulto[13], M. Schutten[2] & A.D.M.E. Osterhaus[1,2]*
PLoS Pathogens 2013; 9: e1003343

Affiliations
[1] Viroclinics Biosciences B.V., Rotterdam, The Netherlands
[2]Department of Viroscience, Erasmus Medical Center, Rotterdam, The Netherlands
[3]Eurocine Vaccines AB, Karolinska Institutet Science Park, Solna, Sweden
[4]Department of Radiology, Erasmus Medical Center, Rotterdam, The Netherlands
[5]Retroscreen Virology, London, United Kingdom
[6]Archimedes Development Limited, Nottingham, United Kingdom
[7]University of Siena, Siena, Italy
[8]VisMederi LifeSciences, srl, Siena, Italy
[9]Evicom, Teddington, United Kingdom
[10]Department of Clinical Science, University of Bergen; Department of R&D, Haukeland University Hospital, Bergen, Norway
[11]Department of Paediatrics, Erasmus Medical Center Sophia, Rotterdam, The Netherlands
[12]Department of Neurology, Erasmus Medical Center, Rotterdam, The Netherlands
[13]Department of Hospital Pharmacy, Erasmus Medical Center, Rotterdam, The Netherlands
[14]GlaxoSmithKline Biologicals, Rixensart, Belgium

INTRODUCTION

This chapter describes the practical applications of the ferret model in four influenza intervention studies that assessed novel adjuvant-antigen formulations and immunosuppression strategies. The results regarding pathological interpretation and evaluation are summarised.

METHODOLOGY

The ferrets were normally healthy outbred females (390, 632) or males (633, 634) of 8-12 months of age, seronegative for circulating influenza viruses and ADV, and housed in standard cages and/or in negatively pressurised glovebox BSL-3 isolator cages in groups of six individuals. Commercial food and fresh drinking water were provided *ad libitum*. A body temperature logger (DST micro-T ultra-small temperature logger; Star-Oddi, Reykjavik, Iceland) was surgically implanted within the peritoneal cavity of each ferret. Routinely, ferrets were challenged by intratracheal (IT) inoculation with IAV, but in one study by intranasal (IN) inoculation as well (633). All procedures were conducted in compliance with European guidelines (EU directive on animal testing 86/609/EEC) and Dutch legislation (Experiments on Animals Act, 1997).

The body weights were recorded during the experiments and at autopsy. Post-mortem examinations were performed and all abnormalities were recorded. The lungs were examined and weighed. The percentages of affected lung parenchyma were visually estimated. The relative lung weights (RLW) were expressed as the ratio between the lung weight and the body weight at autopsy. Sampled organs/tissues were fixed in 10% neutral-buffered formalin for histopathology. After fixation, four samples from the left cranial and caudal lung lobes were embedded in paraffin and the tissue sections were stained with haematoxylin and eosin (H&E) for histological examination. The extent of alveolitis/alveolar damage (0%, <25%, 25–50%, >50% of section) and the severity of alveolitis/bronchitis/tracheitis/rhinitis (infiltration of no, few, moderate number of, or many inflammatory cells) were scored from 0 to 3. In the study from Baras and colleagues 2011, the histology score for alveolitis (including both the extent and severity of alveolitis) corresponded to the sum of both scores (score 0–6) (390).

STUDIES

In the first study (632), the efficacy of IN **Endocine^{TM}-adjuvanted** split virion and whole virus pH1N1/09 candidate vaccines challenged IT by homologous wildtype H1N1 A/

NL/602/2009 (wt-pH1N1) virus was evaluated. Endocine™ is a mucosal anionic lipid-based adjuvant composed of mono-olein and oleic acid, which are endogenous lipids in humans and other animals (635, 636). Known advantages of this novel IN application of Endocine™ mixed with inactivated IAV antigens include induction of local and systemic immunity protective against homologous IAV challenge in mice (637) and safe needle-free application. In contrast to live-attenuated influenza vaccines (LAIV), this application of inactivated IAV antigens may prove suitable for people < 2 years and > 59 years of age as well.

Nasal vaccine drops (0.2 ml) containing Endocine™ (20 mg/ml) and inactivated H1N1/California/2009 split virion antigen at 5, 15 or 30 µg HA or whole virus antigen H1N1/California/2009 whole virus antigen containing 15 µg HA (Eurocine Vaccines AB, Stockholm, Sweden) were given thrice with three-week intervals to ferret groups 3, 4, 5, and 6, respectively. These treatments induced high levels of serum antibody titres. Control group 1 was similarly sham-vaccinated with PBS (150 mM, pH 7.4). Group 2 was subcutaneously (s.c.) vaccinated twice with a non-adjuvanted inactivated trivalent influenza vaccine (TIV) containing 15 µg HA each of H1N1/California/7/2009, H3N2/A/Victoria/210/2009, and B/Brisbane/60/2008 (Fluarix® 2010/2011, GSK). IN sham-vaccination and TIV vaccinations induced no neutralising serum antibody titres. All animals were homologously IT challenged with 10^6 $TCID_{50}$ IAV H1N1/NL/602/2009 four weeks after the last vaccinations, and autopsied at 4 dpi.

The IN immunised ferrets were protected from virus replication in the lungs and largely protected from virus replication in the URT, and from major body weight loss (≤ 4.7%). In comparison, sham-vaccinated and TIV-vaccinated ferrets showed high viral titres in lung (mean titres; 5.7 and 5.5 $log_{10}TCID_{50}$/gram tissue, respectively) and nasal turbinates (mean titres: 7.2 and 6.9 $log_{10}TCID_{50}$/gram tissue, respectively), and most pronounced body weight losses (mean body weight loss of 18.0% and 11.5%, respectively). Fever was observed throughout all groups, with the highest body temperature increase in the sham-vaccinated animals (**Table 6.3.1**).

Pathological examination revealed lung lesions consisting of focal or multifocal pulmonary consolidation, characterised by well delineated reddening of the parenchyma. All ferrets in control group 1 (sham-vaccine) and group 2 (TIV) showed affected lung tissue with a mean percentage of 50% and 37%, respectively, and corresponded with a mean relative lung weight (RLW) of 1.5 and 1.3, respectively (**Table 6.3.1**). One animal from group 2 was found dead on 4 dpi; it suffered from an acute extensive viral pneumonia or DAD, which was the likely cause of death as no other lesions were evident. In contrast, lungs in groups 3–6 (Endocine™ vaccines) were much less affected with mean percentages of affected lung tissue of 7–8% and low RLWs within a close range of 0.8 to 0.9.

The pulmonary consolidation corresponded with an acute broncho-interstitial pneumonia. The histological parameters that were scored are summarised in **Table 6.3.2**. The most severe alveolar lesions were found in the control groups 1 (sham-vaccine) and 2 (TIV). All parameters of alveolar lesions scored lowest in group 5, but in fact the differences between the groups 3–6 were not significant.

The novel formulation of Endocine^{TM}-adjuvanted IN vaccines has shown to protect against significant lesions of the respiratory tract following IT challenge with pH1N1 IAV compared to sham-vaccination and TIV-vaccination in the ferret model. Furthermore, no significant differences among dosage or type of HA-antigen used as vaccine constituent regarding the conferred protection against respiratory lesions resulted from Endocine^{TM}-adjuvantad IN vaccinations.

Table 6.3.1 Efficacy of Endocine™-formulated 2009 H1N1 vaccines in ferrets demonstrated by clinical, virological and gross-pathology parameters.

		Group [a]					
		1	2	3	4	5	6
Clinical score	Survival	**6/6**	**5/6**	**6/6**	**6/6**	**6/6**	**6/6**
	Fever	**1.7 ± 0.6** (6/6)	**1.1 ± 0.4** (6/6)	**1.3 ± 0.3** (6/6)	**1.2 ± 0.6** (4/5*)	**1.1 ± 0.6** (6/6)	**1.3 ± 0.2** (6/6)
	Body weight loss	**18.0 ± 4.6** (6/6)	**11.5 ± 2.1** (6/6)	**−2.2 ± 2.6** (1/6)	**1.7 ± 1.5** (4/6)	**2.7 ± 3.3** (4/6)	**4.7 ± 3.1** (6/6)
Virology	Lung virus load [$log_{10}TCID_{50}/g$]	**5.7 ± 0.5** (6/6)	**5.5 ± 0.9** (6/6)	**≤1.5** (0/6)	**≤1.4** (0/6)	**≤1.3** (0/6)	**≤1.3** (0/6)
	Turbinates virus load [$log_{10}TCID_{50}/g$]	**7.2 ± 2.4** (6/6)	**6.9 ± 1.5** (6/6)	**≤1.9** (0/6)	**≤1.7** (0/6)	**≤1.7** (0/6)	**4.1 ± 2.7** (3/6)
	Virus shedding in nasal swabs	**2.6** (5/6)	**1.2** (4/6)	**0.058** (1/6)	**0.0** (0/6)	**0.0** (0/6)	**1.4** (3/6)
	Virus shedding in throat swabs	**10** (6/6)	**10** (6/6)	**0.0** (1/6)	**0.14** (1/6)	**0.0** (1/6)	**4.2** (5/6)
Gross pathology	Affected lung tissue [%]	**50 ± 25** (6/6)	**37 ± 21** (6/6)	**8 ± 4** (5/6)	**7 ± 5** (4/6)	**7 ± 5** (4/6)	**8 ± 4** (5/6)
	Relative lung weight	**1.5 ± 0.5**	**1.3 ± 0.1**	**0.8 ± 0.1**	**0.8 ± 0.1**	**0.8 ± 0.2**	**0.9 ± 0.1**

[a] Group 1 (control, IN PBS sham-vaccine), group 2 (s.c. TIV), group 3 (IN Endocine™-adjuvanted split antigen at 5 µg HA), group 4 (IN Endocine™-adjuvanted split antigen at 15 µg HA), group 5 (IN Endocine™-adjuvanted split antigen at 30 µg HA) and group 6 (IN Endocine™-adjuvanted inactivated whole virus antigen at 15 µg HA).

Clinical Scores. Survival, number of animals that survived up to 4 dpi; fever (°C), maximum temperature increase presented as average with standard deviation, number of animals in which fever was observed in parentheses, (*), body temperature of 1 animal in group 4 was not available due to malfunction of the recorder; % body weight loss between 0 and 4 dpi presented as average with standard deviation, number of animals with body weight loss in parentheses. *Virology*. Virus shedding in nose and throat swab samples, area under the curve (AUC) for titration results 1–4 dpi, number of animals showing 1 or more virus positive swab in parentheses; virus load in lung and turbinates ($log_{10}TCID_{50}/g$) on 4 dpi presented as average with standard deviation, or the lower limit of detection in case all animals in the group were virus negative, number of animals with lung/turbinate virus in parentheses. *Gross pathology*. % of estimated affected lung parenchyma by visual examination during autopsy on 4 dpi presented as average with standard deviation, number of animals with affected lung in parentheses; lung/body weight ratio ($\times 10^2$) on 4 dpi presented as average with standard deviation.

Table 6.3.2 Semi-quantitative scoring for histopathological parameters on 4 dpi.

		Group [a]					
		1	2	3	4	5	6
Histopathology	Extent of alveolitis/alveolar damage (score 0–3)	**2.08 ± 0.74** (6/6)	**1.88 ± 0.54** (6/6)	**0.42 ± 0.52** (3/6)	**0.08 ± 0.20** (1/6)	**0.04 ± 0.10** (1/6)	**0.42 ± 0.41** (4/6)
	Severity of alveolitis (score 0–3)	**2.04 ± 0.68** (6/6)	**1.63 ± 0.31** (6/6)	**0.50 ± 0.69** (3/6)	**0.08 ± 0.20** (1/6)	**0.04 ± 0.10** (1/6)	**0.46 ± 0.46** (4/6)
	Alveolar oedema (% slides positive)	**29 ± 29** (4/6)	**21 ± 19** (4/6)	**4 ± 10** (1/6)	**0 ± 0** (0/6)	**0 ± 0** (0/6)	**8 ± 13** (2/6)
	Alveolar hemorrhage (% slides positive)	**21 ± 40** (2/6)	**17 ± 26** (2/6)	**0 ± 0** (0/6)	**0 ± 0** (0/6)	**0 ± 0** (0/6)	**0 ± 0** (0/6)
	Type II pneumocyte hyperplasia (% slides positive)	**42 ± 34** (4/6)	**46 ± 37** (4/6)	**8 ± 20** (1/6)	**4 ± 10** (1/6)	**0 ± 0** (0/6)	**4 ± 10** (1/6)

[a] Group 1 (control, IN PBS sham-vaccine), group 2 (s.c. TIV), group 3 (IN Endocine™-adjuvanted split antigen at 5 µg HA), group 4 (IN Endocine™-adjuvanted split antigen at 15 µg HA), group 5 (IN Endocine™-adjuvanted split antigen at 30 µg HA) and group 6 (IN Endocine™-adjuvanted inactivated whole virus antigen at 15 µg HA).

Histopathology. Semi-quantitative scoring for histopathological parameters on 4 dpi. Extent of alveolitis/alveolar damage, score: 0, 0%; 1, 25%; 2, 25–50%; 3, > 50%; severity of alveolitis, score: no inflammatory cells (0); few inflammatory cells (1); moderate numbers of inflammatory cells (2); many inflammatory cells (3); alveolar oedema, alveolar hemorrhage and type II pneumocyte hyperplasia were scored as positive slides (no = 0, yes = 1); All histopathology results are presented as average with standard deviation, number of affected animals per group of six in parentheses.

In the second study (633), the efficacy of two **IN Chitosan (CSN)-adjuvanted** H5N1 Influenza vaccines against HPAIV was evaluated. Challenge consisted of IT and IN inoculation of IAV H5N1/Vietnam/1194/2004. Chitosan is a co-polymer of D-glucosamine and N-acetyl-D-glucosamine. Chitosan is available commercially in water-soluble (< pH 6) salt forms, such as CSN glutamate and CSN hydrochloride. Methylation of amine groups of CSN as in trimethyl-CSN (TM-CSN) provides increased solubility in neutral and basic environments (638). The effectiveness of CSN as vaccine adjuvant correlates with its degree of solubility. CSN improves the adhesion of vaccine antigens to the mucosa of the nasal cavity.

IN vaccines or PBS as sham vaccine were given (0.2 ml) to ferret groups twice with a 3-week interval as follows, followed by intratracheal (IT) or intranasal (IN) virus challenge: group 1, PBS sham (IT); group 2, non-adjuvanted-antigen (IT); group 3, CSN-antigen (IT); group 4, TM-CSN-antigen (IT); group 5, PBS sham (IN); group 6, CSN-antigen (IN). The inactivated subunit antigen (15 µg HA) was from vaccine seed strain NIBRG-14, a reassortant of PR8 IAV and H5N1 AIV A/Vietnam/1194/2004 (Batch#1090/10, Novartis, Italy). The CSN-adjuvanted and TM-CSN-adjuvanted vaccinations induced high levels of serum antibody titres, while the sham-vaccinations and non-adjuvanted vaccinations induced no detectable antibody titres. All animals were challenged with 10^5 $TCID_{50}$ IAV H5N1/Vietnam/1194/2004 four weeks after the last vaccinations, and autopsied at 5 dpi.

CSN-adjuvanted vaccinated group 3 and TM-CSN-adjuvanted vaccinated group 4 showed reduced viral replication of the LRT and reduced disease, and were protected from death following IT viral challenge. In comparison, in non-adjuvanted vaccinated IT-challenged group 2 showed extensive viral replication of the LRT, and two of six animals were not protected from death.

IN viral challenge of sham-vaccinated group 5 induced virus replication predominantly in the URT and CNS, without causing mortalities. In comparison, IT viral challenge of sham-vaccinated group 1 resulted predominantly in a LRT infection, which was associated with a high mortality rate, as five of six animals were either found dead or had to be euthanised because of severe illness. Interestingly, all mortalities were associated with IT viral challenge and not with IN viral challenge regardless of the type of vaccination or sham-vaccination.

The viral infection of the LRT in sham-vaccinated group 1 especially, resulted in severe tissue damage, which was characterised by multifocal to coalescing well-delineated intense reddening of consolidated lung parenchyma. The most severely and extensively affected lungs had copious amounts of frothy fluid (oedema) oozing from the bronchi, and several had peripheral emphysema also. Related to pneumonia were enlarged tracheobronchial lymph nodes. Histopathological examination of the H5N1 IAV affected lungs revealed flooding of alveolar lumina with macrophages, neutrophils,

and erythrocytes, mixed with protein strands and fibrin, oedema fluid, and cellular debris. The alveolar septa were thickened, and epithelial cells were swollen or sloughed. Subsequent type II pneumocyte hyperplasia was generally observed in cases of mild to moderate of alveolar damage. The ferrets that died spontaneously or those that had to be euthanised prematurely suffered from similar very severe viral interstitial pneumonia or DAD. Both CSN-adjuvanted and TM-CSN-adjuvanted vaccinations strongly reduced lesions of the LRT compared to sham-vaccination and non-adjuvanted vaccination following IT viral challenge.

IN viral challenge in both sham-vaccinated group 5 and CSN-adjuvanted vaccinated group 6 equally induced predominantly mild rhinitis (URT), which was characterised by infiltration of mostly neutrophils and fewer lymphocytes and occasional eosinophils in the epithelium and *lamina propria* of the respiratory nasal mucosae.

Five animals were diagnosed with an encephalitis, yet remarkably none of these died or had to be euthanised prematurely. All but one of these originated from IN-challenged animals (one CSN-adjuvanted vaccinated animal from group 6 and three sham-vaccinated animals from group 5). The one IT-challenged animal from non-adjuvanted vaccinated group 2 had an inflammation of the brainstem, whereas all IN-challenged animals had an inflammation of the olfactory bulb, which is in close anatomical proximity to the nasal cavity. All these encephalitides were characterised by lymphohistiocytic perivascular cuffing, gliosis, and swelling of endothelial cells.

The novel formulation of TM-CSN-adjuvanted IN vaccines has shown to protect against significant lesions of the LRT (**Figure 6.3.1**) and mortality following IT challenge with H5N1 IAV in the ferret model. Furthermore, the CSN-adjuvanted IN vaccine showed partial protection against alveolitis following IT viral challenge and no protection against rhinitis following IN viral challenge.

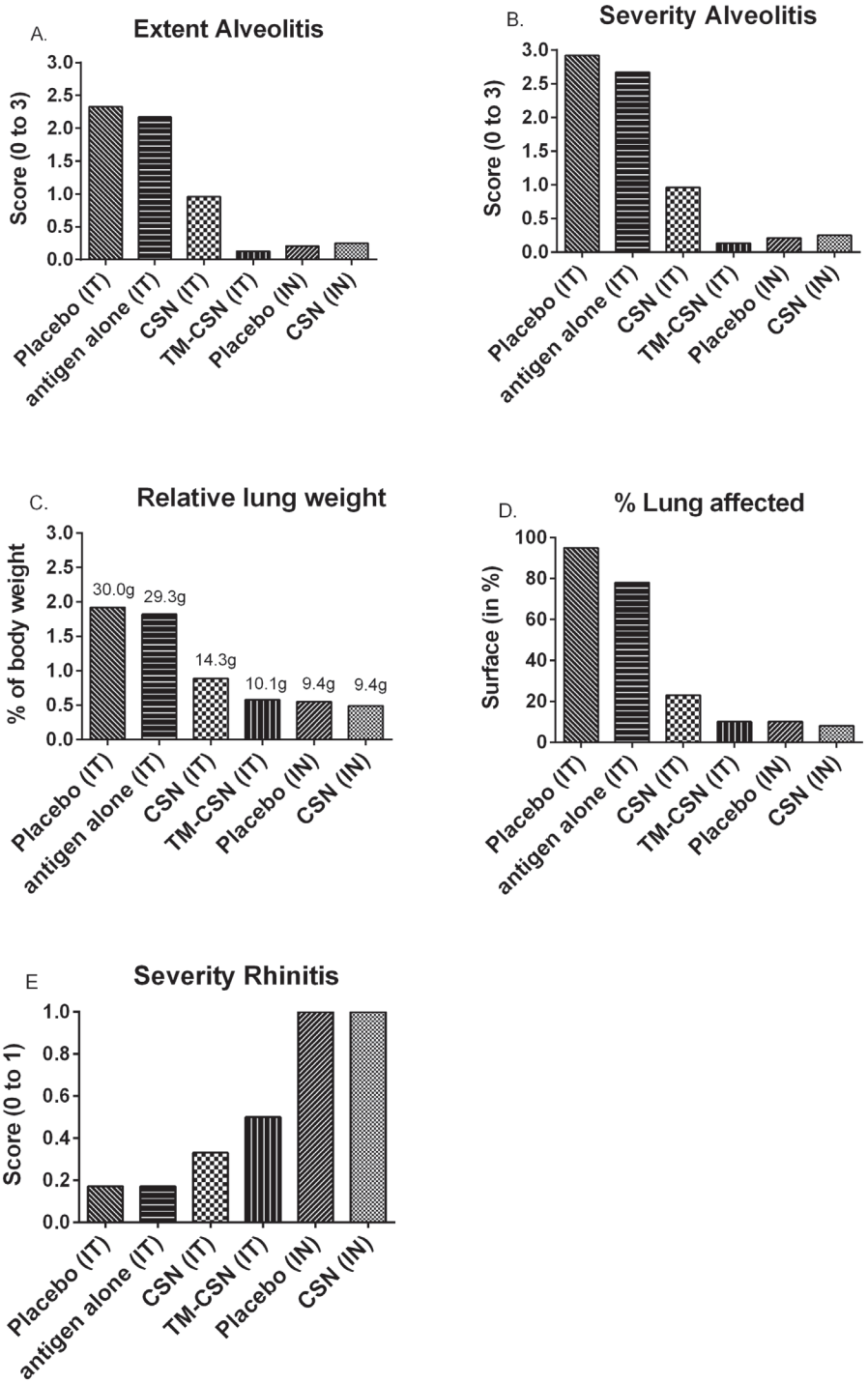

Figure 6.3.1 Histopathology in control and vaccinated ferrets post challenge.

← **Figure 6.3.1 Histopathology in control and vaccinated ferrets post challenge.** Histopathology was performed on ferrets that were euthanised according to schedule as well as animals euthanised prematurely on welfare groups and any decedents. In those ferrets that were not euthanised according to the schedule all had acute severe pneumonia or diffuse alveolar damage, which was considered the likely cause of death. The panels represent: (A) extent of alveolitis, (B) severity of alveolitis, (C) relative weight of lung, (D) percentage lung affected, and (E) severity of rhinitis.

In the third study (390), the efficacy of a pH1N1 A/California/7/09 split vaccine with or without the **adjuvant AS03**, against challenge with pH1N1 IAV A/NL/602/09 was evaluated. AS03 is an oil-in-water-based adjuvant system containing α-tocopherol, which showed to increase the immunogenicity in a clinical trial involving an H1N1 strain (639).

In this study, AS03 was formulated in two concentrations, 11.86 mg/ml tocopherol ($AS03_A$) and 5.93 mg/ml tocopherol ($AS03_B$). Intramuscular vaccines (1.0 ml) with and without AS03 or PBS as sham vaccine were given to ferret groups once or twice with a 3-week interval as follows: groups 2, 4 and 6 received two vaccinations with 15, 3.75 or 1.9 µg HA of $AS03_A$-adjuvanted pH1N1 A/California/7/09 split vaccine, respectively; groups 3 and 5 received one vaccination with 3.75 or 1.9 µg HA of $AS03_A$-adjuvanted pH1N1 A/California/7/09 split vaccine, respectively; group 7 received two vaccinations with 1.9 µg HA of $AS03_B$-adjuvanted pH1N1 A/California/7/09 split vaccine; control groups 1 and 8 received two vaccinations with 15 µg HA of the non-adjuvanted pH1N1 A/California/7/09 split vaccine or two sham-vaccinations, respectively. Two vaccinations of AS03-adjuvanted A/pH1N1 induced substantial levels of neutralising serum antibody titres with 100% of animals achieving titres ≥40 against the challenge strain (**Table 6.3.3**). Single vaccination with AS03-adjuvanted A/pH1N1 (groups 3 and 5) induced in 60–67% of animals neutralising serum antibody responses ≥40, while single non-adjuvanted vaccination induced no detectable neutralising antibody titres (≤4). All animals were challenged IT with 10^6 $TCID_{50}$ pH1N1 influenza virus A/NL/602/2009 four weeks after the last vaccinations, and all survived until autopsy at 4 dpi.

In the AS03-adjuvanted vaccinated animals, compared to non-adjuvanted vaccinated and sham-vaccinated animals, the RLWs were lower, and the percentages of visually affected consolidated lung tissue were much lower (**Table 6.3.3**). Histopathological examination revealed that the pulmonary consolidation corresponded with an acute broncho-interstitial pneumonia. The extent of damage and inflammation was consistently lowest in the lungs of ferrets that received two vaccinations with 15 µg of $AS03_A$-adjuvanted HA (group 2) and consistently highest in ferrets in the control groups (groups 1 and 8). With the exception of group 3, histopathologic scores among all ferrets immunised with the AS03-adjuvanted vaccine were significantly lower compared to those in ferrets immunised with the non-adjuvanted vaccine or sham vaccine with PBS (**Table 6.3.3**).

These findings suggested a critical role for adjuvantation and two vaccinations with the 2009 A/H1N1 pandemic influenza vaccine intended for human use. Especially so, if to protect unprimed children who were at high risk of developing severe complications from 2009 A/H1N1 infection.

In the fourth study (634), it was evaluated whether **immunosuppression** with prolonged IAV shedding and antiviral resistance of pH1N1 IAV could be modelled in the ferret.

Immunosuppression in the ferret was achieved with a multidrug treatment comprised of: mycophenolate mofetil (MMF), tacrolimus, and prednisolone. Advantages of this treatment are efficacious immunosuppression in ferrets by means of the same cocktail of drugs used in humans to suppress immunity. Disadvantages of this treatment include disease from facultative pathogens, which may influence results. Hence all animals received antibiotic prophylaxis of amoxicillin and clavulanic acid.

Four days before virus inoculation, all 6 groups received oral amoxicillin/clavulanic acid (10/2.5 mg/kg, Pharmachemie BV, Haarlem, NL). One day later, groups 2, 3, 5 and 6 were treated orally with MMF (20 mg/kg, CellCept, Roche, NL), tacrolimus (0.5 mg/kg, Prograft, Astellas Pharma BV, Leiderdorp, NL), and prednisolone sodium phosphate (8 mg/kg, Hospital Pharmacy, UMCN, Nijmegen, NL) during the remainder of the study. Prednisolone dosage was halved every 7 days from 8 mg/kg in the first to 1 mg/kg in the last week. One day after virus inoculation, groups 3 and 6 were treated with oseltamivir phosphate (10 mg/kg, Tamiflu, Hoffman-La Roche, Basel, Switzerland) for the remaining 20 days of the study.

The animals of groups 1, 2 and 3 were IT inoculated with 10^4 $TCID_{50}$ oseltamivir sensitive pH1N1 IAV (A/NL/1715b/2009 wild type; H275) and the animals in groups 4, 5 and 6 were IT inoculated with 10^4 $TCID_{50}$ oseltamivir resistant pH1N1 IAV (mutant; H275Y) and autopsied on days of spontaneous death or at 21 dpi.

Pathological examination revealed, in all MMF/tacrolimus/prednisolone-treated groups 2, 3, 5, and 6, prolonged virus replication (≥ 7 dpi) evidenced by IAV NP positive cells by IHC, whilst oseltamivir treatment in groups 3 and 6 reduced IHC positivity and favoured reduced body weight loss and survival until 21 dpi. Additionally, opportunistic infections became florid in all these treated groups evidenced by several cases (n=8) of bacterial bronchopneumonia (**Figure 6.3.2**) and few cases (n=3) of mycotic bronchopneumonia (**Figure 6.3.3**). The bacterial infections appeared associated with reduced survival. None of the untreated animals showed IAV NP positivity in IHC nor opportunistic infections of the respiratory tract at 21 dpi. MMF/tacrolimus/prednisolone-treated animals showed cellular depletion of lymphoid (**Figure 6.3.4**) and hemopoietic tissues (lymph nodes, tonsils, BALT, GALT, spleen, and bone marrow) in comparison to untreated animals.

Table 6.3.3 Neutralising antibody responses against the challenge strain after immunisation with the H1N1 A/California/7/09 split vaccine, lung pathology, viral load in the lung and viral shedding in the nose of ferrets after challenge with H1N1 A/The Netherlands/602/09 (10^6 $TCID_{50}$).

Group no.[a]	Vaccination regimen H1N1 A/California/7/09	Anti-A/NL/602/09 neutralising antibody titres[b]		Lung pathology			Viral load lung[f]		Viral shedding in nasal swabs	
		GMT (95%CI)	% Responders (titres ≥ 40)	Affected lung parenchyma[c] (%)	RLW[d] ($\times10^{-2}$)	Histology score[e]	$TCID_{50}$/g	%[g]	$TCID_{50}$/ml[h]	%[i]
1	15 µg, unadjuvanted (2×)	**4** (4–4)	**0**	**22.5**	**1.54**	**2.79**	**239883**	**100**	**1950**	**83**
2	15 µg, $AS03_A$ (2×)	**376** (145–974)	**100**	**0.6**	**0.99**	**0.26**	**<10**	**0**	**<10**	**0**
3	3.75 µg, $AS03_A$ (1×)	**63** (12–322)	**67**	**0.2**	**1.06**	**1.42**	**166**	**33**	**32**	**33**
4	3.75 µg, $AS03_A$ (2×)	**794** (289–2184)	**100**	**0.5**	**0.93**	**0.50**	**<10**	**0**	**83**	**60**
5	1.9 µg, $AS03_A$ (1×)	**76** (15–375)	**60**	**0.5**	**1.25**	**0.90**	**15**	**17**	**32**	**40**
6	1.9 µg, $AS03_A$ (2×)	**352** (156–795)	**100**	**0.3**	**1.07**	**0.42**	**<10**	**0**	**20**	**33**
7	1.9 µg, $AS03_B$ (2×)	**697** (236–2059)	**100**	**1.0**	**1.01**	**0.58**	**<10**	**0**	**200**	**67**
8	PBS	**13** (10–16)	**0**	**33**	**1.81**	**3.88**	**478630**	**100**	**2399**	**100**

[a] Five (groups 4 and 5) or six (groups 1–3 and 6–8) animals per group.

[b] Anti-A/The Netherlands/602/09 neutralizing antibody titres on day 48 (the day before the challenge).

[c] Average percentage of affected lung parenchyma by visual examination during autopsy.

[d] Relative lung weight, average lung/body weight ratio ($\times10^{-2}$).

[e] Average extent and severity of alveolitis/alveolar damage (score 0–6).

[f] Virus isolation ($TCID_{50}$ per gram) on MDCK of lung tissue collected four days after challenge. Limit of detection is standardised as 5.62 $TCID_{50}$ per gram.

[g] Percentage of ferrets with detectable viral load in the Lung.

[h] Virus isolation ($TCID_{50}$ per ml of swab) on MDCK of nasal swabs collected four days after challenge (peak of viral shedding). Limit of detection is standardised as 5.62 $TCID_{50}$ per ml.

[i] Percentage of ferrets with detectable viral shedding in nasal swabs at one or more time points after challenge.

Indicators of immunosuppression in MMF/tacrolimus/prednisolone-treated ferrets according to pathological examination included: (a) reduction of lymphocyte proliferation and follicle formation in lymphoid tissues, (b) prolonged virus replication in lungs and noses, and (c) disease from facultative pathogens.

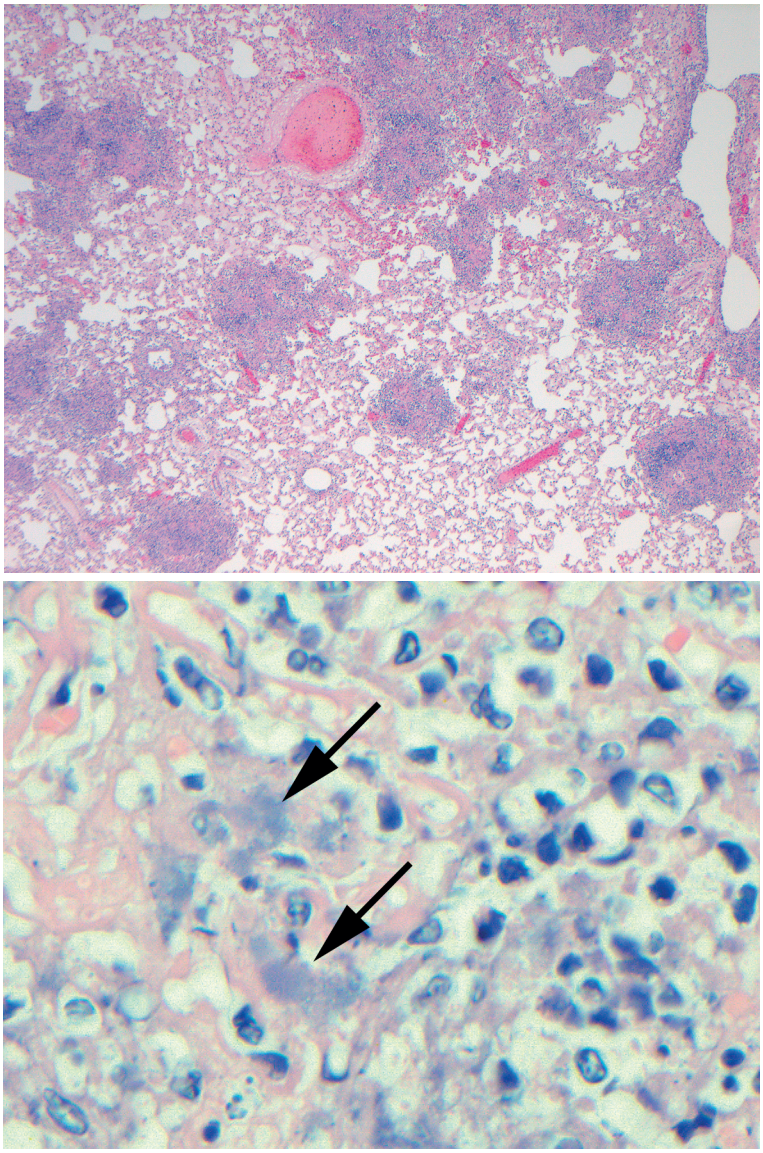

Figure 6.3.2 Bacterial bronchopneumonia in a MMF/tacrolimus/prednisolone-treated ferret with pH1N1 IAV infection, at 10 dpi. On the right is a close-up photomicrograph showing intrabronchial presence of bluish finely granular colonies of bacteria (arrows). H&E stains, original magnifications 25× and 800×.

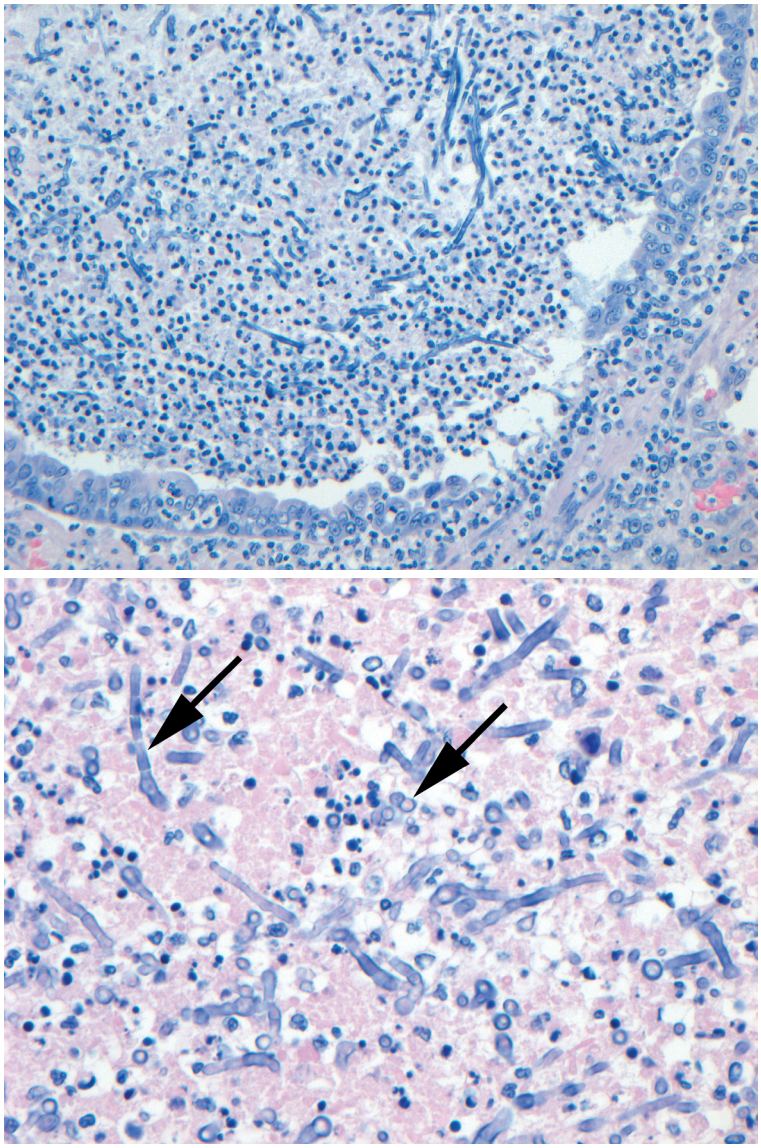

Figure 6.3.3 Mycotic bronchopneumonia in a MMF/tacrolimus/prednisolone-treated ferret with pH1N1 IAV infection, at 21 d dpi. On the right is a close-up photomicrograph showing intrabronchial presence of longitudinal sections and cross sections of septate fungal hyphae (arrows) amidst necrosuppurative exudates. H&E stains, original magnifications 200× and 400×.

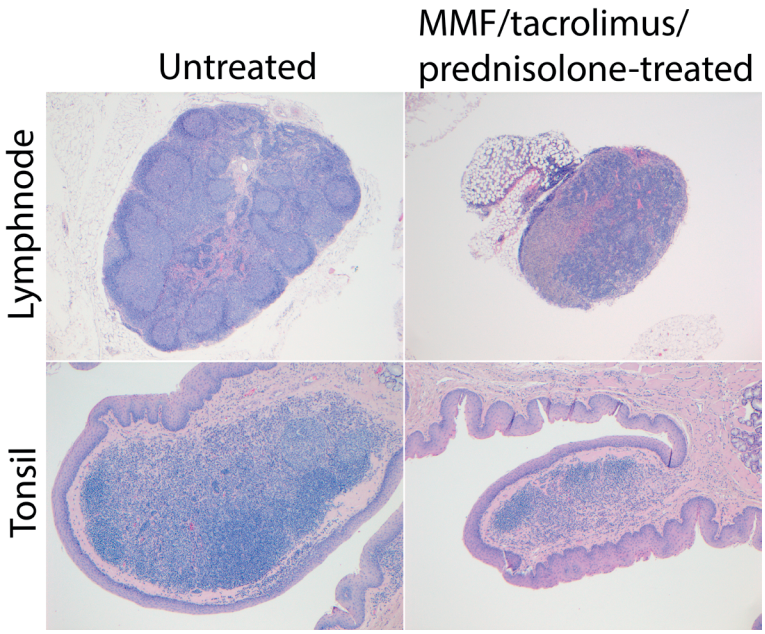

Figure 6.3.4 Reduced lymphoid follicle formation in tracheobronchial lymph nodes and lymphodepletion in the tonsils of MMF/tacrolimus/prednisolone-treated ferrets (MMF, mycophenolate mofetil) compared to untreated ferrets. Representative photomicrographs of tracheobronchial lymph nodes (original magnification 25×) and tonsils (original magnification 50×). H&E stains.

In conclusion of this synopsis, pathological examinations revealed the protective systemic immunity against intratracheal IAV challenge induced by novel adjuvanted influenza vaccines with a novel innovative intranasal administration route such as Endocine-pH1N1 and Chitosan-H5N1, or induced by novel adjuvanted influenza vaccine formulations as AS03-pH1N1 by reduced lesions of the ferrets' respiratory tract. Additionally the efficacious development of immunosuppression with prolonged IAV replication was shown in ferrets' respiratory tract and lymphoid tissues. These assessments were successfully performed in the ferret model, thus expanding its possibilities and confirming its suitability to test protective and therapeutic treatments against influenza-induced disease.

CHAPTER 7

Summarising Discussion

This final chapter begins with a summary part of the main findings of the research performed in these studies and described in the previous chapters, which collectively expand on and contribute to the current scientific knowledge on the pathogenesis and prevention of influenza. Subsequently, knowledge gaps in the pathogenesis of influenza-induced ARDS are discussed, together with recommendations for future research. Finally, the overall conclusions and perspectives of this thesis are summarised.

SUMMARY OF THE PERFORMED RESEARCH

The findings from **chapter 2.1** indicate that in an infectious respiratory disease like influenza the alveolar epithelial cell layer is the most important constituent of the EEB in the pathogenesis of influenza-induced ARDS and alveolar oedema formation. Not only are these epithelial cells the initial target of viral infection and replication; they also constitute the strongest layer of the EEB in preventing alveolar oedema to develop. Thus alveolar epithelial cells should be the primary research focus regarding both pathogenesis and therefore probably also therapeutic approaches for influenza-induced ARDS and alveolar oedema.

In contrast to most mammals' (including humans) and wild waterbirds' epithelial cells being the main target of AIV infections, the findings of **chapter 2.2** indicated the tropism of HPAIVs for endothelial cells in chickens and black swans. Furthermore, enteric inoculation of H5N1 HPAIV in domestic cats also led to endothelial cell involvement. The mechanisms involved in these species-specific differences in tropism for epithelial cells versus endothelial cells of IAV remain unclear. Regardless whether endothelial cells are infected by influenza virus, additional findings from **chapters 2.1 and 2.2** point to the important role of the endothelium of the alveolar EEB in the pathogenesis of influenza-induced ARDS as significant contributors to the pro-inflammatory response. Reducing the synthesis of pro-inflammatory cytokines and chemokines in endothelial cells should mitigate the pulmonary inflammatory response significantly.

In **chapter 3.1** we showed that many animal species are susceptible to IAV infections. The host range of IAVs includes many more animal species, including humans, than the host ranges of influenza B, C, and D viruses. The majority of this broad host range of IAV is accounted for by sporadic short-lived infections. Yet, the host range of endemic infections is gradually expanding as new IAVs from wild birds or via intermediate hosts are introduced and become established infections in humans, pigs, horses, and, most recently (2005), in dogs. Canine Influenza is caused by equine-origin H3N8 IAV predominantly in North America or caused by avian-origin H3N2 IAV predominantly in Asia. However, since April 2015 avian-origin H3N2 IAV has been detected as etiology of canine influenza in the USA as well (640). There is ongoing concern that zoonotic

transmission of IAVs from animals to humans may give rise to new epidemics or even pandemics in the human population. Conversely, anthroponotic transmission of 2009 pH1N1 IAV from people to few individual pet ferrets, cats, and dogs, and several zoo animals has been recorded, yet without becoming endemic in these animals.

Ferrets and carnivores in general, have shown to be highly susceptible to IAV infection and to be very sensitive to develop subsequent disease. However in many other animal species, the susceptibility to infection does not equal or imply a sensitivity to develop disease, as it may induce subclinical infections only.

Risk factors involved in severe influenza outbreaks in novel host species such as groups of carnivores (and not in infections of individual animals) were: introductions of a new IAV into cohorts of immunologically naïve carnivores housed in confined spaces, as kennels, farms, and zoos. Remarkably, such outbreaks are not apparent in cattle under similar conditions at all.

The sensitivity to develop disease after infection seems mostly inherent to attributes of a particular order or family of animal species. However, there are virus-specific attributes that influence the propensity to develop disease, too. For example, H5N1 HPAIV induces more severe pneumonia in a ferret than a seasonal H3N2 IAV. In **figure 7.1.1** the sensitivity of several mammals to natural H5N1 HPAIV-induced disease is plotted against their reported incidences.

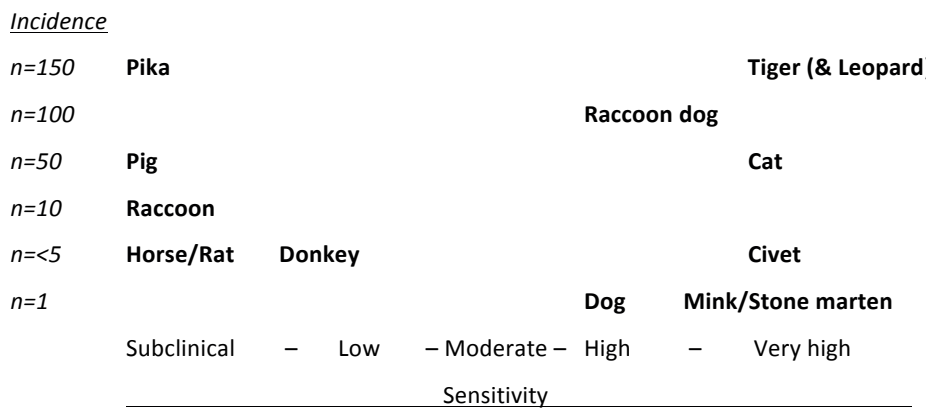

Figure 7.1.1 Sensitivity of mammalian animal species to natural H5N1 HPAIV infections and induced disease with corresponding reported incidences (641).

In **chapters 3.2** and **chapters 4 to 6**, the ferret model was further characterised and developed as a model for influenza-induced ARDS and alveolar oedema in humans.

In **chapters 4 to 6**, intratracheal inoculation of several different IAVs was applied to reproducibly induce the required acute and severe pneumonia in the ferret as model for ARDS and alveolar oedema. The intratracheal route was essential to cause broncho-

interstitial pneumonia, as intranasal inoculations of H5N1 HPAIV caused evident neurological signs (642), and meningo-encephalitis (549).

In **chapters 4.1** and **4.2**, the ferret model was used to characterise the pathogenicity of the newly emerged virus 2013 H7N9 LPAIV from humans, and to characterise the pathogenicity and transmission of new escape mutants of 2009 pH1N1 IAV. In contrast to the low pathogenicity of this H7N9 AIV in poultry, **chapter 4.1** illustrated the high pathogenicity of this H7N9 IAV in the ferret, similar to natural infections in humans. The finding that H7N9 LPAIV induced a rhinitis in these ferrets was corroborated by the virus' attachment to the URT (68), and by a limited airborne transmission between ferrets (643). Studies performed in **chapter 4.2** indicated that a neuraminidase-resistant mutant virus isolate (NL/2631-R223) had slightly lower, albeit not significant, pathogenicity but comparable replicative ability and transmissibility to reference pH1N1 (NL/602) IAV in ferrets, and thus indicated a potential spread of this neuraminidase-resistant mutant virus in human population.

In **chapter 5** the technical development and advancement of implementing *in vivo* CT-scanning of pH1N1 IAV-inoculated ferrets was successfully performed as 'proof of principle' and showed its additional value in successive monitoring of influenza-induced ARDS development in this animal model. This methodology revealed reductions in aerated lung volume that were replaced by pulmonary oedema and inflammatory cells, visible as ground glass opacities.

Consecutive *in vivo* CT-scanning yielded several additional benefits over conventional (time course) studies: (a) the inter-individual variation in inflammatory responses was reduced as the day-to-day scanned animal served as its own base-line control animal; thereby (b) reducing the number of animals needed; and (c) no need to artificially lump together pathology results of ferrets that had been euthanised or had died on different days after inoculation; (d) establishment of the optimal time point of maximal pulmonary consolidation allowed for performing autopsies in subsequent trials for antivirals and vaccines at the time point of the biggest possible spread in values between control group and treatment group (3 dpi for pH1N1 IAV in the ferret model).

The subsequent practical application of measuring altered ALV by CT-scanning as read-out parameter in a vaccine efficacy study was described in **chapter 6.1.** These findings confirmed the suitability of the ferret model in evaluating the degrees of daily altered ALV as correlate of protection against influenza virus challenge in vaccinated ferrets compared to controls and classical virology and pathology. The findings of **chapter 6.2** confirmed the suitability of the ferret model to study and compare the efficacies of several intranasally applied live-attenuated-influenza-vaccines against intratracheal pH1N1 IAV challenge. These vaccine viruses exhibited controlled replication limited to the nasal epithelium of ferrets, yet thereby inducing a strong systemic protective immune response without the need of an adjuvant. The findings of **chapter 6.3** indicated

the possibilities and limitations of use of ferrets to study novel adjuvant formulations with novel administration routes, and to develop an immunosuppression model. The intranasal administration of mucosal adjuvants or immunomodulators combined with either intranasal or intramuscular immunisation (against IAVs pH1N1 and H5N1) in the ferret model had the advantage of successfully inducing strong systemic protective immune responses, as is intended for future use in humans. In the immunosuppression study, the ferret model had the advantage that the same drugs used to suppress immunity in humans worked equivalently in ferrets, and IAV inoculation lead to prolonged viral replication compared to placebo. A disadvantage was that opportunistic infections became florid in the ferrets.

DISCUSSION OF THE PATHOGENESIS OF INFLUENZA-INDUCED ARDS AND OEDEMA FORMATION ACCORDING TO INVOLVED CELL TYPES WITH RECOMMENDATIONS FOR FUTURE RESEARCH

In this section, the pathogenesis of influenza-induced ARDS and alveolar oedema with future perspectives for further research are discussed according to the main structural and inflammatory cell types that constitute and influence the alveolar EEB in influenza-induced ARDS, as described in **chapter 2.1**.

Historically, the pathogeneses of ARDS and pulmonary oedema have been studied mainly as outcomes of bacterial sepsis. Such studies focused on modelling endothelial disruption by bacterial LPS as a starting point of the cascade. However, in IAV infections in humans and most other mammals, the initial target constitutes the epithelial cell layer of the alveolar EEB. Moreover the alveolar epithelial lining, in which tight junctions (TJs) interconnect the epithelial cells, is considered more important as fluid barrier than the vascular endothelial lining of the alveolar EEB. Therefore, emphasis is put on the epithelial cells lining the alveolus as the major target of aerogenous influenza virus infections. Influenza virus infection directly and indirectly leads to damage, and ultimately death of epithelial cells, permitting alveolar fluid leakage and respiratory insufficiency, which are hallmarks of the pathogenesis of influenza-induced ARDS. However, it should not be forgotten that, under some conditions, highly pathogenic avian influenza viruses can exhibit endotheliotropism as well, as described in **chapter 2.2.**

Epithelium

Two types of epithelial cells line the pulmonary alveoli: **type I and type II pneumocytes**. Type II pneumocytes outnumber type I pneumocytes (in the order of 60% vs 40%), whilst remarkably, type I pneumocytes cover 95% of the alveolar surface by spanning multiple alveoli with their flat cytoplasmic projections. This thin lining allows for easy

gas diffusion between air and blood. Type II pneumocytes are not flat but cuboidal cells that play a role in re-epithelisation of denuded alveoli. The epithelial layer constitutes the main fluid barrier in the EEB as it accounts for more than 90% of the resistance to protein transport across this barrier. The thus maintained gradient in colloid osmotic pressure across the EEB passively prevents water leakage into the alveolar lumen, and subsequently prevents pulmonary oedema.

ARDS is a clinical syndrome and term, which corresponds to the pathological term of **diffuse alveolar damage** (DAD). One of the histopathological hallmarks of DAD is the presence of alveolar oedema, caused by damage to the alveolar EEB. However, the presence of alveolar oedema only is not adequate to make the diagnosis DAD. By definition this requires additional detection of hyaline membranes, as visible evidence of epithelial necrosis. Disruption of the normally continuous epithelial layer of the EBB and presence of consequent alveolar oedema, as important features of DAD, can be detected and scored by histopathology. Microscopic identification of damaged pneumocytes in direct conjunction with presence of alveolar oedema will ascertain and emphasise the essential role of the epithelial lining in the pathogenesis of ARDS. The gradation of histological damage to alveolar pneumocytes may range from subtle disruptions in the normally continuous epithelial layer to completely denuded alveoli. Recognition of such subtle disruptions is aided when stained with an epithelium-specific antibody such as pankeratin by IHC. Therefore, as a recommendation for future research in the ferret model, the correlation that anticipatedly exists between damaged pneumocytes and alveolar oedema should be investigated in sufficient numbers of slides. As practical recommendation for a set-up of acutely IAV-inoculated ferrets, 25 alveoli (or 25 microscopic fields of alveoli at 100x magnification) per lung slide that contain alveolar proteinaceous fluid are scored for the presence or absence of damaged pneumocytes. If a total of four lung slides per animal in a total of six animals per group are evaluated and added it amounts to a percentage of damaged epithelium in alveolar oedema and should allow for sufficient statistical power and significance. Other variables that could be included and simultaneously assessed are for example: the degree of pneumocyte damage in relation to the degree of alveolar oedema and possibly even the protein contents of the fluid (according to the intensity of eosinophilia of the fluid in H&E-stains), and/or the grade of pneumocyte damage in relation to the number and type of inflammatory cells present within the epithelium or alveoli. Preferably this set-up entails analyses of ferret lungs sampled at different dpi with different strains of IAVs at various viral inoculum dosages to complete a comprehensive dataset. Logically, these data are to be compared to equally assessed sham-inoculated control ferrets.

Tight junctions (TJs) firmly interconnect alveolar epithelial cells, and are composed of various proteins, including claudins, and zona occludens 1, 2, and 3. As shown some time before by Wang and colleagues in 2003 in rats, these proteins were stained

specifically by IHC to measure differences in TJ proteins expression (644). Reduction of expression likely relates to a degree of loosening of epithelial cells (645), and a consequent increase in alveolar EEB permeability. As recommendation for future research, a presumed correlation between reduced TJ-proteins expression (qualitative and/or quantitative alterations in IHC staining) and the degree of alveolar oedema can be evaluated in the ferret model, and should reveal the proportional significance of alveolar epithelial TJs in the pathogenesis of influenza-induced ARDS. However, the poor availability of ferret-specific antibodies for IHC may prove problematic.

Alveolar amiloride-sensitive epithelial sodium channels (**ENaCs**) on both type I and type II pneumocytes maintain, in conjunction with endogenous energy consuming basolateral Na^+/K^+ ATPase pumps, an osmotic gradient across the alveolar EEB. Luminal alveolar water passively follows the gradient through epithelial aquaporins (**AQP**) and intracellular pathways towards the interstitium and bloodstream, thus preventing pulmonary oedema. As the name of this ion channel suggests, it can be blocked directly by amiloride. H1N1 IAV PR/8/1934 has shown to posses the ability to inhibit type II pneumocytes' ENaCs *in vitro* also (103, 104). As recommendation for future research, in order to assess the relative importance of these sodium pumps in influenza-induced ARDS/lung oedema, suitable animals like the ferret should be experimentally inoculated with an IAV, and treated with amiloride and compared to placebo-treated controls. If the outcome of this set-up would amount to significantly increased pulmonary oedema in the amiloride-treated group in comparison to the placebo-treated group, it implies a trivial role of the pump in influenza-induced pulmonary oedema. Or *vice versa*, if the degree of pulmonary oedema were to be similar for both infected animal groups, irrespective of amiloride blockade or not it implies an important role of sodium channel and pump in influenza-induced pulmonary oedema.

Aquaporin 5 (AQP5) is expressed in the apical plasma membrane of alveolar type I pneumocytes (646, 647). Reduced AQP5 expression of mouse type I pneumocytes was shown *in vitro* after exposure to TNF-α (648) and after exposure to NO (649), suggesting down-regulation in viral infection and in neutrophil-dominated alveolitis *in vivo*. Reduced apical expression of AQP5 likely impairs passive flow of alveolar water back to the interstitial blood stream. However, alveolar water clearance was not decreased in AQP5 knock-out mice (650), suggesting alternative ways of passive water transport across the EEB. Nonetheless, development of anti-AQP5 antibodies optimised for IHC on ferret tissues is recommended for future research, as it should reveal the relative importance of epithelial AQP5 in influenza-induced ARDS in the ferret model.

As described previously, ferrets inoculated with H5N1 HPAIV showed extensive alveolar epithelial necrosis, yet without abundant **type II pneumocyte hyperplasia**. In contrast, less pathogenic IAVs such as the 2009 pandemic H1N1 IAV induced more abundant type

II pneumocyte hyperplasia in ferrets. A possible explanation for this observation may be that the most abundantly present type of pneumocyte in the (ferret) lung is the type II pneumocyte, which expresses the 'avian-type' SA-alpha-2,3-Gal receptor on its apical surface and is responsible for regeneration of damaged epithelial cells. Regeneration of pneumocytes indicates lung repair and is evidenced by type II pneumocyte hyperplasia. The high pathogenicity of H5N1 AIV in many mammals including ferrets may be explained by the virus' tropism for these type II pneumocytes. Because incapacitation of this cell type restricts repair and would logically result in more severe alveolar damage than infection of readily replenishable type I pneumocytes, which express the 'human-type' SA-alpha-2,6-Gal receptor targeted by intrinsic less pathogenic seasonal IAVs.

Type II pneumocyte hyperplasia, recognisable by microscopy as alveolar septal-lining rows of contiguous cuboidal-to-columnar pneumocytes, is indicative of replenishing lost type I (and type II) pneumocytes, and as argued above also indicative of remaining viable cells capable of regeneration. Essential steps in the process of alveolar re-epithelisation involve proliferation and migration of type II pneumocytes, remodelling of the basement membrane, and differentiation of type II into type I epithelial cells. In order to migrate, the hemi-desmosomes that normally connect pneumocytes to the **basement membrane (BM)** are degraded by matrix metalloproteinases (MMPs) secreted by involved epithelial and mesenchymal cells, and subsequent upregulated expression of cell surface integrins then allows the loosened cells to move along the scaffold of BMs. A damaged BM hampers re-epithelisation, as it needs to be resynthesised first by the proliferating pneumocytes aided by interstitial fibroblasts that secrete growth factors and BM matrix constituents (651). If alveolar necrosis is very extensive it may be beyond functional repair capacity and replacement fibrosis forming scar tissue will ensue. Interstitial fibrosis may develop if fibrinous exudates persist in alveoli, inciting proliferation and ingrowth of fibroblasts that deposit collagenous matrix, followed by inclusion to the alveolar interstitium by overgrowth of proliferating epithelial cells and BM formation (652, 653). An intact alveolar epithelial cell layer suppresses fibroblast proliferation and collagenous matrix deposition (654). Thus enhancement of alveolar re-epithelisation in ARDS may reduce fibrosis by restoring alveolar fluid clearance preventing proteineacous fluid to accumulate, and by suppression of fibroblasts to proliferate (655).

As recommendation for future research on subacute to chronic IAV-induced pneumonias (e.g., > 7 dpi) and subsequent repair capacity, the ferret model can serve to score the degree of re-epithelisation (type II pneumocyte hyperplasia) in relation to the degree of scar tissue (fibroblasts and collagenous matrix) by histopathological assessment. Damage of the BM, caused by degrading enzymes from neutrophils and macrophages, may be detected more easily in histopathology stained by silver-precipitation stains or specific immuno(fluorescent) stains. By these methods BMs are

routinely stained and evaluated in nephropathology for lesions such as disruptions and splitting. As additional future recommendation for future research and histological assessments, noticeable defects in the alveolar network of BMs or large areas of denuded alveolar BM could be additional microscopic parameters to score present lung damage and/or future impaired repair.

Substances with **therapeutic** potential in lung repair by stimulating re-epithelisation of type II pneumocytes are **growth factors** (GF). GFs such as HGF, KGF and granulocyte macrophage colony-stimulating factor (GM-CSF) are specific cytokines synthesised by various cell types that drive cellular proliferation and differentiation. Biochemically synthesised analogues of such GFs are available and have been shown to stimulate re-epithelisation of denuded alveolar BMs in influenza-damaged lungs of mice (656). HGF induced type II pneumocytes to proliferate and to synthesise BM remodelling enzymes such as matrix metalloproteinase-9 (MMP9) and urokinase-type plasminogen activator (uPA) *in vitro*. These enzymes could be inhibited by tissue inhibitor of matrix metalloproteinase-1 (TIMP1) and by transforming growth factor-β1 (TGF-β1) (657), involved in re-epithelisation *in vivo* as well.

Although not yet assessed in the ferret model, application of GFs will likely improve the re-epithelisation in damaged ferret lungs as well. So as prospective research topic, therapeutic treatment of GFs is recommended to be evaluated in experimentally influenza-infected ferrets. The potential benefits such as enhanced type II pneumocyte hyperplasia and reduced fibrosis can be evaluated by histopathological examination compared to placebo-treated controls. A more comprehensive and functional prospective approach to monitor potential therapeutic effects of GFs is implementation of extra-corporeal membrane oxygenation (**ECMO**) in ferrets with influenza-induced ARDS. Possible improved amelioration from ARDS should be evidenced by normalised blood oxygenation, and normalised respiratory rates and heart rates. The feasibility of long-term ECMO implementation in respiratory research has been shown before in sheep and recently in rabbits (658).

Besides type II pneumocytes, other **progenitor cells** like distal airway stem cells (DASCs) residing in peribronchiolar niches, and bone marrow derived mesenchymal stem cells (MSCs) capable of structural pulmonary self-renewal have been identified in mice (659-661). The MSCs could be stimulated *in vitro* and *in vivo* to differentiate into type II pneumocytes by administration of Wnt ligand Wnt5a. *In vivo* lung repair was enhanced by transplantation of cloned DASCs in IAV inoculated syngeneic mice (659). Hopefully future availability of ferret-specific bioreagents will expand research possibilities on stem cell based re-epithelisation of influenza-induced lung damage in the ferret model. More specifically, administration of Wnt ligand Wnt5a may induce

MSCs of ferrets as well, in order to study pathogenesis or therapeutic options of influenza-induced ARDS.

In addition to light microscopy, histological assessments by **electron microscopy** (EM) is suggested for future research in the ferret model as it may corroborate lesions or reveal ultrastructural lesions of the EEB (in particular pneumocytes and constituents: TJs, ENaCs, AQPs, and BM) associated with leakage of plasma fluid. However, the infinitesimal tissue samples analysed by regular EM may not represent the majority of involved pneumocytes and constituents. To overcome this issue, the implementation of complementary microscope techniques collectively named 'correlative light and electron microscopy' (CLEM) that integrates and overlays larger tissue areas, should allow EM suitable for representative assessment of lesions of the EEB. Briefly in CLEM, cells, organelles or proteins of interest are localised first by fluorescent markers in light microscopy and subsequently evaluated in ultra-high resolution by EM (662, 663). Plasma proteins as constituents of oedema fluid within alveoli can be labelled and detected by EM also. The combined morphologic evaluations of light and electron microscopy, would contribute without doubt to insights in the role that the EEB and especially the alveolar epithelial layer plays in the pathogenesis of influenza-induced ARDS and oedema formation.

Cytokines (CK) produced by epithelial cells during IAV infections are discussed since they can damage the EEB, by targeting epithelial cells and their TJs and ENaCs. As recently performed by K.R. Short (personal communication), the amount of cytokines induced depended largely on the type of IAV and seemed less correlated to the speed of replication. H5N8 HPAIV appeared *in vitro* a greater proinflammatory CK inducer than H5N1 at comparable replication rates. This suggests that this phenomenon may be present *in vivo* as well. pH1N1 IAV showed to be a greater proinflammatory CK inducer than seasonal H1N1 IAV in homogenised ferret lung tissues (664). Thus as recommendation for future research on influenza-induced ARDS, the role of these cytokines should be examined in the ferret model, in which different extents of ALI at comparable rates of replication of different viruses should be noticeable. Furthermore, molecular techniques can detect and compare the changes of induced cytokines in overtly inflamed lungs vs. lungs without lesions. Quantifying increased proinflammatory CK mRNA expression in homogenates of IAV-inoculated fresh ferret lung tissue by PCR was shown before (664). More recent PCR techniques can be applied also on formalin-fixed and paraffin-embedded lung tissues to detect upregulated gene expression of several cytokines (665). However, a disadvantage of examining lung tissues as a whole is the inherent simultaneous gathering of several other cell types, each with an unknown contribution to CK expression profiles. A way around this could be implementation of **laser-capture microdissection** (LCM) techniques on paraffin embedded lung tissue slides

in which cell types can be isolated specifically followed by quantitative-PCR analysis of that specific cell type. If several ferret-specific antibodies for cell sorting by FACS analysis would be available these PCR techniques could be applied on fresh lung tissue homogenates like commonly performed in mice (666, 667). Future molecular research on influenza-induced ARDS would benefit from using LCM and from developing ferret cell-specific antibodies. The combined knowledge of which cell types account for which type and amount of cytokines will contribute to understanding the role of cytokines in the pathogenesis of influenza-induced ARDS.

The following paragraph that describes methods of functional analyses of the integrity of the alveolar EEB is included in this section about epithelium. Since failure of the essential epithelial layer will overwhelm the weaker components of the EEB such as interstitium to allow leakage of fluid too.

As described for the various ferret studies in this thesis, **functional analysis** of the integrity of the pulmonary EEB is performed routinely by measuring RLWs of IAV-inoculated ferrets compared with non-infected control animals. Influenza-induced acute inflamed lungs are heavier from oedema and influx of inflammatory cells like macrophages and neutrophils, whereas body weights are relatively stable over the course of an acute infection and inflammation. Alternatively proven methods of functional analysis of the EEB in IAV-inoculated animal models is measuring the amounts of alveolar FITC-labelled albumin leaked from the circulation (668). Although not reported yet, this method could be implemented likewise in ferrets. As recommendation for future research, FITC-labelled albumin in BAL fluids should be measured in the ferret model as alternative to CT-scanning to quantify influenza-induced pulmonary oedema and EEB function. Although, BAL fluid sampling during pathogenesis studies has several disadvantages also. First, flushing the respiratory tract with fluids will alter the amounts of inflammatory cells and oedema present in the distal airways, interfering with pathogenesis and obscuring histopathological changes. Secondly, exposure of the epithelial cells lining the respiratory tract to excess amounts of exogenous fluids may influence their state and morphology, again interfering with pathogenesis and obscuring histopathological changes. Lastly, intermittent BAL sampling during the course of an infection experiment will spread infectious virus particles more widely in the lungs than would have occurred otherwise, which certainly will interfere with the pathogenesis.

Another important question concerning the alveolar epithelium and the pathogenesis of influenza-induced ARDS that should be addressed: Is **influenza virus replication in pneumocytes** required to increase the EEB permeability resulting in oedema? Or does inactivated replication-deficient IAV exert toxic effects to the EEB permitting oedema to develop? Shown before by Imai and colleagues, inactivated H5N1 IAV induced

ARDS in mice via toll-like receptor (TLR)-4 signalling on macrophages producing ROS (203). To address this question, UV-light or radiation-inactivated IAVs can be evaluated on respiratory epithelial cell cultures for CK induction or for altered trans epithelial resistance (TER) as measure cell barrier strength (645). *In vivo* confirmation of potential proinflammatory and/or toxic effects of inactivated IAVs on the delicate EEB should well suit the ferret model, and is as such recommended for future research. Presumably, results will show damaging capacity related to the type of inactivated IAV, as was shown for greater pathogenicity of HA from H5N1 HPAIV than from less pathogenic IAVs.

Macrophages

Macrophages are abundantly present inflammatory cells, resident within the normal alveolus or recruited to inflamed lungs. They can exert phagocytic and CK producing functions, and as such play an important role in ARDS pathogenesis. Recruited macrophages can damage the EEB in influenza-induced pneumonia. They can release tumour-necrosis-factor-related apoptosis-inducing ligand (TRAIL, also known as TNFSF10), NO, and produce proinflammatory cytokines. These substances can induce epithelial cell damage and cell death. As mentioned previously in the section on epithelium, granulocyte-macrophage colony-stimulating factor (GM-CSF) is a growth factor that stimulates pulmonary stem cells and type II pneumocytes to increase and accelerate re-epithelisation of injured alveoli. Classically, hence the name, GM-CSF stimulates stem cells to generate differentiated granulocytes and monocytes/macrophages. Whether GM-CSF leads to increased numbers of recruited macrophages in lungs of experimentally influenza-infected ferrets is not known. However, there may well be a conceivable equilibrium between beneficial effects of lung repair or deleterious effects potentially induced by recruited activated macrophages by GM-CSF which can be assessed in prospective research by histological examination of treated ferrets compared with placebo-treated controls. Preferably an additional animal group would be included treated with monoclonal antibodies that block TRAIL (anti-TRAIL Ab's), and assess if this leads to noticeable differences in re-epithelisation by histopathology.

In experimental IAV inoculations, *in vivo* depletion of resident alveolar macrophages (AM) by means intratracheal instillation of clodronate-liposomes have been performed in ferrets (Kim 2013), permitting increased viral replication and more severe lung lesions and disease compared to placebo-treated controls. Under normal circumstances, inhaled aerosolised infectious IAV particles will reach deep into lungs, to be subjected to innate antiviral immune responses from AMs. Depletion of AM in ferrets would lead to a higher 'take' of the virus, i.e., a higher infectivity of the virus, hereby potentially modelling seasonal influenza-induced ARDS in immune compromised patients. Previous methods to increase ferrets' susceptibility to seasonal IAVs and respiratory disease required either very high infectious titers (669) or required immunosuppressive medication as

described in chapter 6.3. Modulation of the innate or adaptive immune system in the ferret model, either by macrophage depletion and/or immunosuppressive medication, plausibly resembles more naturally immune compromised patients than unnaturally high infectious viral doses would. Considering these approaches, pre-infectious depletion of resident AMs is recommended to be intensified in future research as it may well improve the applicability of this model, without the poorly controllable drawbacks, such as the general deleterious catabolic effects of corticosteroids including, but not limited to opportunistic secondary infections, of systemic immunosuppressive medication.

Neutrophils

Neutrophils, or more accurately, neutrophilic granulocytes are short-lived inflammatory cells rapidly recruited to inflamed lungs. They can exert phagocytic and microbiocidal functions by aspecific degranulation of lysozymes and release of ROS, and by CK production. These substances are additionally toxic to IAV-infected and non-infected cells that constitute and uphold the alveolar EEB. Especially, matrix metalloproteinases (MMPs) secreted by neutrophils (and macrophages) can cause proteolytic damage of the alveolar BM. Furthermore neutrophils can undergo cell death called netosis in which extruded DNA forms extracellular traps (NETs) foremost involved in killing pathogens and thus less likely in damaging the EBB. NETs may contribute to ARDS indirectly by vascular damage and thrombus formation (155). However, the specific significance of neutrophils in the pathogenesis of influenza-induced ARDS in relation to other inflammatory cells and inflammatory processes is not known. Shown by van den Brand and colleagues, in the acute stages (<24 hpi) of H5N1 AIV induced ARDS in ferrets, alveolar protein-rich oedema fluid was already present before evident influx of neutrophils (316). This suggests that neutrophils are not essential in initial stages of alveolar oedema formation. However, when in the subsequent stages many activated neutrophils are recruited to IAV-infected lungs, and undergo burst degranulation, ROS and proteolytic lysozymes (MMPs) are released that can cause major bystander damage to the EEB. This may weaken the barrier and MMPs especially, may disrupt the BM leading to impaired re-epithelisation.

Therefore as recommendation for prospective research topic, to assess the significance and role of the neutrophil and its MMP in the acute inflammatory process and subsequent repair process in the ferret model, neutrophils and/or MMPs should be extracted from influenza-induced pneumonia and compared with controls. Experimental treatments with monoclonal antibodies to selectively deplete neutrophils followed by IAV inoculation in mice in different studies resulted, contrastingly, in increased mortality and pneumonia (670-672) and in less severe morbidity and mild pneumonia without ARDS (155), suggesting both beneficial and disadvantageous roles of neutrophils in acute IAV infection and inflammation. Blockade of MMPs may theoretically lead to less severe disease by reduced proteolysis and enhanced alveolar re-epithelisation.

Endothelium

Endothelial cells are flattened mesenchymal cells that line blood vessels, and as such form the direct blood border as structural constituent of the alveolar EEB. As elaborated on previously, about 10% of the strength in upholding the colloid osmotic pressure across the alveolar EBB is provided by the endothelial cells and interstitium. Endothelial cells are not as firmly interconnected with TJs as pneumocytes. They are the most abundant cell type present in the lung (30%), and have shown to participate in the pathogenesis of influenza-induced ARDS.

Mostly in mammals (except for domestic cats intestinally exposed to H5N1 HPAIV), IAV infections are primarily epitheliotropic, infecting and replicating in epithelial cells of the respiratory tract. However, in several bird species, such as chickens and black swans, HPAIV infections have shown to be primarily endotheliotropic, infecting and replicating systemically in vascular endothelial cells. This particular cellular tropism of AIVs has consequences for the pathogenesis, virulence, viral excretion and transmission in those specific animal species.

The role that endothelial cells play in the pathogenesis of ARDS seems foremost indirect through production of pro-inflammatory cytokines when activated by adjoining IAV-infected epithelial cells, and not caused by direct structural damage of endothelial cells of infection of endothelial cells. These cytokines augment and perpetuate the inflammatory response, resulting in damage to the alveolar epithelial cells and weakening of the EEB. By some researchers, endothelial cells were proposed to act as the central orchestrators in cytokine amplification in the pathogenesis of influenza-induced ARDS (135). This proposition is likely because of the abundance of endothelial cells in lungs as well as their capacity to produce large amounts of many of pro-inflammatory cytokines, and likely also because of their strategic location, by which they can trap inflammatory cells passing through the blood vessel and direct them towards the site of inflammation in the pulmonary alveoli. The major driving forces in the pathogenesis of influenza-induced ARDS may be unravelled by selectively blocking pro-inflammatory mechanisms orchestrated by endothelial cells such as the coagulation cascade, chemotaxis and diapedesis of inflammatory cells, and complement activation. Although the alveolar endothelium does not constitute the strongest layer of EBB, further studies in cats with endotheliotropic IAVs such as H5N1 HPAIV might provide further insights in the pathogenesis of influenza-induced ARDS and oedema formation. Besides infections in chickens and swans, H5N1 HPAIV showed a remarkable yet not fully understood endotheliotropism and generalisation of infection after intestinal inoculation with infected capsules of cats (144). Interestingly, these cats developed neither ARDS nor pulmonary oedema, in contrast to intratracheally H5N1 inoculated cats (249). Together, these findings suggest that local endothelial activation plays a more important part than does direct endothelial cell damage by rare mammalian IAV infections. Gastro-

intestinal inoculations with H5N1 HPAIV have been performed in ferrets by feeding meat from infected chickens (673) and by infected capsules (274), resulting in systemic virus spread, yet endothelial cell infections were not reported. Recommended future research on the role of endothelial cells in ARDS should focus on blocking their active state, including blockade of permissive selectins and integrins. Preferably such studies should be performed in the ferret model, although the lack of ferret specific antibodies might prove to be a hurdle. Nonetheless, potential results from ferret studies would likely provide additional insights in the pathogenesis of influenza-induced ARDS likely valuable for influenza-intervention options.

Lymphocytes

Lymphocytes are inflammatory cells mostly involved in adaptive immune responses. In immunologically naïve people and animals, both subtypes (B- and T-lymphocytes) need specific antigen priming and activation before they infiltrate and proliferate in influenza-inflamed lungs. This process takes several days and as such lymphocytes are deemed less relevant in the (per)acute stages of influenza-induced ARDS pathogenesis in naïve animal models, and were not discussed extensively previously. However, natural killer (NK) cells, being of lymphocytic progeny, are discussed in this section about acute inflammation since they function as effector cells of the innate immune response. They can kill IAV-infected cells by enzymatic degradation (by granzymes and perforins), or by inducing apoptosis by expressing Fas ligand or TRAIL on their cell surface, without the necessity of prior activation by antigen presentation (674). As such, they can kill infected pneumocytes, and likely influence the integrity of the alveolar EEB. However, the role of NK cells in the pathogenesis in acute influenza-induced disease is less straightforward than this. Early reports by Nogusa and colleagues (675) and Stein-Streilein and colleagues (676) showed that IAV infection in NK-depleted mice and hamsters induced increased morbidity and mortality. These finding seem to corroborate a protective effect of NK cells following IAV infection. *In vitro* studies showed that even NK cells could be infected by IAV and be killed by apoptosis (677). Conversely, more recent work by Zhou and colleagues (678) and Abdul-Careem and colleagues (679) showed that NK cells exacerbated the severity of inflammation after influenza inoculation of mice, which suggests that NK cells may damage the alveolar EEB by killing influenza-infected epithelial cells.

In summary, though NK cells have shown to participate in the anti-influenza innate immunity, their relative significance in potentially weakening the EEB by killing IAV-infected pneumocytes remains unknown. Speculatively, their role is limited as the low numbers of NK cells residing in the normal lung could be overwhelmed by the rapid viral replication peaking at 2-3 dpi, whilst significant recruitment of NK cells to the lungs occurs from 5 dpi onwards (680), which is also about the same time when the very first specific T and B cells appear on the scene (680). If not many pneumocytes are infected by

Table 7.2.1 Knowledge gaps in the pathogenesis of IAV-induced damage to the alveolar epithelial-endothelial barrier (EEB). Recommendations for prospective research topics and methodologies in the IAV-inoculated ferret model to tackle these knowledge gaps are listed. These prospective methodologies may supplement typical implemented clinical (fever, CT-scanning), virological (tissue viral loads), and (histo)pathological (relative lung weights [RLW], H&E stains) analysis methods.

Knowledge Gap Detailed role of:	Prospective Research Topic Assessment of:	Prospective Methodology Score effects by/of:
Epithelium in EEB	1-Damage to lining **Pneumocytes** ~* presence/ degree alveolar oedema	•**LM, IHC cytokeratin stains**; **EM/CLEM****
	2-Damage to interepithelial **Tight Junctions** ~ presence/degree alveolar oedema	•**LM, IHC/Fluorescence Claudin-4 stains**; **EM/CLEM**
	3-Epithelial **Amiloride-sensitive Sodium Pumps (ENaCs)** ~ presence/degree alveolar oedema	•**Amiloride** treatment on amount of **FIT-C-labeled Albumin in BAL-fluid*****
	4-Expression of type I pneumocytes' **Aquaporin 5 (AQP5)** ~ presence/degree alveolar oedema	•**LM, IHC AQP5 stains; EM/CLEM**
	5-Damage to epithelial **Basement Membrane (BM)** ~ presence/ degree alveolar oedema and repair of epithelium (type II pneumocyte hyperplasia vs interstitial fibrosis)	•**LM, IHC/Silver-Collagen stains; EM/CLEM**
	6-**Enhancement Epithelial Repair** ~ presence/ degree alveolar oedema	•**GF-therapy** (HGF, KGF, GM-CSF, Wnt5a) monitored by **ECMO** and **LM, Collagen/IHC cytokeratin stains**[#]
	7-Increase **Proinflammatory Cytokines** ~ presence/ degree alveolar oedema	•Concentrations Cytokines (**TNFα, ILs, IFNs**) by **PCR/LCM** ~ **LM/EM/CLEM lesions**[##]
	8-**Integrity of EEB** by **functional analysis to prevent/permit** development alveolar oedema	•Amount of **FIT-C-labeled Albumin in BAL fluids**

Table 7.2.1 Knowledge gaps in the pathogenesis of IAV-induced damage to the alveolar epithelial-endothelial barrier (EEB). Recommendations for prospective research topics and methodologies in the IAV-inoculated ferret model to tackle these knowledge gaps are listed. These prospective methodologies may supplement typical implemented clinical (fever, CT-scanning), virological (tissue viral loads), and (histo)pathological (relative lung weights [RLW], H&E stains) analysis methods. (continued)

Knowledge Gap Detailed role of:	Prospective Research Topic Assessment of:	Prospective Methodology Score effects by/of:
	9-**Necessity of IAV replication** ~ presence/ degree alveolar oedema and epithelial damage	•Inoculation of radiation-**inactivated** (UV, gamma) **IAV (H5N1/pH1N1)** ~ **LM/EM/CLEM lesions**
Endothelium in EEB	1-**Blockade of Proinflammatory mechanisms** ~ presence/ degree alveolar oedema	•Specific **Antibody** (α-selectins, α-integrins) treatment ~ **LM/EM/CLEM lesions**
Macrophages on EEB	1-**Enhancement** and/or **Depletion of Macrophages** ~ presence/ degree alveolar oedema	•Enhancing **GM-CSF** treatment ~ **LM/EM/CLEM lesions** •Depletion by **Clodronate-Liposomes** or specific **Antibody** treatments ~ **LM/EM/CLEM lesions**
Neutrophils on EEB	1-**Depletion of Neutrophils** and/or **Blockade Hydrolytic Enzymes** ~ presence/degree alveolar oedema	•Depletion by specific **Antibody** treatment ~ **LM/EM/CLEM lesions** •Blockade of MMPs by treatment with synthetic **MMPs-inhibitors** ~ **LM/EM/CLEM lesions** ###
Lymphocytes (NK cells) on EEB	1-**Depletion of NK cells** ~ presence/degree alveolar oedema	•Depletion by specific **Antibody** treatment ~ **LM/EM/CLEM lesions**

* **~**, in relation to.

** **LM**, light microscopy; **IHC**, immunohistochemistry; **EM**, electron microscopy; **CLEM**, correlative light-electron microscopy.

*** **BAL**, broncho-alveolar lavage.

GF, growth factor; **HGF**, hepatocyte growth factor; **KGF**, keratinocyte growth factor; **GM-CSF**, granulocyte-macrophage colony-stimulating factor, **ECMO**, extracorporeal membrane oxygenation.

TNFα, tumour necrosis factor; **ILs**, interleukins; **IFNs**, interferons; **LCM**, laser-capture microdissection.

MMPs, matrix metalloproteinases.

initial inoculation, there may be sufficient NK cells to destroy the infected pneumocytes before the virus has a chance to complete the infection cycle and cause a second wave of infection among pneumocytes. This also may explain the apparently contradicting results of above experiments. If inoculation dose is low, NK cells would be protective and be able to abrogate infection. If inoculation dose is high, NK cells would be damaging yet not be able to abrogate infection. However to assess the relative significance of NK cells in influenza-induced ARDS, prospectively ferrets as apt animal model should be depleted of NK cells by treatment with specific monoclonal antibodies, as was performed successfully before in other animal models such as mice (675, 676, 681, 682) and hamsters (676).

CONCLUSIONS & PERSPECTIVES

In conclusion, although influenza-induced ARDS is largely preventable by vaccination, permissive conditions such as immunosuppression, zoonotic infections with new pathogenic IAVs, and IAV mutants escaping anti-viral drugs, dictate the exploration into the pathogenesis and novel therapeutic approaches of ARDS. The need for such exploration is accentuated by the fact that once people develop ARDS, case fatality rate is high. Classically, interventions and therapies against influenza-induced ARDS were focused on reducing viral replication. Except for prolonged infections in immunosuppressed patients, the duration of the replicative phase of IAVs is limited to only five days on avergae, rendering a narrow window of therapeutic opportunity to abrogate viral replication. The longer lasting recovery phase from diffusely damaged alveolar epithelial-endothelial barrier (EEB), and impaired gas exchange by pulmonary oedema will benefit from enhanced convalescence. Therefore future treatments of influenza-induced ARDS should shift their focus towards an augmented recovery phase of ARDS rather than trying to limit viral replication. Given our considerations on the importance of the alveolar epithelium in influenza-induced ARDS and alveolar oedema, this should be attempted by actively stimulating re-epithelisation in order to expedite repair of the EEB thereby safeguarding the osmotic gradient allowing restored imperative gas exchange across the delicate structure of the pulmonary alveolus. Additionally, accelerated re-epithelisation may reduce pulmonary fibrosis in survivors of ARDS. Overall, recommendations given in this thesis for prospective research topics in influenza-induced ARDS include: visualise and understand microscopic lesions in the alveolar EEB, deplete and measure levels of pro-inflammatory cytokines and key inflammatory cells, and treatment with drugs like growth factors to enhance lung repair. These proposed topics can and should be studied in the ferret model, in order to appropriately assess each factor and/or mechanism for its relative significance in the pathogenesis and intervention of influenza-induced ARDS.

CHAPTER 8

Nederlandse Samenvatting

NEDERLANDSE SAMENVATTING

In dit hoofdstuk wordt het proefschrift samengevat. **Hoofdstuk 1** geeft achtergrondinformatie om de rest van het proefschrift te kunnen begrijpen. Infectie met een influenzavirus kan de ziekte griep (influenza) bij mens en diverse andere diersoorten veroorzaken. Vier genera van influenzavirussen worden op basis van antigene en structurele verschillen erkend: influenza A, B, C, en D virussen. Deze genera verschillen in gastheerspectrum. Influenza A virussen (**IAVs**) komen endemisch voor bij diverse zoogdieren (voor zover bekend bij mensen, varkens, paarden, honden, en vleermuizen) en bij vogels. De IAVs die endemisch bij mensen vóórkomen veroorzaken elk jaar griepepidemieën; in gematigde klimaatzones vinden deze doorgaans gedurende de wintermaanden plaats. Infecties met een nieuw IAV, waartegen mensen of dieren geen of geringe immuniteit hebben, kunnen in zeldzame gevallen leiden tot individuele infecties, lokale epidemieën en zelfs tot een wereldwijde uitbraak of pandemie. Dergelijke infecties met nieuwe IAVs kunnen afkomstig zijn van vogels of van zoogdieren zoals varkens. Influenza B virussen (twee soorten) kunnen bij de mens vergelijkbare seizoensgebonden griep veroorzaken als IAVs, en kunnen ook zeehonden en varkens infecteren. Influenza C virus kan bij de mens een milde bovenste luchtweginfectie veroorzaken, en infecteert ook varkens. Influenza D virus is alleen bij varkens en runderen aangetoond.

De rest van dit proefschrift beperkt zich tot studies met IAVs. Deze virussen hebben een negatief enkelstrengs RNA genoom van acht segmenten, waarvan twee coderen voor de oppervlakte-eiwitten haemagglutinine (**HA**) en neuraminidase (**NA**). Terwijl HA de aanhechting van een IAV partikel aan een gastheercel mogelijk maakt, is NA verantwoordelijk voor het losmaken ervan. Subtypering van IAVs geschiedt op basis van hun HA en NA eiwitten: tegenwoordig worden 18 HA subtypen (H1-H18) en 11 NA subtypen (N1-N11) erkend, die in vrijwel elke combinatie van HA en NA kunnen voorkomen. IAVs kunnen gensegmenten uitwisselen en vormen zo nieuwe IAVs. Bij watervogels, die beschouwd worden als het natuurlijke reservoir van IAVs, komen IAVs, bestaande uit combinaties van de subtypes H1-H16 en N1-N9, in het darmkanaal voor, doorgaans zonder duidelijke klinische verschijnselen te veroorzaken (laagpathogene aviaire influenzavirussen; LPAIVs). In pluimvee kunnen de subtypen H5 en H7 echter muteren tot hoog pathogene vogelgriepvirussen (hoogpathogene aviaire influenzavirussen; HPAIVs), die systemische infecties met een aanzienlijke sterfte (mortaliteit) kunnen induceren. H17N10 en H18N11 zijn de meest recente IAVs geïsoleerd uit gezonde fruitetende vleermuizen (*Sturnira sp.* en *Artibeus sp.*) uit Midden- en Zuid-Amerika.

Bij mensen circuleren tegenwoordig de seizoensgriepvirussen (H3N2 en H1N1). Deze virussen kunnen jaarlijks aan de bestaande immuniteit van de wereldbevolking

ontsnappen door continu optredende kleine mutaties in de HA en/of NA gensegmenten ("**antigenic drift**"), en kunnen zo tot nieuwe infecties en jaarlijkse epidemieën leiden. Wereldwijd overlijden per jaar naar schatting 250.000 tot 500.000 mensen aan griep tijdens griepepidemieën.

In zeldzame gevallen kan een mens geïnfecteerd worden met een IAV, waarvan sommige of alle gensegmenten anders zijn dan die van de seizoensgriepvirussen ("**antigenic shift**"). Deze nieuwe gensegmenten zijn afkomstig van een andere diersoort. Een dergelijk nieuw IAV kan een pandemie veroorzaken door ontwikkeling van een efficiënte overdraagbaarheid (transmissibiliteit) van mens naar mens in een relatief immunologisch naïeve populatie, wat leidt tot een hoge infectiegraad, een hoog ziektecijfer (morbiditeit) en soms hoge mortaliteit. Gedurende de laatste eeuw zijn er vier belangrijke pandemieën voorgekomen: de Spaanse griep (H1N1) met piek in 1918, de Aziatische griep (H2N2) in 1957, de Hong Kong griep (H3N2) in 1968, en de Mexicaanse griep (H1N1) in 2009. De Spaanse griep was zeer ernstig vanwege, naar schatting, ernstige ziekte bij een kwart van de wereldbevolking, en zo'n 50 miljoen sterfgevallen.

Vogelgriepvirussen zoals H5N1 en H7N9 kunnen tot infecties bij mensen leiden door nauw contact met pluimvee of met hun producten en hun excreta. Vooral in Zuidoost-Azië en Egypte hebben dergelijke infecties in de afgelopen jaren geleid tot ernstige en soms dodelijke griepgevallen met longontsteking. Deze vogelgriepvirussen worden praktisch niet van mens op mens overgedragen. Echter, mocht een vogelgriepvirus zich zodanig ontwikkelen dat dergelijke overdracht wel efficiënt plaatsvindt, dan kan dit tot een pandemie leiden.

Ongecompliceerde influenza is een ziekte ten gevolge van infectie met een influenzavirus, meestal een seizoensgriepvirus, en wordt gekenmerkt door ontsteking van slijmvliezen van de bovenste luchtwegen zoals neus- en bijholten en keel, maar ook van de luchtpijp (trachea) en grotere vertakkende luchtwegen (bronchiën), en voorts algemene malaise en koorts. Seizoensgebonden IAVs kunnen zich hechten aan epitheelcellen met humane type IAV-receptoren (zogenaamde α-2,6 siaalzuurgebonden receptoren), welke vooral in de bovenste luchtwegen voorkomen. Na virusaanhechting kunnen deze epitheelcellen worden geïnfecteerd gevolgd door virusreplicatie welke piekt op zo'n twee dagen na infectie om in de daaropvolgende dagen geleidelijk af te nemen. Virusreplicatie resulteert gewoonlijk in het verlies van de geïnfecteerde epitheelcellen en inductie van een ontstekingsreactie met lokale en gegeneraliseerde ziekteverschijnselen. De ontstekingsreactie van ongecompliceerde influenza is doorgaans mild en van vlot voorbijgaande aard en wordt histologisch gekenmerkt door epitheliale degeneratie en loslating (desquamatie). Voorts kan er sprake zijn van bloedrijkdom (hyperaemie), vochtophoping (oedeem), en lymphohistiocytaire ontstekingsinfiltraten in de direct onderliggende slijmvlieslagen.

IAV infectie kan zich onder bepaalde omstandigheden uitbreiden naar de longen, waardoor er dan sprake is van een **gecompliceerde influenza**, die wordt gekenmerkt door een ernstiger ziektebeeld met longontsteking (pneumonie). Belangrijke risicofactoren voor het ontwikkelen van ernstige griep met longontsteking zijn: onderliggende hart- en vaatziekten, andere longaandoeningen, verminderde weerstand, stofwisselings- en tumorziekten, vetzucht en zwangerschap. De diep gelegen longblaasjes (alveoli) zijn bekleed met epitheelcellen bestaande uit type I longcellen (pneumocyten) die de wanden van de alveoli bekleden met een flinterdunne doch waterdichte laag, en uit type II pneumocyten die o.a. een rol spelen in herstel na beschadiging. Rondom de alveoli circuleert bloed door een netwerk van haarvaten (capillairen), die bekleed worden door endotheelcellen. Gezamenlijk vormen deze epitheel- en endotheelcellen de begrenzing (epithelio-endotheliale barrière; **EEB**) tussen de luchthoudende alveoli en de bloedstroom, waarin de epitheelcellen de sterkste laag vormen. Een ontsteking van de alveoli tijdens IAV infectie beschadigt het epitheel en belemmert de levensbelangrijke gasuitwisseling van zuurstof en koolzuurgas tussen lucht en bloed, door zwelling van de EEB en door lekkage van vocht (alveolair oedeem) uit de bloedstroom naar de alveoli. Dit kan aanleiding geven tot het ontstaan van acuut longfalen, en het daarop volgende “acute respiratory distress syndrome” (**ARDS**). De ziekteverschijnselen en symptomen van een door influenza geïnduceerde virale pneumonie en ARDS worden gekenmerkt door hoge koorts, algehele malaise, benauwdheid (dyspneu), zuurstoftekort (hypoxie), blauwzucht van o.a. slijmvliezen en vingertoppen (cyanose) en ophoesten van bloed (haemoptysis). Tekenen van multi-orgaan falen en sterfte kunnen optreden reeds 48 uur na de eerste symptomen. Veelal worden virale pneumonieën verergerd door secundaire opportunistische bacteriële infecties. Een door influenza geïnduceerde pneumonie wordt macroscopisch gekenmerkt door gezwollen, zware, en vochtrijke paars-rode longen met ribafdrukken, en een histologisch beeld van een uitgebreide alveolaire celdood (necrose) en ontsteking, zogenaamde “diffuse alveolar damage” (**DAD**) met bloedingen (haemorrhagie), oedeem, hyaliene membranen en acute ontstekingsinfiltraten. Een laag van zich vermeerderende type II pneumocyten (hyperplasie), die zich kunnen differentiëren in type I pneumocyten om zo de EEB te herstellen, kan aanwezig zijn.

In tegenstelling tot menselijke seizoensgriepvirussen, hecht het H5N1 vogelgriepvirus zich bij de mens bij voorkeur aan de zogenaamde α-2,3 siaalzuurgebonden receptoren, die vooral bij vogels voorkomen en bij de mens vooral op de epitheelcellen in de diepere delen van het ademhalingsstelsel (respiratietractus), zoals de kleinste vertakkende luchtwegen (bronchioli) en alveoli. Het H7N9 vogelgriepvirus en het Mexicaanse H1N1 griepvirus van de pandemie in 2009 kunnen zich zowel aan humane α-2,6 siaalzuurgebonden receptoren, als aan aviaire type α-2,3 receptoren hechten in de bovenste delen en in de diepe delen van de respiratietractus. De aanhechtingspatronen

van deze virussen worden weerspiegeld door de presentatievormen van influenza die ze veroorzaken, waarbij veelal sprake is van gecompliceerde virale pneumonieën.

Manieren om influenza te voorkomen (profylaxe) zijn **vaccinatie** en behandeling met **antivirale middelen** die zowel profylactisch als genezend (therapie) kunnen worden toegepast. Jaarlijks moet het seizoensgriepvaccin worden aangepast aan de circulerende virussen. Voorbeelden van antivirale middelen zijn de bestaande neuraminidaseremmers, waaronder oseltamivir (Tamiflu®) en zanamivir (Relenza®) en de in ontwikkeling zijnde specifieke antilichaampreparaten. Diermodellen zijn nodig om vaccins en antivirale middelen op hun werkzaamheid te toetsen. Voor de evaluatie van de gecompliceerde processen van de ziekteontwikkeling (pathogenese) of het juist het veelal beoogde voorkómen van ziekte, en transmissibiliteit van een IAV volgende op een infectie bestaan geen proefdiervrije (*in vitro*) alternatieven. Diverse **proefdiersoorten** (o.a. muis, cavia, fret) worden gebruikt in dergelijke evaluaties. De fret is als proefdiersoort voor veel experimenten het meest geschikt gebleken om als model te dienen om influenza bij de mens na te bootsen.

Hoewel influenza, in zowel de ongecompliceerde als de gecompliceerde vorm, een bekend ziektebeeld is, is de pathogenese ervan slechts ten dele bekend. Het **doel van dit proefschrift** was, middels onderzoek naar de pathogenese van influenza in het frettenmodel, opheldering van de belangrijkste pathogenetische factor(en) in het ontstaan van door influenza geïnduceerd ARDS en het optredend longoedeem. Inzicht in de pathogenese is van het grootste belang om deze acute aandoening gericht en adequaat te kunnen bestrijden of wellicht zelfs te voorkomen.

Hoofdstuk 2 van dit proefschrift is een literatuurstudie naar de kennis over de pathogenese van door influenza geïnduceerd ARDS op het moment dat de studies in het kader van dit proefschrift werden aangevangen. De diverse betrokken structurele elementen van de EEB, ontstekingscellen en ontstekingsfactoren (cytokinen en chemokinen) werden betrokken in de analyse. Met name de bevindingen uit **hoofdstuk 2.1** hebben geleid tot het inzicht dat bij door influenza geïnduceerd ARDS in het bijzonder de alveolaire epitheelcellen van groot belang zijn. Niet alleen worden deze cellen direct geïnfecteerd via de inademingslucht en vindt de virusvermeerdering er plaats, maar ook vormen deze alveolaire epitheelcellen onder normale omstandigheden de meest waterdichte cellaag van de EEB. Eerdere onderzoeken naar de pathogenese van ARDS hebben zich veelal primair gericht op alveolaire endotheelschade door toxinen via de bloedcirculatie als startpunt van dit proces. Derhalve moest de focus van het onderzoek en behandeling van door influenza geïnduceerd ARDS en longoedeem juist gericht worden op het alveolaire epitheel.

Onder bepaalde omstandigheden bij diverse diersoorten vertoont IAV ook een systemisch tropisme voor endotheelcellen. Zo wordt in **hoofdstuk 2.2** beschreven dat HPAIVs in bepaalde vogelsoorten (o.a. de kip en de zwarte zwaan) juist de endotheelcellen primair infecteren en niet de epitheelcellen zoals bij de meeste zoogdieren en andere vogelsoorten. Een uitzondering binnen de zoogdieren is een experimentele inoculatie van H5N1 HPAIV in het darmkanaal van katten, die leidt tot systemische endotheliale infecties en ziekte zonder ARDS. Dit is een tegenstelling tot intratracheale inoculatie van katten met hetzelfde virus, hetgeen wel leidt tot infectie van respiratoir epitheel. Hoewel IAV de endotheelcellen van de EEB van zoogdieren meestal niet infecteert, spelen deze endotheelcellen wel degelijk een rol in de pathogenese van door influenza geïnduceerd ARDS en longoedeem. Dit komt doordat geactiveerde endotheelcellen middels hun kwalitatieve en kwantitatieve cytokineproductie beschouwd worden als belangrijke stuwers van een pro-inflammatoire ontstekingsreactie. Medicamenteuze remming van endotheelactivatie en cytokineproductie bij influenza zou een ontstekingsremmend effect moeten hebben in de pathogenese van ARDS.

In **hoofdstuk 3.1** wordt beschreven dat vele diersoorten gevoelig zijn voor IAV infecties. De meeste infecties zijn kortdurend en voorbijgaand echter het gastheerspectrum van endemische infecties breidt zich uit. Onderzoek dat leidt tot beter begrip van de omstandigheden waaronder en de wijze waarop nieuwe IAVs naar een andere diersoort worden overgedragen, en hoe het virus zich vervolgens efficiënt kan verspreiden in de populatie van de nieuwe gastheersoort, is van groot belang. Met dit wetenschappelijk inzicht zouden mogelijk griepepidemieën of zelfs pandemieën beter kunnen worden bestreden. Waarom in de ene diersoort een IAV endemisch kan worden en ziekte kan veroorzaken en in de andere diersoort niet is grotendeels onbekend. Groepshuisvesting met hoge bezettingsgraad van immunologisch naïeve individuen zijn wel als risicofactoren aangemerkt voor ernstige influenzauitbraken na introductie van nieuwe IAVs. In het algemeen zijn van zoogdieren de carnivoren en omnivoren gevoeliger voor IAV infecties en ziekte dan herbivoren onder vergelijkbare omstandigheden. Opmerkelijk genoeg zijn paarden en kamelen een uitzondering en juist wel gevoelig voor endemische en epidemische IAV infecties en ziekte. De geschiktheid van fretten (ook carnivoren), zoals beschreven in **hoofdstuk 3.2**, voor onderzoek naar influenzapathogenese wordt deels toegeschreven aan het met de mens vergelijkbare, aanhechtingspatroon van IAVs in de respiratietractus. De fret is ook zeer gevoelig voor natuurlijke en experimentele infecties met onveranderde humane en aviaire IAVs. Deze induceren na intratracheale inoculatie in de fret een vergelijkbaar ziektebeeld en vergelijkbare longlaesies als bij de mens met dezelfde infecties. In dit proefschrift worden intratracheale inoculatie van IAVs in fretten als model voor influenza bij de mens verkort aangeduid met “het frettenmodel”. Diverse andere proefdiersoorten gebruikt voor influenzaonderzoek hebben allen hun

diersoortspecifieke voor- en nadelen, die zorgvuldig dienen te worden afgewogen vóór het opzetten van studies, met een gerichte wetenschappelijke vraagstelling.

In **hoofdstuk 4** wordt het frettenmodel gebruikt om het ziekteverwekkende vermogen (pathogeniciteit) en transmissibiliteit van nieuwe IAVs te evalueren. Zo wordt in **hoofdstuk 4.1** beschreven hoe de fret wordt ingezet voor modelontwikkeling om pathogenese- en interventiestudies te kunnen verrichten naar het H7N9 vogelgriepvirus, dat bij mensen in China vanaf 2013 een nieuwe influenzauitbraak met hoge morbiditeit en mortaliteit induceerde. De resultaten van deze studie bevestigen de geschiktheid van het frettenmodel, en ook toonden zij aan dat dit laagpathogene vogelgriepvirus juist een hoge pathogeniciteit in de fret vertoonde, wat overeenkwam met de hoge morbiditeit en mortaliteit bij de mens. Tijdens de pandemie van 2009 werden bij immuungecompromitteerde, persistent geïnfecteerde en met neuraminidaseremmers behandelde patiënten gemuteerde resistente virusstammen van het nieuwe Mexicaanse H1N1 griepvirus in een hoog percentage aangetroffen. Omdat het risico voor introductie en verspreiding van deze therapieresistente virusstammen te evalueren werden de pathogeniciteit en potentiële transmissibiliteit in het frettenmodel bestudeerd. In **hoofdstuk 4.2** wordt beschreven dat deze therapieresistente virusmutant in vergelijking met het wildtype pandemische Mexicaanse griepvirus een vergelijkbare transmissibiliteit en pathogeniciteit in het frettenmodel vertoonde.

In **hoofdstuk 5** is beschreven hoe voor het eerst “computed tomography”(CT)-scanning succesvol en herhaaldelijk toegepast op levende fretten, om de pathogenese van ARDS door het destijds pandemische Mexicaanse H1N1 griepvirus in het frettenmodel in beeld te brengen. Het was mogelijk om de mate van verandering van luchthoudendheid van de frettenlong in procenten te kwantificeren en tevens bleek op 3 dagen na virusinoculatie de piek van witte longversluiering aanwezig die reeds vanaf de volgende dag herstellende was. Middels histologische identificatie bleek deze versluiering te bestaan uit longoedeem en ontstekingsinfiltraten ter plaatse van virusgeïnfecteerde epitheelcellen van alveoli en bronchioli. Voordelen van deze nieuwe analysemethode t.o.v. conventionele studies met meerdaagse sectiemomenten zijn: (a) vermindering van het aantal benodigde proefdieren, daar (b) het gescande dier ook fungeert als zijn eigen controledier, (c) geen noodzaak om pathologiedata verkregen van verschillende sectiemomenten van verschillende proefdieren met elkaar te moeten vergelijken, (d) vaststelling van het optimale sectiemoment met maximale longversluiering zodat in volgende influenza-interventiestudies optimaal gebruik gemaakt kan worden van de maximale spreiding in longlaesies tussen behandelde dieren en onbehandelde controledieren. Op dit sectiemoment zal namelijk de mate van werkzaamheid van het te toetsen vaccin of antivirale middel het meest evident zijn.

In **hoofdstuk 6** worden diverse influenza-interventiestudies beschreven waarbij het frettenmodel veelal voor het eerst wordt toegepast. In **hoofdstuk 6.1** werden middels

dagelijkse *in vivo* CT-scanning veranderingen in luchthoudendheid van de frettenlong na experimentele influenza-inoculatie gekwantificeerd om de werkzaamheid van een influenzavaccin uit te lezen. De bevindingen van deze studie bevestigden de geschiktheid van het frettenmodel om een vaccinwerkzaamheid te toetsen aan de hand van de mate van luchthoudendheid van de longen, naast de traditionele virologische en pathologische uitleesparameters. **In hoofdstuk 6.2** wordt beschreven hoe het frettenmodel werd toegepast om de werkzaamheid van verschillende nieuwe zogenaamde levend-geattenueerde vaccins tegen het Mexicaanse H1N1 griepvirus te evalueren. Deze vaccins worden intranasaal toegediend, alwaar het vaccinvirus beperkt kan repliceren om zodoende toch een adequate immuniteit tegen Mexicaanse griep te induceren, zonder noodzaak van een additioneel immuunstimulerend bestanddeel (adjuvans).

Hoofdstuk 6.3 vat de praktische inzetbaarheid van het frettenmodel aan de hand van de pathologische bevindingen in een viertal van influenza-interventiestudies samen. Telkens werden verminderingen van laesies van de respiratietractus in gevaccineerde dieren t.o.v. schijngevaccineerde (sham-vaccinated) controledieren aangetroffen. Tevens werd beschreven hoe met pathologische evaluatie de geslaagde opzet van een medicamenteuze immuunsuppressie in het frettenmodel is beoordeeld. Aanwijzingen hiervoor waren een histologische afname van het aantal immuuncellen in lymfoide en bloedvormende (haemopoietische) organen, zoals lymfknopen, tonsillen, milt, en beenmerg, en verder ook het optreden van een verlengde virusexcretie en het opkomen van opportunistische bacteriële en mycotische infecties van de longen. Dit model is van belang bij het bestuderen van influenza bij immuungecompromitteerde individuen, zoals geriatrische patiënten en mensen na orgaantransplantatie.

Hoofdstuk 7 bevat de samenvattende discussie van de belangrijkste bevindingen van dit proefschrift. Ondanks dat seizoensinfluenza grotendeels voorkomen kan worden door vaccinatie, is pathogeneseonderzoek relevant vanwege het voortdurend optreden van factoren die predisponeren voor een ernstig beloop van influenza zoals bij patiënten met een verhoogd risico op complicaties zoals genoemd in hoofdstukken 1 en 6.3, zoönotische infecties met nieuwe pathogene IAVs, en het ontstaan van therapieresistente virusmutanten. Voorts bestaan er nog steeds hiaten in de kennis over specifieke eigenschappen van de EEB (zie **tabel 7.2.1**) die een rol spelen bij het ontstaan van ARDS, dat ondanks de beste geneeskundige zorg nog altijd tot hoge mortaliteit leidt. Pathogeneseonderzoek geeft kennis en inzicht die van groot belang kunnen zijn voor de ontwikkeling van nieuwe behandelmethoden van ARDS. De belangrijke rol die het frettenmodel in het influenzaonderzoek kan spelen wordt bevestigd bij nieuwe toepassingen zoals CT-scannen, bij de bestudering van nieuwe IAVs, maar ook bij het testen van nieuwe geadjuveerde influenzavaccins, antivirale therapieën en de effecten van medicamenteuze immuunsuppressie. De belangrijkste celtypen betrokken bij de

pathogenese van influenza werden besproken in de discussie. Concluderend kan de alveolaire epitheelcel in de EEB niet alleen als een zeer belangrijk celtype beschouwd worden in de pathogenese van door influenza geïnduceerd ARDS en longoedeem, maar dit zeker ook als doelwit voor het ontwikkelen van interventiesstrategieën. Waar conventionele interventies zich richten op afremming van influenzavirusreplicatie, wordt in dit proefschrift de aandacht tevens gevestigd op de mogelijke rol van medicamenteuze toepassing van lichaamseigen groeifactoren, zoals HGF*, KGF en GM-CSF (CSF2). Deze zouden het herstel van ARDS kunnen bespoedigen door het bevorderen van reparatie van het alveolaire epitheel, hetgeen zou kunnen leiden tot versneld functioneel herstel van de EEB, resorptie van longoedeem, en op de lange termijn een vermindering van het ontstaan van longfibrose.

*HGF, hepatocyte growth factor; KGF, keratinocyte growth factor; GM-CSF, granulocyte-macrophage colony stimulating factor, syn. CSF2, colony stimulating factor 2.

CHAPTER 9

References

REFERENCES

1. **Osterhaus AD, Rimmelzwaan GF, Martina BE, Bestebroer TM, Fouchier RA.** 2000. Influenza B virus in seals. Science **288:**1051-1053.
2. **Bodewes R, Morick D, de Mutsert G, Osinga N, Bestebroer T, van der Vliet S, Smits SL, Kuiken T, Rimmelzwaan GF, Fouchier RA, Osterhaus AD.** 2013. Recurring influenza B virus infections in seals. Emerg Infect Dis **19:**511-512.
3. **Ran Z, Shen H, Lang Y, Kolb EA, Turan N, Zhu L, Ma J, Bawa B, Liu Q, Liu H, Quast M, Sexton G, Krammer F, Hause BM, Christopher-Hennings J, Nelson EA, Richt J, Li F, Ma W.** 2015. Domestic pigs are susceptible to infection with influenza B viruses. J Virol **89:**4818-4826.
4. **Guo YJ, Jin FG, Wang P, Wang M, Zhu JM.** 1983. Isolation of influenza C virus from pigs and experimental infection of pigs with influenza C virus. J Gen Virol **64 (Pt 1):**177-182.
5. **Ducatez MF, Pelletier C, Meyer G.** 2015. Influenza D virus in cattle, France, 2011-2014. Emerg Infect Dis **21:**368-371.
6. **Tong S, Li Y, Rivailler P, Conrardy C, Castillo DA, Chen LM, Recuenco S, Ellison JA, Davis CT, York IA, Turmelle AS, Moran D, Rogers S, Shi M, Tao Y, Weil MR, Tang K, Rowe LA, Sammons S, Xu X, Frace M, Lindblade KA, Cox NJ, Anderson LJ, Rupprecht CE, Donis RO.** 2012. A distinct lineage of influenza A virus from bats. Proc Natl Acad Sci U S A **109:**4269-4274.
7. **Tong S, Zhu X, Li Y, Shi M, Zhang J, Bourgeois M, Yang H, Chen X, Recuenco S, Gomez J, Chen LM, Johnson A, Tao Y, Dreyfus C, Yu W, McBride R, Carney PJ, Gilbert AT, Chang J, Guo Z, Davis CT, Paulson JC, Stevens J, Rupprecht CE, Holmes EC, Wilson IA, Donis RO.** 2013. New world bats harbor diverse influenza A viruses. PLoS Pathog **9:**e1003657.
8. **Wu Y, Wu Y, Tefsen B, Shi Y, Gao GF.** 2014. Bat-derived influenza-like viruses H17N10 and H18N11. Trends Microbiol **22:**183-191.
9. **Zhu X, Yu W, McBride R, Li Y, Chen LM, Donis RO, Tong S, Paulson JC, Wilson IA.** 2013. Hemagglutinin homologue from H17N10 bat influenza virus exhibits divergent receptor-binding and pH-dependent fusion activities. Proc Natl Acad Sci U S A **110:**1458-1463.
10. **Zhu X, Yang H, Guo Z, Yu W, Carney PJ, Li Y, Chen LM, Paulson JC, Donis RO, Tong S, Stevens J, Wilson IA.** 2012. Crystal structures of two subtype N10 neuraminidase-like proteins from bat influenza A viruses reveal a diverged putative active site. Proc Natl Acad Sci U S A **109:**18903-18908.
11. **Garcia-Sastre A.** 2012. The neuraminidase of bat influenza viruses is not a neuraminidase. Proc Natl Acad Sci U S A **109:**18635-18636.
12. **Anonymous.** 1980. A revision of the system of nomenclature for influenza viruses: a WHO memorandum. Bull World Health Organ **58:**585-591.
13. **Geraci JR, St Aubin DJ, Barker IK, Webster RG, Hinshaw VS, Bean WJ, Ruhnke HL, Prescott JH, Early G, Baker AS, Madoff S, Schooley RT.** 1982. Mass mortality of harbor seals: pneumonia associated with influenza A virus. Science **215:**1129-1131.
14. **Callan RJ, Early G, Kida H, Hinshaw VS.** 1995. The appearance of H3 influenza viruses in seals. J Gen Virol **76 (Pt 1):**199-203.
15. **Anthony SJ, St Leger JA, Pugliares K, Ip HS, Chan JM, Carpenter ZW, Navarrete-Macias I, Sanchez-Leon M, Saliki JT, Pedersen J, Karesh W, Daszak P, Rabadan R, Rowles T, Lipkin WI.** 2012. Emergence of fatal avian influenza in New England harbor seals. MBio **3:**e00166-00112.
16. **Fiers W, De Filette M, Birkett A, Neirynck S, Min Jou W.** 2004. A "universal" human influenza A vaccine. Virus Res **103:**173-176.

17. **Shah ML, Palese P.** 2013. Orthomyxoviridae: Stages of viral replication, p 1155-1175. *In* Knipe DM, Howley PM (ed), Fields Virology, 6 ed. Lippincott, Williams & Wilkins, Philadelphia, PA.

18. **Herold S, Becker C, Ridge KM, Budinger GR.** 2015. Influenza virus-induced lung injury: pathogenesis and implications for treatment. Eur Respir J **45:**1463-1478.

19. **Wright PF, Neumann G, Kawaoka Y.** 2013. Orthomyxoviruses: Influenza in humans-Epidemiology, p 1201. *In* Knipe DM, Howley PM (ed), Fields Virology. Lippincott, Williams & Wilkins, Philadelphia, PA.

20. **Garten RJ, Davis CT, Russell CA, Shu B, Lindstrom S, Balish A, Sessions WM, Xu X, Skepner E, Deyde V, Okomo-Adhiambo M, Gubareva L, Barnes J, Smith CB, Emery SL, Hillman MJ, Rivailler P, Smagala J, de Graaf M, Burke DF, Fouchier RA, Pappas C, Alpuche-Aranda CM, Lopez-Gatell H, Olivera H, Lopez I, Myers CA, Faix D, Blair PJ, Yu C, Keene KM, Dotson PD, Jr., Boxrud D, Sambol AR, Abid SH, St George K, Bannerman T, Moore AL, Stringer DJ, Blevins P, Demmler-Harrison GJ, Ginsberg M, Kriner P, Waterman S, Smole S, Guevara HF, Belongia EA, Clark PA, Beatrice ST, Donis R, et al.** 2009. Antigenic and genetic characteristics of swine-origin 2009 A(H1N1) influenza viruses circulating in humans. Science **325:**197-201.

21. **Noymer A, Garenne M.** 2000. The 1918 influenza epidemic's effects on sex differentials in mortality in the United States. Popul Dev Rev **26:**565-581.

22. **Brundage JF, Shanks GD.** 2008. Deaths from bacterial pneumonia during 1918-19 influenza pandemic. Emerg Infect Dis **14:**1193-1199.

23. **Chien YW, Klugman KP, Morens DM.** 2009. Bacterial pathogens and death during the 1918 influenza pandemic. N Engl J Med **361:**2582-2583.

24. **Dawood FS, Iuliano AD, Reed C, Meltzer MI, Shay DK, Cheng PY, Bandaranayake D, Breiman RF, Brooks WA, Buchy P, Feikin DR, Fowler KB, Gordon A, Hien NT, Horby P, Huang QS, Katz MA, Krishnan A, Lal R, Montgomery JM, Molbak K, Pebody R, Presanis AM, Razuri H, Steens A, Tinoco YO, Wallinga J, Yu H, Vong S, Bresee J, Widdowson MA.** 2012. Estimated global mortality associated with the first 12 months of 2009 pandemic influenza A H1N1 virus circulation: a modelling study. Lancet Infect Dis **12:**687-695.

25. **Rothberg MB, Haessler SD, Brown RB.** 2008. Complications of viral influenza. Am J Med **121:**258-264.

26. **Hancock K, Veguilla V, Lu X, Zhong W, Butler EN, Sun H, Liu F, Dong L, DeVos JR, Gargiullo PM, Brammer TL, Cox NJ, Tumpey TM, Katz JM.** 2009. Cross-reactive antibody responses to the 2009 pandemic H1N1 influenza virus. N Engl J Med **361:**1945-1952.

27. **Skountzou I, Koutsonanos DG, Kim JH, Powers R, Satyabhama L, Masseoud F, Weldon WC, Martin Mdel P, Mittler RS, Compans R, Jacob J.** 2010. Immunity to pre-1950 H1N1 influenza viruses confers cross-protection against the pandemic swine-origin 2009 A (H1N1) influenza virus. J Immunol **185:**1642-1649.

28. **Miller AC, Subramanian RA, Safi F, Sinert R, Zehtabchi S, Elamin EM.** 2012. Influenza A 2009 (H1N1) virus in admitted and critically ill patients. J Intensive Care Med **27:**25-31.

29. **Shieh WJ, Blau DM, Denison AM, Deleon-Carnes M, Adem P, Bhatnagar J, Sumner J, Liu L, Patel M, Batten B, Greer P, Jones T, Smith C, Bartlett J, Montague J, White E, Rollin D, Gao R, Seales C, Jost H, Metcalfe M, Goldsmith CS, Humphrey C, Schmitz A, Drew C, Paddock C, Uyeki TM, Zaki SR.** 2010. 2009 pandemic influenza A (H1N1): pathology and pathogenesis of 100 fatal cases in the United States. Am J Pathol **177:**166-175.

30. **Louie JK, Acosta M, Winter K, Jean C, Gavali S, Schechter R, Vugia D, Harriman K, Matyas B, Glaser CA, Samuel MC, Rosenberg J, Talarico J, Hatch D, California Pandemic Working G.** 2009. Factors associated with death or hospitalization due to pandemic 2009 influenza A(H1N1) infection in California. JAMA **302:**1896-1902.

31. **Claas EC, Osterhaus AD, van Beek R, De Jong JC, Rimmelzwaan GF, Senne DA, Krauss S, Shortridge KF, Webster RG.** 1998. Human influenza A H5N1 virus related to a highly pathogenic avian influenza virus. Lancet **351:**472-477.

32. **Subbarao K, Klimov A, Katz J, Regnery H, Lim W, Hall H, Perdue M, Swayne D, Bender C, Huang J, Hemphill M, Rowe T, Shaw M, Xu X, Fukuda K, Cox N.** 1998. Characterization of an avian influenza A (H5N1) virus isolated from a child with a fatal respiratory illness. Science **279:**393-396.

33. **WHO.** 2016. Cumulative number of confirmed human cases for avian influenza A(H5N1) reported to WHO, 2003-2016. http://www.who.int/influenza/human_animal_interface/2016_07_19_tableH5N1.pdf?ua=1 Accessed 19 July 2016.

34. **Herfst S, Schrauwen EJ, Linster M, Chutinimitkul S, de Wit E, Munster VJ, Sorrell EM, Bestebroer TM, Burke DF, Smith DJ, Rimmelzwaan GF, Osterhaus AD, Fouchier RA.** 2012. Airborne transmission of influenza A/H5N1 virus between ferrets. Science **336:**1534-1541.

35. **Imai M, Watanabe T, Hatta M, Das SC, Ozawa M, Shinya K, Zhong G, Hanson A, Katsura H, Watanabe S, Li C, Kawakami E, Yamada S, Kiso M, Suzuki Y, Maher EA, Neumann G, Kawaoka Y.** 2012. Experimental adaptation of an influenza H5 HA confers respiratory droplet transmission to a reassortant H5 HA/H1N1 virus in ferrets. Nature **486:**420-428.

36. **Webster RG, Govorkova EA.** 2006. H5N1 influenza--continuing evolution and spread. N Engl J Med **355:**2174-2177.

37. **WHO.** 2016. Influenza at the human-animal interface. http://www.who.int/influenza/human_animal_interface/Influenza_Summary_IRA_HA_interface_07_19_2016.pdf?ua=1. Accessed 19 July 2016.

38. **Gao R, Cao B, Hu Y, Feng Z, Wang D, Hu W, Chen J, Jie Z, Qiu H, Xu K, Xu X, Lu H, Zhu W, Gao Z, Xiang N, Shen Y, He Z, Gu Y, Zhang Z, Yang Y, Zhao X, Zhou L, Li X, Zou S, Zhang Y, Li X, Yang L, Guo J, Dong J, Li Q, Dong L, Zhu Y, Bai T, Wang S, Hao P, Yang W, Zhang Y, Han J, Yu H, Li D, Gao GF, Wu G, Wang Y, Yuan Z, Shu Y.** 2013. Human infection with a novel avian-origin influenza A (H7N9) virus. N Engl J Med **368:**1888-1897.

39. **Horby P.** 2013. H7N9 is a virus worth worrying about. Nature **496:**399.

40. **Hayden F, Croisier A.** 2005. Transmission of avian influenza viruses to and between humans. J Infect Dis **192:**1311-1314.

41. **Shinya K, Ebina M, Yamada S, Ono M, Kasai N, Kawaoka Y.** 2006. Avian flu: influenza virus receptors in the human airway. Nature **440:**435-436.

42. **Connor RJ, Kawaoka Y, Webster RG, Paulson JC.** 1994. Receptor specificity in human, avian, and equine H2 and H3 influenza virus isolates. Virology **205:**17-23.

43. **van Riel D, den Bakker MA, Leijten LM, Chutinimitkul S, Munster VJ, de Wit E, Rimmelzwaan GF, Fouchier RA, Osterhaus AD, Kuiken T.** 2010. Seasonal and pandemic human influenza viruses attach better to human upper respiratory tract epithelium than avian influenza viruses. Am J Pathol **176:**1614-1618.

44. **Wright PF, Neumann G, Kawaoka Y.** 2013. Orthomyxoviruses: Clinical features and pathogenesis in humans, p 1220-1225. *In* Knipe DM, Howley PM (ed), Fields Virology, 6 ed. Lippincott, Williams & Wilkins, Philadelphia, PA.

45. **Eccles R.** 2005. Understanding the symptoms of the common cold and influenza. Lancet Infect Dis **5:**718-725.

46. **Hayden FG, Fritz R, Lobo MC, Alvord W, Strober W, Straus SE.** 1998. Local and systemic cytokine responses during experimental human influenza A virus infection. Relation to symptom formation and host defense. J Clin Invest **101:**643-649.

47. **Taubenberger JK, Morens DM.** 2008. The pathology of influenza virus infections. Annu Rev Pathol **3:**499-522.

48. **Taubenberger JK, Layne SP.** 2001. Diagnosis of influenza virus: coming to grips with the molecular era. Mol Diagn **6:**291-305.

49. **CDC.** 2000. Update: influenza activity--United States and worldwide, 1999-2000 season, and composition of the 2000-01 influenza vaccine. MMWR Morb Mortal Wkly Rep **49:**375-381.

50. **van Riel D, Munster VJ, de Wit E, Rimmelzwaan GF, Fouchier RA, Osterhaus AD, Kuiken T.** 2007. Human and avian influenza viruses target different cells in the lower respiratory tract of humans and other mammals. Am J Pathol **171:**1215-1223.

51. **Kuiken T, Taubenberger JK.** 2008. Pathology of human influenza revisited. Vaccine **26 Suppl 4:**D59-66.

52. **Walsh JJ, Dietlein LF, Low FN, Burch GE, Mogabgab WJ.** 1961. Bronchotracheal response in human influenza. Type A, Asian strain, as studied by light and electron microscopic examination of bronchoscopic biopsies. Arch Intern Med **108:**376-388.

53. **Lopez A, Prior M, Yong S, Lillie L, Lefebvre M.** 1988. Nasal lesions in rats exposed to hydrogen sulfide for four hours. Am J Vet Res **49:**1107-1111.

54. **Bruder D, Srikiatkhachorn A, Enelow RI.** 2006. Cellular immunity and lung injury in respiratory virus infection. Viral Immunol **19:**147-155.

55. **Wright PF, Neumann G, Kawaoka Y.** 2013. Orthomyxoviruses, p 1186-1342. *In* Knipe DM, Howley PM (ed), Fields virology, 6 ed. Lippincott, Williams & Wilkins, Philidelphia, PA.

56. **Renegar KB, Small PA, Jr., Boykins LG, Wright PF.** 2004. Role of IgA versus IgG in the control of influenza viral infection in the murine respiratory tract. J Immunol **173:**1978-1986.

57. **Couch RB, Kasel JA.** 1983. Immunity to influenza in man. Annu Rev Microbiol **37:**529-549.

58. **Ito R, Ozaki YA, Yoshikawa T, Hasegawa H, Sato Y, Suzuki Y, Inoue R, Morishima T, Kondo N, Sata T, Kurata T, Tamura S.** 2003. Roles of anti-hemagglutinin IgA and IgG antibodies in different sites of the respiratory tract of vaccinated mice in preventing lethal influenza pneumonia. Vaccine **21:**2362-2371.

59. **Craighead JE.** 2000. Pathology and pathogenesis of human viral disease. Academic Press, San Diego, CA.

60. **McCullers JA.** 2006. Insights into the interaction between influenza virus and pneumococcus. Clin Microbiol Rev **19:**571-582.

61. **Hers JF, Masurel N, Mulder J.** 1958. Bacteriology and histopathology of the respiratory tract and lungs in fatal Asian influenza. Lancet **2:**1141-1143.

62. **van Riel D, Munster VJ, de Wit E, Rimmelzwaan GF, Fouchier RA, Osterhaus AD, Kuiken T.** 2006. H5N1 Virus Attachment to Lower Respiratory Tract. Science **312:**399.

63. **Korteweg C, Gu J.** 2008. Pathology, molecular biology, and pathogenesis of avian influenza A (H5N1) infection in humans. Am J Pathol **172:**1155-1170.

64. **Beal AL, Cerra FB.** 1994. Multiple organ failure syndrome in the 1990s. Systemic inflammatory response and organ dysfunction. JAMA **271:**226-233.

65. **Schat KA, Bingham J, Butler JM, Chen LM, Lowther S, Crowley TM, Moore RJ, Donis RO, Lowenthal JW.** 2012. Role of position 627 of PB2 and the multibasic cleavage site of the hemagglutinin in the virulence of H5N1 avian influenza virus in chickens and ducks. PLoS One **7:**e30960.

66. **Fukuyama S, Kawaoka Y.** 2011. The pathogenesis of influenza virus infections: the contributions of virus and host factors. Curr Opin Immunol **23:**481-486.

67. **de Jong MD, Simmons CP, Thanh TT, Hien VM, Smith GJ, Chau TN, Hoang DM, Chau NV, Khanh TH, Dong VC, Qui PT, Cam BV, Ha do Q, Guan Y, Peiris JS, Chinh NT, Hien TT, Farrar J.** 2006. Fatal outcome of human influenza A (H5N1) is associated with high viral load and hypercytokinemia. Nat Med **12:**1203-1207.

68. **Siegers JY, Short KR, Leijten LM, de Graaf M, Spronken MI, Schrauwen EJ, Marshall N, Lowen AC, Gabriel G, Osterhaus AD, Kuiken T, van Riel D.** 2014. Novel avian-origin

influenza A (H7N9) virus attachment to the respiratory tract of five animal models. J Virol **88:**4595-4599.

69. **van Riel D, Leijten LM, de Graaf M, Siegers JY, Short KR, Spronken MI, Schrauwen EJ, Fouchier RA, Osterhaus AD, Kuiken T.** 2013. Novel avian-origin influenza A (H7N9) virus attaches to epithelium in both upper and lower respiratory tract of humans. Am J Pathol **183:**1137-1143.
70. **Knepper J, Schierhorn KL, Becher A, Budt M, Tonnies M, Bauer TT, Schneider P, Neudecker J, Ruckert JC, Gruber AD, Suttorp N, Schweiger B, Hippenstiel S, Hocke AC, Wolff T.** 2013. The novel human influenza A(H7N9) virus is naturally adapted to efficient growth in human lung tissue. MBio **4:**e00601-00613.
71. **Beigel JH, Farrar J, Han AM, Hayden FG, Hyer R, de Jong MD, Lochindarat S, Nguyen TK, Nguyen TH, Tran TH, Nicoll A, Touch S, Yuen KY, Writing Committee of the World Health Organization Consultation on Human Influenza AH.** 2005. Avian influenza A (H5N1) infection in humans. N Engl J Med **353:**1374-1385.
72. **Writing Committee of the Second World Health Organization Consultation on Clinical Aspects of Human Infection with Avian Influenza AV, Abdel-Ghafar AN, Chotpitayasunondh T, Gao Z, Hayden FG, Nguyen DH, de Jong MD, Naghdaliyev A, Peiris JS, Shindo N, Soeroso S, Uyeki TM.** 2008. Update on avian influenza A (H5N1) virus infection in humans. N Engl J Med **358:**261-273.
73. **CDC.** 2006. High levels of adamantane resistance among influenza A (H3N2) viruses and interim guidelines for use of antiviral agents--United States, 2005-06 influenza season. MMWR Morb Mortal Wkly Rep **55:**44-46.
74. **Harvala H, Gunson R, Simmonds P, Hardie A, Bennett S, Scott F, Roddie H, McKnight J, Walsh T, Rowney D, Clark A, Bremner J, Aitken C, Templeton K.** 2010. The emergence of oseltamivir-resistant pandemic influenza A (H1N1) 2009 virus amongst hospitalised immunocompromised patients in Scotland, November-December, 2009. Euro Surveill **15**.
75. **van der Vries E, Stelma FF, Boucher CA.** 2010. Emergence of a multidrug-resistant pandemic influenza A (H1N1) virus. N Engl J Med **363:**1381-1382.
76. **Law M, Stromberg P, Meuten D, Cullen J.** 2012. Necropsy or autopsy? It's all about communication! Vet Pathol **49:**271-272.
77. **Merriam-Webster T.** 1993. Websters' Third New International Dictionary. Merriam-Webster Inc. publishers, Springfield, MA.
78. **Johnson NP, Mueller J.** 2002. Updating the accounts: global mortality of the 1918-1920 "Spanish" influenza pandemic. Bull Hist Med **76:**105-115.
79. **Webster RG, Peiris M, Chen H, Guan Y.** 2006. H5N1 outbreaks and enzootic influenza. Emerg Infect Dis **12:**3-8.
80. **Morens DM, Taubenberger JK, Fauci AS.** 2008. Predominant role of bacterial pneumonia as a cause of death in pandemic influenza: implications for pandemic influenza preparedness. J Infect Dis **198:**962-970.
81. **Palacios G, Hornig M, Cisterna D, Savji N, Bussetti AV, Kapoor V, Hui J, Tokarz R, Briese T, Baumeister E, Lipkin WI.** 2009. Streptococcus pneumoniae coinfection is correlated with the severity of H1N1 pandemic influenza. PLoS One **4:**e8540.
82. **Okada T, Morozumi M, Matsubara K, Komiyama O, Ubukata K, Takahashi T, Iwata S.** 2011. Characteristic findings of pediatric inpatients with pandemic (H1N1) 2009 virus infection among severe and nonsevere illnesses. J Infect Chemother **17:**238-245.
83. **Morens DM, Fauci AS.** 2007. The 1918 influenza pandemic: insights for the 21st century. J Infect Dis **195:**1018-1028.
84. **Chotpitayasunondh T, Ungchusak K, Hanshaoworakul W, Chunsuthiwat S, Sawanpanyalert P, Kijphati R, Lochindarat S, Srisan P, Suwan P, Osotthanakorn Y, Anantasetagoon T, Kanjanawasri S, Tanupattarachai S, Weerakul J, Chaiwirattana R, Maneerattanaporn**

M, Poolsavathitikool R, Chokephaibulkit K, Apisarnthanarak A, Dowell SF. 2005. Human disease from influenza A (H5N1), Thailand, 2004. Emerg Infect Dis **11:**201-209.

85. **To KK, Hung IF, Li IW, Lee KL, Koo CK, Yan WW, Liu R, Ho KY, Chu KH, Watt CL, Luk WK, Lai KY, Chow FL, Mok T, Buckley T, Chan JF, Wong SS, Zheng B, Chen H, Lau CC, Tse H, Cheng VC, Chan KH, Yuen KY.** 2010. Delayed clearance of viral load and marked cytokine activation in severe cases of pandemic H1N1 2009 influenza virus infection. Clin Infect Dis **50:**850-859.
86. **Ramsey C, Kumar A.** 2011. H1N1: viral pneumonia as a cause of acute respiratory distress syndrome. Curr Opin Crit Care **17:**64-71.
87. **Husain AN, Kumar V.** 2010. The lung, p 715–716. *In* Kumar V, Abbas A, Fausto N (ed), Robbins & Cotran Pathologic Basis of Disease 8ed. Elsevier, Pennsylvania, PA.
88. **Piantadosi CA, Schwartz DA.** 2004. The acute respiratory distress syndrome. Ann Intern Med **141:**460-470.
89. **Bannerman DD, Goldblum SE.** 2003. Mechanisms of bacterial lipopolysaccharide-induced endothelial apoptosis. Am J Physiol Lung Cell Mol Physiol **284:**L899-914.
90. **Matthay MA, Zemans RL.** 2011. The acute respiratory distress syndrome: pathogenesis and treatment. Annu Rev Pathol **6:**147-163.
91. **Basler CF, Aguilar PV.** 2008. Progress in identifying virulence determinants of the 1918 H1N1 and the Southeast Asian H5N1 influenza A viruses. Antiviral Res **79:**166-178.
92. **Peiris JS, Cheung CY, Leung CY, Nicholls JM.** 2009. Innate immune responses to influenza A H5N1: friend or foe? Trends Immunol **30:**574-584.
93. **Koval M.** 2013. Claudin heterogeneity and control of lung tight junctions. Annu Rev Physiol **75:**551-567.
94. **Gorin AB, Stewart PA.** 1979. Differential permeability of endothelial and epithelial barriers to albumin flux. J Appl Physiol Respir Environ Exerc Physiol **47:**1315-1324.
95. **Folkesson HG, Matthay MA.** 2006. Alveolar epithelial ion and fluid transport: recent progress. Am J Respir Cell Mol Biol **35:**10-19.
96. **Berthiaume Y, Matthay MA.** 2007. Alveolar edema fluid clearance and acute lung injury. Respir Physiol Neurobiol **159:**350-359.
97. **Nakajima N, Van Tin N, Sato Y, Thach HN, Katano H, Diep PH, Kumasaka T, Thuy NT, Hasegawa H, San LT, Kawachi S, Liem NT, Suzuki K, Sata T.** 2013. Pathological study of archival lung tissues from five fatal cases of avian H5N1 influenza in Vietnam. Mod Pathol **26:**357-369.
98. **Uiprasertkul M, Puthavathana P, Sangsiriwut K, Pooruk P, Srisook K, Peiris M, Nicholls JM, Chokephaibulkit K, Vanprapar N, Auewarakul P.** 2005. Influenza A H5N1 replication sites in humans. Emerg Infect Dis **11:**1036-1041.
99. **Guarner J, Falcon-Escobedo R.** 2009. Comparison of the pathology caused by H1N1, H5N1, and H3N2 influenza viruses. Arch Med Res **40:**655-661.
100. **Childs RA, Palma AS, Wharton S, Matrosovich T, Liu Y, Chai W, Campanero-Rhodes MA, Zhang Y, Eickmann M, Kiso M, Hay A, Matrosovich M, Feizi T.** 2009. Receptor-binding specificity of pandemic influenza A (H1N1) 2009 virus determined by carbohydrate microarray. Nat Biotechnol **27:**797-799.
101. **Stevens J, Blixt O, Paulson JC, Wilson IA.** 2006. Glycan microarray technologies: tools to survey host specificity of influenza viruses. Nat Rev Microbiol **4:**857-864.
102. **Chutinimitkul S, van Riel D, Munster VJ, van den Brand JM, Rimmelzwaan GF, Kuiken T, Osterhaus AD, Fouchier RA, de Wit E.** 2010. In vitro assessment of attachment pattern and replication efficiency of H5N1 influenza A viruses with altered receptor specificity. J Virol **84:**6825-6833.

103. **Chen XJ, Seth S, Yue G, Kamat P, Compans RW, Guidot D, Brown LA, Eaton DC, Jain L.** 2004. Influenza virus inhibits ENaC and lung fluid clearance. Am J Physiol Lung Cell Mol Physiol **287:**L366-373.

104. **Kunzelmann K, Beesley AH, King NJ, Karupiah G, Young JA, Cook DI.** 2000. Influenza virus inhibits amiloride-sensitive Na+ channels in respiratory epithelia. Proc Natl Acad Sci U S A **97:**10282-10287.

105. **Lazrak A, Iles KE, Liu G, Noah DL, Noah JW, Matalon S.** 2009. Influenza virus M2 protein inhibits epithelial sodium channels by increasing reactive oxygen species. FASEB J **23:**3829-3842.

106. **Wolk KE, Lazarowski ER, Traylor ZP, Yu EN, Jewell NA, Durbin RK, Durbin JE, Davis IC.** 2008. Influenza A virus inhibits alveolar fluid clearance in BALB/c mice. Am J Respir Crit Care Med **178:**969-976.

107. **Mauad T, Hajjar LA, Callegari GD, da Silva LF, Schout D, Galas FR, Alves VA, Malheiros DM, Auler JO, Jr., Ferreira AF, Borsato MR, Bezerra SM, Gutierrez PS, Caldini ET, Pasqualucci CA, Dolhnikoff M, Saldiva PH.** 2010. Lung pathology in fatal novel human influenza A (H1N1) infection. Am J Respir Crit Care Med **181:**72-79.

108. **Uiprasertkul M, Kitphati R, Puthavathana P, Kriwong R, Kongchanagul A, Ungchusak K, Angkasekwinai S, Chokephaibulkit K, Srisook K, Vanprapar N, Auewarakul P.** 2007. Apoptosis and pathogenesis of avian influenza A (H5N1) virus in humans. Emerg Infect Dis **13:**708-712.

109. **Brydon EW, Smith H, Sweet C.** 2003. Influenza A virus-induced apoptosis in bronchiolar epithelial (NCI-H292) cells limits pro-inflammatory cytokine release. J Gen Virol **84:**2389-2400.

110. **Arndt U, Wennemuth G, Barth P, Nain M, Al-Abed Y, Meinhardt A, Gemsa D, Bacher M.** 2002. Release of macrophage migration inhibitory factor and CXCL8/interleukin-8 from lung epithelial cells rendered necrotic by influenza A virus infection. J Virol **76:**9298-9306.

111. **Lam WY, Tang JW, Yeung AC, Chiu LC, Sung JJ, Chan PK.** 2008. Avian influenza virus A/HK/483/97(H5N1) NS1 protein induces apoptosis in human airway epithelial cells. J Virol **82:**2741-2751.

112. **Takizawa T, Ohashi K, Nakanishi Y.** 1996. Possible involvement of double-stranded RNA-activated protein kinase in cell death by influenza virus infection. J Virol **70:**8128-8132.

113. **Schultz-Cherry S, Hinshaw VS.** 1996. Influenza virus neuraminidase activates latent transforming growth factor beta. J Virol **70:**8624-8629.

114. **Kash JC, Goodman AG, Korth MJ, Katze MG.** 2006. Hijacking of the host-cell response and translational control during influenza virus infection. Virus Res **119:**111-120.

115. **Golebiewski L, Liu H, Javier RT, Rice AP.** 2011. The avian influenza virus NS1 ESEV PDZ binding motif associates with Dlg1 and Scribble to disrupt cellular tight junctions. J Virol **85:**10639-10648.

116. **Peiris JS, Yu WC, Leung CW, Cheung CY, Ng WF, Nicholls JM, Ng TK, Chan KH, Lai ST, Lim WL, Yuen KY, Guan Y.** 2004. Re-emergence of fatal human influenza A subtype H5N1 disease. Lancet **363:**617-619.

117. **Choi AM, Jacoby DB.** 1992. Influenza virus A infection induces interleukin-8 gene expression in human airway epithelial cells. FEBS Lett **309:**327-329.

118. **Chan MC, Cheung CY, Chui WH, Tsao SW, Nicholls JM, Chan YO, Chan RW, Long HT, Poon LL, Guan Y, Peiris JS.** 2005. Proinflammatory cytokine responses induced by influenza A (H5N1) viruses in primary human alveolar and bronchial epithelial cells. Respir Res **6:**135.

119. **Herold S, von Wulffen W, Steinmueller M, Pleschka S, Kuziel WA, Mack M, Srivastava M, Seeger W, Maus UA, Lohmeyer J.** 2006. Alveolar epithelial cells direct monocyte transepithelial migration upon influenza virus infection: impact of chemokines and adhesion molecules. J Immunol **177:**1817-1824.

120. **Guillot L, Le Goffic R, Bloch S, Escriou N, Akira S, Chignard M, Si-Tahar M.** 2005. Involvement of toll-like receptor 3 in the immune response of lung epithelial cells to double-stranded RNA and influenza A virus. J Biol Chem **280:**5571-5580.

121. **Zeng H, Goldsmith CS, Maines TR, Belser JA, Gustin KM, Pekosz A, Zaki SR, Katz JM, Tumpey TM.** 2013. Tropism and infectivity of influenza virus, including highly pathogenic avian H5N1 virus, in ferret tracheal differentiated primary epithelial cell cultures. J Virol **87:**2597-2607.

122. **Bernasconi D, Amici C, La Frazia S, Ianaro A, Santoro MG.** 2005. The IkappaB kinase is a key factor in triggering influenza A virus-induced inflammatory cytokine production in airway epithelial cells. J Biol Chem **280:**24127-24134.

123. **Veckman V, Osterlund P, Fagerlund R, Melen K, Matikainen S, Julkunen I.** 2006. TNF-alpha and IFN-alpha enhance influenza-A-virus-induced chemokine gene expression in human A549 lung epithelial cells. Virology **345:**96-104.

124. **Adachi M, Matsukura S, Tokunaga H, Kokubu F.** 1997. Expression of cytokines on human bronchial epithelial cells induced by influenza virus A. Int Arch Allergy Immunol **113:**307-311.

125. **Matsukura S, Kokubu F, Noda H, Tokunaga H, Adachi M.** 1996. Expression of IL-6, IL-8, and RANTES on human bronchial epithelial cells, NCI-H292, induced by influenza virus A. J Allergy Clin Immunol **98:**1080-1087.

126. **Roux J, Kawakatsu H, Gartland B, Pespeni M, Sheppard D, Matthay MA, Canessa CM, Pittet JF.** 2005. Interleukin-1beta decreases expression of the epithelial sodium channel alpha-subunit in alveolar epithelial cells via a p38 MAPK-dependent signaling pathway. J Biol Chem **280:**18579-18589.

127. **Mullin JM, Snock KV.** 1990. Effect of tumor necrosis factor on epithelial tight junctions and transepithelial permeability. Cancer Res **50:**2172-2176.

128. **Wyble CW, Hynes KL, Kuchibhotla J, Marcus BC, Hallahan D, Gewertz BL.** 1997. TNF-alpha and IL-1 upregulate membrane-bound and soluble E-selectin through a common pathway. J Surg Res **73:**107-112.

129. **Pinkerton KE, Gehr P, Crapo JD.** 1992. Architecture and cellular composition of the air-blood barrier. , p 121–128. *In* Parent RA (ed), Comparative biology of the lung. CRC Press,, Boca Raton, FL.

130. **Zeng H, Pappas C, Belser JA, Houser KV, Zhong W, Wadford DA, Stevens T, Balczon R, Katz JM, Tumpey TM.** 2012. Human pulmonary microvascular endothelial cells support productive replication of highly pathogenic avian influenza viruses: possible involvement in the pathogenesis of human H5N1 virus infection. J Virol **86:**667-678.

131. **Ocana-Macchi M, Bel M, Guzylack-Piriou L, Ruggli N, Liniger M, McCullough KC, Sakoda Y, Isoda N, Matrosovich M, Summerfield A.** 2009. Hemagglutinin-dependent tropism of H5N1 avian influenza virus for human endothelial cells. J Virol **83:**12947-12955.

132. **Perrone LA, Plowden JK, Garcia-Sastre A, Katz JM, Tumpey TM.** 2008. H5N1 and 1918 pandemic influenza virus infection results in early and excessive infiltration of macrophages and neutrophils in the lungs of mice. PLoS Pathog **4:**e1000115.

133. **Visseren FL, Verkerk MS, Bouter KP, Diepersloot RJ, Erkelens DW.** 1999. Interleukin-6 production by endothelial cells after infection with influenza virus and cytomegalovirus. J Lab Clin Med **134:**623-630.

134. **Ishiguro N, Takada A, Yoshioka M, Ma X, Kikuta H, Kida H, Kobayashi K.** 2004. Induction of interferon-inducible protein-10 and monokine induced by interferon-gamma from human endothelial cells infected with Influenza A virus. Arch Virol **149:**17-34.

135. **Teijaro JR, Walsh KB, Cahalan S, Fremgen DM, Roberts E, Scott F, Martinborough E, Peach R, Oldstone MB, Rosen H.** 2011. Endothelial cells are central orchestrators of cytokine amplification during influenza virus infection. Cell **146:**980-991.

136. **Armstrong SM, Wang C, Tigdi J, Si X, Dumpit C, Charles S, Gamage A, Moraes TJ, Lee WL.** 2012. Influenza infects lung microvascular endothelium leading to microvascular leak: role of apoptosis and claudin-5. PLoS One **7:**e47323.

137. **Armstrong SM, Darwish I, Lee WL.** 2013. Endothelial activation and dysfunction in the pathogenesis of influenza A virus infection. Virulence **4:**537-542.

138. **Alexander DJ.** 2000. A review of avian influenza in different bird species. Vet Microbiol **74:**3-13.

139. **Wiener-Kronish JP, Albertine KH, Matthay MA.** 1991. Differential responses of the endothelial and epithelial barriers of the lung in sheep to Escherichia coli endotoxin. J Clin Invest **88:**864-875.

140. **Sumikoshi M, Hashimoto K, Kawasaki Y, Sakuma H, Suzutani T, Suzuki H, Hosoya M.** 2008. Human influenza virus infection and apoptosis induction in human vascular endothelial cells. J Med Virol **80:**1072-1078.

141. **Chan MC, Chan RW, Yu WC, Ho CC, Chui WH, Lo CK, Yuen KM, Guan YI, Nicholls JM, Peiris JS.** 2009. Influenza H5N1 virus infection of polarized human alveolar epithelial cells and lung microvascular endothelial cells. Respir Res **10:**102.

142. **Gu J, Xie Z, Gao Z, Liu J, Korteweg C, Ye J, Lau LT, Lu J, Gao Z, Zhang B, McNutt MA, Lu M, Anderson VM, Gong E, Yu AC, Lipkin WI.** 2007. H5N1 infection of the respiratory tract and beyond: a molecular pathology study. Lancet **370:**1137-1145.

143. **Kuiken T, van den Brand J, van Riel D, Pantin-Jackwood M, Swayne DE.** 2010. Comparative pathology of select agent influenza a virus infections. Vet Pathol **47:**893-914.

144. **Reperant LA, van de Bildt MW, van Amerongen G, Leijten LM, Watson S, Palser A, Kellam P, Eissens AC, Frijlink HW, Osterhaus AD, Kuiken T.** 2012. Marked endotheliotropism of highly pathogenic avian influenza virus H5N1 following intestinal inoculation in cats. J Virol **86:**1158-1165.

145. **Huber D, Balda MS, Matter K.** 1998. Transepithelial migration of neutrophils. Invasion Metastasis **18:**70-80.

146. **Walker DC, Behzad AR, Chu F.** 1995. Neutrophil migration through preexisting holes in the basal laminae of alveolar capillaries and epithelium during streptococcal pneumonia. Microvasc Res **50:**397-416.

147. **Martin TR, Pistorese BP, Chi EY, Goodman RB, Matthay MA.** 1989. Effects of leukotriene B4 in the human lung. Recruitment of neutrophils into the alveolar spaces without a change in protein permeability. J Clin Invest **84:**1609-1619.

148. **Jaeschke H, Smith CW.** 1997. Mechanisms of neutrophil-induced parenchymal cell injury. J Leukoc Biol **61:**647-653.

149. **Tapper H.** 1996. The secretion of preformed granules by macrophages and neutrophils. J Leukoc Biol **59:**613-622.

150. **Stinchcombe JC, Griffiths GM.** 1999. Regulated secretion from hemopoietic cells. J Cell Biol **147:**1-6.

151. **von Kockritz-Blickwede M, Nizet V.** 2009. Innate immunity turned inside-out: antimicrobial defense by phagocyte extracellular traps. J Mol Med (Berl) **87:**775-783.

152. **Tate MD, Deng YM, Jones JE, Anderson GP, Brooks AG, Reading PC.** 2009. Neutrophils ameliorate lung injury and the development of severe disease during influenza infection. J Immunol **183:**7441-7450.

153. **Weiland JE, Davis WB, Holter JF, Mohammed JR, Dorinsky PM, Gadek JE.** 1986. Lung neutrophils in the adult respiratory distress syndrome. Clinical and pathophysiologic significance. Am Rev Respir Dis **133:**218-225.

154. **Sakai S, Kawamata H, Mantani N, Kogure T, Shimada Y, Terasawa K, Sakai T, Imanishi N, Ochiai H.** 2000. Therapeutic effect of anti-macrophage inflammatory protein 2 antibody on influenza virus-induced pneumonia in mice. J Virol **74:**2472-2476.

155. **Narasaraju T, Yang E, Samy RP, Ng HH, Poh WP, Liew AA, Phoon MC, van Rooijen N, Chow VT.** 2011. Excessive neutrophils and neutrophil extracellular traps contribute to acute lung injury of influenza pneumonitis. Am J Pathol **179:**199-210.

156. **Amulic B, Cazalet C, Hayes GL, Metzler KD, Zychlinsky A.** 2012. Neutrophil function: from mechanisms to disease. Annu Rev Immunol **30:**459-489.

157. **Bandyopadhyay U, Das D, Banerjee RK.** 1999. Reactive oxygen species: oxidative damage and pathogenesis. Current science-bangalore- **77:**658-666.

158. **Fang FC.** 2004. Antimicrobial reactive oxygen and nitrogen species: concepts and controversies. Nat Rev Microbiol **2:**820-832.

159. **Oda T, Akaike T, Hamamoto T, Suzuki F, Hirano T, Maeda H.** 1989. Oxygen radicals in influenza-induced pathogenesis and treatment with pyran polymer-conjugated SOD. Science **244:**974-976.

160. **Snelgrove RJ, Edwards L, Rae AJ, Hussell T.** 2006. An absence of reactive oxygen species improves the resolution of lung influenza infection. Eur J Immunol **36:**1364-1373.

161. **Lefkowitz DL, Mills K, Lefkowitz SS, Bollen A, Moguilevsky N.** 1995. Neutrophil-macrophage interaction: a paradigm for chronic inflammation. Med Hypotheses **44:**58-62.

162. **Yamamoto K, Miyoshi-Koshio T, Utsuki Y, Mizuno S, Suzuki K.** 1991. Virucidal activity and viral protein modification by myeloperoxidase: a candidate for defense factor of human polymorphonuclear leukocytes against influenza virus infection. J Infect Dis **164:**8-14.

163. **Vissers MC, Pullar JM, Hampton MB.** 1999. Hypochlorous acid causes caspase activation and apoptosis or growth arrest in human endothelial cells. Biochem J **344 Pt 2:**443-449.

164. **Sugamata R, Dobashi H, Nagao T, Yamamoto K, Nakajima N, Sato Y, Aratani Y, Oshima M, Sata T, Kobayashi K, Kawachi S, Nakayama T, Suzuki K.** 2012. Contribution of neutrophil-derived myeloperoxidase in the early phase of fulminant acute respiratory distress syndrome induced by influenza virus infection. Microbiol Immunol **56:**171-182.

165. **Wang JP, Bowen GN, Padden C, Cerny A, Finberg RW, Newburger PE, Kurt-Jones EA.** 2008. Toll-like receptor-mediated activation of neutrophils by influenza A virus. Blood **112:**2028-2034.

166. **Ichikawa A, Kuba K, Morita M, Chida S, Tezuka H, Hara H, Sasaki T, Ohteki T, Ranieri VM, dos Santos CC, Kawaoka Y, Akira S, Luster AD, Lu B, Penninger JM, Uhlig S, Slutsky AS, Imai Y.** 2013. CXCL10-CXCR3 enhances the development of neutrophil-mediated fulminant lung injury of viral and nonviral origin. Am J Respir Crit Care Med **187:**65-77.

167. **Cameron CM, Cameron MJ, Bermejo-Martin JF, Ran L, Xu L, Turner PV, Ran R, Danesh A, Fang Y, Chan PK, Mytle N, Sullivan TJ, Collins TL, Johnson MG, Medina JC, Rowe T, Kelvin DJ.** 2008. Gene expression analysis of host innate immune responses during Lethal H5N1 infection in ferrets. J Virol **82:**11308-11317.

168. **Hemmers S, Teijaro JR, Arandjelovic S, Mowen KA.** 2011. PAD4-mediated neutrophil extracellular trap formation is not required for immunity against influenza infection. PLoS One **6:**e22043.

169. **Valberg PA, Blanchard JD.** 1992. Pulmonary macrophage physiology:origin, motility, endocytosis, p 681–724. *In* Parent RA (ed), Comparative biologyof the lung. CRC Press, Boca Raton, FL.

170. **Holt PG.** 1986. Down-regulation of immune responses in the lower respiratory tract: the role of alveolar macrophages. Clin Exp Immunol **63:**261-270.

171. **Tate MD, Pickett DL, van Rooijen N, Brooks AG, Reading PC.** 2010. Critical role of airway macrophages in modulating disease severity during influenza virus infection of mice. J Virol **84:**7569-7580.

172. **Dawson TC, Beck MA, Kuziel WA, Henderson F, Maeda N.** 2000. Contrasting effects of CCR5 and CCR2 deficiency in the pulmonary inflammatory response to influenza A virus. Am J Pathol **156:**1951-1959.

173. **Herold S, Steinmueller M, von Wulffen W, Cakarova L, Pinto R, Pleschka S, Mack M, Kuziel WA, Corazza N, Brunner T, Seeger W, Lohmeyer J.** 2008. Lung epithelial apoptosis in influenza virus pneumonia: the role of macrophage-expressed TNF-related apoptosis-inducing ligand. J Exp Med **205:**3065-3077.

174. **Hogner K, Wolff T, Pleschka S, Plog S, Gruber AD, Kalinke U, Walmrath HD, Bodner J, Gattenlohner S, Lewe-Schlosser P, Matrosovich M, Seeger W, Lohmeyer J, Herold S.** 2013. Macrophage-expressed IFN-beta contributes to apoptotic alveolar epithelial cell injury in severe influenza virus pneumonia. PLoS Pathog **9:**e1003188.

175. **Padalko E, Ohnishi T, Matsushita K, Sun H, Fox-Talbot K, Bao C, Baldwin WM, 3rd, Lowenstein CJ.** 2004. Peroxynitrite inhibition of Coxsackievirus infection by prevention of viral RNA entry. Proc Natl Acad Sci U S A **101:**11731-11736.

176. **Szabo C.** 2003. Multiple pathways of peroxynitrite cytotoxicity. Toxicol Lett **140-141:**105-112.

177. **Akaike T, Noguchi Y, Ijiri S, Setoguchi K, Suga M, Zheng YM, Dietzschold B, Maeda H.** 1996. Pathogenesis of influenza virus-induced pneumonia: involvement of both nitric oxide and oxygen radicals. Proc Natl Acad Sci U S A **93:**2448-2453.

178. **Karupiah G, Chen JH, Mahalingam S, Nathan CF, MacMicking JD.** 1998. Rapid interferon gamma-dependent clearance of influenza A virus and protection from consolidating pneumonitis in nitric oxide synthase 2-deficient mice. J Exp Med **188:**1541-1546.

179. **Pirhonen J, Sareneva T, Kurimoto M, Julkunen I, Matikainen S.** 1999. Virus infection activates IL-1 beta and IL-18 production in human macrophages by a caspase-1-dependent pathway. J Immunol **162:**7322-7329.

180. **Cheung CY, Poon LL, Lau AS, Luk W, Lau YL, Shortridge KF, Gordon S, Guan Y, Peiris JS.** 2002. Induction of proinflammatory cytokines in human macrophages by influenza A (H5N1) viruses: a mechanism for the unusual severity of human disease? Lancet **360:**1831-1837.

181. **Lehmann C, Sprenger H, Nain M, Bacher M, Gemsa D.** 1996. Infection of macrophages by influenza A virus: characteristics of tumour necrosis factor-alpha (TNF alpha) gene expression. Res Virol **147:**123-130.

182. **Hui KP, Lee SM, Cheung CY, Ng IH, Poon LL, Guan Y, Ip NY, Lau AS, Peiris JS.** 2009. Induction of proinflammatory cytokines in primary human macrophages by influenza A virus (H5N1) is selectively regulated by IFN regulatory factor 3 and p38 MAPK. J Immunol **182:**1088-1098.

183. **Matikainen S, Pirhonen J, Miettinen M, Lehtonen A, Govenius-Vintola C, Sareneva T, Julkunen I.** 2000. Influenza A and sendai viruses induce differential chemokine gene expression and transcription factor activation in human macrophages. Virology **276:**138-147.

184. **Geiler J, Michaelis M, Sithisarn P, Cinatl J, Jr.** 2011. Comparison of pro-inflammatory cytokine expression and cellular signal transduction in human macrophages infected with different influenza A viruses. Med Microbiol Immunol **200:**53-60.

185. **Woo PC, Tung ET, Chan KH, Lau CC, Lau SK, Yuen KY.** 2010. Cytokine profiles induced by the novel swine-origin influenza A/H1N1 virus: implications for treatment strategies. J Infect Dis **201:**346-353.

186. **Yu WC, Chan RW, Wang J, Travanty EA, Nicholls JM, Peiris JS, Mason RJ, Chan MC.** 2011. Viral replication and innate host responses in primary human alveolar epithelial cells and alveolar macrophages infected with influenza H5N1 and H1N1 viruses. J Virol **85:**6844-6855.

187. **Michaelis M, Geiler J, Naczk P, Sithisarn P, Leutz A, Doerr HW, Cinatl J, Jr.** 2011. Glycyrrhizin exerts antioxidative effects in H5N1 influenza A virus-infected cells and inhibits virus replication and pro-inflammatory gene expression. PLoS One **6:**e19705.

188. **Osterlund P, Pirhonen J, Ikonen N, Ronkko E, Strengell M, Makela SM, Broman M, Hamming OJ, Hartmann R, Ziegler T, Julkunen I.** 2010. Pandemic H1N1 2009 influenza A virus induces weak cytokine responses in human macrophages and dendritic cells and is highly sensitive to the antiviral actions of interferons. J Virol **84:**1414-1422.

189. **Friesenhagen J, Boergeling Y, Hrincius E, Ludwig S, Roth J, Viemann D.** 2012. Highly pathogenic avian influenza viruses inhibit effective immune responses of human blood-derived macrophages. J Leukoc Biol **92:**11-20.

190. **Mok KP, Wong CH, Cheung CY, Chan MC, Lee SM, Nicholls JM, Guan Y, Peiris JS.** 2009. Viral genetic determinants of H5N1 influenza viruses that contribute to cytokine dysregulation. J Infect Dis **200:**1104-1112.

191. **van Riel D, Leijten LM, van der Eerden M, Hoogsteden HC, Boven LA, Lambrecht BN, Osterhaus AD, Kuiken T.** 2011. Highly pathogenic avian influenza virus H5N1 infects alveolar macrophages without virus production or excessive TNF-alpha induction. PLoS Pathog **7:**e1002099.

192. **Hale BG, Albrecht RA, Garcia-Sastre A.** 2010. Innate immune evasion strategies of influenza viruses. Future Microbiol **5:**23-41.

193. **Seo SH, Hoffmann E, Webster RG.** 2002. Lethal H5N1 influenza viruses escape host anti-viral cytokine responses. Nat Med **8:**950-954.

194. **Salomon R, Hoffmann E, Webster RG.** 2007. Inhibition of the cytokine response does not protect against lethal H5N1 influenza infection. Proc Natl Acad Sci U S A **104:**12479-12481.

195. **Szretter KJ, Gangappa S, Lu X, Smith C, Shieh WJ, Zaki SR, Sambhara S, Tumpey TM, Katz JM.** 2007. Role of host cytokine responses in the pathogenesis of avian H5N1 influenza viruses in mice. J Virol **81:**2736-2744.

196. **Sevransky JE, Martin GS, Shanholtz C, Mendez-Tellez PA, Pronovost P, Brower R, Needham DM.** 2009. Mortality in sepsis versus non-sepsis induced acute lung injury. Crit Care **13:**R150.

197. **Sheu CC, Gong MN, Zhai R, Chen F, Bajwa EK, Clardy PF, Gallagher DC, Thompson BT, Christiani DC.** 2010. Clinical characteristics and outcomes of sepsis-related vs non-sepsis-related ARDS. Chest **138:**559-567.

198. **Brunkhorst FM, Eberhard OK, Brunkhorst R.** 1999. Discrimination of infectious and noninfectious causes of early acute respiratory distress syndrome by procalcitonin. Crit Care Med **27:**2172-2176.

199. **Budinger GR, Sznajder JI.** 2006. The alveolar-epithelial barrier: a target for potential therapy. Clin Chest Med **27:**655-669; abstract ix.

200. **Darwish I, Mubareka S, Liles WC.** 2011. Immunomodulatory therapy for severe influenza. Expert Rev Anti Infect Ther **9:**807-822.

201. **Narasaraju T, Ng HH, Phoon MC, Chow VT.** 2010. MCP-1 antibody treatment enhances damage and impedes repair of the alveolar epithelium in influenza pneumonitis. Am J Respir Cell Mol Biol **42:**732-743.

202. **Vlahos R, Stambas J, Bozinovski S, Broughton BR, Drummond GR, Selemidis S.** 2011. Inhibition of Nox2 oxidase activity ameliorates influenza A virus-induced lung inflammation. PLoS Pathog **7:**e1001271.

203. **Imai Y, Kuba K, Neely GG, Yaghubian-Malhami R, Perkmann T, van Loo G, Ermolaeva M, Veldhuizen R, Leung YH, Wang H, Liu H, Sun Y, Pasparakis M, Kopf M, Mech C, Bavari S, Peiris JS, Slutsky AS, Akira S, Hultqvist M, Holmdahl R, Nicholls J, Jiang C, Binder CJ, Penninger JM.** 2008. Identification of oxidative stress and Toll-like receptor 4 signaling as a key pathway of acute lung injury. Cell **133:**235-249.

204. **Zheng BJ, Chan KW, Lin YP, Zhao GY, Chan C, Zhang HJ, Chen HL, Wong SS, Lau SK, Woo PC, Chan KH, Jin DY, Yuen KY.** 2008. Delayed antiviral plus immunomodulator treatment still

reduces mortality in mice infected by high inoculum of influenza A/H5N1 virus. Proc Natl Acad Sci U S A **105:**8091-8096.

205. **Bellingan GJ.** 2002. The pulmonary physician in critical care * 6: The pathogenesis of ALI/ARDS. Thorax **57:**540-546.

206. **Hooper P, Selleck P.** 2003. Pathology of Low and High Virulent Influenza Virus Infections. Avian Diseases **47:**134-141.

207. **Brown CC, Olander HJ, Senne DA.** 1992. A pathogenesis study of highly pathogenic avian influenza virus H5N2 in chickens, using immunohistochemistry. J Comp Pathol **107:**341-348.

208. **Suarez DL, Perdue ML, Cox N, Rowe T, Bender C, Huang J, Swayne DE.** 1998. Comparisons of highly virulent H5N1 influenza A viruses isolated from humans and chickens from Hong Kong. J Virol **72:**6678-6688.

209. **Ito T, Kobayashi Y, Morita T, Horimoto T, Kawaoka Y.** 2002. Virulent influenza A viruses induce apoptosis in chickens. Virus Res **84:**27-35.

210. **Jones YL, Swayne DE.** 2004. Comparative pathobiology of low and high pathogenicity H7N3 Chilean avian influenza viruses in chickens. Avian Dis **48:**119-128.

211. **Nakatani H, Nakamura K, Yamamoto Y, Yamada M, Yamamoto Y.** 2005. Epidemiology, pathology, and immunohistochemistry of layer hens naturally affected with H5N1 highly pathogenic avian influenza in Japan. Avian Dis **49:**436-441.

212. **Muramoto Y, Ozaki H, Takada A, Park CH, Sunden Y, Umemura T, Kawaoka Y, Matsuda H, Kida H.** 2006. Highly pathogenic H5N1 influenza virus causes coagulopathy in chickens. Microbiol Immunol **50:**73-81.

213. **Swayne DE.** 2007. Understanding the complex pathobiology of high pathogenicity avian influenza viruses in birds. Avian Dis **51:**242-249.

214. **Nakamura K, Imada T, Imai K, Yamamoto Y, Tanimura N, Yamada M, Mase M, Tsukamoto K, Yamaguchi S.** 2008. Pathology of specific-pathogen-free chickens inoculated with H5N1 avian influenza viruses isolated in Japan in 2004. Avian Dis **52:**8-13.

215. **Wibawa H, Bingham J, Nuradji H, Lowther S, Payne J, Harper J, Wong F, Lunt R, Junaidi A, Middleton D, Meers J.** 2013. The pathobiology of two Indonesian H5N1 avian influenza viruses representing different clade 2.1 sublineages in chickens and ducks. Comp Immunol Microbiol Infect Dis **36:**175-191.

216. **van Riel D, van den Brand JM, Munster VJ, Besteboer TM, Fouchier RA, Osterhaus AD, Kuiken T.** 2009. Pathology and virus distribution in chickens naturally infected with highly pathogenic avian influenza A virus (H7N7) During the 2003 outbreak in The Netherlands. Vet Pathol **46:**971-976.

217. **Perkins LE, Swayne DE.** 2001. Pathobiology of A/chicken/Hong Kong/220/97 (H5N1) avian influenza virus in seven gallinaceous species. Vet Pathol **38:**149-164.

218. **Perkins LE, Swayne DE.** 2003. Comparative susceptibility of selected avian and mammalian species to a Hong Kong-origin H5N1 high-pathogenicity avian influenza virus. Avian Dis **47:**956-967.

219. **Lee CW, Suarez DL, Tumpey TM, Sung HW, Kwon YK, Lee YJ, Choi JG, Joh SJ, Kim MC, Lee EK, Park JM, Lu X, Katz JM, Spackman E, Swayne DE, Kim JH.** 2005. Characterization of highly pathogenic H5N1 avian influenza A viruses isolated from South Korea. J Virol **79:**3692-3702.

220. **Bertran K, Perez-Ramirez E, Busquets N, Dolz R, Ramis A, Darji A, Abad FX, Valle R, Chaves A, Vergara-Alert J, Barral M, Hofle U, Majo N.** 2011. Pathogenesis and transmissibility of highly (H7N1) and low (H7N9) pathogenic avian influenza virus infection in red-legged partridge (Alectoris rufa). Vet Res **42:**24.

221. **Bertran K, Dolz R, Busquets N, Gamino V, Vergara-Alert J, Chaves AJ, Ramis A, Abad FX, Hofle U, Majo N.** 2013. Pathobiology and transmission of highly and low pathogenic avian influenza viruses in European quail (Coturnix c. coturnix). Vet Res **44:**23.

222. **Feldmann A, Schafer MK, Garten W, Klenk HD.** 2000. Targeted infection of endothelial cells by avian influenza virus A/FPV/Rostock/34 (H7N1) in chicken embryos. J Virol **74:**8018-8027.

223. **Perkins LE, Swayne DE.** 2002. Pathogenicity of a Hong Kong-origin H5N1 highly pathogenic avian influenza virus for emus, geese, ducks, and pigeons. Avian Dis **46:**53-63.

224. **Suzuki K, Okada H, Itoh T, Tada T, Mase M, Nakamura K, Kubo M, Tsukamoto K.** 2009. Association of increased pathogenicity of Asian H5N1 highly pathogenic avian influenza viruses in chickens with highly efficient viral replication accompanied by early destruction of innate immune responses. J Virol **83:**7475-7486.

225. **Pantin-Jackwood MJ, Swayne DE.** 2009. Pathogenesis and pathobiology of avian influenza virus infection in birds. Rev Sci Tech **28:**113-136.

226. **Mutinelli F, Capua I, Terregino C, Cattoli G.** 2003. Clinical, gross, and microscopic findings in different avian species naturally infected during the H7N1 low- and high-pathogenicity avian influenza epidemics in Italy during 1999 and 2000. Avian Dis **47:**844-848.

227. **Webster RG, Bean WJ, Gorman OT, Chambers TM, Kawaoka Y.** 1992. Evolution and ecology of influenza A viruses. Microbiol Rev **56:**152-179.

228. **Becker WB.** 1966. The isolation and classification of Tern virus: influenza A-Tern South Africa--1961. J Hyg (Lond) **64:**309-320.

229. **Kwon YK, Joh SJ, Kim MC, Sung HW, Lee YJ, Choi JG, Lee EK, Kim JH.** 2005. Highly pathogenic avian influenza (H5N1) in the commercial domestic ducks of South Korea. Avian Pathol **34:**367-370.

230. **Pasick J, Berhane Y, Embury-Hyatt C, Copps J, Kehler H, Handel K, Babiuk S, Hooper-McGrevy K, Li Y, Mai Le Q, Lien Phuong S.** 2007. Susceptibility of Canada Geese (Branta canadensis) to highly pathogenic avian influenza virus (H5N1). Emerg Infect Dis **13:**1821-1827.

231. **Brojer C, Agren EO, Uhlhorn H, Bernodt K, Morner T, Jansson DS, Mattsson R, Zohari S, Thoren P, Berg M, Gavier-Widen D.** 2009. Pathology of natural highly pathogenic avian influenza H5N1 infection in wild tufted ducks (Aythya fuligula). J Vet Diagn Invest **21:**579-587.

232. **Daoust PY, Kibenge FS, Fouchier RA, van de Bildt MW, van Riel D, Kuiken T.** 2011. Replication of low pathogenic avian influenza virus in naturally infected Mallard ducks (Anas platyrhynchos) causes no morphologic lesions. J Wildl Dis **47:**401-409.

233. **Brown JD, Stallknecht DE, Swayne DE.** 2008. Experimental infection of swans and geese with highly pathogenic avian influenza virus (H5N1) of Asian lineage. Emerg Infect Dis **14:**136-142.

234. **Ellis TM, Bousfield RB, Bissett LA, Dyrting KC, Luk GS, Tsim ST, Sturm-Ramirez K, Webster RG, Guan Y, Malik Peiris JS.** 2004. Investigation of outbreaks of highly pathogenic H5N1 avian influenza in waterfowl and wild birds in Hong Kong in late 2002. Avian Pathol **33:**492-505.

235. **Teifke JP, Klopfleisch R, Globig A, Starick E, Hoffmann B, Wolf PU, Beer M, Mettenleiter TC, Harder TC.** 2007. Pathology of natural infections by H5N1 highly pathogenic avian influenza virus in mute (Cygnus olor) and whooper (Cygnus cygnus) swans. Vet Pathol **44:**137-143.

236. **Kalthoff D, Breithaupt A, Teifke JP, Globig A, Harder T, Mettenleiter TC, Beer M.** 2008. Highly pathogenic avian influenza virus (H5N1) in experimentally infected adult mute swans. Emerg Infect Dis **14:**1267-1270.

237. **Kwon YK, Thomas C, Swayne DE.** 2010. Variability in pathobiology of South Korean H5N1 high-pathogenicity avian influenza virus infection for 5 species of migratory waterfowl. Vet Pathol **47:**495-506.

238. **Neufeld JL, Embury-Hyatt C, Berhane Y, Manning L, Ganske S, Pasick J.** 2009. Pathology of highly pathogenic avian influenza virus (H5N1) infection in Canada geese (Branta canadensis): preliminary studies. Vet Pathol **46:**966-970.

239. **Yamamoto Y, Nakamura K, Kitagawa K, Ikenaga N, Yamada M, Mase M, Narita M.** 2007. Severe nonpurulent encephalitis with mortality and feather lesions in call ducks (Anas platyrhyncha var. domestica) inoculated intravenously with H5N1 highly pathogenic avian influenza virus. Avian Dis **51:**52-57.

240. **Zhou JY, Shen HG, Chen HX, Tong GZ, Liao M, Yang HC, Liu JX.** 2006. Characterization of a highly pathogenic H5N1 influenza virus derived from bar-headed geese in China. J Gen Virol **87:**1823-1833.

241. **Pantin-Jackwood MJ, Swayne DE.** 2007. Pathobiology of Asian highly pathogenic avian influenza H5N1 virus infections in ducks. Avian Dis **51:**250-259.

242. **Londt BZ, Nunez A, Banks J, Nili H, Johnson LK, Alexander DJ.** 2008. Pathogenesis of highly pathogenic avian influenza A/turkey/Turkey/1/2005 H5N1 in Pekin ducks (Anas platyrhynchos) infected experimentally. Avian Pathol **37:**619-627.

243. **Brown JD, Stallknecht DE, Beck JR, Suarez DL, Swayne DE.** 2006. Susceptibility of North American ducks and gulls to H5N1 highly pathogenic avian influenza viruses. Emerg Infect Dis **12:**1663-1670.

244. **Perkins LE, Swayne DE.** 2002. Susceptibility of laughing gulls (Larus atricilla) to H5N1 and H5N3 highly pathogenic avian influenza viruses. Avian Dis **46:**877-885.

245. **Ogiwara H, Yasui F, Munekata K, Takagi-Kamiya A, Munakata T, Nomura N, Shibasaki F, Kuwahara K, Sakaguchi N, Sakoda Y, Kida H, Kohara M.** 2014. Histopathological evaluation of the diversity of cells susceptible to H5N1 virulent avian influenza virus. Am J Pathol **184:**171-183.

246. **Wang S, Le TQ, Kurihara N, Chida J, Cisse Y, Yano M, Kido H.** 2010. Influenza virus-cytokine-protease cycle in the pathogenesis of vascular hyperpermeability in severe influenza. J Infect Dis **202:**991-1001.

247. **Babinska A, Kedees MH, Athar H, Ahmed T, Batuman O, Ehrlich YH, Hussain MM, Kornecki E.** 2002. F11-receptor (F11R/JAM) mediates platelet adhesion to endothelial cells: role in inflammatory thrombosis. Thromb Haemost **88:**843-850.

248. **Bunce PE, High SM, Nadjafi M, Stanley K, Liles WC, Christian MD.** 2011. Pandemic H1N1 influenza infection and vascular thrombosis. Clin Infect Dis **52:**e14-17.

249. **Rimmelzwaan GF, van Riel D, Baars M, Bestebroer TM, van Amerongen G, Fouchier RA, Osterhaus AD, Kuiken T.** 2006. Influenza A virus (H5N1) infection in cats causes systemic disease with potential novel routes of virus spread within and between hosts. Am J Pathol **168:**176-183; quiz 364.

250. **Desvaux S, Marx N, Ong S, Gaidet N, Hunt M, Manuguerra JC, Sorn S, Peiris M, Van der Werf S, Reynes JM.** 2009. Highly pathogenic avian influenza virus (H5N1) outbreak in captive wild birds and cats, Cambodia. Emerg Infect Dis **15:**475-478.

251. **Keawcharoen J, Oraveerakul K, Kuiken T, Fouchier RA, Amonsin A, Payungporn S, Noppornpanth S, Wattanodorn S, Theambooniers A, Tantilertcharoen R, Pattanarangsan R, Arya N, Ratanakorn P, Osterhaus DM, Poovorawan Y.** 2004. Avian influenza H5N1 in tigers and leopards. Emerg Infect Dis **10:**2189-2191.

252. **Kiss I, Gyarmati P, Zohari S, Ramsay KW, Metreveli G, Weiss E, Brytting M, Stivers M, Lindstrom S, Lundkvist A, Nemirov K, Thoren P, Berg M, Czifra G, Belak S.** 2008. Molecular characterization of highly pathogenic H5N1 avian influenza viruses isolated in Sweden in 2006. Virol J **5:**113.

253. **Klopfleisch R, Wolf PU, Uhl W, Gerst S, Harder T, Starick E, Vahlenkamp TW, Mettenleiter TC, Teifke JP.** 2007. Distribution of lesions and antigen of highly pathogenic avian influenza virus A/Swan/Germany/R65/06 (H5N1) in domestic cats after presumptive infection by wild birds. Vet Pathol **44:**261-268.

254. **Klopfleisch R, Wolf PU, Wolf C, Harder T, Starick E, Niebuhr M, Mettenleiter TC, Teifke JP.** 2007. Encephalitis in a stone marten (Martes foina) after natural infection with highly pathogenic avian influenza virus subtype H5N1. J Comp Pathol **137:**155-159.

255. **Leschnik M, Weikel J, Mostl K, Revilla-Fernandez S, Wodak E, Bago Z, Vanek E, Benetka V, Hess M, Thalhammer JG.** 2007. Subclinical infection with avian influenza A (H5N1) virus in cats. Emerg Infect Dis **13:**243-247.

256. **Mushtaq MH, Juan H, Jiang P, Li Y, Li T, Du Y, Mukhtar MM.** 2008. Complete genome analysis of a highly pathogenic H5N1 influenza A virus isolated from a tiger in China. Arch Virol **153:**1569-1574.

257. **ProMed-mail.** 2006. Avian influenza - worldwide (70): Asia, Europe [4] Sweden, mink: H5. http://www.promedmail.org/direct.php?id=20060328.0943. Accessed 16 January 2015.

258. **Qi X, Li X, Rider P, Fan W, Gu H, Xu L, Yang Y, Lu S, Wang H, Liu F.** 2009. Molecular characterization of highly pathogenic H5N1 avian influenza A viruses isolated from raccoon dogs in China. PLoS One **4:**e4682.

259. **Roberton SI, Bell DJ, Smith GJ, Nicholls JM, Chan KH, Nguyen DT, Tran PQ, Streicher U, Poon LL, Chen H, Horby P, Guardo M, Guan Y, Peiris JS.** 2006. Avian influenza H5N1 in viverrids: implications for wildlife health and conservation. Proc Biol Sci **273:**1729-1732.

260. **Songserm T, Amonsin A, Jam-on R, Sae-Heng N, Meemak N, Pariyothorn N, Payungporn S, Theamboonlers A, Poovorawan Y.** 2006. Avian influenza H5N1 in naturally infected domestic cat. Emerg Infect Dis **12:**681-683.

261. **Songserm T, Amonsin A, Jam-on R, Sae-Heng N, Pariyothorn N, Payungporn S, Theamboonlers A, Chutinimitkul S, Thanawongnuwech R, Poovorawan Y.** 2006. Fatal avian influenza A H5N1 in a dog. Emerg Infect Dis **12:**1744-1747.

262. **Thanawongnuwech R, Amonsin A, Tantilertcharoen R, Damrongwatanapokin S, Theamboonlers A, Payungporn S, Nanthapornphiphat K, Ratanamungklanon S, Tunak E, Songserm T, Vivatthanavanich V, Lekdumrongsak T, Kesdangsakonwut S, Tunhikorn S, Poovorawan Y.** 2005. Probable tiger-to-tiger transmission of avian influenza H5N1. Emerg Infect Dis **11:**699-701.

263. **Yingst SL, Saad MD, Felt SA.** 2006. Qinghai-like H5N1 from domestic cats, northern Iraq. Emerg Infect Dis **12:**1295-1297.

264. **Zohari S, Gyarmati P, Thoren P, Czifra G, Brojer C, Belak S, Berg M.** 2008. Genetic characterization of the NS gene indicates co-circulation of two sub-lineages of highly pathogenic avian influenza virus of H5N1 subtype in Northern Europe in 2006. Virus Genes **36:**117-125.

265. **Li H, Yu K, Yang H, Xin X, Chen J, Zhao P, Bi Y, Chen H.** 2004. Isolation and characterization of H5N1 and H9N2 influenza viruses from pigs in China. Chin J Prev Vet Med **26:**1-6.

266. **Zhou J, Sun W, Wang J, Guo J, Yin W, Wu N, Li L, Yan Y, Liao M, Huang Y, Luo K, Jiang X, Chen H.** 2009. Characterization of the H5N1 highly pathogenic avian influenza virus derived from wild pikas in China. J Virol **83:**8957-8964.

267. **Abdel-Moneim AS, Abdel-Ghany AE, Shany SA.** 2010. Isolation and characterization of highly pathogenic avian influenza virus subtype H5N1 from donkeys. J Biomed Sci **17:**25.

268. **El-Sayed A, Prince A, Fawzy A, Nadra E, Abdou MI, Omar L, Fayed A, Salem M.** 2013. Sero-prevalence of avian influenza in animals and human in Egypt. Pak J Biol Sci **16:**524-529.

269. **Shortridge KF, Gao P, Guan Y, Ito T, Kawaoka Y, Markwell D, Takada A, Webster RG.** 2000. Interspecies transmission of influenza viruses: H5N1 virus and a Hong Kong SAR perspective. Vet Microbiol **74:**141-147.

270. **Horimoto T, Maeda K, Murakami S, Kiso M, Iwatsuki-Horimoto K, Sashika M, Ito T, Suzuki K, Yokoyama M, Kawaoka Y.** 2011. Highly pathogenic avian influenza virus infection in feral raccoons, Japan. Emerg Infect Dis **17:**714-717.

271. **Gubareva LV, McCullers JA, Bethell RC, Webster RG.** 1998. Characterization of influenza A/HongKong/156/97 (H5N1) virus in a mouse model and protective effect of zanamivir on H5N1 infection in mice. J Infect Dis **178:**1592-1596.

272. **Lu X, Tumpey TM, Morken T, Zaki SR, Cox NJ, Katz JM.** 1999. A mouse model for the evaluation of pathogenesis and immunity to influenza A (H5N1) viruses isolated from humans. J Virol **73:**5903-5911.

273. **Maines TR, Lu XH, Erb SM, Edwards L, Guarner J, Greer PW, Nguyen DC, Szretter KJ, Chen LM, Thawatsupha P, Chittaganpitch M, Waicharoen S, Nguyen DT, Nguyen T, Nguyen HH, Kim JH, Hoang LT, Kang C, Phuong LS, Lim W, Zaki S, Donis RO, Cox NJ, Katz JM, Tumpey TM.** 2005. Avian influenza (H5N1) viruses isolated from humans in Asia in 2004 exhibit increased virulence in mammals. J Virol **79:**11788-11800.

274. **Shinya K, Makino A, Tanaka H, Hatta M, Watanabe T, Le MQ, Imai H, Kawaoka Y.** 2011. Systemic dissemination of H5N1 influenza A viruses in ferrets and hamsters after direct intragastric inoculation. J Virol **85:**4673-4678.

275. **Shortridge KF, Zhou NN, Guan Y, Gao P, Ito T, Kawaoka Y, Kodihalli S, Krauss S, Markwell D, Murti KG, Norwood M, Senne D, Sims L, Takada A, Webster RG.** 1998. Characterization of avian H5N1 influenza viruses from poultry in Hong Kong. Virology **252:**331-342.

276. **Govorkova EA, Rehg JE, Krauss S, Yen HL, Guan Y, Peiris M, Nguyen TD, Hanh TH, Puthavathana P, Long HT, Buranathai C, Lim W, Webster RG, Hoffmann E.** 2005. Lethality to ferrets of H5N1 influenza viruses isolated from humans and poultry in 2004. J Virol **79:**2191-2198.

277. **Zitzow LA, Rowe T, Morken T, Shieh WJ, Zaki S, Katz JM.** 2002. Pathogenesis of avian influenza A (H5N1) viruses in ferrets. J Virol **76:**4420-4429.

278. **Kuiken T, Rimmelzwaan GF, Van Amerongen G, Osterhaus AD.** 2003. Pathology of human influenza A (H5N1) virus infection in cynomolgus macaques (Macaca fascicularis). Vet Pathol **40:**304-310.

279. **Rimmelzwaan GF, Kuiken T, van Amerongen G, Bestebroer TM, Fouchier RA, Osterhaus AD.** 2001. Pathogenesis of influenza A (H5N1) virus infection in a primate model. J Virol **75:**6687-6691.

280. **Rimmelzwaan GF, Kuiken T, van Amerongen G, Bestebroer TM, Fouchier RA, Osterhaus AD.** 2003. A primate model to study the pathogenesis of influenza A (H5N1) virus infection. Avian Dis **47:**931-933.

281. **Reperant LA, van Amerongen G, van de Bildt MW, Rimmelzwaan GF, Dobson AP, Osterhaus AD, Kuiken T.** 2008. Highly pathogenic avian influenza virus (H5N1) infection in red foxes fed infected bird carcasses. Emerg Infect Dis **14:**1835-1841.

282. **Kalthoff D, Hoffmann B, Harder T, Durban M, Beer M.** 2008. Experimental infection of cattle with highly pathogenic avian influenza virus (H5N1). Emerg Infect Dis **14:**1132-1134.

283. **Amonsin A, Payungporn S, Theamboonlers A, Thanawongnuwech R, Suradhat S, Pariyothorn N, Tantilertcharoen R, Damrongwantanapokin S, Buranathai C, Chaisingh A, Songserm T, Poovorawan Y.** 2006. Genetic characterization of H5N1 influenza A viruses isolated from zoo tigers in Thailand. Virology **344:**480-491.

284. **Thornley M.** 2004. Avian influenza ravages Thai tigers. Aust Vet J **82:**652.

285. **Romvary J, Rozsa J, Farkas E.** 1975. Infection of dogs and cats with the Hong Kong influenza A (H3N2) virus during an epidemic period in Hungary. Acta Vet Acad Sci Hung **25:**255-259.

286. **Chang CP, New AE, Taylor JF, Chiang HS.** 1976. Influenza virus isolations from dogs during a human epidemic in Taiwan. Int J Zoonoses **3:**61-64.

287. **Nikitin A, Cohen D, Todd JD, Lief FS.** 1972. Epidemiological studies of A-Hong Kong-68 virus infection in dogs. Bull World Health Organ **47:**471-479.

288. **Paniker CK, Nair CM.** 1972. Experimental infection of animals with influenzavirus types A and B. Bull World Health Organ **47:**461-463.

289. **Song D, Moon HJ, An DJ, Jeoung HY, Kim H, Yeom MJ, Hong M, Nam JH, Park SJ, Park BK, Oh JS, Song M, Webster RG, Kim JK, Kang BK.** 2012. A novel reassortant canine H3N1 influenza virus between pandemic H1N1 and canine H3N2 influenza viruses in Korea. J Gen Virol **93:**551-554.

290. **Promed-mail.** 2009. Influenza pandemic (H1N1) 2009, animal (30): China, canine http://www.promedmail.org/direct.php?id=20091128.4079. Accessed 16 January 2015.

291. **Promed-mail.** 2009. Influenza pandemic (H1N1) 2009, animal (40): USA (NY) canine http://www.promedmail.org/direct.php?id=20091222.4305. Accessed 16 January 2015.

292. **Lin D, Sun S, Du L, Ma J, Fan L, Pu J, Sun Y, Zhao J, Sun H, Liu J.** 2012. Natural and experimental infection of dogs with pandemic H1N1/2009 influenza virus. J Gen Virol **93:**119-123.

293. **Zhan GJ, Ling ZS, Zhu YL, Jiang SJ, Xie ZJ.** 2012. Genetic characterization of a novel influenza A virus H5N2 isolated from a dog in China. Vet Microbiol **155:**409-416.

294. **Song QQ, Zhang FX, Liu JJ, Ling ZS, Zhu YL, Jiang SJ, Xie ZJ.** 2013. Dog to dog transmission of a novel influenza virus (H5N2) isolated from a canine. Vet Microbiol **161:**331-333.

295. **Hai-xia F, Yuan-yuan L, Qian-qian S, Zong-shuai L, Feng-xia Z, Yan-li Z, Shi-jin J, Zhi-jing X.** 2014. Interspecies transmission of canine influenza virus H5N2 to cats and chickens by close contact with experimentally infected dogs. Vet Microbiol **170:**414-417.

296. **Sun X, Xu X, Liu Q, Liang D, Li C, He Q, Jiang J, Cui Y, Li J, Zheng L, Guo J, Xiong Y, Yan J.** 2013. Evidence of avian-like H9N2 influenza A virus among dogs in Guangxi, China. Infect Genet Evol **20:**471-475.

297. **Moon H, Hong M, Kim JK, Seon B, Na W, Park SJ, An DJ, Jeoung HY, Kim DJ, Kim JM, Kim SH, Webby RJ, Webster RG, Kang BK, Song D.** 2014. H3N2 canine influenza virus with the matrix gene from the pandemic A/H1N1 virus: infection dynamics in dogs and ferrets. Epidemiol Infect doi:S0950268814001617 [pii] 10.1017/S0950268814001617**:**1-9.

298. **FAO.** 2006. Incursion of H5N1 'Asian lineage' virus into Europe: source of introduction? http://www.fao.org/avianflu/conferences/rome_avian/documents/I.Brown.pdf. Accessed 16 January 2015.

299. **Li D, Zhu L, Cui H, Ling S, Fan S, Yu Z, Zhou Y, Wang T, Qian J, Xia X, Xu Z, Gao Y, Wang C.** 2014. Influenza A(H1N1)pdm09 virus infection in giant pandas, China. Emerg Infect Dis **20:**480-483.

300. **Britton AP, Sojonky KR, Scouras AP, Bidulka JJ.** 2010. Pandemic (H1N1) 2009 in skunks, Canada. Emerg Infect Dis **16:**1043-1045.

301. **Schrenzel MD, Tucker TA, Stalis IH, Kagan RA, Burns RP, Denison AM, Drew CP, Paddock CD, Rideout BA.** 2011. Pandemic (H1N1) 2009 virus in 3 wildlife species, San Diego, California, USA. Emerg Infect Dis **17:**747-749.

302. **Klingeborn B, Englund L, Rott R, Juntti N, Rockborn G.** 1985. An avian influenza A virus killing a mammalian species--the mink. Brief report. Arch Virol **86:**347-351.

303. **Gagnon CA, Spearman G, Hamel A, Godson DL, Fortin A, Fontaine G, Tremblay D.** 2009. Characterization of a Canadian mink H3N2 influenza A virus isolate genetically related to triple reassortant swine influenza virus. J Clin Microbiol **47:**796-799.

304. **Larsen LE, Breum SØ, Trebbien R, Bradstad K, Nielsen LP, Chriél M, Jensen TH, Hjulsager CK, Handberg K, Jørgensen PH, Le Févre Harslund J, Rangstrup-Christensen L, Peterson B, Hammer AS.** Outbreaks of influenza A virus in farmed mink (Neovison vison) in Denmark: molecular characterization of the viruses, p 153-156. *In* Larsen PF, Møller SH, Clausen T,

Hammer AS, Lássen TM, Nielsen VH, Tauson AH, Jeppesen LL, Hansen SW, Elnif J, Malmkvist J (ed), Wageningen Academic Publishers,

305. **Chriél M, Jensen TH, Hjulsager C, Larsen LE, Jørgensen PH, Le Févre Harslund J, Rangstrup-Christensen L, Peterson B, Hammer AS.** Consequences of outbreaks of influenza A virus in farmed mink (Neovison vison) in Denmark in 2009 and 2010, p 186-189. *In* Larsen PF, Møller SH, Clausen T, Hammer AS, Lássen TM, Nielsen VH, Tauson AH, Jeppesen LL, Hansen SW, Elnif J, Malmkvist J (ed), Wageningen Academic Publishers,

306. **Yoon KJ, Schwartz K, Sun D, Zhang J, Hildebrandt H.** 2012. Naturally occurring Influenza A virus subtype H1N2 infection in a Midwest United States mink (Mustela vison) ranch. J Vet Diagn Invest **24:**388-391.

307. **Åkerstedt J, Valheim M, Germundsson A, Moldal T, Lie KI, Falk M, Hungnes O.** 2012. Pneumonia caused by influenza A H1N1 2009 virus in farmed American mink (Neovison vison). Vet Rec **170:**362.

308. **Kleyn van Willigen FC, Dijkman R.** Influenza on Dutch mink farms in 2011, p 180-185. *In* Larsen PF, Møller SH, Clausen T, Hammer AS, Lássen TM, Nielsen VH, Tauson AH, Jeppesen LL, Hansen SW, Elnif J, Malmkvist J (ed), Wageningen Academic Publishers,

309. **Fisher JW, Scott P.** 1944. An Epizootic of Influenza A in a Ferret Colony. Can J Public Health/ Revue Canadienne de Santé Publique **35:**364-366.

310. **Bell FR, Dudgeon JA.** 1948. An epizootic in influenza in a ferret colony. J Comp Pathol Ther **58:**167-171.

311. **Patterson AR, Cooper VL, Yoon KJ, Janke BH, Gauger PC.** 2009. Naturally occurring influenza infection in a ferret (Mustela putorius furo) colony. J Vet Diagn Invest **21:**527-530.

312. **ProMed-mail.** 2009. Influenza pandemic (H1N1) 2009, animal health (15): USA (OR) ferret. http://www.promedmail.org/direct.php?id=20091021.3618. Accessed 16 January 2015.

313. **ProMed-mail.** 2009. Influenza pandemic (H1N1) 2009, animal health (16): USA (NE) ferret http://www.promedmail.org/direct.php?id=20091101.3777. Accessed 16 January 2015.

314. **Promed-mail.** 2009. Influenza pandemic (H1N1) 2009, animal (26): USA (OR), ferret http://www.promedmail.org/direct.php?id=20091114.3936. Accessed 16 January 2015.

315. **Promed-mail.** 2009. Influenza pandemic (H1N1) 2009, animal (27): USA (OR) ferret. http://www.promedmail.org/direct.php?id=20091115.3947. Accessed 16 January 2015.

316. **van den Brand JM, Stittelaar KJ, van Amerongen G, Reperant L, de Waal L, Osterhaus AD, Kuiken T.** 2012. Comparison of temporal and spatial dynamics of seasonal H3N2, pandemic H1N1 and highly pathogenic avian influenza H5N1 virus infections in ferrets. PLoS One **7:**e42343.

317. **Lang G, Gagnon A, Geraci JR.** 1981. Isolation of an influenza A virus from seals. Arch Virol **68:**189-195.

318. **Webster RG, Hinshaw VS, Bean WJ, Van Wyke KL, Geraci JR, St Aubin DJ, Petursson G.** 1981. Characterization of an influenza A virus from seals. Virology **113:**712-724.

319. **Webster RG, Geraci J, Petursson G, Skirnisson K.** 1981. Conjunctivitis in human beings caused by influenza A virus of seals. N Engl J Med **304:**911.

320. **Hinshaw VS, Bean WJ, Webster RG, Rehg JE, Fiorelli P, Early G, Geraci JR, St Aubin DJ.** 1984. Are seals frequently infected with avian influenza viruses? J Virol **51:**863-865.

321. **Zohari S, Neimanis A, Harkonen T, Moraeus C, Valarcher J.** 2014. Avian influenza A(H10N7) virus involvement in mass mortality of harbour seals (Phoca vitulina) in Sweden, March through October 2014. Euro Surveill **19**.

322. **Bodewes R, Bestebroer TM, van der Vries E, Verhagen JH, Herfst S, Koopmans MP, Fouchier RAM, Pfankuche VM, Wohlsein P, Siebert U, Baumgärtner W, E. OADM.** 2015. Avian Influenza A (H10N7) Virus–Associated Mass Deaths among Harbor Seals. Emerg Infect Dis **21**.

323. **Krog JS, Hansen MS, Holm E, Hjulsager CK, Chriél M, Pedersen K, Andresen LO, Abildstrøm M, Jensen TH, Larsen LE.** 2015. Influenza A(H10N7) Virus in Dead Harbor Seals, Denmark. Emerg Infect Dis **21**.

324. **Bogomolni AL, Gast RJ, Ellis JC, Dennett M, Pugliares KR, Lentell BJ, Moore MJ.** 2008. Victims or vectors: a survey of marine vertebrate zoonoses from coastal waters of the Northwest Atlantic. Dis Aquat Organ **81:**13-38.

325. **Goldstein T, Mena I, Anthony SJ, Medina R, Robinson PW, Greig DJ, Costa DP, Lipkin WI, Garcia-Sastre A, Boyce WM.** 2013. Pandemic H1N1 influenza isolated from free-ranging Northern Elephant Seals in 2010 off the central California coast. PLoS One **8:**e62259.

326. **OIE.** 2012. Update on highly pathogenic Avian Influenza in animals (Type H5 and H7). http://www.oie.int/animal-health-in-the-world/update-on-avian-influenza/2012/. Accessed 16 January 2015.

327. **ProMed-mail.** 2004. Avian influenza H5N1, mammals - East Asia. http://www.promedmail.org/direct.php?id=20040221.0560. Accessed 16 January 2015.

328. **ProMed-mail.** 2006. Avian influenza (140) - Indonesia (cat). http://www.promedmail.org/direct.php?id=20060620.1700. Accessed 16 January 2015.

329. **Sponseller BA, Strait E, Jergens A, Trujillo J, Harmon K, Koster L, Jenkins-Moore M, Killian M, Swenson S, Bender H, Waller K, Miles K, Pearce T, Yoon KJ, Nara P.** 2010. Influenza A pandemic (H1N1) 2009 virus infection in domestic cat. Emerg Infect Dis **16:**534-537.

330. **Löhr CV, DeBess EE, Baker RJ, Hiett SL, Hoffman KA, Murdoch VJ, Fischer KA, Mulrooney DM, Selman RL, Hammill-Black WM.** 2010. Pathology and viral antigen distribution of lethal pneumonia in domestic cats due to pandemic (H1N1) 2009 influenza A virus. Vet Pathol **47:**378-386.

331. **Fiorentini L, Taddei R, Moreno A, Gelmetti D, Barbieri I, De Marco MA, Tosi G, Cordioli P, Massi P.** 2011. Influenza A pandemic (H1N1) 2009 virus outbreak in a cat colony in Italy. Zoonoses Public Health **58:**573-581.

332. **Song DS, An DJ, Moon HJ, Yeom MJ, Jeong HY, Jeong WS, Park SJ, Kim HK, Han SY, Oh JS, Park BK, Kim JK, Poo H, Webster RG, Jung K, Kang BK.** 2011. Interspecies transmission of the canine influenza H3N2 virus to domestic cats in South Korea, 2010. J Gen Virol **92:**2350-2355.

333. **Jeoung HY, Lim SI, Shin BH, Lim JA, Song JY, Song DS, Kang BK, Moon HJ, An DJ.** 2013. A novel canine influenza H3N2 virus isolated from cats in an animal shelter. Vet Microbiol **165:**281-286.

334. **Crossley B, Hietala S, Hunt T, Benjamin G, Martinez M, Darnell D, Rubrum A, Webby R.** 2012. Pandemic (H1N1) 2009 in captive cheetah. Emerg Infect Dis **18:**315-317.

335. **Weber S, Harder T, Starick E, Beer M, Werner O, Hoffmann B, Mettenleiter TC, Mundt E.** 2007. Molecular analysis of highly pathogenic avian influenza virus of subtype H5N1 isolated from wild birds and mammals in northern Germany. J Gen Virol **88:**554-558.

336. **Starick E, Beer M, Hoffmann B, Staubach C, Werner O, Globig A, Strebelow G, Grund C, Durban M, Conraths FJ, Mettenleiter T, Harder T.** 2008. Phylogenetic analyses of highly pathogenic avian influenza virus isolates from Germany in 2006 and 2007 suggest at least three separate introductions of H5N1 virus. Vet Microbiol **128:**243-252.

337. **Kuiken T, Rimmelzwaan G, van Riel D, van Amerongen G, Baars M, Fouchier R, Osterhaus A.** 2004. Avian H5N1 influenza in cats. Science **306:**241.

338. **Vahlenkamp TW, Harder TC, Giese M, Lin F, Teifke JP, Klopfleisch R, Hoffmann R, Tarpey I, Beer M, Mettenleiter TC.** 2008. Protection of cats against lethal influenza H5N1 challenge infection. J Gen Virol **89:**968-974.

339. **Romvary J, Takatsy G, Barb K, Farkas E.** 1962. Isolation of influenza virus strains from animals. Nature **193:**907-908.

340. **Lopez JW, Woods GT.** 1984. Influenza virus in ruminants: a review. Res Commun Chem Pathol Pharmacol **45:**445-462.

341. **Campbell CH, Easterday BC, Webster RG.** 1977. Strains of Hong Kong influenza virus in calves. J Infect Dis **135:**678-680.

342. **Yamnikova SS, Mandler J, Bekh-Ochir ZH, Dachtzeren P, Ludwig S, Lvov DK, Scholtissek C.** 1993. A reassortant H1N1 influenza A virus caused fatal epizootics among camels in Mongolia. Virology **197:**558-563.

343. **Yondon M, Zayat B, Nelson MI, Heil GL, Anderson BD, Lin X, Halpin RA, McKenzie PP, White SK, Wentworth DE, Gray GC.** 2014. Equine influenza A(H3N8) virus isolated from Bactrian camel, Mongolia. Emerg Infect Dis **20:**2144-2147.

344. **Lvov DK, Zdanov VM, Sazonov AA, Braude NA, Vladimirtceva EA, Agafonova LV, Skljanskaja EI, Kaverin NV, Reznik VI, Pysina TV, Oserovic AM, Berzin AA, Mjasnikova IA, Podcernjaeva RY, Klimenko SM, Andrejev VP, Yakhno MA.** 1978. Comparison of influenza viruses isolated from man and from whales. Bull World Health Organ **56:**923-930.

345. **Van Campen H, Early G.** 2001. Orthomyxovirus and Paramyxovirus Infections, p 271-273. *In* Williams ES, Barker IK (ed), Infectious diseases of wild animals, Third edition ed. Iowa State University Press Ames, USA.

346. **Hinshaw VS, Bean WJ, Geraci J, Fiorelli P, Early G, Webster RG.** 1986. Characterization of two influenza A viruses from a pilot whale. J Virol **58:**655-656.

347. **Groth M, Lange J, Kanrai P, Pleschka S, Scholtissek C, Krumbholz A, Platzer M, Sauerbrei A, Zell R.** 2014. The genome of an influenza virus from a pilot whale: relation to influenza viruses of gulls and marine mammals. Infect Genet Evol **24:**183-186.

348. **Butler D.** 2006. Thai dogs carry bird-flu virus, but will they spread it? Nature **439:**773.

349. **ProMed-mail.** 2007. Avian influenza (17): Indonesia (feline), Japan, Hungary http://www.promedmail.org/direct.php?id=20070126.0347. Accessed 16 January 2015.

350. **Marschall J, Schulz B, Harder Priv-Doz TC, Vahlenkamp Priv-Doz TW, Huebner J, Huisinga E, Hartmann K.** 2008. Prevalence of influenza A H5N1 virus in cats from areas with occurrence of highly pathogenic avian influenza in birds. J Feline Med Surg **10:**355-358.

351. **Paltrinieri S, Spagnolo V, Giordano A, Martin AM, Luppi A.** 2007. Influenza virus type A serosurvey in cats. Emerg Infect Dis **13:**662-664.

352. **Kuiken T, Fouchier R, Rimmelzwaan G, Osterhaus A, Roeder P.** 2006. Feline friend or potential foe? Nature **440:**741-742.

353. **Thiry E, Addie D, Belak S, Boucraut-Baralon C, Egberink H, Frymus T, Gruffydd-Jones T, Hartmann K, Hosie MJ, Lloret A, Lutz H, Marsilio F, Pennisi MG, Radford AD, Truyen U, Horzinek MC.** 2009. H5N1 avian influenza in cats. ABCD guidelines on prevention and management. J Feline Med Surg **11:**615-618.

354. **Maas R, Tacken M, Ruuls L, Koch G, van Rooij E, Stockhofe-Zurwieden N.** 2007. Avian influenza (H5N1) susceptibility and receptors in dogs. Emerg Infect Dis **13:**1219-1221.

355. **Chen Y, Zhong G, Wang G, Deng G, Li Y, Shi J, Zhang Z, Guan Y, Jiang Y, Bu Z, Kawaoka Y, Chen H.** 2010. Dogs are highly susceptible to H5N1 avian influenza virus. Virology **405:**15-19.

356. **Qin Q, Wei F, Li M, Dubovi EJ, Loeffler IK.** 2007. Serosurvey of infectious disease agents of carnivores in captive red pandas (Ailurus fulgens) in China. J Zoo Wildl Med **38:**42-50.

357. **Cha SY, Seo HS, Kang M, Jang HK.** 2013. Serologic survey for antibodies to canine parvovirus and influenza virus in wild raccoon dogs (Nyctereutes procyonoides) in South Korea. J Wildl Dis **49:**200-202.

358. **ProMed-mail.** 2005. Avian influenza - Asia (12): Viet Nam, civets, H5N1 http://www.promedmail.org/direct.php?id=20050826.2527. Accessed 16 January 2015.

359. **Chen H, Smith GJ, Zhang SY, Qin K, Wang J, Li KS, Webster RG, Peiris JS, Guan Y.** 2005. Avian flu: H5N1 virus outbreak in migratory waterfowl. Nature **436:**191-192.

360. **Liu J, Xiao H, Lei F, Zhu Q, Qin K, Zhang XW, Zhang XL, Zhao D, Wang G, Feng Y, Ma J, Liu W, Wang J, Gao GF.** 2005. Highly pathogenic H5N1 influenza virus infection in migratory birds. Science **309:**1206.

361. **Daly JM, Blunden AS, Macrae S, Miller J, Bowman SJ, Kolodziejek J, Nowotny N, Smith KC.** 2008. Transmission of equine influenza virus to English foxhounds. Emerg Infect Dis **14:**461-464.

362. **Crawford PC, Dubovi EJ, Castleman WL, Stephenson I, Gibbs EP, Chen L, Smith C, Hill RC, Ferro P, Pompey J, Bright RA, Medina MJ, Johnson CM, Olsen CW, Cox NJ, Klimov AI, Katz JM, Donis RO.** 2005. Transmission of equine influenza virus to dogs. Science **310:**482-485.

363. **Song D, Kang B, Lee C, Jung K, Ha G, Kang D, Park S, Park B, Oh J.** 2008. Transmission of avian influenza virus (H3N2) to dogs. Emerg Infect Dis **14:**741-746.

364. **Li S, Shi Z, Jiao P, Zhang G, Zhong Z, Tian W, Long LP, Cai Z, Zhu X, Liao M, Wan XF.** 2010. Avian-origin H3N2 canine influenza A viruses in Southern China. Infect Genet Evol **10:**1286-1288.

365. **Bunpapong N, Nonthabenjawan N, Chaiwong S, Tangwangvivat R, Boonyapisitsopa S, Jairak W, Tuanudom R, Prakairungnamthip D, Suradhat S, Thanawongnuwech R, Amonsin A.** 2014. Genetic characterization of canine influenza A virus (H3N2) in Thailand. Virus Genes **48:**56-63.

366. **Ado AD, Titova SM.** 1959. [Studies on experimental influenza in dogs] Izuchenie eksperimental'nogo grippa u sobak. Vopr Virusol **4:**165-169.

367. **Fyson RE, Westwood JC, Brunner AH.** 1975. An immunoprecipitin study of the incidence of influenza A antibodies in animal sera in the Ottawa area. Can J Microbiol **21:**1089-1101.

368. **Kilbourne ED, Kehoe JM.** 1975. Demonstration of antibodies to both hemagglutinin and neuraminidase antigens of H3N2 influenza A virus in domestic dogs. Intervirology **6:**315-318.

369. **Houser RE, Heuschele WP.** 1980. Evidence of prior infection with influenza A/Texas/77 (H3N2(virus in dogs with clinical parainfluenza. Can J Comp Med **44:**396-402.

370. **Todd JD, Cohen D.** 1968. Studies of influenza in dogs. I. Susceptibility of dogs to natural and experimental infection with human A2 and B strains of influenza virus. Am J Epidemiol **87:**426-439.

371. **Bao L, Xu L, Zhan L, Deng W, Zhu H, Gao H, Sun H, Ma C, Lv Q, Li F, Chen H, Zhang L, Qin C.** 2010. Challenge and polymorphism analysis of the novel A (H1N1) influenza virus to normal animals. Virus Res **151:**60-65.

372. **Zhang K, Zhang Z, Yu Z, Li L, Cheng K, Wang T, Huang G, Yang S, Zhao Y, Feng N.** 2013. Domestic cats and dogs are susceptible to H9N2 avian influenza virus. Virus research **175:**52-57.

373. **Amirsalehy H, Nili H, Mohammadi A.** 2012. Can dogs carry the global pandemic candidate avian influenza virus H9N2? Aust Vet J **90:**341-345.

374. **Vahlenkamp TW, Greene CE, Hartmann K.** 2012. Influenza Virus Infections, p 202-209. *In* Greene CE (ed), Infectious Diseases of the Dog and Cat Fourth Edition ed. Saunders, St. Louis, USA.

375. **Madic J, Huber D, Lugovic B.** 1993. Serologic survey for selected viral and rickettsial agents of brown bears (Ursus arctos) in Croatia. J Wildl Dis **29:**572-576.

376. **Harding LE, Smith FA.** 2009. Mustela or Vison? Evidence for the taxonomic status of the American mink and a distinct biogeographic radiation of American weasels. Mol Phylogenet Evol **52:**632-642.

377. **Okazaki K, Yanagawa R, Kida H, Noda H.** 1983. Human influenza virus infection in mink: serological evidence of infection in summer and autumn. Vet Microbiol **8:**251-257.

378. **Onta T, Kida H, Kawano J, Matsuoka Y, Yanagawa R.** 1978. Distribution of antibodies against various influenza A viruses in animals. Nihon Juigaku Zasshi **40:**451-454.

379. **Matsuura Y, Yanagawa R, Noda H.** 1979. Experimental infection of mink with influenza A viruses. Brief report. Arch Virol **62:**71-76.

380. **Okazaki K, Yanagawa R, Kida H.** 1983. Contact infection of mink with 5 subtypes of avian influenza virus. Brief report. Arch Virol **77:**265-269.

381. **Yagyu K, Yanagawa R, Matsuura Y, Noda H.** 1981. Contact infection of mink with influenza A viruses of avian and mammalian origin. Arch Virol **68:**143-145.

382. **Englund L.** 2000. Studies on influenza viruses H10N4 and H10N7 of avian origin in mink. Vet Microbiol **74:**101-107.

383. **Englund L, Hård af Segerstad C.** 1998. Two avian H10 influenza A virus strains with different pathogenicity for mink (Mustela vison). Arch Virol **143:**653-666.

384. **Zohari S, Metreveli G, Kiss I, Belak S, Berg M.** 2010. Full genome comparison and characterization of avian H10 viruses with different pathogenicity in Mink (Mustela vison) reveals genetic and functional differences in the non-structural gene. Virol J **7:**145.

385. **Smith W, Andrewes CH, Laidlaw PP.** 1933. A virus obtained from influenza patients. Lancet **222:**66-68.

386. **Shope RE.** 1934. The Infection of Ferrets with Swine Influenza Virus. J Exp Med **60:**49-61.

387. **Smith W, Stuart-Harris CH.** 1936. Influenza infection of man from the ferret. Lancet **228:**121-123.

388. **Stuart-Harris CH, Francis T.** 1938. Studies on the Nasal Histology of Epidemic Influenza Virus Infection in the Ferret : Ii. The Resistance of Regenerating Respiratory Epithelium to Reinfection and to Physicochemical Injury. J Exp Med **68:**803-812.

389. **Andrewes CH, Glover RE.** 1941. Spread of infection from the respiratory tract of the ferret. I. Transmission of influenza A virus. Br J Exp Pathol **22:**91.

390. **Baras B, de Waal L, Stittelaar KJ, Jacob V, Giannini S, Veldhuis Kroeze EJ, van den Brand JM, van Amerongen G, Simon JH, Hanon E, Mossman SP, Osterhaus AD.** 2011. Pandemic H1N1 vaccine requires the use of an adjuvant to protect against challenge in naive ferrets. Vaccine **29:**2120-2126.

391. **Basarab O, Smith H.** 1969. Quantitative studies on the tissue localization of influenza virus in ferrets after intranasal and intravenous or intracardial inoculation. Br J Exp Pathol **50:**612-618.

392. **Dimmock NJ, Dove BK, Scott PD, Meng B, Taylor I, Cheung L, Hallis B, Marriott AC, Carroll MW, Easton AJ.** 2012. Cloned defective interfering influenza virus protects ferrets from pandemic 2009 influenza A virus and allows protective immunity to be established. PLoS One **7:**e49394.

393. **Hinshaw VS, Webster RG, Easterday BC, Bean WJ, Jr.** 1981. Replication of avian influenza A viruses in mammals. Infect Immun **34:**354-361.

394. **Huang SS, Banner D, Fang Y, Ng DC, Kanagasabai T, Kelvin DJ, Kelvin AA.** 2011. Comparative analyses of pandemic H1N1 and seasonal H1N1, H3N2, and influenza B infections depict distinct clinical pictures in ferrets. PLoS One **6:**e27512.

395. **Itoh Y, Shinya K, Kiso M, Watanabe T, Sakoda Y, Hatta M, Muramoto Y, Tamura D, Sakai-Tagawa Y, Noda T, Sakabe S, Imai M, Hatta Y, Watanabe S, Li C, Yamada S, Fujii K, Murakami S, Imai H, Kakugawa S, Ito M, Takano R, Iwatsuki-Horimoto K, Shimojima M, Horimoto T, Goto H, Takahashi K, Makino A, Ishigaki H, Nakayama M, Okamatsu M, Takahashi K, Warshauer D, Shult PA, Saito R, Suzuki H, Furuta Y, Yamashita M, Mitamura K, Nakano K, Nakamura M, Brockman-Schneider R, Mitamura H, Yamazaki M, Sugaya N, Suresh M, Ozawa M, Neumann G, Gern J, Kida H, et al.** 2009. In vitro and in vivo characterization of new swine-origin H1N1 influenza viruses. Nature **460:**1021-1025.

396. **Jackson S, Van Hoeven N, Chen LM, Maines TR, Cox NJ, Katz JM, Donis RO.** 2009. Reassortment between avian H5N1 and human H3N2 influenza viruses in ferrets: a public health risk assessment. J Virol **83:**8131-8140.

397. **Kimble JB, Angel M, Wan H, Sutton TC, Finch C, Perez DR.** 2014. Alternative reassortment events leading to transmissible H9N1 influenza viruses in the ferret model. J Virol **88:**66-71.

398. **Kreijtz JH, Veldhuis Kroeze EJ, Stittelaar KJ, de Waal L, van Amerongen G, van Trierum S, van Run P, Bestebroer T, Kuiken T, Fouchier RA, Rimmelzwaan GF, Osterhaus AD.** 2013. Low pathogenic avian influenza A(H7N9) virus causes high mortality in ferrets upon intratracheal challenge: a model to study intervention strategies. Vaccine **31:**4995-4999.

399. **Smith JH, Nagy T, Driskell E, Brooks P, Tompkins SM, Tripp RA.** 2011. Comparative pathology in ferrets infected with H1N1 influenza A viruses isolated from different hosts. J Virol **85:**7572-7581.

400. **Toms GL, Sweet C, Smith H.** 1977. Behaviour in ferrets of swine influenza virus isolated from man. Lancet **1:**68-71.

401. **Li ZN, Ip HS, Trost JF, White CL, Murray MJ, Carney PJ, Sun XJ, Stevens J, Levine MZ, Katz JM.** 2014. Serologic evidence of influenza A(H1N1)pdm09 virus infection in northern sea otters. Emerg Infect Dis **20:**915-917.

402. **Hall JS, Bentler KT, Landolt G, Elmore SA, Minnis RB, Campbell TA, Barras SC, Root JJ, Pilon J, Pabilonia K, Driscoll C, Slate D, Sullivan H, McLean RG.** 2008. Influenza infection in wild raccoons. Emerg Infect Dis **14:**1842-1848.

403. **Root JJ, Bentler KT, Shriner SA, Mooers NL, VanDalen KK, Sullivan HJ, Franklin AB.** 2014. Ecological routes of avian influenza virus transmission to a common mesopredator: an experimental evaluation of alternatives. PLoS One **9:**e102964.

404. **Murphy BR, Harper J, Sly DL, London WT, Miller NT, Webster RG.** 1983. Evaluation of the A/Seal/Mass/1/80 virus in squirrel monkeys. Infect Immun **42:**424-426.

405. **Czudai-Matwich V, Otte A, Matrosovich M, Gabriel G, Klenk HD.** 2014. PB2 mutations D701N and S714R promote adaptation of an influenza H5N1 virus to a mammalian host. J Virol **88:**8735-8742.

406. **Salomon R, Franks J, Govorkova EA, Ilyushina NA, Yen HL, Hulse-Post DJ, Humberd J, Trichet M, Rehg JE, Webby RJ, Webster RG, Hoffmann E.** 2006. The polymerase complex genes contribute to the high virulence of the human H5N1 influenza virus isolate A/Vietnam/1203/04. J Exp Med **203:**689-697.

407. **Ohishi K, Kishida N, Ninomiya A, Kida H, Takada Y, Miyazaki N, Boltunov AN, Maruyama T.** 2004. Antibodies to human-related H3 influenza A virus in Baikal seals (Phoca sibirica) and ringed seals (Phoca hispida) in Russia. Microbiol Immunol **48:**905-909.

408. **Ohishi K, Ninomiya A, Kida H, Park CH, Maruyama T, Arai T, Katsumata E, Tobayama T, Boltunov AN, Khuraskin LS, Miyazaki N.** 2002. Serological evidence of transmission of human influenza A and B viruses to Caspian seals (Phoca caspica). Microbiol Immunol **46:**639-644.

409. **Stuen S, Have P, Osterhaus AD, Arnemo JM, Moustgaard A.** 1994. Serological investigation of virus infections in harp seals (Phoca groenlandica) and hooded seals (Cystophora cristata). Vet Rec **134:**502-503.

410. **Fujii K, Kakumoto C, Kobayashi M, Saito S, Kariya T, Watanabe Y, Sakoda Y, Kida H, Suzuki M.** 2007. Serological evidence of influenza A virus infection in Kuril harbor seals (Phoca vitulina stejnegeri) of Hokkaido, Japan. J Vet Med Sci **69:**259-263.

411. **Danner GR, McGregor MW, Zarnke RL, Olsen CW.** 1998. Serologic evidence of influenza virus infection in a ringed seal (Phoca hispida) from Alaska. Marine mammal science **14:**380-384.

412. **Nielsen O, Clavijo A, Boughen JA.** 2001. Serologic evidence of influenza A infection in marine mammals of arctic Canada. J Wildl Dis **37:**820-825.

413. **de Boer GF, Back W, Osterhaus AD.** 1990. An ELISA for detection of antibodies against influenza A nucleoprotein in humans and various animal species. Arch Virol **115:**47-61.

414. **Blanc A, Ruchansky D, Clara M, Achaval F, Le Bas A, Arbiza J.** 2009. Serologic evidence of influenza A and B viruses in South American fur seals (Arctocephalus australis). J Wildl Dis **45:**519-521.

415. **Calle PP, Seagars DJ, McClave C, Senne D, House C, House JA.** 2002. Viral and bacterial serology of free-ranging Pacific walrus. J Wildl Dis **38:**93-100.

416. **Ohishi K, Maruyama T, Ninomiya A, Kida H, Zenitani R, Bando T, Fujise Y, Nakamatsu K, Miyazaki N, Boltunov AN.** 2006. Serologic investigation of Influenza A virus infection in cetaceans from the Western North Pacific and the Southern Oceans. Marine mammal science **22:**214-221.

417. **Ramis AJ, van Riel D, van de Bildt MW, Osterhaus A, Kuiken T.** 2012. Influenza A and B virus attachment to respiratory tract in marine mammals. Emerg Infect Dis **18:**817-820.

418. **Harder TC, Vahlenkamp TW.** 2010. Influenza virus infections in dogs and cats. Vet Immunol Immunopathol **134:**54-60.

419. **Paniker CK, Nair CM.** 1970. Infection with A2 Hong Kong influenza virus in domestic cats. Bull World Health Organ **43:**859-862.

420. **Campagnolo ER, Rankin JT, Daverio SA, Hunt EA, Lute JR, Tewari D, Acland HM, Ostrowski SR, Moll ME, Urdaneta VV, Ostroff SM.** 2011. Fatal pandemic (H1N1) 2009 influenza A virus infection in a Pennsylvania domestic cat. Zoonoses Public Health **58:**500-507.

421. **Pigott AM, Haak CE, Breshears MA, Linklater AK.** 2014. Acute bronchointerstitial pneumonia in two indoor cats exposed to the H1N1 influenza virus. J Vet Emerg Crit Care (San Antonio) doi:10.1111/vec.12179.

422. **ProMed-mail.** 2009. Influenza pandemic (H1N1) 2009, animal (21): USA (IA) feline http://www.promedmail.org/direct.php?id=20091105.3816. Accessed 16 January 2015.

423. **Promed-mail.** 2009. Influenza pandemic (H1N1) 2009, animal (28): USA (UT, OR) feline http://www.promedmail.org/direct.php?id=20091121.4008 Accessed 16 January 2015.

424. **Promed-mail.** 2009. Influenza pandemic (H1N1) 2009, animal (37): USA (OR, CA) feline http://www.promedmail.org/direct.php?id=20091211.4213. Accessed 16 January 2015.

425. **LeFigaro.** 2009. H1N1: un chat contaminé en France, *on* Le Figaro, Société du Figaro. http://www.lefigaro.fr/flash-actu/2009/12/08/01011-20091208FILWWW00424-h1n1-un-chat-contamine-en-france.php. Accessed 16 January 2015.

426. **van den Brand JM, Stittelaar KJ, van Amerongen G, van de Bildt MW, Leijten LM, Kuiken T, Osterhaus AD.** 2010. Experimental pandemic (H1N1) 2009 virus infection of cats. Emerg Infect Dis **16:**1745-1747.

427. **Ali A, Daniels JB, Zhang Y, Rodriguez-Palacios A, Hayes-Ozello K, Mathes L, Lee CW.** 2011. Pandemic and seasonal human influenza virus infections in domestic cats: prevalence, association with respiratory disease, and seasonality patterns. J Clin Microbiol **49:**4101-4105.

428. **McCullers JA, Van De Velde LA, Schultz RD, Mitchell CG, Halford CR, Boyd KL, Schultz-Cherry S.** 2011. Seroprevalence of seasonal and pandemic influenza A viruses in domestic cats. Arch Virol **156:**117-120.

429. **Su S, Yuan L, Li H, Chen J, Xie J, Huang Z, Jia K, Li S.** 2013. Serologic evidence of pandemic influenza virus H1N1 2009 infection in cats in China. Clin Vaccine Immunol **20:**115-117.

430. **Damiani AM, Kalthoff D, Beer M, Muller E, Osterrieder N.** 2012. Serological survey in dogs and cats for influenza A(H1N1)pdm09 in Germany. Zoonoses Public Health **59:**549-552.

431. **Gordy JT, Jones CA, Rue J, Crawford PC, Levy JK, Stallknecht DE, Tripp RA, Tompkins SM.** 2012. Surveillance of feral cats for influenza A virus in north central Florida. Influenza Other Respir Viruses **6:**341-347.

432. **Zhao FR, Liu CG, Yin X, Zhou DH, Wei P, Chang HY.** 2014. Serological report of pandemic (H1N1) 2009 infection among cats in northeastern China in 2012-02 and 2013-03. Virol J **11:**49.

433. **Naidenko SV, Pavlova EV, Kirilyuk VE.** 2014. Detection of seasonal weight loss and a serologic survey of potential pathogens in wild Pallas' cats (Felis [Otocolobus] manul) of the Daurian Steppe, Russia. J Wildl Dis **50:**188-194.

434. **Ehrengut W, Sarateanu DE, Rutter G.** 1980. Influenza A antibodies in cervine animals. Infection **8:**66-69.

435. **Ehrengut W, Sarateanu DE, Rutter G.** 1979. [Influenza A antibodies in deer and elk] Influenza-A-Antikorper bei Rehen und Hirschen. Dtsch Med Wochenschr **104:**1112.

436. **Graves IL, Pyakural S, Sousa VO.** 1974. Susceptibility of a yak to influenza A viruses and presence of H3N2 antibodies in animals in Nepal and India. Bull World Health Organ **51:**173-177.

437. **MacPherson L, Zbitnew A, Ditchfield WJB.** 1963. A Study of the incidence of neutralising antibodies in animal sera to the viruses of the influenza and Para-Influenza groups. Can J Publ Hlth **54:**51.

438. **Rivera H, Madewell BR, Ameghino E.** 1987. Serologic survey of viral antibodies in the Peruvian alpaca (Lama pacos). Am J Vet Res **48:**189-191.

439. **McQueen JL, Davenport FM.** 1963. Experimental influenza in sheep. Proc Soc Exp Biol Med **112:**1004-1006.

440. **Meenan PN, Boyd MR.** 1962. Effect of an influenza epidemic on a city population The Lancet **279:**96-98.

441. **Meenan PN, Boyd MR, Mullaney R.** 1962. Human Influenza Viruses in Domesticated Animals. Br Med J **2:**86-89.

442. **Sousa VO, Graves IL, Pyakural S.** 1974. Spread of influenzaviruses A/ENGLAND/42/72 AND A/Hong Kong/1/68. Bull World Health Organ **50:**475-478.

443. **Brown IH, Crawshaw TR, Harris PA, Alexander DJ.** 1998. Detection of antibodies to influenza A virus in cattle in association with respiratory disease and reduced milk yield. Vet Rec **143:**637-638.

444. **Crawshaw TR, Brown IH, Essen SC, Young SC.** 2008. Significant rising antibody titres to influenza A are associated with an acute reduction in milk yield in cattle. Vet J **178:**98-102.

445. **Graham DA, Calvert V, McLaren E.** 2002. Retrospective analysis of serum and nasal mucus from cattle in Northern Ireland for evidence of infection with influenza A virus. Vet Rec **150:**201-204.

446. **Gunning RF, Brown IH, Crawshaw TR.** 1999. Evidence of influenza A virus infection in dairy cows with sporadic milk drop syndrome. Vet Rec **145:**556-557.

447. **Anchlan D, Ludwig S, Nymadawa P, Mendsaikhan J, Scholtissek C.** 1996. Previous H1N1 influenza A viruses circulating in the Mongolian population. Arch Virol **141:**1553-1569.

448. **ProMed-mail.** 2009. Influenza pandemic (H1N1) 2009, animal (25): domestic, Hajj http://www.promedmail.org/direct.php?id=20091110.3889. Accessed 16 January 2015.

449. **Intisar KS, Ali YH, Khalafalla AI, Rahman ME, Amin AS.** 2010. Respiratory infection of camels associated with parainfluenza virus 3 in Sudan. J Virol Methods **163:**82-86.

450. **Barbieri ES, Rodriguez DV, Marin RE, Setti W, Romero S, Barrandeguy M, Parreno V.** 2014. [Serological survey of antibodies against viral diseases of public health interest in llamas (Lama glama) from Jujuy province, Argentina] Relevamiento serologico de anticuerpos

contra enfermedades virales de interes sanitario en llamas (Lama glama) de la provincia de Jujuy, Argentina. Rev Argent Microbiol **46:**53-57.

451. **Marcoppido G, Parreno V, Vila B.** 2010. Antibodies to pathogenic livestock viruses in a wild vicuna (Vicugna vicugna) population in the Argentinean Andean altiplano. J Wildl Dis **46:**608-614.

452. **Haynes TB, Campbell MA, Neilson JL, López JA.** 2013. Molecular identification of seabird remains found in humpback whale feces. Marine Ornithology **41:**161-166.

453. **Slijper EJ.** 1958. Walvissen. D. B. Centen, Amsterdam, The Netherlands.

454. **Johnsen DO, Wooding WL, Tanticharoenyos P, Karnjanaprakorn C.** 1971. An epizootic of A2/Hong Kong/68 influenza in gibbons. J Infect Dis **123:**365-370.

455. **Malherbe H, Strickland-Cholmley M, Smith GC.** 1975. Letter: Isolation of myxovirus-like agent from baboons. Lancet **2:**41-42.

456. **Karlsson EA, Engel GA, Feeroz MM, San S, Rompis A, Lee BP, Shaw E, Oh G, Schillaci MA, Grant R, Heidrich J, Schultz-Cherry S, Jones-Engel L.** 2012. Influenza virus infection in nonhuman primates. Emerg Infect Dis **18:**1672-1675.

457. **L'Vov D K, Easterday B, Hinshow W, Dandurov Iu V, Arkhipov PN.** 1979. [Isolation of strains of the Hong Kong complex (H3N2) influenza virus from Nyctalus noctula bats in Kazakhstan] Vydelenie shtammov virusa grippa gongongskogo kompleksa (H3N2) ot letuchikh myshei Nyctalus noctula v Kazakhstane. Vopr Virusol**:**338-341.

458. **Isaeva EI, Belkina TS, Rovnova ZI, Kosiakov PN, Selivanov Ia M.** 1982. [Antigenic determinants of human influenza viruses among the influenza viruses isolated from animals] Antigennye determinanty virusov grippa cheloveka v sostave grippoznykh virusov, vydelennykh ot zhivotnykh. Vopr Virusol **27:**681-686.

459. **Dochez AR, Shibley GS, Mills KC.** 1930. Studies in the Common Cold : Iv. Experimental Transmission of the Common Cold to Anthropoid Apes and Human Beings by Means of a Filtrable Agent. J Exp Med **52:**701-716.

460. **Long PH, Bliss EA, Carpenter HM.** 1931. Etiology of Influenza. Transmission experiments in chimpanzees with filtered material derived from human influenza. J Am Med Assoc **97:**1122-1127.

461. **Kalter SS, Heberling RL, Vice TE, Lief FS, Rodriguez AR.** 1969. Influenza (A2-Hong Kong-68) in the baboon (Papio sp.). Proc Soc Exp Biol Med **132:**357-361.

462. **Berendt RF, Hall WC.** 1977. Reaction of squirrel monkeys to intratracheal inoculation with influenza/A/New Jersey/76 (swine) virus. Infect Immun **16:**476-479.

463. **Murphy BR, Hinshaw VS, Sly DL, London WT, Hosier NT, Wood FT, Webster RG, Chanock RM.** 1982. Virulence of avian influenza A viruses for squirrel monkeys. Infect Immun **37:**1119-1126.

464. **Scott GH, Stephen EL, Berendt RF.** 1978. Activity of amantadine, rimantadine, and ribavirin against swine influenza in mice and squirrel monkeys. Antimicrob Agents Chemother **13:**284-288.

465. **Snyder MH, Stephenson EH, Young H, York CG, Tierney EL, London WT, Chanock RM, Murphy BR.** 1986. Infectivity and antigenicity of live avian-human influenza A reassortant virus: comparison of intranasal and aerosol routes in squirrel monkeys. J Infect Dis **154:**709-711.

466. **Snyder MH, Buckler-White AJ, London WT, Tierney EL, Murphy BR.** 1987. The avian influenza virus nucleoprotein gene and a specific constellation of avian and human virus polymerase genes each specify attenuation of avian-human influenza A/Pintail/79 reassortant viruses for monkeys. J Virol **61:**2857-2863.

467. **Stephen EL, Walker JS, Dominik JW, Young HW, Berendt RF.** 1977. Aerosol therapy of influenza infections of mice and primates with rimantadine, ribavirin, and related compounds. Ann N Y Acad Sci **284:**264-271.

468. **Treanor JJ, Snyder MH, London WT, Murphy BR.** 1989. The B allele of the NS gene of avian influenza viruses, but not the A allele, attenuates a human influenza A virus for squirrel monkeys. Virology **171:**1-9.

469. **Berendt RF.** 1974. Simian model for the evaluation of immunity to influenza. Infect Immun **9:**101-105.

470. **Baskin CR, Garcia-Sastre A, Tumpey TM, Bielefeldt-Ohmann H, Carter VS, Nistal-Villan E, Katze MG.** 2004. Integration of clinical data, pathology, and cDNA microarrays in influenza virus-infected pigtailed macaques (Macaca nemestrina). J Virol **78:**10420-10432.

471. **Brown JN, Palermo RE, Baskin CR, Gritsenko M, Sabourin PJ, Long JP, Sabourin CL, Bielefeldt-Ohmann H, Garcia-Sastre A, Albrecht R, Tumpey TM, Jacobs JM, Smith RD, Katze MG.** 2010. Macaque proteome response to highly pathogenic avian influenza and 1918 reassortant influenza virus infections. J Virol **84:**12058-12068.

472. **Go JT, Belisle SE, Tchitchek N, Tumpey TM, Ma W, Richt JA, Safronetz D, Feldmann H, Katze MG.** 2012. 2009 pandemic H1N1 influenza virus elicits similar clinical course but differential host transcriptional response in mouse, macaque, and swine infection models. BMC Genomics **13:**627.

473. **Herfst S, van den Brand JM, Schrauwen EJ, de Wit E, Munster VJ, van Amerongen G, Linster M, Zaaraoui F, van Ijcken WF, Rimmelzwaan GF, Osterhaus AD, Fouchier RA, Andeweg AC, Kuiken T.** 2010. Pandemic 2009 H1N1 influenza virus causes diffuse alveolar damage in cynomolgus macaques. Vet Pathol **47:**1040-1047.

474. **Jegaskanda S, Weinfurter JT, Friedrich TC, Kent SJ.** 2013. Antibody-dependent cellular cytotoxicity is associated with control of pandemic H1N1 influenza virus infection of macaques. J Virol **87:**5512-5522.

475. **Josset L, Engelmann F, Haberthur K, Kelly S, Park B, Kawoaka Y, Garcia-Sastre A, Katze MG, Messaoudi I.** 2012. Increased viral loads and exacerbated innate host responses in aged macaques infected with the 2009 pandemic H1N1 influenza A virus. J Virol **86:**11115-11127.

476. **Marois P, Boudreault A, DiFranco E, Pavilanis V.** 1971. Response of ferrets and monkeys to intranasal infection with human, equine and avian influenza viruses. Can J Comp Med **35:**71-76.

477. **Watanabe T, Shinya K, Watanabe S, Imai M, Hatta M, Li C, Wolter BF, Neumann G, Hanson A, Ozawa M, Yamada S, Imai H, Sakabe S, Takano R, Iwatsuki-Horimoto K, Kiso M, Ito M, Fukuyama S, Kawakami E, Gorai T, Simmons HA, Schenkman D, Brunner K, Capuano SV, 3rd, Weinfurter JT, Nishio W, Maniwa Y, Igarashi T, Makino A, Travanty EA, Wang J, Kilander A, Dudman SG, Suresh M, Mason RJ, Hungnes O, Friedrich TC, Kawaoka Y.** 2011. Avian-type receptor-binding ability can increase influenza virus pathogenicity in macaques. J Virol **85:**13195-13203.

478. **Zhang K, Xu W, Zhang Z, Wang T, Sang X, Cheng K, Yu Z, Zheng X, Wang H, Zhao Y, Huang G, Yang S, Qin C, Gao Y, Xia X.** 2013. Experimental infection of non-human primates with avian influenza virus (H9N2). Arch Virol **158:**2127-2134.

479. **Olsen B, Munster VJ, Wallensten A, Waldenstrom J, Osterhaus AD, Fouchier RA.** 2006. Global patterns of influenza a virus in wild birds. Science **312:**384-388.

480. **Kalter SS, Ratner J, Kalter GV, Rodriguez AR, Kim CS.** 1967. A survey of primate sera for antibodies to viruses of human and simian origin. Am J Epidemiol **86:**552-568.

481. **Buitendijk H, Fagrouch Z, Niphuis H, Bogers WM, Warren KS, Verschoor EJ.** 2014. Retrospective serology study of respiratory virus infections in captive great apes. Viruses **6:**1442-1453.

482. **Atoynatan T, Hsiung GD.** 1969. Epidemiologic studies of latent virus infections in captive monkeys and baboons. II. Serologic evidence of myxovirus infections with special reference to SV5. Am J Epidemiol **89:**472-479.

483. **Jones-Engel L, Engel GA, Schillaci MA, Babo R, Froehlich J.** 2001. Detection of antibodies to selected human pathogens among wild and pet macaques (Macaca tonkeana) in Sulawesi, Indonesia. Am J Primatol **54:**171-178.

484. **Fereidouni S, Kwasnitschka L, Balkema Buschmann A, Muller T, Freuling C, Schatz J, Pikula J, Bandouchova H, Hoffmann R, Ohlendorf B, Kerth G, Tong S, Donis R, Beer M, Harder T.** 2014. No Virological Evidence for an Influenza A - like Virus in European Bats. Zoonoses Public Health doi:10.1111/zph.12131.

485. **Li Q, Sun X, Li Z, Liu Y, Vavricka CJ, Qi J, Gao GF.** 2012. Structural and functional characterization of neuraminidase-like molecule N10 derived from bat influenza A virus. Proc Natl Acad Sci U S A **109:**18897-18902.

486. **Sun X, Shi Y, Lu X, He J, Gao F, Yan J, Qi J, Gao GF.** 2013. Bat-derived influenza hemagglutinin H17 does not bind canonical avian or human receptors and most likely uses a unique entry mechanism. Cell Rep **3:**769-778.

487. **Tefsen B, Lu G, Zhu Y, Haywood J, Zhao L, Deng T, Qi J, Gao GF.** 2014. The N-terminal domain of PA from bat-derived influenza-like virus H17N10 has endonuclease activity. J Virol **88:**1935-1941.

488. **Calisher CH, Childs JE, Field HE, Holmes KV, Schountz T.** 2006. Bats: important reservoir hosts of emerging viruses. Clin Microbiol Rev **19:**531-545.

489. **Kohl C, Kurth A.** 2014. European bats as carriers of viruses with zoonotic potential. Viruses **6:**3110-3128.

490. **Drexler JF, Corman VM, Muller MA, Maganga GD, Vallo P, Binger T, Gloza-Rausch F, Cottontail VM, Rasche A, Yordanov S, Seebens A, Knornschild M, Oppong S, Adu Sarkodie Y, Pongombo C, Lukashev AN, Schmidt-Chanasit J, Stocker A, Carneiro AJ, Erbar S, Maisner A, Fronhoffs F, Buettner R, Kalko EK, Kruppa T, Franke CR, Kallies R, Yandoko ER, Herrler G, Reusken C, Hassanin A, Kruger DH, Matthee S, Ulrich RG, Leroy EM, Drosten C.** 2012. Bats host major mammalian paramyxoviruses. Nat Commun **3:**796.

491. **Drexler JF, Seelen A, Corman VM, Fumie Tateno A, Cottontail V, Melim Zerbinati R, Gloza-Rausch F, Klose SM, Adu-Sarkodie Y, Oppong SK, Kalko EK, Osterman A, Rasche A, Adam A, Muller MA, Ulrich RG, Leroy EM, Lukashev AN, Drosten C.** 2012. Bats worldwide carry hepatitis E virus-related viruses that form a putative novel genus within the family Hepeviridae. J Virol **86:**9134-9147.

492. **Wilson DE, Reeder DMe.** 2005. Mammal Species of the World: a taxonomic and geographic reference. 3rd ed. , vol 2 Vols. The Johns Hopkins University Press, Baltimore.

493. **Shriner SA, VanDalen KK, Mooers NL, Ellis JW, Sullivan HJ, Root JJ, Pelzel AM, Franklin AB.** 2012. Low-pathogenic avian influenza viruses in wild house mice. PLoS One **7:**e39206.

494. **Nofs S, Abd-Eldaim M, Thomas KV, Toplon D, Rouse D, Kennedy M.** 2009. Influenza virus A (H1N1) in giant anteaters (Myrmecophaga tridactyla). Emerg Infect Dis **15:**1081-1083.

495. **Davis LM, Spackman E.** 2008. Do crocodilians get the flu? Looking for influenza A in captive crocodilians. J Exp Zool A Ecol Genet Physiol **309:**571-580.

496. **Mancini DA, Mendonca RM, Cianciarullo AM, Kobashi LS, Trindade HG, Fernandes W, Pinto JR.** 2004. [Influenza in heterothermic animals] Influenza em animais heterotermicos. Rev Soc Bras Med Trop **37:**204-209.

497. **Herfst S, Chutinimitkul S, Ye J, de Wit E, Munster VJ, Schrauwen EJ, Bestebroer TM, Jonges M, Meijer A, Koopmans M, Rimmelzwaan GF, Osterhaus AD, Perez DR, Fouchier RA.** 2010. Introduction of virulence markers in PB2 of pandemic swine-origin influenza virus does not result in enhanced virulence or transmission. J Virol **84:**3752-3758.

498. **Munster VJ, de Wit E, van Riel D, Beyer WE, Rimmelzwaan GF, Osterhaus AD, Kuiken T, Fouchier RA.** 2007. The molecular basis of the pathogenicity of the Dutch highly pathogenic human influenza A H7N7 viruses. J Infect Dis **196:**258-265.

499. **de Wit E, Munster VJ, Spronken MI, Bestebroer TM, Baas C, Beyer WE, Rimmelzwaan GF, Osterhaus AD, Fouchier RA.** 2005. Protection of mice against lethal infection with highly pathogenic H7N7 influenza A virus by using a recombinant low-pathogenicity vaccine strain. J Virol **79:**12401-12407.

500. **Bodewes R, Kreijtz JH, Baas C, Geelhoed-Mieras MM, de Mutsert G, van Amerongen G, van den Brand JM, Fouchier RA, Osterhaus AD, Rimmelzwaan GF.** 2009. Vaccination against human influenza A/H3N2 virus prevents the induction of heterosubtypic immunity against lethal infection with avian influenza A/H5N1 virus. PLoS One **4:**e5538.

501. **Kreijtz JH, Suezer Y, de Mutsert G, van Amerongen G, Schwantes A, van den Brand JM, Fouchier RA, Lower J, Osterhaus AD, Sutter G, Rimmelzwaan GF.** 2009. MVA-based H5N1 vaccine affords cross-clade protection in mice against influenza A/H5N1 viruses at low doses and after single immunization. PLoS One **4:**e7790.

502. **Kreijtz JH, Bodewes R, van den Brand JM, de Mutsert G, Baas C, van Amerongen G, Fouchier RA, Osterhaus AD, Rimmelzwaan GF.** 2009. Infection of mice with a human influenza A/H3N2 virus induces protective immunity against lethal infection with influenza A/H5N1 virus. Vaccine **27:**4983-4989.

503. **Kreijtz JH, Suezer Y, van Amerongen G, de Mutsert G, Schnierle BS, Wood JM, Kuiken T, Fouchier RA, Lower J, Osterhaus AD, Sutter G, Rimmelzwaan GF.** 2007. Recombinant modified vaccinia virus Ankara-based vaccine induces protective immunity in mice against infection with influenza virus H5N1. J Infect Dis **195:**1598-1606.

504. **Kreijtz JH, Bodewes R, van Amerongen G, Kuiken T, Fouchier RA, Osterhaus AD, Rimmelzwaan GF.** 2007. Primary influenza A virus infection induces cross-protective immunity against a lethal infection with a heterosubtypic virus strain in mice. Vaccine **25:**612-620.

505. **Bodewes R, Kreijtz JH, van Amerongen G, Geelhoed-Mieras MM, Verburgh RJ, Heldens JG, Bedwell J, van den Brand JM, Kuiken T, van Baalen CA, Fouchier RA, Osterhaus AD, Rimmelzwaan GF.** 2010. A single immunization with CoVaccine HT-adjuvanted H5N1 influenza virus vaccine induces protective cellular and humoral immune responses in ferrets. J Virol **84:**7943-7952.

506. **van den Brand JM, Stittelaar KJ, van Amerongen G, Rimmelzwaan GF, Simon J, de Wit E, Munster V, Bestebroer T, Fouchier RA, Kuiken T, Osterhaus AD.** 2010. Severity of pneumonia due to new H1N1 influenza virus in ferrets is intermediate between that due to seasonal H1N1 virus and highly pathogenic avian influenza H5N1 virus. J Infect Dis **201:**993-999.

507. **Friesen RH, Koudstaal W, Koldijk MH, Weverling GJ, Brakenhoff JP, Lenting PJ, Stittelaar KJ, Osterhaus AD, Kompier R, Goudsmit J.** 2010. New class of monoclonal antibodies against severe influenza: prophylactic and therapeutic efficacy in ferrets. PLoS One **5:**e9106.

508. **Munster VJ, de Wit E, van den Brand JM, Herfst S, Schrauwen EJ, Bestebroer TM, van de Vijver D, Boucher CA, Koopmans M, Rimmelzwaan GF, Kuiken T, Osterhaus AD, Fouchier RA.** 2009. Pathogenesis and transmission of swine-origin 2009 A(H1N1) influenza virus in ferrets. Science **325:**481-483.

509. **Kreijtz JH, Suezer Y, de Mutsert G, van den Brand JM, van Amerongen G, Schnierle BS, Kuiken T, Fouchier RA, Lower J, Osterhaus AD, Sutter G, Rimmelzwaan GF.** 2009. Preclinical evaluation of a modified vaccinia virus Ankara (MVA)-based vaccine against influenza A/H5N1 viruses. Vaccine **27:**6296-6299.

510. **Kreijtz JH, Suezer Y, de Mutsert G, van den Brand JM, van Amerongen G, Schnierle BS, Kuiken T, Fouchier RA, Lower J, Osterhaus AD, Sutter G, Rimmelzwaan GF.** 2009. Recombinant modified vaccinia virus Ankara expressing the hemagglutinin gene confers protection against homologous and heterologous H5N1 influenza virus infections in macaques. J Infect Dis **199:**405-413.

511. **Stittelaar KJ, Tisdale M, van Amerongen G, van Lavieren RF, Pistoor F, Simon J, Osterhaus AD.** 2008. Evaluation of intravenous zanamivir against experimental influenza A (H5N1) virus infection in cynomolgus macaques. Antiviral Res **80:**225-228.

512. **Rimmelzwaan GF, Baars M, van Amerongen G, van Beek R, Osterhaus AD.** 2001. A single dose of an ISCOM influenza vaccine induces long-lasting protective immunity against homologous challenge infection but fails to protect Cynomolgus macaques against distant drift variants of influenza A (H3N2) viruses. Vaccine **20:**158-163.

513. **Rimmelzwaan GF, Baars M, van Beek R, van Amerongen G, Lovgren-Bengtsson K, Claas EC, Osterhaus AD.** 1997. Induction of protective immunity against influenza virus in a macaque model: comparison of conventional and iscom vaccines. J Gen Virol **78 (Pt 4):**757-765.

514. **Lowen AC, Mubareka S, Tumpey TM, Garcia-Sastre A, Palese P.** 2006. The guinea pig as a transmission model for human influenza viruses. Proc Natl Acad Sci U S A **103:**9988-9992.

515. **Kwon YK, Lipatov AS, Swayne DE.** 2009. Bronchointerstitial pneumonia in guinea pigs following inoculation with H5N1 high pathogenicity avian influenza virus. Vet Pathol **46:**138-141.

516. **Tang X, Chong KT.** 2009. Histopathology and growth kinetics of influenza viruses (H1N1 and H3N2) in the upper and lower airways of guinea pigs. J Gen Virol **90:**386-391.

517. **Mubareka S, Lowen AC, Steel J, Coates AL, Garcia-Sastre A, Palese P.** 2009. Transmission of influenza virus via aerosols and fomites in the guinea pig model. J Infect Dis **199:**858-865.

518. **Lowen AC, Steel J, Mubareka S, Carnero E, Garcia-Sastre A, Palese P.** 2009. Blocking interhost transmission of influenza virus by vaccination in the guinea pig model. J Virol **83:**2803-2818.

519. **Van Hoeven N, Belser JA, Szretter KJ, Zeng H, Staeheli P, Swayne DE, Katz JM, Tumpey TM.** 2009. Pathogenesis of 1918 pandemic and H5N1 influenza virus infections in a guinea pig model: antiviral potential of exogenous alpha interferon to reduce virus shedding. J Virol **83:**2851-2861.

520. **Steel J, Lowen AC, Mubareka S, Palese P.** 2009. Transmission of influenza virus in a mammalian host is increased by PB2 amino acids 627K or 627E/701N. PLoS Pathog **5:**e1000252.

521. **Lowen AC, Mubareka S, Steel J, Palese P.** 2007. Influenza virus transmission is dependent on relative humidity and temperature. PLoS Pathog **3:**1470-1476.

522. **Ottolini MG, Blanco JC, Eichelberger MC, Porter DD, Pletneva L, Richardson JY, Prince GA.** 2005. The cotton rat provides a useful small-animal model for the study of influenza virus pathogenesis. J Gen Virol **86:**2823-2830.

523. **Lange E, Kalthoff D, Blohm U, Teifke JP, Breithaupt A, Maresch C, Starick E, Fereidouni S, Hoffmann B, Mettenleiter TC, Beer M, Vahlenkamp TW.** 2009. Pathogenesis and transmission of the novel swine-origin influenza virus A/H1N1 after experimental infection of pigs. J Gen Virol **90:**2119-2123.

524. **Lipatov AS, Kwon YK, Sarmento LV, Lager KM, Spackman E, Suarez DL, Swayne DE.** 2008. Domestic pigs have low susceptibility to H5N1 highly pathogenic avian influenza viruses. PLoS Pathog **4:**e1000102.

525. **Seo SH, Webby R, Webster RG.** 2004. No apoptotic deaths and different levels of inductions of inflammatory cytokines in alveolar macrophages infected with influenza viruses. Virology **329:**270-279.

526. **Murphy BR, Park EJ, Gottlieb P, Subbarao K.** 1997. An influenza A live attenuated reassortant virus possessing three temperature-sensitive mutations in the PB2 polymerase gene rapidly loses temperature sensitivity following replication in hamsters. Vaccine **15:**1372-1378.

527. **Munster VJ, Schrauwen EJ, de Wit E, van den Brand JM, Bestebroer TM, Herfst S, Rimmelzwaan GF, Osterhaus AD, Fouchier RA.** 2010. Insertion of a multibasic cleavage motif into the hemagglutinin of a low-pathogenic avian influenza H6N1 virus induces a highly pathogenic phenotype. J Virol **84:**7953-7960.

528. **Rimmelzwaan GF, Claas EC, van Amerongen G, de Jong JC, Osterhaus AD.** 1999. ISCOM vaccine induced protection against a lethal challenge with a human H5N1 influenza virus. Vaccine **17:**1355-1358.

529. **Latorre-Margalef N, Gunnarsson G, Munster VJ, Fouchier RA, Osterhaus AD, Elmberg J, Olsen B, Wallensten A, Haemig PD, Fransson T, Brudin L, Waldenstrom J.** 2009. Effects of influenza A virus infection on migrating mallard ducks. Proc Biol Sci **276:**1029-1036.

530. **Keawcharoen J, van Riel D, van Amerongen G, Bestebroer T, Beyer WE, van Lavieren R, Osterhaus AD, Fouchier RA, Kuiken T.** 2008. Wild ducks as long-distance vectors of highly pathogenic avian influenza virus (H5N1). Emerg Infect Dis **14:**600-607.

531. **Rowe T, Leon AJ, Crevar CJ, Carter DM, Xu L, Ran L, Fang Y, Cameron CM, Cameron MJ, Banner D, Ng DC, Ran R, Weirback HK, Wiley CA, Kelvin DJ, Ross TM.** 2010. Modeling host responses in ferrets during A/California/07/2009 influenza infection. Virology **401:**257-265.

532. **Porter HG, Porter DD, Larsen AE.** 1982. Aleutian disease in ferrets. Infect Immun **36:**379-386.

533. **Philippa J, Baas C, Beyer W, Bestebroer T, Fouchier R, Smith D, Schaftenaar W, Osterhaus A.** 2007. Vaccination against highly pathogenic avian influenza H5N1 virus in zoos using an adjuvanted inactivated H5N2 vaccine. Vaccine **25:**3800-3808.

534. **Seo SH, Peiris M, Webster RG.** 2002. Protective cross-reactive cellular immunity to lethal A/Goose/Guangdong/1/96-like H5N1 influenza virus is correlated with the proportion of pulmonary CD8(+) T cells expressing gamma interferon. J Virol **76:**4886-4890.

535. **Rimmelzwaan GF, Baars M, Claas EC, Osterhaus AD.** 1998. Comparison of RNA hybridization, hemagglutination assay, titration of infectious virus and immunofluorescence as methods for monitoring influenza virus replication in vitro. J Virol Methods **74:**57-66.

536. **Kärber G.** 1931. Beitrag zur kollektiven Behandlung pharmakologischer Reihenversuche. Naunyn-Schmiedebergs Archiv für experimentelle pathologie und pharmakologie **162:**480-483.

537. **Reed LJ, Muench H.** 1938. A simple method of estimating fifty per cent endpoints. Am J Epidemiol **27:**493-497.

538. **de Wit E, Spronken MI, Bestebroer TM, Rimmelzwaan GF, Osterhaus AD, Fouchier RA.** 2004. Efficient generation and growth of influenza virus A/PR/8/34 from eight cDNA fragments. Virus Res **103:**155-161.

539. **Bodewes R, Rimmelzwaan GF, Osterhaus AD.** 2010. Animal models for the preclinical evaluation of candidate influenza vaccines. Expert Rev Vaccines **9:**59-72.

540. **Wiersma LC, Kreijtz JH, Vogelzang-van Trierum SE, van Amerongen G, van Run P, Ladwig M, Banneke S, Schaefer H, Fouchier RA, Kuiken T, Osterhaus AD, Rimmelzwaan GF.** 2015. Virus replication kinetics and pathogenesis of infection with H7N9 influenza virus in isogenic guinea pigs upon intratracheal inoculation. Vaccine doi:S0264-410X(15)01177-9 [pii] 10.1016/j.vaccine.2015.08.050.

541. **Wiersma LC, Vogelzang-van Trierum SE, van Amerongen G, van Run P, Nieuwkoop NJ, Ladwig M, Banneke S, Schaefer H, Kuiken T, Fouchier RA, Osterhaus AD, Rimmelzwaan GF.** 2015. Pathogenesis of infection with 2009 pandemic H1N1 influenza virus in isogenic guinea pigs after intranasal or intratracheal inoculation. Am J Pathol **185:**643-650.

542. **Liu D, Shi W, Shi Y, Wang D, Xiao H, Li W, Bi Y, Wu Y, Li X, Yan J, Liu W, Zhao G, Yang W, Wang Y, Ma J, Shu Y, Lei F, Gao GF.** 2013. Origin and diversity of novel avian influenza A H7N9 viruses causing human infection: phylogenetic, structural, and coalescent analyses. Lancet **381:**1926-1932.

543. **Koopmans M, de Jong MD.** 2013. Avian influenza A H7N9 in Zhejiang, China. Lancet **381:**1882-1883.

544. **Jonges M, Meijer A, Fouchier RA, Koch G, Li J, Pan JC, Chen H, Shu YL, Koopmans MP.** 2013. Guiding outbreak management by the use of influenza A(H7Nx) virus sequence analysis. Euro Surveill **18:**20460.

545. **Li Q, Zhou L, Zhou M, Chen Z, Li F, Wu H, Xiang N, Chen E, Tang F, Wang D, Meng L, Hong Z, Tu W, Cao Y, Li L, Ding F, Liu B, Wang M, Xie R, Gao R, Li X, Bai T, Zou S, He J, Hu J, Xu Y, Chai C, Wang S, Gao Y, Jin L, Zhang Y, Luo H, Yu H, He J, Li Q, Wang X, Gao L, Pang X, Liu G, Yan Y, Yuan H, Shu Y, Yang W, Wang Y, Wu F, Uyeki TM, Feng Z.** 2014. Epidemiology of human infections with avian influenza A(H7N9) virus in China. N Engl J Med **370:**520-532.

546. **Arima Y, Zu R, Murhekar M, Vong S, Shimada T.** 2013. Author Response: Human infections with avian influenza A(H7N9): preliminary assessments of the age and sex distribution. Western Pac Surveill Response J **4:**24-25.

547. **Skowronski DM, Janjua NZ, Kwindt TL, De Serres G.** 2013. Virus-host interactions and the unusual age and sex distribution of human cases of influenza A(H7N9) in China, April 2013. Euro Surveill **18:**20465.

548. **WHO.** 2013. Number of confirmed human cases of avian influenza A(H7N9) reported to WHO (2013) http://www.who.int/influenza/human_animal_interface/influenza_h7n9/06_ReportWebH7N9Number.pdf Accessed 18 May 2013.

549. **Bodewes R, Kreijtz JH, van Amerongen G, Fouchier RA, Osterhaus AD, Rimmelzwaan GF, Kuiken T.** 2011. Pathogenesis of Influenza A/H5N1 virus infection in ferrets differs between intranasal and intratracheal routes of inoculation. Am J Pathol **179:**30-36.

550. **van den Brand JM, Kreijtz JH, Bodewes R, Stittelaar KJ, van Amerongen G, Kuiken T, Simon J, Fouchier RA, Del Giudice G, Rappuoli R, Rimmelzwaan GF, Osterhaus AD.** 2011. Efficacy of vaccination with different combinations of MF59-adjuvanted and nonadjuvanted seasonal and pandemic influenza vaccines against pandemic H1N1 (2009) influenza virus infection in ferrets. J Virol **85:**2851-2858.

551. **Sorrell EM, Schrauwen EJ, Linster M, De Graaf M, Herfst S, Fouchier RA.** 2011. Predicting 'airborne' influenza viruses: (trans-) mission impossible? Curr Opin Virol **1:**635-642.

552. **Monto AS.** 2003. The role of antivirals in the control of influenza. Vaccine **21:**1796-1800.

553. **Bautista E, Chotpitayasunondh T, Gao Z, Harper SA, Shaw M, Uyeki TM, Zaki SR, Hayden FG, Hui DS, Kettner JD, Kumar A, Lim M, Shindo N, Penn C, Nicholson KG.** 2010. Clinical aspects of pandemic 2009 influenza A (H1N1) virus infection. N Engl J Med **362:**1708-1719.

554. **Lee VJ, Yap J, Cook AR, Chen MI, Tay JK, Tan BH, Loh JP, Chew SW, Koh WH, Lin R, Cui L, Lee CW, Sung WK, Wong CW, Hibberd ML, Kang WL, Seet B, Tambyah PA.** 2010. Oseltamivir ring prophylaxis for containment of 2009 H1N1 influenza outbreaks. N Engl J Med **362:**2166-2174.

555. **Dominguez-Cherit G, Lapinsky SE, Macias AE, Pinto R, Espinosa-Perez L, de la Torre A, Poblano-Morales M, Baltazar-Torres JA, Bautista E, Martinez A, Martinez MA, Rivero E, Valdez R, Ruiz-Palacios G, Hernandez M, Stewart TE, Fowler RA.** 2009. Critically Ill patients with 2009 influenza A(H1N1) in Mexico. JAMA **302:**1880-1887.

556. **WHO.** 2011. Update on oseltamivir resistance to influenza H1N1 (2009) viruses. http://www.who.int/csr/disease/influenza/2011_07_15_weekly_web_update_oseltamivir_resistance.pdf. Accessed 10 October 2106.

557. **Gaur AH, Bagga B, Barman S, Hayden R, Lamptey A, Hoffman JM, Bhojwani D, Flynn PM, Tuomanen E, Webby R.** 2010. Intravenous zanamivir for oseltamivir-resistant 2009 H1N1 influenza. N Engl J Med **362:**88-89.

558. **Monto AS, McKimm-Breschkin JL, Macken C, Hampson AW, Hay A, Klimov A, Tashiro M, Webster RG, Aymard M, Hayden FG, Zambon M.** 2006. Detection of influenza viruses resistant to neuraminidase inhibitors in global surveillance during the first 3 years of their use. Antimicrob Agents Chemother **50:**2395-2402.

559. **Kiso M, Mitamura K, Sakai-Tagawa Y, Shiraishi K, Kawakami C, Kimura K, Hayden FG, Sugaya N, Kawaoka Y.** 2004. Resistant influenza A viruses in children treated with oseltamivir: descriptive study. Lancet **364:**759-765.

560. **Hauge SH, Dudman S, Borgen K, Lackenby A, Hungnes O.** 2009. Oseltamivir-resistant influenza viruses A (H1N1), Norway, 2007-08. Emerg Infect Dis **15:**155-162.

561. **Meijer A, Lackenby A, Hungnes O, Lina B, van-der-Werf S, Schweiger B, Opp M, Paget J, van-de-Kassteele J, Hay A, Zambon M, European Influenza Surveillance S.** 2009. Oseltamivir-resistant influenza virus A (H1N1), Europe, 2007-08 season. Emerg Infect Dis **15:**552-560.

562. **Ives JA, Carr JA, Mendel DB, Tai CY, Lambkin R, Kelly L, Oxford JS, Hayden FG, Roberts NA.** 2002. The H274Y mutation in the influenza A/H1N1 neuraminidase active site following oseltamivir phosphate treatment leave virus severely compromised both in vitro and in vivo. Antiviral Res **55:**307-317.

563. **Carr J, Ives J, Kelly L, Lambkin R, Oxford J, Mendel D, Tai L, Roberts N.** 2002. Influenza virus carrying neuraminidase with reduced sensitivity to oseltamivir carboxylate has altered properties in vitro and is compromised for infectivity and replicative ability in vivo. Antiviral Res **54:**79-88.

564. **Herlocher ML, Carr J, Ives J, Elias S, Truscon R, Roberts N, Monto AS.** 2002. Influenza virus carrying an R292K mutation in the neuraminidase gene is not transmitted in ferrets. Antiviral Res **54:**99-111.

565. **van der Vries E, van den Berg B, Schutten M.** 2008. Fatal oseltamivir-resistant influenza virus infection. N Engl J Med **359:**1074-1076.

566. **Bouvier NM, Lowen AC, Palese P.** 2008. Oseltamivir-resistant influenza A viruses are transmitted efficiently among guinea pigs by direct contact but not by aerosol. J Virol **82:**10052-10058.

567. **Baz M, Abed Y, Simon P, Hamelin ME, Boivin G.** 2010. Effect of the neuraminidase mutation H274Y conferring resistance to oseltamivir on the replicative capacity and virulence of old and recent human influenza A(H1N1) viruses. J Infect Dis **201:**740-745.

568. **Bloom JD, Gong LI, Baltimore D.** 2010. Permissive secondary mutations enable the evolution of influenza oseltamivir resistance. Science **328:**1272-1275.

569. **Collins PJ, Haire LF, Lin YP, Liu J, Russell RJ, Walker PA, Martin SR, Daniels RS, Gregory V, Skehel JJ, Gamblin SJ, Hay AJ.** 2009. Structural basis for oseltamivir resistance of influenza viruses. Vaccine **27:**6317-6323.

570. **Duan S, Boltz DA, Seiler P, Li J, Bragstad K, Nielsen LP, Webby RJ, Webster RG, Govorkova EA.** 2010. Oseltamivir-resistant pandemic H1N1/2009 influenza virus possesses lower transmissibility and fitness in ferrets. PLoS Pathog **6:**e1001022.

571. **Hamelin ME, Baz M, Abed Y, Couture C, Joubert P, Beaulieu E, Bellerose N, Plante M, Mallett C, Schumer G, Kobinger GP, Boivin G.** 2010. Oseltamivir-resistant pandemic A/H1N1 virus is as virulent as its wild-type counterpart in mice and ferrets. PLoS Pathog **6:**e1001015.

572. **Kiso M, Shinya K, Shimojima M, Takano R, Takahashi K, Katsura H, Kakugawa S, Le MT, Yamashita M, Furuta Y, Ozawa M, Kawaoka Y.** 2010. Characterization of oseltamivir-resistant 2009 H1N1 pandemic influenza A viruses. PLoS Pathog **6:**e1001079.

573. **Memoli MJ, Davis AS, Proudfoot K, Chertow DS, Hrabal RJ, Bristol T, Taubenberger JK.** 2011. Multidrug-resistant 2009 pandemic influenza A(H1N1) viruses maintain fitness and transmissibility in ferrets. J Infect Dis **203:**348-357.

574. **Seibert CW, Kaminski M, Philipp J, Rubbenstroth D, Albrecht RA, Schwalm F, Stertz S, Medina RA, Kochs G, Garcia-Sastre A, Staeheli P, Palese P.** 2010. Oseltamivir-resistant variants of the 2009 pandemic H1N1 influenza A virus are not attenuated in the guinea pig and ferret transmission models. J Virol **84:**11219-11226.

575. **Nguyen HT, Fry AM, Loveless PA, Klimov AI, Gubareva LV.** 2010. Recovery of a multidrug-resistant strain of pandemic influenza A 2009 (H1N1) virus carrying a dual H275Y/I223R mutation from a child after prolonged treatment with oseltamivir. Clin Infect Dis **51:**983-984.

576. **Matrosovich M, Matrosovich T, Carr J, Roberts NA, Klenk HD.** 2003. Overexpression of the alpha-2,6-sialyltransferase in MDCK cells increases influenza virus sensitivity to neuraminidase inhibitors. J Virol **77:**8418-8425.

577. **Fouchier RA, Bestebroer TM, Herfst S, Van Der Kemp L, Rimmelzwaan GF, Osterhaus AD.** 2000. Detection of influenza A viruses from different species by PCR amplification of conserved sequences in the matrix gene. J Clin Microbiol **38:**4096-4101.

578. **Squires B, Macken C, Garcia-Sastre A, Godbole S, Noronha J, Hunt V, Chang R, Larsen CN, Klem E, Biersack K, Scheuermann RH.** 2008. BioHealthBase: informatics support in the elucidation of influenza virus host pathogen interactions and virulence. Nucleic Acids Res **36:**D497-503.

579. **CDC.** 2009. Oseltamivir-resistant 2009 pandemic influenza A (H1N1) virus infection in two summer campers receiving prophylaxis--North Carolina, 2009. MMWR Morb Mortal Wkly Rep **58:**969-972.

580. **Hurt AC, Lee RT, Leang SK, Cui L, Deng YM, Phuah SP, Caldwell N, Freeman K, Komadina N, Smith D, Speers D, Kelso A, Lin RT, Maurer-Stroh S, Barr IG.** 2011. Increased detection in Australia and Singapore of a novel influenza A(H1N1)2009 variant with reduced oseltamivir and zanamivir sensitivity due to a S247N neuraminidase mutation. Euro Surveill **16**.

581. **McCaw JM, Arinaminpathy N, Hurt AC, McVernon J, McLean AR.** 2011. A mathematical framework for estimating pathogen transmission fitness and inoculum size using data from a competitive mixtures animal model. PLoS Comput Biol **7:**e1002026.

582. **Schrauwen EJ, Herfst S, Chutinimitkul S, Bestebroer TM, Rimmelzwaan GF, Osterhaus AD, Kuiken T, Fouchier RA.** 2011. Possible increased pathogenicity of pandemic (H1N1) 2009 influenza virus upon reassortment. Emerg Infect Dis **17:**200-208.

583. **CDC.** 2009. Update: infections with a swine-origin influenza A (H1N1) virus--United States and other countries, April 28, 2009. MMWR Morb Mortal Wkly Rep **58:**431-433.

584. **Osterhaus AD.** 2008. New respiratory viruses of humans. Pediatr Infect Dis J **27:**S71-74.

585. **Del Giudice G, Stittelaar KJ, van Amerongen G, Simon J, Osterhaus AD, Stohr K, Rappuoli R.** 2009. Seasonal influenza vaccine provides priming for A/H1N1 immunization. Sci Transl Med **1:**12re11.

586. **Zhou B, Li Y, Belser JA, Pearce MB, Schmolke M, Subba AX, Shi Z, Zaki SR, Blau DM, Garcia-Sastre A, Tumpey TM, Wentworth DE.** 2010. NS-based live attenuated H1N1 pandemic vaccines protect mice and ferrets. Vaccine **28:**8015-8025.

587. **Gill JR, Sheng ZM, Ely SF, Guinee DG, Beasley MB, Suh J, Deshpande C, Mollura DJ, Morens DM, Bray M, Travis WD, Taubenberger JK.** 2010. Pulmonary pathologic findings of fatal 2009 pandemic influenza A/H1N1 viral infections. Arch Pathol Lab Med **134:**235-243.

588. **Li P, Su DJ, Zhang JF, Xia XD, Sui H, Zhao DH.** 2011. Pneumonia in novel swine-origin influenza A (H1N1) virus infection: high-resolution CT findings. Eur J Radiol **80:**e146-152.

589. **Marchiori E, Zanetti G, Hochhegger B, Rodrigues RS, Fontes CA, Nobre LF, Mancano AD, Meirelles GS, Irion KL.** 2010. High-resolution computed tomography findings from adult patients with Influenza A (H1N1) virus-associated pneumonia. Eur J Radiol **74:**93-98.

590. **Mollura DJ, Asnis DS, Crupi RS, Conetta R, Feigin DS, Bray M, Taubenberger JK, Bluemke DA.** 2009. Imaging findings in a fatal case of pandemic swine-origin influenza A (H1N1). AJR Am J Roentgenol **193:**1500-1503.

591. **Perez-Padilla R, de la Rosa-Zamboni D, Ponce de Leon S, Hernandez M, Quinones-Falconi F, Bautista E, Ramirez-Venegas A, Rojas-Serrano J, Ormsby CE, Corrales A, Higuera A,**

Mondragon E, Cordova-Villalobos JA, Influenza IWGo. 2009. Pneumonia and respiratory failure from swine-origin influenza A (H1N1) in Mexico. N Engl J Med **361:**680-689.

592. **Ellebedy AH, Fabrizio TP, Kayali G, Oguin TH, 3rd, Brown SA, Rehg J, Thomas PG, Webby RJ.** 2010. Contemporary seasonal influenza A (H1N1) virus infection primes for a more robust response to split inactivated pandemic influenza A (H1N1) Virus vaccination in ferrets. Clin Vaccine Immunol **17:**1998-2006.

593. **Hossain MJ, Bourgeois M, Quan FS, Lipatov AS, Song JM, Chen LM, Compans RW, York I, Kang SM, Donis RO.** 2011. Virus-like particle vaccine containing hemagglutinin confers protection against 2009 H1N1 pandemic influenza. Clin Vaccine Immunol **18:**2010-2017.

594. **Martel CJ, Agger EM, Poulsen JJ, Hammer Jensen T, Andresen L, Christensen D, Nielsen LP, Blixenkrone-Moller M, Andersen P, Aasted B.** 2011. CAF01 potentiates immune responses and efficacy of an inactivated influenza vaccine in ferrets. PLoS One **6:**e22891.

595. **Jones FR, Gabitzsch ES, Xu Y, Balint JP, Borisevich V, Smith J, Smith J, Peng BH, Walker A, Salazar M, Paessler S.** 2011. Prevention of influenza virus shedding and protection from lethal H1N1 challenge using a consensus 2009 H1N1 HA and NA adenovirus vector vaccine. Vaccine **29:**7020-7026.

596. **Yang P, Duan Y, Wang C, Xing L, Gao X, Tang C, Luo D, Zhao Z, Jia W, Peng D, Liu X, Wang X.** 2011. Immunogenicity and protective efficacy of a live attenuated vaccine against the 2009 pandemic A H1N1 in mice and ferrets. Vaccine **29:**698-705.

597. **Pearce MB, Belser JA, Houser KV, Katz JM, Tumpey TM.** 2011. Efficacy of seasonal live attenuated influenza vaccine against virus replication and transmission of a pandemic 2009 H1N1 virus in ferrets. Vaccine **29:**2887-2894.

598. **Pillet S, Kobasa D, Meunier I, Gray M, Laddy D, Weiner DB, von Messling V, Kobinger GP.** 2011. Cellular immune response in the presence of protective antibody levels correlates with protection against 1918 influenza in ferrets. Vaccine **29:**6793-6801.

599. **Veldhuis Kroeze EJ, van Amerongen G, Dijkshoorn ML, Simon JH, de Waal L, Hartmann IJ, Krestin GP, Kuiken T, Osterhaus AD, Stittelaar KJ.** 2011. Pulmonary pathology of pandemic influenza A/H1N1 virus (2009)-infected ferrets upon longitudinal evaluation by computed tomography. J Gen Virol **92:**1854-1858.

600. **Stittelaar KJ, Veldhuis Kroeze EJ, Rudenko L, Dhere R, Thirapakpoomanunt S, Kieny MP, Osterhaus AD.** 2011. Efficacy of live attenuated vaccines against 2009 pandemic H1N1 influenza in ferrets. Vaccine **29:**9265-9270.

601. **De Swart RL, Kuiken T, Timmerman HH, van Amerongen G, Van Den Hoogen BG, Vos HW, Neijens HJ, Andeweg AC, Osterhaus AD.** 2002. Immunization of macaques with formalin-inactivated respiratory syncytial virus (RSV) induces interleukin-13-associated hypersensitivity to subsequent RSV infection. J Virol **76:**11561-11569.

602. **Black CP.** 2003. Systematic review of the biology and medical management of respiratory syncytial virus infection. Respir Care **48:**209-231; discussion 231-203.

603. **Baras B, Stittelaar KJ, Kuiken T, Jacob V, Bernhard R, Giannini S, de Waal L, van Amerongen G, Simon JH, Osterhaus AD, Hanon E, Mossman SP.** 2011. Longevity of the protective immune response induced after vaccination with one or two doses of AS03A-adjuvanted split H5N1 vaccine in ferrets. Vaccine **29:**2092-2099.

604. **CDC.** 2009. Serum cross-reactive antibody response to a novel influenza A (H1N1) virus after vaccination with seasonal influenza vaccine. MMWR Morb Mortal Wkly Rep **58:**521-524.

605. **Girard MP, Tam JS, Assossou OM, Kieny MP.** 2010. The 2009 A (H1N1) influenza virus pandemic: A review. Vaccine **28:**4895-4902.

606. **CDC.** 2009. Hospitalized patients with novel influenza A (H1N1) virus infection - California, April-May, 2009. MMWR Morb Mortal Wkly Rep **58:**536-541.

607. **Kobinger GP, Meunier I, Patel A, Pillet S, Gren J, Stebner S, Leung A, Neufeld JL, Kobasa D, von Messling V.** 2010. Assessment of the efficacy of commercially available and candidate vaccines against a pandemic H1N1 2009 virus. J Infect Dis **201:**1000-1006.

608. **Fraser C, Donnelly CA, Cauchemez S, Hanage WP, Van Kerkhove MD, Hollingsworth TD, Griffin J, Baggaley RF, Jenkins HE, Lyons EJ, Jombart T, Hinsley WR, Grassly NC, Balloux F, Ghani AC, Ferguson NM, Rambaut A, Pybus OG, Lopez-Gatell H, Alpuche-Aranda CM, Chapela IB, Zavala EP, Guevara DM, Checchi F, Garcia E, Hugonnet S, Roth C, Collaboration WHORPA.** 2009. Pandemic potential of a strain of influenza A (H1N1): early findings. Science **324:**1557-1561.

609. **WHO.** 2009. WHO recommendations on pandemic (H1N1) 2009 vaccines, Pandemic (H1N1) 2009 briefing note 2. http://www.who.int/csr/disease/swineflu/notes/h1n1_vaccine_20090713/en/print.html. Accessed 10 October 2016.

610. **Murphy BR, Coelingh K.** 2002. Principles underlying the development and use of live attenuated cold-adapted influenza A and B virus vaccines. Viral Immunol **15:**295-323.

611. **Wareing MD, Marsh GA, Tannock GA.** 2002. Preparation and characterisation of attenuated cold-adapted influenza A reassortants derived from the A/Leningrad/134/17/57 donor strain. Vaccine **20:**2082-2090.

612. **Mendelman PM, Cordova J, Cho I.** 2001. Safety, efficacy and effectiveness of the influenza virus vaccine, trivalent, types A and B, live, cold-adapted (CAIV-T) in healthy children and healthy adults. Vaccine **19:**2221-2226.

613. **Glezen WP.** 2004. Cold-adapted, live attenuated influenza vaccine. Expert Rev Vaccines **3:**131-139.

614. **Watanabe S, Watanabe T, Kawaoka Y.** 2009. Influenza A virus lacking M2 protein as a live attenuated vaccine. J Virol **83:**5947-5950.

615. **Richt JA, Garcia-Sastre A.** 2009. Attenuated influenza virus vaccines with modified NS1 proteins. Curr Top Microbiol Immunol **333:**177-195.

616. **Akarsu H, Iwatsuki-Horimoto K, Noda T, Kawakami E, Katsura H, Baudin F, Horimoto T, Kawaoka Y.** 2011. Structure-based design of NS2 mutants for attenuated influenza A virus vaccines. Virus Res **155:**240-248.

617. **Rudenko LG, Lonskaya NI, Klimov AI, Vasilieva RI, Ramirez A.** 1996. Clinical and epidemiological evaluation of a live, cold-adapted influenza vaccine for 3-14-year-olds. Bull World Health Organ **74:**77-84.

618. **Rudenko LG, Slepushkin AN, Monto AS, Kendal AP, Grigorieva EP, Burtseva EP, Rekstin AR, Beljaev AL, Bragina VE, Cox N, et al.** 1993. Efficacy of live attenuated and inactivated influenza vaccines in schoolchildren and their unvaccinated contacts in Novgorod, Russia. J Infect Dis **168:**881-887.

619. **Rudenko LG, Arden NH, Grigorieva E, Naychin A, Rekstin A, Klimov AI, Donina S, Desheva J, Holman RC, DeGuzman A, Cox NJ, Katz JM.** 2000. Immunogenicity and efficacy of Russian live attenuated and US inactivated influenza vaccines used alone and in combination in nursing home residents. Vaccine **19:**308-318.

620. **Hickling J, D'Hondt E.** 2011. Review of production technologies for influenza virus vaccines and their suitability in developing countries for influenza pandemic preparedness. www.who.int/influenza/resources/technical_studies_under_resolution_wha63_1_en.pdf Accessed 10 October 2016.

621. **Tamura S, Tanimoto T, Kurata T.** 2005. Mechanisms of broad cross-protection provided by influenza virus infection and their application to vaccines. Jpn J Infect Dis **58:**195-207.

622. **Maassab HF, Bryant ML.** 1999. The development of live attenuated cold-adapted influenza virus vaccine for humans. Rev Med Virol **9:**237-244.

623. **Subbarao EK, Park EJ, Lawson CM, Chen AY, Murphy BR.** 1995. Sequential addition of temperature-sensitive missense mutations into the PB2 gene of influenza A transfectant

viruses can effect an increase in temperature sensitivity and attenuation and permits the rational design of a genetically engineered live influenza A virus vaccine. J Virol **69:**5969-5977.

624. **Bracco Neto H, Farhat CK, Tregnaghi MW, Madhi SA, Razmpour A, Palladino G, Small MG, Gruber WC, Forrest BD, Group DPLS.** 2009. Efficacy and safety of 1 and 2 doses of live attenuated influenza vaccine in vaccine-naive children. Pediatr Infect Dis J **28:**365-371.

625. **Rudenko L, Desheva J, Korovkin S, Mironov A, Rekstin A, Grigorieva E, Donina S, Gambaryan A, Katlinsky A.** 2008. Safety and immunogenicity of live attenuated influenza reassortant H5 vaccine (phase I-II clinical trials). Influenza Other Respir Viruses **2:**203-209.

626. **Chen Z, Wang W, Zhou H, Suguitan AL, Jr., Shambaugh C, Kim L, Zhao J, Kemble G, Jin H.** 2010. Generation of live attenuated novel influenza virus A/California/7/09 (H1N1) vaccines with high yield in embryonated chicken eggs. J Virol **84:**44-51.

627. **Chen GL, Min JY, Lamirande EW, Santos C, Jin H, Kemble G, Subbarao K.** 2011. Comparison of a live attenuated 2009 H1N1 vaccine with seasonal influenza vaccines against 2009 pandemic H1N1 virus infection in mice and ferrets. J Infect Dis **203:**930-936.

628. **Kiseleva I, Larionova N, Kuznetsov V, Rudenko L.** 2010. Phenotypic characteristics of novel swine-origin influenza A/California/07/2009 (H1N1) virus. Influenza Other Respir Viruses **4:**1-5.

629. **WHO.** 2009. Update of WHO biosafety risk assessment and guidelines for the production and quality control of human influenza pandemic vaccines; 2009. http://www.who.int/biologicals/publications/trs/areas/vaccines/influenza/H1N1_vaccine_production_biosafety_SHOC.27May2009.pdf. Accessed 10 October 2016.

630. **Friede M, Palkonyay L, Alfonso C, Pervikov Y, Torelli G, Wood D, Kieny MP.** 2011. WHO initiative to increase global and equitable access to influenza vaccine in the event of a pandemic: supporting developing country production capacity through technology transfer. Vaccine **29 Suppl 1:**A2-7.

631. **Webb SA, Seppelt IM, Investigators AI.** 2009. Pandemic (H1N1) 2009 influenza ("swine flu") in Australian and New Zealand intensive care. Crit Care Resusc **11:**170-172.

632. **Maltais AK, Stittelaar KJ, Veldhuis Kroeze EJ, van Amerongen G, Dijkshoorn ML, Krestin GP, Hinkula J, Arwidsson H, Lindberg A, Osterhaus AD.** 2014. Intranasally administered Endocine formulated 2009 pandemic influenza H1N1 vaccine induces broad specific antibody responses and confers protection in ferrets. Vaccine **32:**3307-3315.

633. **Mann AJ, Noulin N, Catchpole A, Stittelaar KJ, de Waal L, Veldhuis Kroeze EJ, Hinchcliffe M, Smith A, Montomoli E, Piccirella S, Osterhaus AD, Knight A, Oxford JS, Lapini G, Cox R, Lambkin-Williams R.** 2014. Intranasal H5N1 vaccines, adjuvanted with chitosan derivatives, protect ferrets against highly pathogenic influenza intranasal and intratracheal challenge. PLoS One **9:**e93761.

634. **van der Vries E, Stittelaar KJ, van Amerongen G, Veldhuis Kroeze EJ, de Waal L, Fraaij PL, Meesters RJ, Luider TM, van der Nagel B, Koch B, Vulto AG, Schutten M, Osterhaus AD.** 2013. Prolonged influenza virus shedding and emergence of antiviral resistance in immunocompromised patients and ferrets. PLoS Pathog **9:**e1003343.

635. **Millican RC, Brown JB.** 1944. The isolation and properties of some naturally occuring octadecenoic (Oleic) acids. Journal of Biological Chemistry **154:**437-450.

636. **Bourre JM, Dumont OL, Clement ME, Durand GA.** 1997. Endogenous synthesis cannot compensate for absence of dietary oleic acid in rats. J Nutr **127:**488-493.

637. **Petersson P, Hedenskog M, Alves D, Brytting M, Schroder U, Linde A, Lundkvist A.** 2010. The Eurocine L3 adjuvants with subunit influenza antigens induce protective immunity in mice after intranasal vaccination. Vaccine **28:**6491-6497.

638. **Sahni JK, Chopra S, Ahmad FJ, Khar RK.** 2008. Potential prospects of chitosan derivative trimethyl chitosan chloride (TMC) as a polymeric absorption enhancer: synthesis, characterization and applications. J Pharm Pharmacol **60:**1111-1119.

639. **Roman F, Vaman T, Gerlach B, Markendorf A, Gillard P, Devaster JM.** 2010. Immunogenicity and safety in adults of one dose of influenza A H1N1v 2009 vaccine formulated with and without AS03A-adjuvant: preliminary report of an observer-blind, randomised trial. Vaccine **28:**1740-1745.

640. **CDC.** 2015. Update on Canine Influenza (Dog Flu) Outbreak Reported in Chicago Area. http://www.cdc.gov/flu/news/canine-influenza-update.htm. Accessed 10 October 2016.

641. **Veldhuis Kroeze EJB, Kuiken T.** 2016. Sporadic Influenza A Virus Infections of Miscellaneous Mammal Species *In* Swayne DE (ed), Animal Influenza, 2nd ed. Wiley-Blackwell, Hoboken, New Jersey.

642. **Belser JA, Tumpey TM.** 2013. H5N1 pathogenesis studies in mammalian models. Virus Res **178:**168-185.

643. **Richard M, Schrauwen EJ, de Graaf M, Bestebroer TM, Spronken MI, van Boheemen S, de Meulder D, Lexmond P, Linster M, Herfst S, Smith DJ, van den Brand JM, Burke DF, Kuiken T, Rimmelzwaan GF, Osterhaus AD, Fouchier RA.** 2013. Limited airborne transmission of H7N9 influenza A virus between ferrets. Nature **501:**560-563.

644. **Wang F, Daugherty B, Keise LL, Wei Z, Foley JP, Savani RC, Koval M.** 2003. Heterogeneity of claudin expression by alveolar epithelial cells. Am J Respir Cell Mol Biol **29:**62-70.

645. **Short KR, Kasper J, van der Aa S, Andeweg AC, Zaaraoui-Boutahar F, Goeijenbier M, Richard M, Herold S, Becker C, Scott DP, Limpens RW, Koster AJ, Barcena M, Fouchier RA, Kirkpatrick CJ, Kuiken T.** 2016. Influenza virus damages the alveolar barrier by disrupting epithelial cell tight junctions. Eur Respir J **47:**954-966.

646. **Kreda SM, Gynn MC, Fenstermacher DA, Boucher RC, Gabriel SE.** 2001. Expression and localization of epithelial aquaporins in the adult human lung. Am J Respir Cell Mol Biol **24:**224-234.

647. **Verkman AS.** 2005. More than just water channels: unexpected cellular roles of aquaporins. J Cell Sci **118:**3225-3232.

648. **Towne JE, Krane CM, Bachurski CJ, Menon AG.** 2001. Tumor necrosis factor-alpha inhibits aquaporin 5 expression in mouse lung epithelial cells. J Biol Chem **276:**18657-18664.

649. **Nagai K, Watanabe M, Seto M, Hisatsune A, Miyata T, Isohama Y.** 2007. Nitric oxide decreases cell surface expression of aquaporin-5 and membrane water permeability in lung epithelial cells. Biochem Biophys Res Commun **354:**579-584.

650. **Ma T, Fukuda N, Song Y, Matthay MA, Verkman AS.** 2000. Lung fluid transport in aquaporin-5 knockout mice. J Clin Invest **105:**93-100.

651. **Furuyama A, Mochitate K.** 2000. Assembly of the exogenous extracellular matrix during basement membrane formation by alveolar epithelial cells in vitro. J Cell Sci **113 (Pt 5):**859-868.

652. **Geiser T.** 2003. Mechanisms of alveolar epithelial repair in acute lung injury--a translational approach. Swiss Med Wkly **133:**586-590.

653. **Ware LB, Matthay MA.** 2000. The acute respiratory distress syndrome. N Engl J Med **342:**1334-1349.

654. **Adamson IY, Young L, Bowden DH.** 1988. Relationship of alveolar epithelial injury and repair to the induction of pulmonary fibrosis. Am J Pathol **130:**377-383.

655. **Berthiaume Y, Lesur O, Dagenais A.** 1999. Treatment of adult respiratory distress syndrome: plea for rescue therapy of the alveolar epithelium. Thorax **54:**150-160.

656. **Cakarova L, Marsh LM, Wilhelm J, Mayer K, Grimminger F, Seeger W, Lohmeyer J, Herold S.** 2009. Macrophage tumor necrosis factor-alpha induces epithelial expression of granulocyte-macrophage colony-stimulating factor: impact on alveolar epithelial repair. Am J Respir Crit Care Med **180:**521-532.

657. **Furuyama A, Mochitate K.** 2004. Hepatocyte growth factor inhibits the formation of the basement membrane of alveolar epithelial cells in vitro. Am J Physiol Lung Cell Mol Physiol **286:**L939-946.

658. **Lu S, Pan S, Wang C, Hu K, Hong T.** 2012. Establishment of an animal model of extracorporeal membrane oxygenation in rabbits. Perfusion **27:**414-418.

659. **Zuo W, Zhang T, Wu DZ, Guan SP, Liew AA, Yamamoto Y, Wang X, Lim SJ, Vincent M, Lessard M, Crum CP, Xian W, McKeon F.** 2015. p63(+)Krt5(+) distal airway stem cells are essential for lung regeneration. Nature **517:**616-620.

660. **Liu A, Chen S, Cai S, Dong L, Liu L, Yang Y, Guo F, Lu X, He H, Chen Q, Hu S, Qiu H.** 2014. Wnt5a through noncanonical Wnt/JNK or Wnt/PKC signaling contributes to the differentiation of mesenchymal stem cells into type II alveolar epithelial cells in vitro. PLoS One **9:**e90229.

661. **Liu AR, Liu L, Chen S, Yang Y, Zhao HJ, Liu L, Guo FM, Lu XM, Qiu HB.** 2013. Activation of canonical wnt pathway promotes differentiation of mouse bone marrow-derived MSCs into type II alveolar epithelial cells, confers resistance to oxidative stress, and promotes their migration to injured lung tissue in vitro. J Cell Physiol **228:**1270-1283.

662. **Mironov AA, Beznoussenko GV.** 2009. Correlative microscopy: a potent tool for the study of rare or unique cellular and tissue events. J Microsc **235:**308-321.

663. **Hellstrom K, Vihinen H, Kallio K, Jokitalo E, Ahola T.** 2015. Correlative light and electron microscopy enables viral replication studies at the ultrastructural level. Methods **90:**49-56.

664. **Kang YM, Song BM, Lee JS, Kim HS, Seo SH.** 2011. Pandemic H1N1 influenza virus causes a stronger inflammatory response than seasonal H1N1 influenza virus in ferrets. Arch Virol **156:**759-767.

665. **Xiao YL, Kash JC, Beres SB, Sheng ZM, Musser JM, Taubenberger JK.** 2013. High-throughput RNA sequencing of a formalin-fixed, paraffin-embedded autopsy lung tissue sample from the 1918 influenza pandemic. J Pathol **229:**535-545.

666. **Herold S, Ludwig S, Pleschka S, Wolff T.** 2012. Apoptosis signaling in influenza virus propagation, innate host defense, and lung injury. J Leukoc Biol **92:**75-82.

667. **Quantius J, Schmoldt C, Vazquez-Armendariz AI, Becker C, El Agha E, Wilhelm J, Morty RE, Vadasz I, Mayer K, Gattenloehner S, Fink L, Matrosovich M, Li X, Seeger W, Lohmeyer J, Bellusci S, Herold S.** 2016. Influenza Virus Infects Epithelial Stem/Progenitor Cells of the Distal Lung: Impact on Fgfr2b-Driven Epithelial Repair. PLoS Pathog **12:**e1005544.

668. **Buchackert Y, Rummel S, Vohwinkel CU, Gabrielli NM, Grzesik BA, Mayer K, Herold S, Morty RE, Seeger W, Vadasz I.** 2012. Megalin mediates transepithelial albumin clearance from the alveolar space of intact rabbit lungs. J Physiol **590:**5167-5181.

669. **van den Brand JM, Stittelaar KJ, Leijten LM, van Amerongen G, Simon JH, Osterhaus AD, Kuiken T.** 2012. Modification of the ferret model for pneumonia from seasonal human influenza A virus infection. Vet Pathol **49:**562-568.

670. **Tate MD, Brooks AG, Reading PC.** 2008. The role of neutrophils in the upper and lower respiratory tract during influenza virus infection of mice. Respir Res **9:**57.

671. **Fujisawa H.** 2008. Neutrophils play an essential role in cooperation with antibody in both protection against and recovery from pulmonary infection with influenza virus in mice. J Virol **82:**2772-2783.

672. **Tate MD, Ioannidis LJ, Croker B, Brown LE, Brooks AG, Reading PC.** 2011. The role of neutrophils during mild and severe influenza virus infections of mice. PLoS One **6:**e17618.

673. **Lipatov AS, Kwon YK, Pantin-Jackwood MJ, Swayne DE.** 2009. Pathogenesis of H5N1 influenza virus infections in mice and ferret models differs according to respiratory tract or digestive system exposure. J Infect Dis **199:**717-725.

674. **Mandelboim O, Lieberman N, Lev M, Paul L, Arnon TI, Bushkin Y, Davis DM, Strominger JL, Yewdell JW, Porgador A.** 2001. Recognition of haemagglutinins on virus-infected cells by NKp46 activates lysis by human NK cells. Nature **409:**1055-1060.

675. **Nogusa S, Ritz BW, Kassim SH, Jennings SR, Gardner EM.** 2008. Characterization of age-related changes in natural killer cells during primary influenza infection in mice. Mech Ageing Dev **129:**223-230.

676. **Stein-Streilein J, Guffee J.** 1986. In vivo treatment of mice and hamsters with antibodies to asialo GM1 increases morbidity and mortality to pulmonary influenza infection. J Immunol **136:**1435-1441.

677. **Mao H, Tu W, Qin G, Law HK, Sia SF, Chan PL, Liu Y, Lam KT, Zheng J, Peiris M, Lau YL.** 2009. Influenza virus directly infects human natural killer cells and induces cell apoptosis. J Virol **83:**9215-9222.

678. **Zhou G, Juang SW, Kane KP.** 2013. NK cells exacerbate the pathology of influenza virus infection in mice. Eur J Immunol **43:**929-938.

679. **Abdul-Careem MF, Mian MF, Yue G, Gillgrass A, Chenoweth MJ, Barra NG, Chew MV, Chan T, Al-Garawi AA, Jordana M, Ashkar AA.** 2012. Critical role of natural killer cells in lung immunopathology during influenza infection in mice. J Infect Dis **206:**167-177.

680. **Guo H, Kumar P, Malarkannan S.** 2011. Evasion of natural killer cells by influenza virus. J Leukoc Biol **89:**189-194.

681. **Cook KD, Whitmire JK.** 2013. The depletion of NK cells prevents T cell exhaustion to efficiently control disseminating virus infection. J Immunol **190:**641-649.

682. **Nishikado H, Mukai K, Kawano Y, Minegishi Y, Karasuyama H.** 2011. NK cell-depleting anti-asialo GM1 antibody exhibits a lethal off-target effect on basophils in vivo. J Immunol **186:**5766-5771.

ADDENDA

Abbreviations

Curriculum Vitae

PhD portfolio

List of publications

Dankwoord

ABBREVIATIONS

ADV	-	Aleutian Disease Virus
AEC	-	[1]Alveolar Epithelial Cell, [2]3-Amino-9-Ethylcarbazole
AGID	-	Agar Gel Immunodiffusion (assay)
AIV	-	Avian Influenza Virus
ALI	-	Acute Lung Injury
ALV	-	Aerated Lung Volume
ARDS	-	Acute Respiratory Distress Syndrome
AUC	-	Area Under Curve
BAL	-	Bronchoalveolar Lavage
BALB/c	-	'Bagg's Albinos' inbred mouse strain
BALT	-	Bronchus-associated Lymphoid Tissue
BM	-	Basement Membrane
BSA	-	Bovine Serum Albumin
BSL	-	Biosafety Level
ca	-	Cold Adapted
CCL	-	CC motif (two adjacent cysteines) Chemokine Ligand (several subtypes are recognised)
CDC	-	Centers for Disease Control and Prevention
CFSE	-	Carboxyfluorescein Diacetate Succinimidyl Ester
CIV	-	Canine Influenzavirus
CNS	-	Central Nervous System
CO	-	Corticosteroid
CSF	-	Colony stimulating factor (several subtypes are recognised)
CT	-	Computed Tomography
CXCL	-	CXC motif (two N-terminal Cysteines separated by one amino acid X) Chemokine Ligand (several subtypes are recognised)
CXCR	-	CXC motif (two N-terminal Cysteines separated by one amino acid X) Chemokine Ligand Receptor (several subtypes are recognised)
C57BL/6	-	'C57-Black 6' inbred mouse strain
DAB	-	2,3-diaminobenzidine
DID	-	Double agar Immunodiffusion
DIC	-	Disseminated Intravascular Coagulation
DLG1	-	Disks large homolog 1, also known as synapse-associated protein 97 or SAP97
dpe	-	Days Post Exposure
dpi	-	Days Post Infection
DR5	-	Death Receptor 5

ECMO	-	Extra Corporeal Membrane Oxygenation
EMEM	-	Eagle's Minimal Essential Medium
ENaCs	-	amiloride-sensitive Epithelial Sodium Channels
ESEV	-	ligand sequence Glu-Ser-Glu-Val, at C-terminal of NS1 proteins of most AIVs
ECG	-	Electrocardiogram
EDTA	-	Ethylenediaminetetraacetic Acid
EID_{50}	-	Median Egg Infective Dose
ELISA	-	Enzyme-Linked Immunosorbent Assay
FITC	-	Fluorescein Isothiocyanate
HA	-	Haemagglutinin, receptor-binding glycoprotein
HI	-	Hemagglutination Inhibition
ENaC	-	Amiloride-sensitive Epithelial Sodium Channel
FCS	-	Fetal Calf Serum
Gal	-	Galactose
HEPA	-	High Efficiency Particulate Air (filter)
HMPV	-	Human Metapneumovirus
HPAIV	-	Highly Pathogenic(ity) Avian Influenza Virus
hpi	-	Hours Post Infection
HU	-	Hounsfield Units
HGF	-	Hepatocyte Growth Factor
H&E	-	Haematoxylin & Eosin
GALT	-	Gut-associated Lymphoid Tissue
GGO	-	Ground Glass Opacity
GM-CSF	-	Granulocyte Macrophage Colony Stimulating Factor
IAV	-	Influenza A virus
IBV	-	Influenza B virus
ICAM	-	Intercellular Adhesion Molecule (several subtypes are recognised)
ICV	-	Influenza C virus
IFN	-	Interferon (several subtypes are recognised)
Ig	-	Immunoglobulin (several subtypes are recognised)
IHC	-	Immunohistochemistry
IL	-	Interleukin (several subtypes are recognised)
ILI	-	Influenza-Like Illness
i.m.	-	Intramuscular
IN	-	Intranasal
ISH	-	In Situ Hybridisation
IT	-	Intratracheal
IVPI	-	Intravenous Pathogenicity Index

KGF	-	Keratinocyte Growth Factor
LAIV	-	Live Attenuated Influenza Vaccine
LLF	-	Lung Lavage Fluid
LPAIV	-	Low Pathogenic(ity) Avian Influenza Virus
LPS	-	Lipopolysaccharide
LRT	-	Lower Respiratory Tract
MDCK cells	-	Madin-Darby Canine Kidney cells
MEM	-	Minimal Esential Medium
MK cells	-	Monkey Kidney cells
MMF	-	Mycophenolate Mofetil (CellCept®)
MMP	-	Matrix metalloproteinase (several subtypes are recognised)
MODS	-	Multi-Organ Dysfunction Syndrome
MPO	-	Myeloperoxidase
MRI	-	Magnetic Resonance Imaging
M1	-	Matrix 1, ribonucleoprotein-interacting matrix protein
M2	-	Matrix 2, ion channel protein
NA	-	Neuraminidase, sialic acid (SA)-destroying enzyme
NADPH	-	Nicotinamide adenine dinucleotide phosphate
NAI	-	Neuraminidase inhibitor
Na^+/K^+	-	ATPase-Sodium-Potassium Adenosine Triphosphatase, also known as the Na^+/K^+ pump or Sodium-Potassium pump
NAL	-	NA-like (protein)
NET	-	Neutrophil Extracellular Trap
NHP	-	Non-Human Primate
NO	-	Nitric Oxide
NOS2	-	Nitric Oxide Synthase 2
NP	-	Nucleoprotein, RNA-binding protein
NS	-	[1]Non-Structural (protein), [2]Nose Swab
NS1	-	Non-Structural 1 (protein), interferon (IFN)-antagonising protein
NS2	-	Non-Structural 2 (protein) nuclear export protein
OS	-	[1]Oseltamivir (Tamiflu®), [2]Oropharyngeal Swab
PA	-	Polymerase Acidic
PB1	-	Polymerase Basic 1
PB1-F2	-	Polymerase Basic 1-F2, pro-apoptotic protein
PB2	-	Polymerase Basic 2
PBM	-	PDZ-ligand Binding Motif
PBMC	-	Peripheral Blood Mononuclear Cell
PBS	-	Phosphate-Buffered Saline
PCR	-	Polymerase Chain Reaction

Pdm09	-	2009 pandemic
PDZ	-	Acronym of three proteins, **P**ost synaptic density protein (PSD95), **D**rosophila disc large tumor suppressor (Dlg1), and **Z**onula occludens-1 protein (ZO1). A common structural domain anchoring receptors.
PFU	-	Plague Forming Unit
pH1N1	-	2009 pandemic H1N1 IAV
PIP	-	Pandemic Influenza Preparedness
PIV	-	Parainfluenza Virus
RBC	-	Red Blood Cell (=erythrocyte)
rg	-	Reverse Genetic
RLW	-	Relative Lung Weight (=lung weight / body weight * 100)
ROS	-	Reactive Oxygen Species
RPMI	-	Roswell Park Memorial Institute (medium)
RSV	-	Respiratory Syncytial Virus
SA	-	Sialic Acid
SARI	-	Severe Acute Respiratory Infection
SARS	-	Severe Acute Respiratory Syndrome
s.c.	-	Subcutaneous
SD	-	Standard Deviation
SEM	-	Standard Error of Mean
SPF	-	Specified Pathogens-Free
$TCID_{50}$	-	Median Tissue Culture Infective Dose
TGF β	-	Transforming Growth Factor β
TIMP	-	Tissue Inhibitor of Metalloproteinases (several subtypes are recognised)
TIV	-	Trivalent Influenza Vaccine
TJ	-	Tight Junction
TNF	-	Tumour Necrosis Factor (several subtypes are recognised, α β γ)
TRAIL	-	Tumour-necrosis-factor-Related Apoptosis-Inducing Ligand, also known as TNFSF10
URT	-	Upper Respiratory Tract
VCAM	-	Vascular Cell Adhesion Molecule
VN	-	Virus Neutralisation
vWF (F8)	-	von Willebrand Factor (=Factor 8)
WT	-	Wild Type

CURRICULUM VITAE

The author of this thesis, Edwin Johannes Bertus Veldhuis Kroeze, was born on the 18th of September 1970 in The Hague, The Netherlands. After secondary school at 't Groen van Prinsterercollege' in The Hague, he started studying veterinary medicine at Utrecht University in 1991. After graduating in 2000 with a doctoral thesis 'Bijzondere fysiologische kenmerken en veterinaire aspecten van de Europesche bruine beer (*Ursus a. arctos*)' together with Dr M.A.D. Vente, he gained hands-on research experience by investigating the digestibility of macronutrients in polar bears at Ouwehand's Zoo in Rhenen, The Netherlands. Subsequently, for a short period he worked in a companion animal clinic in Eersel, The Netherlands. He started his residency in veterinary pathology at the Department of Veterinary Pathology at the Faculty of Veterinary Medicine, Utrecht University in 2000, and passed the board examinations of the European College of Veterinary Pathology (ECVP) in 2008. His work at the Department of Veterinary Pathology (later Department of Pathobiology) in collaboration with Dr J.H. van der Kolk, from the Department of Equine Sciences, Faculty of Veterinary Medicine, Utrecht University, led to publication of the book 'Infectious Diseases of the Horse. Diagnosis, pathology, management, and public health' in 2013. From 2009 onwards he has been working as a veterinary pathologist at Viroclinics Biosciences B.V. and was engaged in a PhD project under supervision of Prof Dr Albert D.M.E. Osterhaus and Prof Dr Thijs Kuiken at the Department of Viroscience at the Erasmus Medical Center that led to this thesis.

Edwin J.B. Veldhuis Kroeze is married to Marcelle Schots and they have a son Ocke Lourens Herman, born in 2011.

PHD PORTFOLIO

Edwin J.B. Veldhuis Kroeze, DVM, Dipl ECVP

Research group:	Erasmus MC, Department of Viroscience
Research school:	Post-graduate Molecular Medicine
PhD period:	2010-2017
Promotores:	Prof dr A.D.M.E. Osterhaus
	Prof dr T. Kuiken

In-depth courses

2010 Molecular Medicine Postgraduate School Animal Imaging Workshop by AMIE (Applied Molecular Imaging Erasmus MC) 'From mouse to man', Erasmus MC Rotterdam, February 3 – 5

Molecular Medicine Postgraduate School Virology Course 2010, Erasmus MC Rotterdam, May 31 – June 4

Bone Marrow Workshop, by Dr Rose Raskin from Purdue University College of Veterinary Medicine USA, Utrecht University, July 10 – 11

2013 Laboratory training influenza induced Alveolar leakage in mice, Prof Dr Susanna Herold at the Department of Internal Medicine II, Section of Infectious Diseases, (Justus Liebig) Universities Giessen & Marburg Lung Center (UGMLC) Germany, August 19 – 22

2014 Course in Good Laboratory Practices (GLP) by the Center for Professional Advancement (CfPA), accredited technical training Worldwide. Amsterdam, February 24 – 25

2015 Molecular Medicine Postgraduate School Workshop on Photoshop and Illustrator CS5 for PhD students and other researchers, Erasmus MC Rotterdam, June 16

2016 Fundamentals of Good Laboratory Practices (GLP) by Alida Bouhuijzen, Quality Assurance Compliance specialist III at WIL Research Den Bosch, Viroclinics Biosciences B.V. Schaijk, February 24

Scientific Presentations

2010 Introduction Veterinary Pathology. General Meeting Viroclinics Biosciences B.V. Rotterdam, January 4

Imaging Influenza. E-lig presentation Department of Radiology Erasmus MC Rotterdam, November 9

2011 Imaging Influenza. Meeting Department of Virology Erasmus MC Rotterdam February 2

Imaging Influenza. Presentation 10th Siemens CT-user day, St. Jansdal hospital Harderwijk, June 9

2012 Autopsy findings in a harbour porpoise. Meeting Department Virology EMC Rotterdam, October 24

2013 Pulmonary pathology; lung oedema and other lesions. General Meeting Viroclinics Biosciences B.V. Rotterdam, November 5

2014 Immunosuppressed ferret model, from a veterinary pathologist's perspective. Werkbespreking Department of Viroscience Erasmus MC Rotterdam, January 29

Attended scientific meetings & lectures

2010 Studium Generale & Erasmus Cultuur, Forensic pathology by NFI pathologist drs Frank van de Goot, Erasmus MC Rotterdam, October 12

2013 XV International Symposium on Respiratory Viral Infections. The Macrae foundation, Blijdorp Zoo Rotterdam, March 14 – 17

Studium Generale & Erasmus Cultuur, Autopsy with live explanation, by pathologist i.o. drs Gül Eker, Eramus MC Rotterdam, March 19

The International Liver Congress EASL, Amsterdam RAI, April 24 – 28

The 31st meeting of the European Society and College of Veterinary Pathologists, London, UK, September 4 – 7

Transvac symposium: 'The pig as model in human vaccine development' CVI Lelystad, September 20

Advances in Comparative Pathology, "Pathology and pathogenesis of influenza and other pulmonary infections" Erasmus MC, Rotterdam, November 25

7th National Zoonoses Symposium - Wildlife Zoonoses: How wild are the Netherlands? RIVM and NVWA, Faculty of Veterinary Medicine, Utrecht University, December 3

2014 Advances in Comparative Pathology, "The Central Nervous System" Erasmus MC, Rotterdam, May 26

Virology in the last 4 decades, breakthroughs and benefits. Ab's farewell symposium. World Trade Center, Rotterdam, July 2

2016 Influenza D virus: Surveillance and Pathogenesis, by Mariette F Ducatez École Nationale Vétérinaire de Toulouse, Utrecht University, November 22

Teaching

Lecturing

2009-2015 ECVP-styled Mock Board Exam Training of residents in veterinary pathology, Utrecht

Tutoring

2009-2010 Tutor of two residents in veterinary pathology, Utrecht

Other

2012 Preparation of photographic display material for opening exhibition for opening exhibition of the new education center Erasmus MC Rotterdam

LIST OF PUBLICATIONS

Relevant to this thesis:

EJB Veldhuis Kroeze & T Kuiken. Chapter 23: Sporadic Influenza A Virus Infections of Miscellaneous Mammal Species. In Animal Influenza, 2nd edition. Editor D.E. Swayne. Wiley-Blackwell, Hoboken, New Jersey, 2016. ISBN: 978-1-118-90746-7.

KR Short, **EJB Veldhuis Kroeze**, LA Reperant, M Richard, T Kuiken. Influenza virus and endothelial cells: a species specific relationship. *Front Microbiol* (2014) 2 Dec. 5: 653. Review.

AK Maltais, KJ Stittelaar, **EJB Veldhuis Kroeze**, G van Amerongen, ML Dijkshoorn, GP Krestin, J Hinkula, H Arwidsson, A Lindberg, ADMO Osterhaus. Intranasally administered Endocine™ formulated 2009 pandemic influenza H1N1 vaccine induces broad specific antibody responses and confers protection in ferrets. *Vaccine* (2014) May 30;32(26):3307-15.

AJ Mann, N Noulin, A Catchpole, KJ Stittelaar, L de Waal, **EJB Veldhuis Kroeze**, M Hinchcliffe, A Smith, E Montomoli, S Piccirella, ADME Osterhaus, A Knight, JS Oxford, R Lambkin-Williams. Intranasal H5N1 Vaccines, Adjuvanted with Chitosan Derivatives, Protect Ferrets against Highly Pathogenic Influenza Intranasal and Intratracheal Challenge. *PLoS ONE* (2014) May 21;9(5):e93761.

KR Short, **EJB Veldhuis Kroeze**, RAM Fouchier, T Kuiken. Pathogenesis of influenza-induced acute respiratory distress syndrome. *Lancet Infect Dis* (2014) Jan;14(1):57-69. Review.

JH Kreijtz*, **EJB Veldhuis Kroeze***, KJ Stittelaar, L de Waal, G van Amerongen, S van Trierum, P van Run, T Bestebroer, T Kuiken, RAM Fouchier, GF Rimmelzwaan, ADME Osterhaus. Low pathogenic avian influenza A(H7N9) virus causes high mortality in ferrets upon intratracheal challenge: A model to study intervention strategies. *Vaccine* (2013) Oct 9;31(43):4995-9.

E van der Vries, KJ Stittelaar, G van Amerongen, **EJB Veldhuis Kroeze**, L de Waal, PLA Fraaij, RJ Meesters, TM Luider, B van der Nagel, B Koch, AG Vulto, M Schutten, ADME Osterhaus. Prolonged influenza virus shedding and emergence of antiviral resistance in immunocompromised patients and ferrets. *PLoS Pathog* (2013) 9(5):e1003343.

EJB Veldhuis Kroeze, KJ Stittelaar, VJ Teeuwsen, ML Dijkshoorn, G van Amerongen, L de Waal, T Kuiken, GP Krestin, J Hinkula, ADME Osterhaus. Consecutive CT *in vivo* lung imaging as quantitative parameter of influenza vaccine efficacy in the ferret model. *Vaccine* (2012) 17. pii: S0264-410X(12)01454-5.

EJB Veldhuis Kroeze, T Kuiken, ADME Osterhaus. Chapter 8: Animal models. Methods Mol Biol. 2012;865:127-46. In Influenza Virus, methods and protocols. Series: Methods in Molecular Biology, Vol 865. Kawaoka, Yoshihiro; Neumann, Gabriele (Eds.) Springer, New York, 2012. ISBN 978-1-61779-620-3.

E van der Vries, **EJB Veldhuis Kroeze**, KJ Stittelaar, M Linster, A van der Linden, EJA Schrauwen, LME Leijten, G van Amerongen, M Schutten, T Kuiken, ADME Osterhaus, RAM Fouchier, CAB Boucher, S Herfst. Multidrug Resistant 2009 A/H1N1 Influenza Clinical Isolate with a Neuraminidase I223R Mutation Retains Its Virulence and Transmissibility in Ferrets. *PLoS Pathog* (2011) 7(9):e1002276.

KJ Stittelaar, **EJB Veldhuis Kroeze**, L Rudenko, R Dhere, S Thirapakpoomanunt, MP Kieny, ADME Osterhaus. Efficacy of live attenuated vaccines against 2009 pandemic H1N1 influenza in ferrets. *Vaccine* (2011) 29(49):9265-70.

EJB Veldhuis Kroeze, G van Amerongen, ML Dijkshoorn, JH Simon, L de Waal, I Hartmann, GP Krestin, T Kuiken, ADME Osterhaus, KJ Stittelaar. Pulmonary pathology of pandemic influenza A/H1N1 virus (2009) infected ferrets upon longitudinal evaluation by computed tomography. *J Gen Virol* (2011) 92(Pt 8):1854-8.

B Baras, L de Waal, KJ Stittelaar, V Jacob, S Giannini, **EJB Veldhuis Kroeze**, JMA van den Brand, G van Amerongen, JH Simon, E Hanon, SP Mossman, ADME Osterhaus. Pandemic H1N1 vaccine requires the use of an adjuvant to protect against challenge in naive ferrets. *Vaccine* (2011) 29(11):2120-6.

* Both authors contributed equally to the results of this study.

Others:

FC Velkers, SJ Blokhuis, **EJB Veldhuis Kroeze**, SA Burt. The role of rodents in Avian Influenza outbreaks in poultry farms: a review. *Vet Quart* (2017) Submitted.

KJ Stittelaar, L de Waal, G van Amerongen, **EJB Veldhuis Kroeze**, PLA Fraaij, C van Baalen, JJ van Kampen, E van der Vries, ADME Osterhaus, RL de Swart. Ferrets as a novel animal

model for studying human respiratory syncytial virus infections in the immunocompetent and immunocompromised host. *Viruses* (2016) Jun 14;8(6). pii: E168.

M Achten-Weiler, **EJB Veldhuis Kroeze**, S Boerma, JH van der Kolk. Hairy cell-like leukemia in a 9-year-old Friesian mare. *Vet Quart* (2016) Jun;36(2):105-8.

N Sleeckx, L Van Brantegem, G Van den Eynden, E Fransen, C Casteleyn, S Van Cruchten, **EJB Veldhuis Kroeze**, C Van Ginneken. Angiogenesis in Canine mammary Tumours: a Morphometric and Prognostic Study. *J Comp Path* (2014) Feb-Apr;150(2-3):175-83.

N Sleeckx, L Van Brantegem, E Fransen, G Van den Eynden, C Casteleyn, **EJB Veldhuis Kroeze**, C Van Ginneken. Lymphangiogenesis in Canine mammary Tumours: a Morphometric and Prognostic Study. *J Comp Path* (2014) Feb-Apr;150(2-3):184-93.

JH van der Kolk & **EJB Veldhuis Kroeze**. Infectious Diseases of the Horse. Diagnosis, pathology, management, and public health. Manson Publishing, London, 2013. ISBN: 978-1-84076-165-8.

N Sleeckx, L Van Brantegem, E Fransen, G Van den Eynden, C Casteleyn, **EJB Veldhuis Kroeze**, C Van Ginneken. Evaluation of Immunohistochemical Markers of Lymphatic and Blood Vessels in Canine Mammary Tumours. *J Comp Pathol* (2013) May;148(4):307-17.

VJ van Essen, JJ Uilenreef, V Szátmari, **EJB Veldhuis Kroeze**, RV Kuiper, J Rothuizen, A de Bruin. Ultrasound-guided serial transabdominal cardiac biopsies in cats. *Vet J* (2012) 191(3):341-6.

N Sleeckx, H de Rooster, **EJB Veldhuis Kroeze**, C Van Ginneken, L Van Brantegem. Canine Mammary Tumours, an Overview. *Reprod Domest Anim* (2011) 46(6):1112-31. Review.

V Szatmári, MW Freund, **EJB Veldhuis Kroeze**, J Strengers. Juxtaductal coarctation of both pulmonary arteries in a cat. *J Vet Diagn Invest* (2010) 22(5):812-6.

JJ Buijtels, J de Gier, HS Kooistra, **EJB Veldhuis Kroeze**, AC Okkens. Alterations of the pituitary-ovarian axis in dogs with a functional granulosa cell tumor. *Theriogenology* (2010) 73(1):11-9.

JJ Buijtels, J de Gier, T van Haeften, HS Kooistra, B Spee, **EJB Veldhuis Kroeze**, C Zijlstra, AC Okkens. Minimal external masculinisation in a SRY-negative XX male Podenco dog. *Reprod Domest Anim* (2009) 44(5):751-6.

EP Reijerkerk, **EJB Veldhuis Kroeze**, MM Sloet van Oldruitenborgh-Oosterbaan. Equine sarcoidosis. *Sarcoidosis Vasc Diffuse Lung Dis* (2009) 26(1):20-3. Review.

F Fracassi, D Shehdula, A Diana, **EJB Veldhuis Kroeze**, BP Meij. Primary Polycythemia in a Dog with Hypercortisolism. *J Vet Clinical Sciences* (2009) 2(2):42-50.

EP Reijerkerk, **EJB Veldhuis Kroeze**, MM Sloet van Oldruitenborgh-Oosterbaan. Generalised sarcoidosis in two horses. *Tijdschr Diergeneeskd* (2008) 133(16):654-61.

R van den Boom, **EJB Veldhuis Kroeze**, WR Klein, DJ Houwers, AG van der Zanden, MM Sloet van Oldruitenborgh-Oosterbaan. Granulomatous pneumonia, lymphadenopathy and hepatopathy in an adult horse with repeated injection of BCG. *J Vet Intern Med* (2008) 22(4):1056-60.

SJ Hernandez-Divers, D Martinez-Jimenez, S Bush, KS Latimer, P Zwart, **EJB Veldhuis Kroeze**. Effects of Allopurinol on plasma uric acid levels in normouricaemic and hyperuricaemic green Iguanas (*Iguana iguana*). *Vet Rec* (2008) 162(4):112-5. Erratum in: *Vet Rec* (2008) 162(24):776.

A Brünott, **EJB Veldhuis Kroeze**, JM Ensink, TTJM Laan, MM Sloet van Oldruitenborgh-Oosterbaan. A colonic epidermoid cyst as a cause of chronic recurrent colic in a horse. *Equine Vet Educ* (2007) 19(3):123-8.

JJ Buijtels, **EJB Veldhuis Kroeze**, G Voorhout, CJ Schellens, JJ van Nes. Cerebellar cortical degeneration in an American Staffordshire terrier. *Tijdschr Diergeneeskd* (2006) 131(14-15):518-22.

EJB Veldhuis Kroeze, J Zentek, A Edixhoven-Bosdijk, J Rothuizen, TSGAM van den Ingh. Transient Erythropoietic Protoporphyria associated with chronic hepatitis and cirrhosis in a cohort of German shepherd dogs. *Vet Rec* (2006) 158(4):120-4.

CM de Bruijn, **EJB Veldhuis Kroeze**, MM Sloet van Oldruitenborgh-Oosterbaan. Yellow fat disease in equids. *Equine Vet Educ* (2006) 18(1):38-44.

JE van Dijk, E Gruys, JMVM Mouwen. (eds.), with contributions of TSGAM van den Ingh, JP Koeman, GCM Grinwis, JJ van der Lugt, **EJB Veldhuis Kroeze**. Color Atlas of Veterinary Pathology: General Morphological Reactions of Organs and Tissues, 2nd ed. Elsevier, 2006. ISBN: 978-0-70202-758-1.

NA Benders, **EJB Veldhuis Kroeze**, JH van der Kolk. Idiopathic muscular hypertrophy of the oesophagus in the horse: a retrospective study of 31 cases. *Equine Vet J* (2004) 36(1):46-50.

EJ Verdegaal, **EJB Veldhuis Kroeze**, KJ Dik, LA van Oijen, MM Sloet van Oldruitenborgh-Oosterbaan. Unilateral facial paralysis and keratitis sicca, signs of temporohyoid osteoarthropathy in the horse. *Tijdschr Diergeneeskd* (2003) 128(24):760-6.

WL Jansen, J Bos, **EJB Veldhuis Kroeze**, A Wellen, AC Beynen. Apparent digestibility of macro-nutrients in captive polar bears (*Ursus maritimus*). *Zool Garten N.F.* (2003) 73(2):111-5.

DANKWOORD

Na lang wachten en veel 'gezwoeg', is het nu dan eindelijk zover! De afronding van dit proefschrift middels het schrijven van mijn dankwoord aan al die personen welke een rol hebben gespeeld in de totstandkoming van dit proefschrift. Bedankt aan alle leden van de lees- en promotiecommissie.

Beste Ab, mijn promotor en 'silverback' van de afdeling waar je mij het vertrouwen en de mogelijkheid gaf te promoveren naast een reguliere aanstelling als veterinair patholoog bij Viroclinics (VC), hartelijk dank hiervoor! Altijd (vaak) had je tijd en gelegenheid voor overleg en reflectie. Ondanks het niet altijd volbrengen van studies met vernieuwende experimentele onderzoeksideeën die opborrelden tijdens brainstormsessies, was het voor mij niet alleen een voorrecht maar vooral een groot plezier om jou, vanwege je immer constructieve en motiverende instelling, als promotor te mogen hebben.

Beste Thijs, mijn promotor, bedankt dat je altijd oprecht, objectief en wetenschappelijk kritisch bent. Jouw insteek als promotor is om de promovendus te onderrichten als wetenschappelijk onderzoeker in brede zin. Zodoende heb ik veel van je geleerd, zelfs meer dan van pathologie en onderzoek alleen. Zo wil ik je bij dezen roemen om je brede scoop, je visie, en ook je vogelgeluidenimitaties zijn legendarisch. Altijd (meestal) maakte je tijd voor overleg, zij het direct probleemoplossend of breder meer holistisch middels enige wetenschapsfilosofie. Het is een privilege van je te hebben mogen leren en met je samen te werken, hopelijk ook nog in de toekomst. En wie had ooit gedacht, ik zeker niet, dat wij jarenlang dezelfde slaapkamer, al zij het niet gelijktijdig, zouden delen!

Hartelijk dank ook aan de directie van VC, met name Hans en Bob (en eerder James), voor de mij geboden mogelijkheid om te promoveren naast mijn reguliere aanstelling bij VC, al ging het niet altijd even vlot als verwacht. Echter het uitgangspunt van het promotietraject was dat het mes aan twee kanten zou snijden, mijn promoveren enerzijds en het proefschrift als uithangbord voor de preklinische capaciteiten met specialistische mogelijkheden van VC anderzijds, en dat is uiteindelijk prima gelukt.

De preklinische groep van VC, Koert ik wil je bedanken voor je nimmer aflatende vasthoudendheid maar vooral voor de plezierige samenwerking tijdens de imagingstudies aan het begin van dit promotieonderzoek, Geert ('zonder Geert geen dierproeven') bedankt voor je professionaliteit, tomeloze inzet en gezelligheid en tijdens het verrichten van de vele secties, ik denk dat ik met niemand meer gelachen heb tijdens het seceren. Beste Leon, Willem, Rob, Cindy, Vera, Ronald, preklinikers van het eerste uur, maar

ook die van meer recente samenstelling, Ikrame, Willem H., Rosalie, Marla, Saskia SB, Saskia SCB, Patricia, Jonneke, Marie, Stephane, Simone, en Susan welke allen direct en indirect hun bijdrage hebben gehad aan dit proefschrift, bedankt. Natuurlijk bedankt ook aan alle andere collega's van VC met wie ik in de afgelopen jaren zeer plezierig heb samengewerkt, al dan niet direct gerelateerd aan de totstandkoming dit proefschrift. Voorts wil ik in deze context ook nog noemen de mensen uit het Bilthoventijdperk, Nico, Hans ook nog bedankt voor de muziek, Jan (†), Wim, en Stephane (thans dus ook 'echte' VC collega), en ook dank aan de medeauteurs van mijn wetenschappelijke publicaties m.n. die van de Afdeling Radiologie van het EMC, Marcel Dijkshoorn, Ieneke Hartmann en Prof Krestin.

Dan de befaamde wildlifegroep alias de comparative-pathologygroep, bedankt voor de gezelligheid en de extra-curriculaire bezigheden zoals etentjes bij collega's thuis en andere uitjes, en ook wil ik een ieder prijzen om het altijd warme welkom dat jullie als groep heten aan nieuwe langdurige of kortere tijdelijke gastkamerbewoners (zoals o.a. Tony, Victor, Ursula, Caroline, Marianna, Rebecca (thans VC collega) en Janneke). Verder specifiek dank aan, Peter altijd vriendelijk, punctueel en perfectionistisch, bedankt voor al je histologische werk met strakke planning (coupes zeker weer z.s.m. klaar…?), Marco bedankt voor de gezellige gesprekken vooral die met autosport-updates, Niels bedankt voor je regelmatige onregelmatige maar altijd opwekkende aanwezigheid op de kamer en ook voor het delen van je werkplek, Lonneke bedankt omdat je altijd zo aardig en behulpzaam bent in nog even snel wat immuno's of in situ's, Debby bedankt voor je wetenschappelijke ambitie dat het naast mijzelf voor velen tot inspiratie mag zijn, jammer dat na af en toe wat 'sparren' het (nog) nooit tot een vruchtbare wetenschappelijke samenwerking of publicatie is gekomen maar wie weet, Leslie bedankt voor je specialistische kennis van kansberekeningsmodellen en enthousiaste uitleg daarover, jammer dat je plots geen kamergenoot meer was, Kirsty bedankt voor onze plezierige en efficiënte samenwerking aan jouw papers met co-auteurschap, en ik waardeer je harde en doelgerichte werken en ook je talenknobbel, Lineke bedankt dat je, nadat je vanuit Utrecht naar elke maandelijkse 'Comparative Pathology Meeting' kwam, na enige tijd gelukkig ook in Rotterdam bleef hangen als, door iedereen en zeker door mij, zeer gewaardeerde aanwinst in de groep (alleen al voor de lekkere koffie), Lidewij bedankt voor ons fijne contact gedurende de laatste jaren zowel in Utrecht als Rotterdam, het lijkt nog maar zo kort geleden dat wij onderweg naar een walvis een gesprek voerden over je komende promotieonderzoek, om daarna als tussenstopje naar Rome in sneltreinvaart even je promotie af te ronden, chapeau! Jurre, je maakt mij altijd aan het lachen, bedankt voor je vrolijkheid op de kamer en het lab, en we gaan hierna echt een biertje doen, beloofd. En natuurlijk mijn paranimf Judith, bedankt voor onze hechte band zowel professioneel als persoonlijk gedurende onze parallel verlopende

loopbaan, bedankt voor de regelmatige gesprekken en gezamenlijke vakinhoudelijke interesse en kennisuitwisseling met als voorbeeld van weleer onze (samen met Jaco) memorabele 'Ten Bells' die onze boards verzekerde.

Verder nog van de afdeling, beste Rogier altijd (hoorbaar) goedlachs en opgewekt, bedankt voor je kunde en tijd die je er voor over had om mij wegwijs te maken met viruskweken, virustitraties en inoculeren van muizen en meer, maar ook voor de goede en amusante gesprekken die we veelal voerden tijdens onze gezamenlijke terugreis naar Utrecht. Voorts, Joost bedankt voor je plezierige en professionele samenwerking met de muizenproeven en later met de frettenstudie, Stella bedankt voor o.a. je spoedhulp bij de H7N9 immunokleuringen, Erhard bedankt voor de prima samenwerking tijdens de vele frettenstudies, Pieter jammer dat ons ECMO initiatief nooit van de grond is gekomen en ook jammer dat de pred-studie dat ook bleek en bleef, echter bedankt voor de goede samenwerking met brainstormen en je gezelligheid en behulpzaamheid, David bedankt voor je onmisbare ondersteuning op statistisch gebied en je opgewektheid in gedagzeggen op de gang.

Verder dank aan de dames van het secretariaat, Simone, Loubna, Maria, en Anouk, bedankt voor de uiteenlopende, tot manuscriptsubmissies aan toe, administratieve ondersteuning. Verder wil ik aan ieder van de afdeling mijn algemene dank uitspreken voor mijn welkom voelen, en wil daarbij, zonder niet genoemden tekort te doen, met naam noemen: Ron, Guus, Jan, Theo, Sander H, Monique, Mathilde, Sander v B, Miranda, Patrick, Rob, Stalin, Petra, Byron, Nella, Sarah, Penelope, Josanne, Rik, Arno, en Marion, en in het bijzonder ook dank aan diegenen van de afdeling die op mijn verzoek een voordracht gaven op een van de 'Comparative Pathology Meetings': Bart, Georges, Rory, Tien, Werner, Cox, Marco G., Corine, en nogmaals Debby/Rogier en ook weer Kirsty.

Frank en Joris van de MolMed PGS bedankt voor de vlekkeloze organisatie en plezierige samenwerking tijdens deze 'Comparative Pathology Meetings' op elke tweede dinsdag van de maand en later tijdens de 'Advances in Comparative Pathology' in voor- en najaar, en in deze context ook hartelijk dank aan Rob Verdijk voor zijn onmisbare 'humane' bijdrage aan de vergelijkende pathologie.

Verder wil ik graag een aantal mensen, allen bevlogen veterinair pathologen, bij naam noemen welke door hun kennis en kunde in de veterinaire pathologie, en dus indirect voor dit proefschrift, van groot belang zijn geweest (en de meesten nog steeds zijn): Ingrid van der Gaag bedankt dat je zo'n enorme motiverende uitwerking op mij hebt gemaakt tijdens de co-schappen in de sectiezaal, voorts heel veel dank aan mijn hoofdopleider Ted van den Ingh, en verder natuurlijk aan Jaap van Dijk, Erik Gruys en Peer Zwart. Beste Erik en beste Peer bedankt voor onze goede en warme contacten,

ook met vakinhoudelijke uitwisseling, die wij tot op de dag vandaag onderhouden. In het bijzonder bedankt Peer voor de vele interessante casuïstieken van exoten die wij gezamenlijk onder de microscoop bestudeerden in mijn tijd in Utrecht, waarbij wij beiden telkens weer bijna kinderlijk zo blij verwonderd waren over de schoonheid van ons vak, zo zal ik nooit de simpele maar functionele perfectie van de bouw van het 'camera obscura-oog' van een nautilus vergeten die je mij onder de microscoop schoof. Verder veel dank aan Guy en Jaco voor jullie bijdrage in mijn vorming als patholoog en ook voor de fijne tijd als directe collega's en voor jullie vriendschap.

Mijn lieve moeder en vader, veel dank voor de steun en ook zeker voor de vrijheid die ik van jullie kreeg tijdens mijn jeugd en later tijdens mijn studie diergeneeskunde te Utrecht. Bedankt voor het stimuleren van mijn interesses in dieren en hun natuur door mij nooit een strobreed in de weg te leggen om deze verder te kunnen ontdekken en te ontwikkelen. Als een voorbeeld van mijn onbezorgde en prima gefaciliteerde jeugd; bedankt mam dat je altijd zo stoïcijns mijn ontsnapte slangen vanuit de wasmand of vanachter verwarmingsradiatoren in een van de vele terraria, waar mijn kinderkamer volledig mee volgebouwd was, terugstopte, of de vanzelfsprekendheid waarmee je jonge slangen uit hun ei hielp uitkomen wanneer ik op pad was, en dat jullie er ook nooit een punt van maakten wanneer je in het vriesvak weer eens misgreep naar een zak vol met eigen gekweekte knaagdieren i.p.v. de beoogde diepvrieszakjes met mensenvoedsel, en ook dat waterteilen vol levende vissen, soms met ook allerhande kikkers en/of salamanders en/of schildpadden het balkon mochten bevolken. Kortom, lieve pap en mam, en ook aan mijn lieve zuster Peggy, bedankt voor mijn warme nest, bedankt voor het beantwoorden van al mijn vragen en bedankt voor de mogelijkheid mij onbezorgd te laten opgroeien en studeren.

Als laatste wil ik mijn lieve vrouw Marcelle bedanken voor alle geduld die ze afgelopen jaren met mij heeft gehad, dank voor je steun en motivatie, dank voor je liefde, dank voor onze zoon Ocke, die ondanks dat hij ons drukke schema wat drukker maakte, het mooiste en grootste geluk in ons leven is.

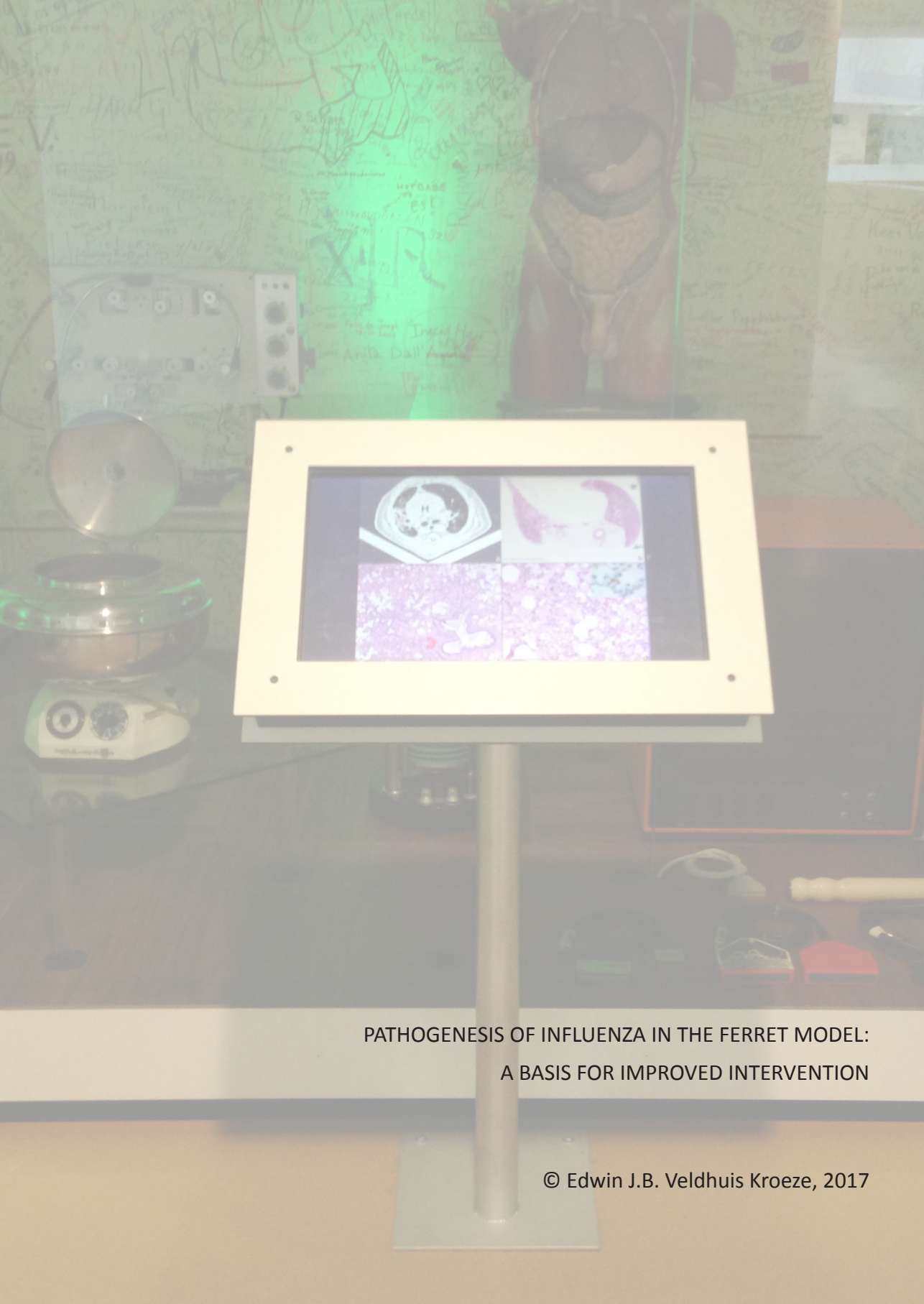

PATHOGENESIS OF INFLUENZA IN THE FERRET MODEL: A BASIS FOR IMPROVED INTERVENTION